BLACK CARBON IN SOIL ORGANIC AND MINERAL MATTER

A Dissertation

Presented to the Faculty of the Graduate School

of Cornell University

In Partial Fulfillment of the Requirements for the Degree of

Doctor of Philosophy

By

Karen Baldovi Heymann

August, 2012

.

BLACK CARBON IN SOIL ORGANIC AND MINERAL MATTER

Karen Baldovi Heymann, Ph. D.

Cornell University 2012

Black carbon (BC) is considered ubiquitous in soil organic matter and therefore plays an important role in soil biogeochemistry. This research largely relied on advanced Near-edge X-ray absorption fine-edge (NEXAFS) spectroscopy to expand our understanding of black carbon chemistry, and to investigate the mechanisms controlling black carbon stability in soil. The international BC ring trial was characterized using NEXAFS; our results indicated that NEXAFS is a reliable approach for spectroscopic characterization of BC in soil. We also evaluated two mathematical modeling approaches to quantify black carbon (BC) in a BC-rich Anthrosol using carbon (C) near-edge X-ray absorption fine-edge structure (NEXAFS) spectroscopy. Best fit results (lowest error) were achieved using BCs formed at 500ºC-600ºC compared with BC produced at at 350ºC-450ºC. BC produced at lower temperatures were characterized by lower aromaticity than those produced at higher temperatures. These differences suggest that assumptions about formation temperature of BC may affect the quantification of BC contained in soil for methods that rely on reference materials. We attempted to verify the existence of BC HS using Scanning Transmission X-ray Microscopy (STXM) coupled with near-edge X-ray absorption fine-edge spectroscopy (NEXAFS) spectroscopy to analyze the spatial composition of a BC rich soil microaggregate at a scale of < 50 μm. However, we were unable to obtain a good fit (RMS = <0.01) for the HS extracts within the spatial map. Our results suggest that HS do not exist in soil as a distinct component class but rather reflect the extraction of various materials at different stages of

decomposition. Near-edge X-ray absorption fine-edge spectroscopy (NEXAFS), scanning electron microscopy (SEM) and scanning transmission electron microscopy (STEM) were used to compare BC exposed to water, nitric acid (HNO_3), kaolinite, pyrophyllite, vermiculite and goethite. that multiple mechanisms such as electrostatic interactions, ligand exchange, electron donor or acid-base reactions play a role in the interaction between BC and clay minerals. High-resolution microscopy revealed that BC-mineral interactions can commence quickly and result in chemical changes to BC.

BIOGRAPHICAL SKETCH

Karen was raised in the suburbs of Boston, Massachusetts. Her earliest introduction to agriculture was through the grandfather, who cultivated enormous gardens at his home outside of Barcelona, Spain. Karen was able to develop her interest in farming when she attended college in the Pioneer Valley of Western Massachusetts and worked on an organic vegetable farm. She earned bachelor's degrees in Social Thought and Political Economy (STPEC) and in Plant, Soil and Insect Sciences at the University of Massachusetts, Amherst. She went on to obtain her Master's Degree at University of Massachusetts, Amherst in Plant, Soil and Insect Sciences.

Karen was awarded an IGERT Fellowship by the National Sciences Foundation and the Department of Biogeochemistry and Environmental Biocomplexity at Cornell Univerity to continue her graduate studies. In January of 2007 she joined the Soil Biogeochemistry group supervised by Dr. Johannes Lehmann, at Cornell. Upon completion of her Ph.D. Karen was awarded a Congressional Science Policy Fellowship by the Soil, Crop and Agronomy Societies of America. Karen is married to Mike Flood and they have a son, William Joseph Flood.

for Rockfish

ACKNOWLEDGMENTS

This study was funded by grants from the NSF IGERT program (BCS-0215890), the NSF-Geobiology (EAR-0819689), USDA-AFRI (2008-35107-04511) and the Department of Crop and Soil Sciences at Cornell University. The NEXAFS spectra were obtained from the Canadian Light Source, University of Saskatoon, Sasketchewan as well as at the National Synchrotron Light Source (NSLS), Brookhaven National Laboratory, at the Beamline X-1A1 developed by the research group of Janos Kirz and Chris Jacobsen at SUNY, Stony Brook. Many thanks to S. di Stasio and A. Braun are thanked for the spectra they provided, and to Jeff Baldock for his assistance with the Molecular Mixing Model. This study was financially supported by grants from the NSF IGERT program (BCS-0215890), the NSF-Geobiology (EAR-0819689), USDA-AFRI (2008-35107-04511) and the Department of Crop and Soil Sciences at Cornell University. Any opinions, findings and conclusions or recommendations expressed in this material are those of the authors and do not necessarily reflect the views of the National Science Foundation.

I would like to recognize the guidance, consel and support from my advisor, Johannes Lehmann, and to my committee, Janice Thies and John Duxbury. I would also like to express my gratitude to Stephen DeGloria for his support and encouragement. A special thank you to Dawit Solomon for all his encouragement and expertise, particularly late at night in remote locations. Many thanks to the soil biogeochemistry laboratory group at Cornell, and a special thank you to Kelly Hanley and Akio Enders for their help in the laboratory, and to all who helped me along the way.

TABLE OF CONTENTS

LIST OF FIGURES

LIST OF TABLES

1. C 1S K-EDGE NEAR-EDGE X-RAY FINE STRUCTURE (NEXAFS) SPECTROSCOPY FOR CHARACTERIZING THE FUNCTIONAL GROUP CHEMISTRY OF BLACK CARBON

Abstract

Black carbon (BC) is considered ubiquitous in soil organic matter and therefore plays an important role in soil biogeochemistry. The complexity of BC, particularly within environmental matrices, presents a challenge to research primarily due to techniques which may favor the detection of certain functional group types rather than capturing total sample C. The objective of this study was to utilize carbon (C) 1s near-edge X-ray absorption fine edge structure (NEXAFS) spectroscopy to characterize the C chemistry of a broad range of BC materials. Characteristic resonances in the NEXAFS spectra allowed for direct molecular speciation of the total C chemistry of BC reference materials, environmental matrices, and potentially interfering materials, obtained from an earlier BC ring trial. Spectral deconvolution was used to further identify the functional group distribution of the materials. BC reference materials and soils were characterized by a large aromatic C region comprising around 40% of total absorption intensity. We were able to distinguish shale and melanoidin from BC reference materials based on their unique spectral characteristics. However, bituminous coal shared chemical characteristics with BC reference materials, namely high aromaticity of more than 40% identified by a broad peak. Lignite coal also shared similar spectra and functional group distributions with BC reference materials and bituminous coal. We compared the results of spectral deconvolution to the functional group distributions obtained by direct polarization magic angle spinning (DPMAS) ^{13}C Nuclear Magnetic Resonance (NMR). Correlations between aromatic type C values for DPMAS ^{13}C NMR and NEXAFS yielded an r^2=0.633

($p<0.05$), and the values for NEXAFS were around 30-40% lower than for ^{13}C NMR. Correlations were also drawn between the aromatic C/O-alkyl C ratio values for the two methods yielding an $r^2= 0.49$ ($p<0.05$). Overall, NEXAFS was applicable for a wide range of environmental materials such as those measured in this study; however, some limitations for this technique are addressed in this study.

1.1. Introduction

The black carbon (BC) continuum describes residues from the incomplete combustion of either biomass or fossil fuels (Schmidt and Noack, 2000; Preston and Schmidt, 2006). These combustion products reside largely in soils and sediments, and therefore play an important role in biogeochemical cycles (Czimczik and Masiello, 2007). BC serves as an important source and sink for global carbon (C) (Kuhlbusch, 1998; Masiello and Druffel, 1998) and is known to affect a multitude of soil properties and processes such as cation exchange capacity (Liang et al., 2006), nutrient dynamics (Lehmann et al., 2003), and microbial habitation (Pietikäinen et al., 2000). The profound sorption of hydrophobic organic contaminants by BC has long been observed in soils and marine sediments (Cornelissen et al., 2004; Xiao et al., 2004). Despite increased attention to BC in the literature over the last decade, many questions remain regarding its chemistry and subsequent influence on reactivity, recalcitrance, residence time, transport and accumulation in terrestrial and aquatic systems.

The forms of BC most relevant to terrestrial and marine biogeochemistry may be divided into two broad categories: soot, which is formed at high temperatures from the condensation of hydrocarbons in the vapor phase (Akhter et al., 1985a; Preston and Schmidt, 2006), and char, which is formed directly from biomass at lower temperatures than soot (<700º C) under oxygen deprived conditions (Fernandes and Brooks, 2003;

Hopkins et al., 2007). Natural and anthropogenic additions of BC strongly affect the chemical signatures of soils (Carter et al., 2002). For example, the accumulation of highly refractory aryl structures in Amazonian Dark Earths, attributed to the additions of biomass derived BC several hundred to a few thousand years ago, was suggested to be responsible for the biochemical recalcitrance and the stability of soil organic C (Solomon et al., 2007). Surface chemistry can strongly influence the fate of BC; for example, the extent of surface oxidation of atmospheric BC (soot, aerosols) can increase oxygen and defective structures at the particles interface, promoting higher chemical reactivity (Chughtai et al., 2002). Organic matter from Amazonian Dark Earths was observed to be enriched with aromatic C, O-rich C (carboxylic, aldehyde, ketone, quinine) and a diverse group of refractory alkyl C moieties. In contrast, organic matter of adjacent soils (unamended with BC) was predominantly composed of O-alkyl C and more labile alkyl C structures (Solomon et al., 2007). This trend of enrichment by BC is seen among a number of soils affected by fire regimes over long time spans (Skjemstad et al., 1999).

The complex surface and bulk chemistries of BC are not yet thoroughly understood due to highly variable formation conditions and until recently, a lack of international reference standards for cross-comparison among different studies and laboratories (Schmidt et al., 2001). The combustion continuum encompasses the chemical and physical properties used to describe BC forms, ranging from partially charred plant biomass to highly ordered soot and graphite (Baldock et al., 2004). The chemical properties of BC are dependent on pyrolysis conditions and fuel type; for example, the charring of even simple components of biomass (lignin, cellulose, wood) yields structural changes that vary with the material, temperature, and duration of charring (Reeves et al., 2007). The major defining characteristic of BC is the presence of fused aromatic C ring structures, which become progressively ordered and condensed with increasing formation

temperature (Schmidt and Noack, 2000). Carbon is a unique and versatile element due to the nearly infinite number of compounds it may form. This owes to the types of possible C bonds, the number of elements it can join in bonding, and the different hybridization states of these bonds (sp^2, sp^3 or mixed hybridization states). Graphite, for example, is comprised of a highly ordered periodic stack of graphene sheets comprised of a hexagonal lattice of C with strong sp^2 bonding, thus representing 100% sp^2 hybridization. Amorphous C, by contrast, has a mixture of sp^2 and sp^3 bonds and displays no long-range order. Brodowski et al. (2005) observed that soil BC occurred as both well-defined and amorphous particles using scanning electron microscopy (SEM). Lignocellulosic biomass is transformed from relatively amorphous C structures into polyaromatic graphene sheets with increasing temperature while low-temperature BC is likely to be a complex mixture of these two main C forms (Nguyen et al., 2010). Thorough characterization of the BC continuum therefore necessitates the detection of all C bonding states present in the sample of interest.

In order to further our understanding of BC chemistry and its role in the environment, the utilization of advanced spectroscopic techniques is required. Many analytical techniques (thermal, chemical, optical) employed for the characterization of BC, soils and sediments, are often optimized to detect only a portion of the chemical species present. For BC, this presents a challenge due to the extremely broad range of characteristics comprising the combustion continuum. Studies have been employed to determine what part of the BC spectrum is actually quantified by different methods (Elmquist et al., 2006). Solid state ^{13}C nuclear magnetic resonance (NMR) spectroscopy is widely used for the study of soils, natural organic matter, BC and marine sediments, and it is considered an accurate, semi-quantitative method for obtaining detailed information about the bulk chemistry of solid samples. Certain difficulties; however, are

encountered in ^{13}C NMR studies of BC which would benefit from the availability of additional spectroscopic techniques. Typical cross polarization (CP) ^{13}C NMR, may not detect 100% of BC carbon. This is due to the lack of protons in the highly aromatic structure of BC, which are necessary to achieve detection (Hedges et al., 2000). Improved Bloch-decay (BD) or direct polarization (DP) techniques are available, but are not yet commonly used due to extensive sample run times (Hedges et al., 2000) or difficulties in obtaining good NMR spectra for biochars produced at high temperatures (Freitas et al., 1999; Bourke et al., 2007). The high electrical conductivity associated with the alignment of aromatic sheets may make measurement difficult, and may also result in peak shifting due to delocalized π-electrons in aromatic structures (Freitas et al., 2002).

NEXAFS spectroscopy is a powerful counterpart for the chemical characterization of BC or other complex environmental materials as it may overcome some of the aforementioned limitations of other techniques. NEXAFS spectroscopy uses the intense, tunable, polarized X-ray beams generated by a synchrotron light source to probe the electronic states of a sample (Watts et al., 2006), and is able to capture total sample C. NEXAFS probes the X-ray absorption cross section of a sample through inner-shell excitation processes; at photon energies close to an atomic absorption edge, inner shell electrons are excited to an unoccupied energy level, thus creating resonance peaks in the absorption spectra (Stöhr, 1992). Detection methods for these resonances include total electron yield (TEY), which can be used for probing sample surfaces (~10 nm), and fluorescence yield (FLY), which is bulk sensitive and can be used to probe ~100 nm into the sample surface. FLY may be particularly useful for environmental samples such as soils, since electron yield from a sample depends on the charge transport properties of that sample.

NEXAFS is particularly suited for the characterization of chemically complex,

heterogeneous samples such as BC, since absorption spectra depend directly on the local bonding environment of atoms (Lehmann and Solomon, 2010). When coupled with scanning transmission X-ray microscopy (STXM), NEXAFS is one of the few approaches to map the nano-scale heterogeneity of soil particles with sub-micron resolution (Kirz et al., 1995; Jacobsen et al., 2000; Lehmann and Solomon, 2010). Determining the functional group chemistry at high spatial resolution has proven vital in demonstrating biogeochemically relevant processes of BC in soils (Lehmann et al., 2005; Liang et al., 2006, 2008). However, little published information exists regarding the characterization of different BC forms using C NEXAFS. Keiluweit et al. (2010) used C NEXAFS to relate chemical changes occurring in char as a function of formation temperature and starting material to observed physical changes. Hopkins et al. (2007) observed that NEXAFS spectra from three soots produced from diffusion flames (ethylene, methane, *n*-hexane) were highly similar to each other, but distinct in functional composition from other types of soots, such as diesel soot. This demonstrates the powerful capabilities of NEXAFS in detecting fine-scale characteristics for distinguishing BC forms.

The main objectives of this research were (1) to characterize the C chemistry of contrasting forms of BC materials; (2) to determine the value of NEXAFS to distinguish different BC types and non-BC organic matter in terrestrial ecosystems; (3) to assess the value of NEXAFS for obtaining spectra of environmentally complex samples such as BC. To date, no NEXAFS study is available that attempts to quantify the functional group chemistry of different BC types relevant for biogeochemical processes in soils and sediments.

1.2. Material and methods

1.2.1 Materials

Reference materials identified by the BC steering committee (Schmidt et al., 2003; Hammes et al., 2007) were used for this study. Descriptions of these reference materials can be found at http://www.geo.uzh.ch/phys/bc. The reference materials are categorized in three groups: (1) BC reference materials: *n*-hexane soot, grass char, and wood char; (2) environmental matrices: aerosol (urban dust NIST 1649a), marine sediment (NIST 1941b), a sand-rich Chernozem, a clay-rich Vertisol, and dissolved organic matter from the Suwannee river; (3) potentially interfering materials: melanoidin, shale, bituminous coal (Pocahontas), lignite coal (Beulah-Zap).

1.2.2 Sample preparation

The reference materials were mixed with C-free nanopure water (1 mg per 2 mL water) in 5-mL Eppendorf vials. The vials were lowered briefly into an ultrasound bath in order to achieve homogeneous wetting of the samples. Using a pipette, approximately 1 mL of the sample solution was deposited onto gold coated silicon wafers. The wafers were prepared by thermally evaporating an optically opaque layer of pure gold onto the unpolished side of commercially available Si wafers. The thermal evaporation used a 0.25-mm thick W filament that was wetted with Au (Lesker, 99.9 % pure). The deposition was done at a pressure of 10^{-5} Torr and once prepared, the substrates were left under vacuum until shortly before the sample preparation and subsequent NEXAFS measurements took place.

1.2.3. Sample Measurement

C (1s) NEXAFS spectra were obtained on beamline 11ID-1 at the Canadian Light Source (CLS) located at the University of Saskatchewan, Saskatoon, Canada. The beamline is equipped with a Spherical Grating Monochromator (SGM) designed for high resolution soft X-ray spectroscopy (Regier et al., 2007). Total fluorescence yield (FLY) was measured using a chevron stacked Micro-Channel Pate (MCP) detector with a bias of -1600 V. The detector is at the same elevation as the sample and makes an angle of 43 degrees with respect to the beam axes. A negatively charged grid in front of the detector was used to repulse electrons from the detector. The prepared sample plate was loaded into a vacuum chamber (1e-7 Torr). The beamline was configured for resolving power of approximately 7500 at the C K edge (exit slit gap of 50 μm) and the photon energy was scanned from 270 to 310 eV. Dwell time was set at 0.5 s. Background measurements were taken by measuring an empty gold wafer on each sample plate loaded into the chamber. A normalization current was also measured during each scan by collecting the TEY from an Au mesh. The mesh was monitored for C contamination and was periodically refreshed using an in-situ Au evaporator that is incorporated into the beamline vacuum system. A Ti filter was used in the beamline to reduce the effects of 2^{nd} order oxygen in the pre-edge region. Two measurements were taken for each sample at different spots on the sample to make sure that the resulting spectra were identical. If inconsistencies were observed, additional measurements were taken. Main 1s-pi* and Rydberg/ mixed valence transitions in the fine structure regions of C K-edge spectra recorded from BC ring trial samples span from an energy range of 284-310 eV. The fine structures in the C (1s) NEXAFS region above 290 eV transitions tend to be broad and overlap with each other (Cody et al., 1998; Schäfer et al., 2003); therefore, only the main 1s-pi* transitions were used for interpretation of the NEXAFS results in this study.

Spectra were background subtracted as follows:

$$I_{sub} = I_{(FLY,\ TEY)} - gold_{(FLY,\ TEY)} / I_o,$$

where I_{sub} corresponded to the subtracted signal, $I_{(FLY,\ TEY)}$ corresponded to the sample current from either FLY or TEY, and Io to the current from a gold mesh-monitor located upstream from the sample. In order to correct for C contamination in the beamline optics, a linear transformation was applied to normalize the pre-edge region of the sample with the pre-edge region of clean gold measured at the beginning of the experimental run. The details of this method can be found in the supplementary online methods.

All data were normalized prior to curve fitting using ATHENA 0.8.052 software (Ravel and Newville, 2005). The photon energy was calibrated to the C 1s-> pi^* resonance in CO gas at 287.38 eV. Spectra were characterized according to the peak assignments listed in Table 1.1.

Table 1.1. C 1s NEXAFS approximate transition energy ranges and assignments of primary absorption peaks; median values are indicated as average values for final fit position for all 12 standards

Organic C forms	Bond	Transition	Peak energy (eV)	Deconvolution Curve	Fit position	Median
Aromatic-C Quinone-C	C=O	1 s-π*	283-284.5	G1	284.5	284.4 (-0.1)
Aromatic C	C=C	1 s-π*	284.9-285.5	G2	285.4	285.4
Aromatic C	C=O	1 s-π*	285.8-286.2	G3	286.1	286.1
Aromatic C with substituent	C=C-OH C=O R-(C=O)-R'	1 s-π*	286-287.4	G4	286.7	286.8 (+0.1)
			287-287.6	G5	287.6	
Alkyl C	C-H	1 s-π*				287.7
Carboxylic C	R-COOH COO C=O	1s-3p/σ*	288- 288.7	G6	288.4	288.4
O-alkyl C	C-OH	1 s-π*	289.2-289.5	G7	289.2	289.2
O-alkyl C/ Carbonyl	COO^-	1 s-π*	289.5-290.2	G8	289.9	289.9

The samples in this study are not expected to have any long range order, since the C in the sample is randomly oriented. Therefore, there should be no polarization effects.

1.2.4 Deconvolution of spectra

Peak resonances with specific bonding environments were assigned based on the spectral signatures of pure chemical standards representative of specific functional groups (Solomon et al., 2009). In order to compare the chemistry of the different samples in a semi-quantitative way, a least-squares fitting scheme was applied to the normalized NEXAFS spectra in the range of 280 to 310 eV. The scheme was based on eight Gaussians (labeled "G-1", etc.) following the procedure suggested by Scheinost et al. (2001), with additional bands to account for substituted aryl C (G3) and an additional carbonyl group (G8) (Liang et al., 2008). Specific positions for the Gaussian bands are described in Table 1.1.

The Gaussian curve component positions were verified by examining the spectra of previously measured chemical standards as representatives of specific functional group chemistries. An arctangent function was used to model the ionization step and was fixed at 290 eV. The full width at half maximum of the bands was set at 0.4 ± 0.2 eV, while the amplitude was floated during the fit. Deconvolution was performed by resolving spectra into individual arctangent and Gaussian curve components (G) using the ATHENA software. Spectral regions represented by Gaussian curves were described as being generally attributed to the following functional groups: overall aromatic type C was represented by the sum of the [G1+G2+G3] peaks (Table 1.1); aromatic C with side chain substituent (such as phenolic C) by the G4 peak; alkyl C by the G5 peak; carboxylic C by the G6 peak, and O-alkyl C by the sum of [G7+G8] peaks (Lehmann et al., 2009). The application of a Gaussian fitting procedure for the extraction of semi-quantitative

information is validated by the diversity of C species in these samples. It is known that the C K edge resonances of individual chemical species measured with resolving powers of ~7500 should show non-Gaussian line shapes. This is due to asymmetric broadening caused by chemically distinct C sites, each in turn broadened out by coupling of the electronic and nuclear degrees of freedom. But when the spectra of many similar but distinct C molecules are added together, as in the case of a complex organic system like a soil, the result will resemble a (Gaussian) broadened peak. Absorption intensity and transition intensity values (percentages) reflect relative concentrations of functional groups, since absolute concentration based on peak intensity cannot be determined with NEXAFS. Deconvolution values used in the context of this study are meant to be a comparative tool, and not as an absolute quantification of functional groups, particularly where comparisons to values obtained by other instrumental methods (such as ^{13}C NMR) are made. Statistical analyses

Linear regressions were calculated for the correlations between NEXAFS and ^{13}C NMR values for total aromatic C and the aromatic/O-alkyl C ratio. The linear regressions were calculated using SigmaPlot software with a $p \leq 0.05$.

1.3. Results

Total electron yield (TEY; Table 1.2, Fig. 1.1) and fluorescence yield (FLY; Table 1.3, Fig.1.2) were measured simultaneously.

Table 1.2. Deconvolution results for BC ring trial standards using C 1s NEXAFS total electron yield; each value represents a percentage of total absorption intensity within the region specified at the top of the column (refer to Table 1.1). Chi2 value is statistical value provided for the model fit by ATHENA.

	Proportion of absorption regions (%)						
	283-286.1	286-287.5	287.6-288.3	288.4-289.1	289.2-289.8	289.9-291.2	chi^2
Wood char	39	6	18	14	16	7	0.458
Grass char	41	12	3	20	9	14	0.019
Soot	47	10	19	7	13	5	0.170
Chernozem	41	7	6	21	13	12	0.176
Vertisol	39	13	16	5	19	9	0.342
Dissolved organic matter	22	17	12	22	12	14	0.023
Aerosol	19	8	16	21	23	13	0.077
Marine sediment	6	8	20	31	35	0	2.510
Bituminous coal	42	13	5	16	18	4	1.140
Lignite coal	34	11	10	20	24	1	0.055
Shale	26	8	25	10	21	9	0.596
Melanoidin	6	18	21	29	15	10	0.073

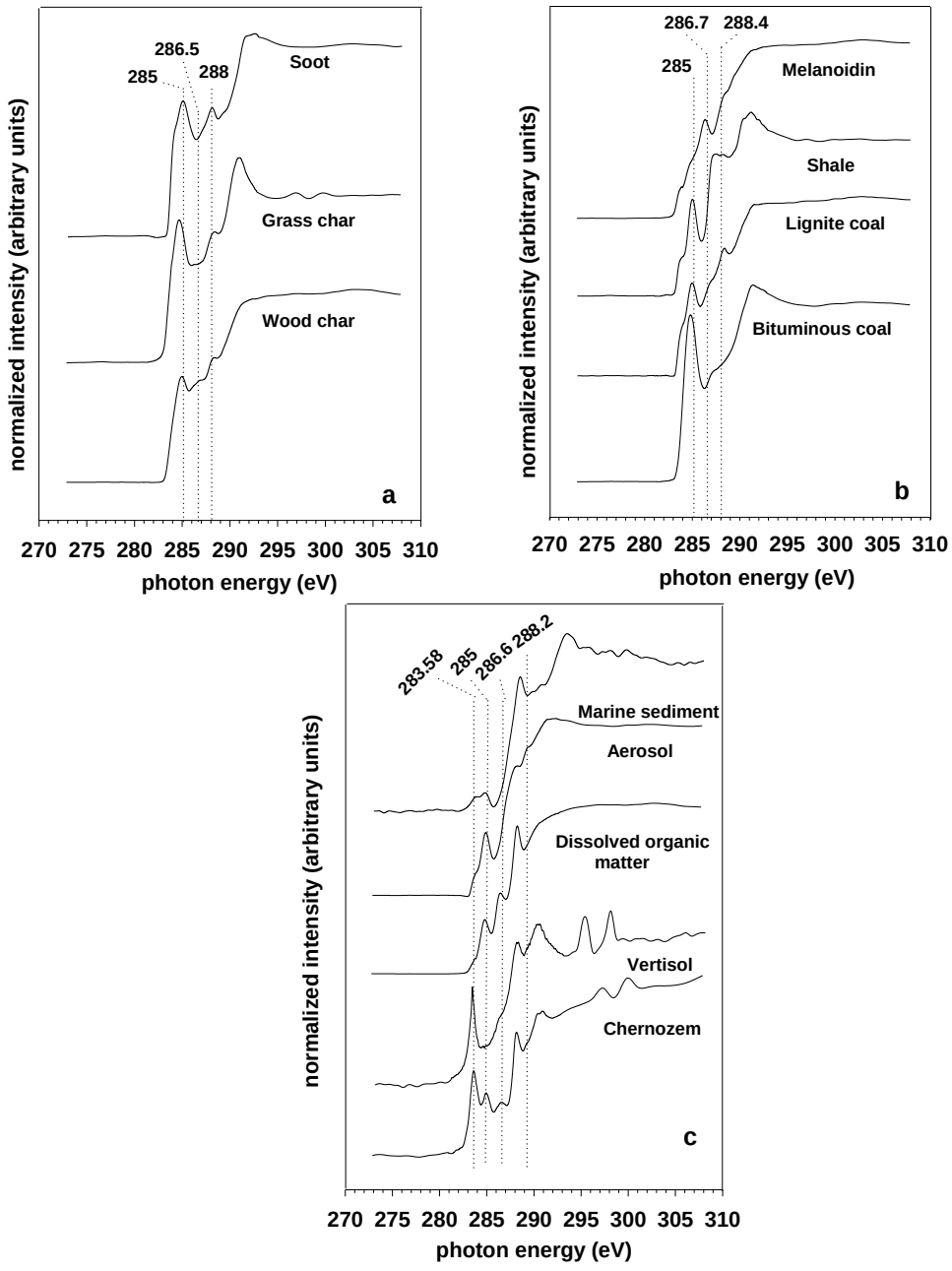

Figure 1.1 C 1s NEXAFS total electron yield (TEY) spectra of (a) BC reference materials, (b) potential interference products, (c) environmental matrices

Table 1.3. Deconvolution results for BC ring trial standards using C 1s NEXAFS fluorescence yield; each value represents a percentage of absorption intensity within the region specified at the top of the column (refer to Table 1.1)

	Proportion of absorption regions (%)						
	283-286.1	286-287.5	287.6-288.3	288.4-289.1	289.2-289.8	289.9-291.2	chi^2
Chernozem	46	6	15	14	11	8	0.846
Vertisol	40	7	8	23	13	8	0.680
Dissolved organic matter	37	14	13	18	6	14	0.489
Aerosol	39	7	17	20	11	6	0.094
Marine sediment	29	5	14	22	19	10	1.215
Shale	33	10	20	16	11	11	0.697
Melanoidin	34	21	23	1	14	6	0.032

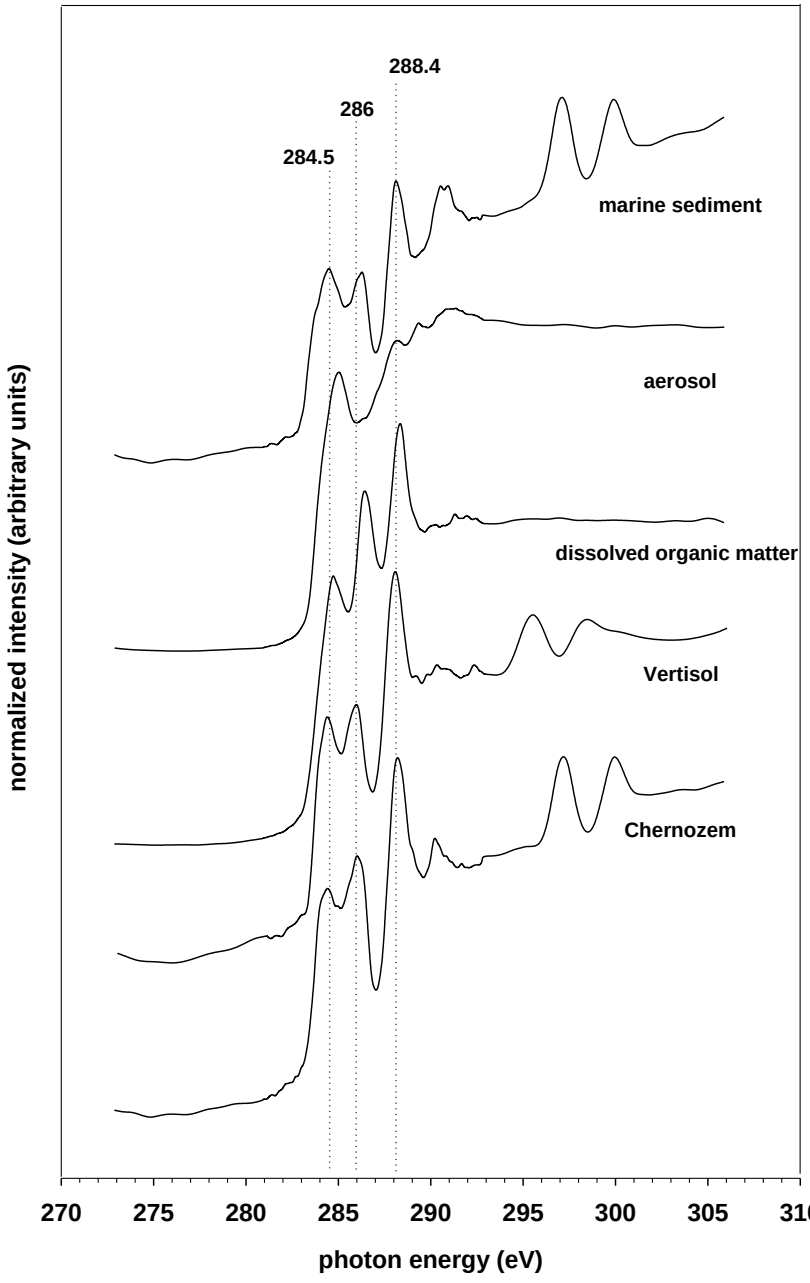

Figure 1.2. C 1s NEXAFS fluorescence yield (FLY) spectra of environmental matrices

We were successful in obtaining TEY data for all measured samples; however, FLY spectra for samples very high in C (all BC reference materials and coals) suffered from distortion due to self-absorption phenomena and were unusable. As a result of these issues, only TEY results were discussed for all BC reference materials, as well as bituminous coal, lignite coal, melanoidin and shale, while both FLY and TEY results were discussed and compared for Vertisol, Chernozem, aerosol, and dissolved organic matter. Comparison of both detection methods was included to illustrate a possible limitation of NEXAFS; the choice of detection method by the user is critical when attempting to obtain quantitative data. A more detailed example of problems occurring during normalization as a result of self-absorption phenomena may be found in the supplementary online material.

1.3.1 Characterization of BC reference materials

NEXAFS revealed a mixture of organic C molecular bonding environments in the BC reference materials (Figure 1a). The main characteristic of all BC reference materials was a broad, well resolved absorption band near 285 eV corresponding to the C 1s-$\pi^*_{C=C}$ transition, which is related to protonated and alkylated to carbonyl substituted aryl-C (C=C) (Cody et al., 1998; Coffey et al., 2002; Lehmann et al., 2005). The broadness of this band can be attributed to multiple resonances, rather than an abundance of one type since additional absorption bands were also observed as shoulders near 284.6 eV and 286.1 eV. The shoulder at 284.6 eV, particularly observable in soot, corresponds to the C 1s-pi* transition of quinone type-C (C=O) structures such as benzoquinone, protonated and alkylated aromatic-C and heteroatom-substituted aromatics (Jokic et al., 2003; Solomon et al., 2005). The broadness of the main aromatic transition suggested a complex chemical structure for BC reference materials (di Stasio and Braun, 2006).

Additional features beyond the aromatic region included multiple absorption bands present as small shoulders near 286.5 eV and 288 eV, corresponding to the C 1s-$\pi^*_{C\text{-}OH}$ and C 1s-$\pi^*_{C=O}$ transitions, representing mainly phenolic and carboxylic C, respectively. Wood char and grass char exhibited a carboxylic region shoulder centered at 288.4 eV, while the similar peak for soot was better resolved and centered at 288 eV. Solomon et al. (2009) identified a well-defined absorption peak at 288.35 eV for benzoic acid reflecting the C 1s-$\pi^*_{C=O}$ transition of carboxyl functional groups bonded to unsaturated C (Cody et al., 1998; Urquhart and Ade, 2002; Braun, 2005). The disparity in peak position between the soot and the chars near 288 eV may be attributed to soot having a more significant presence of two O atoms bonded to saturated C in carboxylic functional groups, rather than carboxylic groups bonded to unsaturated C as in the case of wood and grass char (Solomon et al., 2009). An additional peak near 291 eV was observed for the soot and grass char; this peak has been identified as representing the 1s-σ^* exciton in a previous study by Bernard et al. (2010) of high temperature chars.

Aromatic region values for the BC reference materials ranged from 39-47% (as a proportion of total absorption intensity) for grass char and wood char to a value at the higher end for soot with 46%. Functional group distributions delineated by the individual Gaussian curves within the aromatic C region were similar among the BC reference materials (Table 1.2), ranging from 16-23% for G1, 15-21% for G2 and 3-7% for G3. These values indicated that BC reference materials contain high concentrations of quinone C and aryl type C, compared with O-substituted forms present at higher transitions such as phenolic type C. A significantly lower G5 value of 3% for grass char was observed compared with 18% for wood char and 19% for soot (Table 1.2). G6 region values were higher for grass char (20%) compared with wood char (14%) and soot (7%). O-alkyl regions were similar overall for wood char and grass char (23 %), and soot

(18%).

1.3.2 Characterization of environmental matrices

The aromatic regions of the Chernozem, and Vertisol were characterized by two well resolved peaks near 284.5 and 286 eV (Figure 1c). The aromatic C region was similar for Chernozem (46%) and Vertisol (40%) as detected by FLY (Table 3). Deconvolution values for the aromatic C region detected by TEY were also very similar between soils, with 41% for Chernozem, and 39% for Vertisol detected in the aromatic C region. Despite the similar values for the two soils, functional group distributions were slightly different for the two detection methods, although both TEY and FLY attributed the majority of aromatic type C to the G1 regions for Vertisol and Chernozem. Deconvolution values for the G5-G7 regions were not in agreement among the two detection methods. This made it difficult to interpret the characteristic functional group contributions for the two soils. Adding the values for the 3 regions together, we found that the resulting values were similar between the two detection methods. For the Vertisol and Chernozem, the [G5+G6+G7] values were 34% as detected by TEY; for the FLY data, the Chernozem value was 35% for this entire region, while the Vertisol value for the region was 38%. The complexity of this region, in addition to overlap of spectral bands, may therefore be an obstacle for obtaining more reliable values for environmental matrices. The sharp resonances (doublet) observed in the Vertisol spectra near 300 eV can be assigned to potassium $L_{2,3}$-edge absorption (Yoon et al., 2006).

Dissolved organic matter spectra revealed a highly heterogeneous structure with three strongly resolved absorption bands near 285, 286.5 and 288.4 eV corresponding to multiple C 1s-π^* transitions. The aromatic region comprised 22% (TEY) and 37% (FLY) of total absorption intensity, with the majority of transition intensity (13-20%)

represented by the curve near 284.5 eV. The band near 286.7 eV represented nearly equivalent proportions of C detected by both TEY (17%) and FLY (14%). Similar proportions were also calculated for the band near 287.6 eV, around 12% by both detection methods. The largest proportion of C for an individual band was calculated for the sharp transition near 288.4 eV, with 22% (TEY) and 18% (FLY), indicating a high concentration of acidic functional groups. The spectral signatures for dissolved organic matter were also in agreement for the two detection methods, although FLY peaks were better resolved and had improved intensity compared with TEY.

Aerosol was characterized by one main aromatic C transition at 284.9 eV, and a small carboxylic shoulder at 288.3 eV, with identical spectral patterns for both TEY and FLY. However, the FLY spectra for aerosol revealed a signature highly comparable to the BC reference materials. Deconvolution yielded contrasting results among the two detection methods since FLY attributed 22% of total absorption intensity to the G1 region compared with only 8% by TEY. Overall aromaticity in the aromatic C region was 19% (TEY) and 39% (FLY). Clearly, FLY detected twice the amount of aromatic C compared with TEY in the aromatic C region. Values for the G2-G6 region were similar (within 5% difference) for the two detection methods, but the G7 region and G8 region values were again very different (23% and 13% for TEY compared with 11% and 6% for FLY). In any case, the majority of absorption intensity appeared to fall within the G5-G8 region for aerosol (nearly 60% for TEY, 48% for FLY), indicating lower contributions of aromatic C compared with BC reference materials.

Marine sediment shared spectral characteristics with the two soils; according to FLY, the aromatic region comprised 29% of total absorption intensity. The marine sediment aromatic region accounted for only 6% according to TEY data. Similar to the soils, the marine sediment contained a low proportion of phenolic type C. The carboxylic

C region made up a larger proportion (22%) and O-alkyl C made up 29 % of total absorption intensity. The spectral shapes for both detection methods were in agreement; however the TEY data attributed almost no C to the aromatic region, and the majority to the aliphatic (20%), carboxylic (31%) and O-alkyl (35%) regions.

1.3.3 Characterization of interference products

Bituminous coal, lignite coal and shale exhibited a pronounced absorption band near ~285 eV, corresponding to the C 1s-$\pi^*_{C=C}$ transition related to aromatic C (Figure 1b). This band appearance was broad and well resolved for bituminous coal and shale but relatively weak for lignite by visual comparison. Bituminous coal in particular was remarkably similar in spectral appearance to BC reference materials. The aromatic C region comprised a higher proportion of total absorption intensity for bituminous coal (46%) than lignite coal (34%) or shale (26%) (Tables 1-2 and 1-3). Lignite coal spectra revealed overlapping bands in the 286-289 eV region, while bituminous coal did not appear to present any notable characteristics in this region. A C 1s-$\pi^*_{C=C}$ transition at 287.8 eV for lignite, appeared as a small peak. Shale spectra revealed a large transition near 287 eV, possibly broadly overlapping regions between 287 and 290 eV, since no individual peaks were present in the spectral region. Melanoidin was easily distinguished from other ring trial standards by the absence of a strong aromatic C 1s-$\pi^*_{C=C}$ transition, which was present only as a wide shoulder on a broad peak which had a maximum at 286.3 eV.

1.3.4 Correlations

We were able to utilize TEY data to make correlations between deconvolution data we obtained by NEXAFS, and data collected by DPMAS ^{13} C NMR in a previous

study by Hammes et al. (2008). Correlations between aromatic C (G1-G3) NEXAFS data and aryl C NMR data (Figure 1-3) yielded an r^2 value of 0.63 ($p < 0.05$). The aryl C/O-alkyl C ratio has been recommended as a parameter to compare decomposition of environmental samples (Baldock et al., 2004). We used this parameter to further compare the results of both DPMAS ^{13}C NMR and NEXAFS (Figure 1-4). The [G1+G2+G3] regions were summed to use as the aryl component, while the [G7+G8] regions were summed to use as the O-alkyl component. The r^2 value for this correlation was 0.49 ($p < 0.05$). The correlation values indicated that the ^{13}C NMR values were greater overall than the NEXAFS values. We also correlated the O-alkyl values for the two methods; however, the correlation was very poor, and the r^2 value was around 0.1 ($p < 0.05$; data not shown).

Figure 1.3 (a) Correlation between concentrations of aryl C for ^{13}C NMR data from Hammes et al. (2008), and TEY data calculated in this study for NEXAFS using spectral deconvolution; $p<0.05$; (b) Correlation between aryl C/o-alkyl C values calculated for NEXAFS TEY data using spectral deconvolution, and data from the previous study by Hammes et al. (2008); $p<0.05$

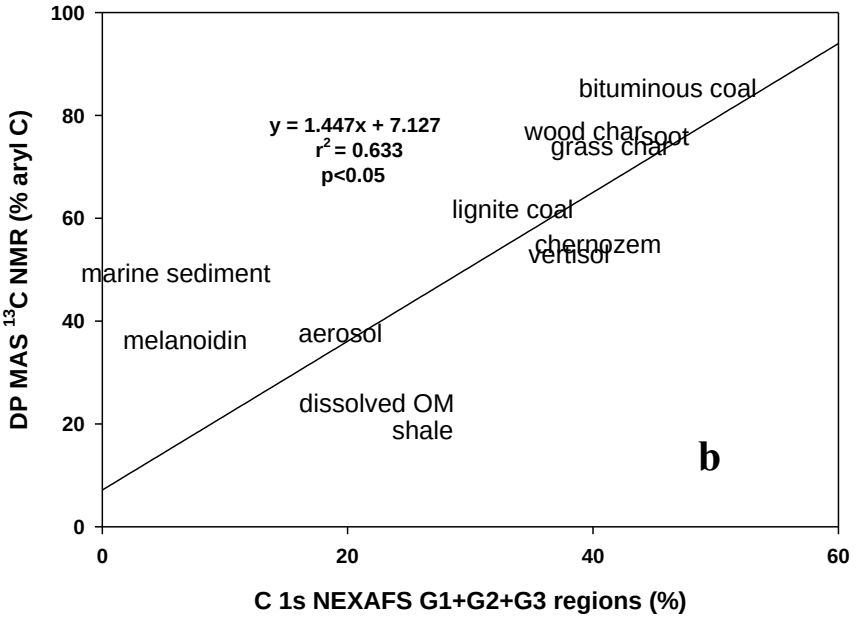
DP MAS 13C NMR (% aryl C)
C 1s NEXAFS G1+G2+G3 regions (%)
y = 1.447x + 7.127
r2 = 0.633
p<0.05
bituminous coal
wood char
soot
grass char
lignite coal
chernozem
vertisol
marine sediment
melanoidin
aerosol
dissolved OM
shale
b
0
20
40
60
80
100

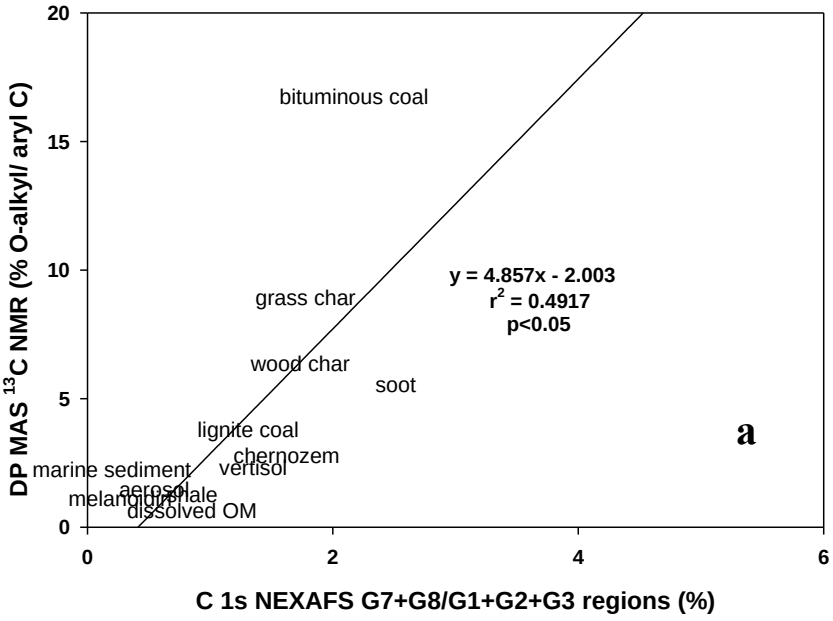
DP MAS 13C NMR (% O-alkyl/ aryl C)
C 1s NEXAFS G7+G8/G1+G2+G3 regions (%)
y = 4.857x - 2.003
r2 = 0.4917
p<0.05
bituminous coal
grass char
wood char
soot
lignite coal
chernozem
vertisol
marine sediment
aerosol
melanoidin
shale
dissolved OM
a
0
2
4
6
0
5
10
15
20

1.4. Discussion

1.4.1. Identification of black carbon within environmental matrices

Aromaticity was the most distinct feature observed for BC in this study, and therefore was a possible signature for BC in more complex matrices such as soils. We observed that the spectral fingerprint in the aromatic C region for the studied soils was similar to the BC reference materials. The overall aromatic region was greater for the soils than for the other environmental matrices, and corresponded with the values for overall aromaticity of the BC reference materials, being nearly 40% of total absorption intensity according to deconvolution performed on TEY data. Upon closer inspection, the BC reference materials and the two soils exhibited similar distributions of transition intensity within the aromatic region (TEY data). However, FLY deconvolution values were not in agreement with TEY and showed all environmental matrices including soils to have similar percentages of absorption intensity within the aromatic region. FLY aromatic C values for environmental matrices could not be compared to those for BC, since FLY data for the BC materials were not obtainable, as discussed previously.

The two soils exhibited individually unique spectral characteristics and functional group distributions, reflecting differences in labile organic matter as well as taxonomy and age. For example, the German Chernozem is a sandy soil that developed around 10,000 years ago. It is much younger than the Australian Vertisol, a clay soil. A previous study quantified the Chernozem as consisting of 50% BC as a fraction of total organic C (Schmidt et al., 1999) and the Vertisol with a comparatively lower BC concentration of 30% using photo-oxidation followed by ^{13}C NMR (Skjemstad et al., 1999). Schmidt et al. (1999) concluded that organic C in the German Chernozem was almost exclusively present as unsubstituted aromatic structures with negligible contributions from other

species using UV photo oxidation followed by ^{13}C NMR. In contrast, previous studies characterized the studied Vertisol as possessing abundant alkyl, O-alkyl, carbonyl and amide C components, attributable to the presence of polymethylene (lipid type) C, polysaccharides (cellulose), proteins and carboxylic acids (Skjemstad et al., 1999).

It was possible to make some observations relevant to BC signatures in the other environmental matrices. Aerosol has been characterized as containing some concentration of soot BC (fossil fuel derived) as well as a range of other materials using chemical and thermal oxidation techniques (Currie et al., 2002). The TEY results were consistent with those findings since the percentage of transition intensity in the aromatic region of aerosol was relatively lower than that of other environmental matrices, particularly when inspecting the values for the individual regions. Dissolved organic matter also indicated low values in the aromatic C region (TEY). Black C has been identified in dissolved organic matter (Hockaday et al., 2006); however, a comparative study (Hammes et al., 2008) found that results for BC quantification in dissolved organic matter were highly variable, with different methods reporting both low (CTO-375) and higher estimates (TOT/R) for the same sample.

1.4.2. Black carbon characterization

We observed spectral signatures among the BC reference materials in this study that were similar to those observed for benzenecarboxylic acids (Fig. S5) observed by Solomon et al. (2009), who utilized C 1s NEXAFS to compile a spectral library of chemical standards relevant to the study of natural organic matter. The transitions observed for BC reference materials were therefore largely related to the C 1s-π^* transition characteristic of C-H sites of unsaturated C bonds (C=C) on aromatic ring structures (Cody et al., 1998). Both Baldock and Smernik (2002) and Fernandes and

Brooks (2003) concurred that carbonaceous straw and wood chars were dominated by highly aromatic (aryl-dominated) structures. di Stasio and Braun (2006) measured several soots using C 1s NEXAFS spectroscopy, and were able to observe different spectral signatures depending on the soot type indicating that NEXAFS is capable of differentiating between BC reference materials. BC reference materials were also characterized by shoulders near 284.5 eV and 286 eV, which we attributed to additional aromatic ring structures similar to benzanthracene, observed at 284.3 eV by Solomon et al. (2009). These transitions represent C atoms with a double bond from benzene or diene structures, which are expected to be present in BC.

The complexity of the aromatic C region in BC has been previously explained as differences in bonding environments for highly aromatic C rings (di Stasio and Braun, 2006). The primary peak at 285 eV arises from the transition of the core (1s) electron to the valence π^* molecular orbital in aromatic C ring structures (Cody et al., 1995a), or from excitonic effects as observed by Bernard et al. (2010). Shifts in electronic transitions around the 285 eV aromatic peak that result from the attachment of other atoms such as O and H into these rings (e.g. quinone) are manifested as peak broadening in the aromatic C region. These energy shifts, which are the result of changes in polarization of the electron clouds around the C atoms, have been observed as a shoulder in ethylene soot attributed to the presence of benzoquinone (two C=O groups in an aromatic ring) (di Stasio and Braun, 2006). However, the shoulder itself is a result of C atoms in the aromatic ring which are not bound to O. The presence of benzoquinone-type C causes C atoms near O to experience a shift of the absorption edge toward higher X-ray energies (oxidation), while the remainder experience a shift to lower energies (di Stasio and Braun, 2006). As a consequence of substitution in aromatic ring structure, peak broadening or even peak splitting may be observed in the aromatic region.

Soot and char spectra reflected the presence of some of O-containing moieties (carbonyl, carboxylic C) likely present on surfaces or edges since most volatile matter has been lost at the formation temperatures for these materials. The presence of O in BC reference materials is an important aspect of their reactivity and long-term stability in soils (Knicker et al., 2007). Fernandes and Brooks (2003) measured both wood and straw charcoal with ^{13}C CPMAS NMR, and observed 78-87% of total C as aromatic C, with small amounts of O-aromatic and O-alkyl C detected. Hammes et al. (2008) utilized ^{13}C NMR to characterize BC reference materials as comprised of around 75% aryl C, and the remaining C as O-alkyl or carbonyl C. *n*-hexane soot was shown to contain a variety of oxygen-containing functional groups, including alkyl ketones, aryl ethers, anhydrides and substituted aromatic groups (Akhter et al., 1985b). Within the C1s NEXAFS region it may be difficult to separate resonances attributed solely to C bonds from those related to C-O bonds within complex environmental materials due to extensive overlapping at the fine edge. In order to obtain finer detail concerning the molecular composition of BC standards, alternative techniques such as STXM may be required (Yoon et al., 2006).

1.4.3. Distinguishing black carbon forms in the environment

Our results indicate that the ability to differentiate between BC and some materials of non-pyrogenic origin may be confounded by observance of C signatures alone, whether by NEXAFS or alternative spectroscopic methods such as ^{13}C NMR. Our observations were in agreement with those made by Hammes et al. (2008), who observed that the high degree of similarity between BC and coal presented difficulties for BC quantification by ^{13}C NMR, and that the H/C and O/C ratios and spectral features of bituminous coal were very similar to BC (chars and soot). While NEXAFS offers an advantage over ^{13}C NMR in its high sensitivity and ability to detect all C bonding

environments, the complexity of resulting spectra may limit the quantitativeness of data analysis unless more sophisticated analyses are developed for complex environmental samples such as soils.

We observed that the bituminous coal spectral signature was nearly identical to that of BC reference materials, and lignite was slightly lower in aromaticity than bituminous coal and exhibited a small additional peak at 288 eV. Therefore, the coals could not be distinguished clearly from BC reference materials according to the deconvolution results. For high-volatile bituminous coal, the concentration of phenol is anticipated to be low, while in low-rank coal a substantial proportion of the aromatic C is bonded to O, implying a complex near-edge structure (Cody et al., 1995b). No differences were detected in the phenolic C region; however, the disparity detected in the functional group distributions between the two coals was in the O-alkyl region, with lignite coal reflecting all band area in the G7 region, while the opposite trend was observed for bituminous coal, with most falling in the G8 region. The sharp peak that lignite coal exhibited in the carboxylic region may explain the higher band area in the G7 region, possibly due to some overlap. Cody et al. (1995b) identified the higher transition of an electron from the core (1s) to a mixed Rydberg valence (C-H*) state in bituminous coal; the intensity of this band correlated with alkyl C. However, deconvolution results in this study showed a relatively small percentage of total absorption intensity attributable to the alkyl C region in either coal, and much higher proportions were observed for carboxylic type C. Cody et al. (1995b) also observed that the intensity of the 288 eV shoulder was greatest for cutinite and lowest for inertinite, a trend consistent with expected variation in chemical structure and composition of macerals in bituminous coal, implying that the absorption at 288 eV is derived principally from the mixed Rydberg/C-H transition of aliphatic C. It is possible that the overlap of these two features confounded

the deconvolution results, and that some percentage of what is observed as carboxylic C in our study is likely a reflection of alkyl C. Overall, we did not observe any clear distinctions between the deconvolution results of bituminous or lignite coal and the BC reference materials; however, we observed unique characteristics in the shale and melanoidin that clearly distinguished them from the BC reference materials. The melanoidin spectral fingerprint lacked the central aromatic C peak near 285 eV, which was the main feature of all BC reference materials. Rather, the most intense peak appeared at 286.3 eV, which was in agreement with previously published NEXAFS spectra of melanoidin by Haberstroh et al. (2006), and was attributed to the presence of aromatic alcohols (phenols). For the shale, NEXAFS spectral deconvolution attributed over half of total absorption intensity to alkyl or O-alkyl type C, which is comparable to the proportion Hammes et al. (2008) were able to distinguish from HF treated kerogen (shale) from BC reference materials on the basis of the alkyl C signal, which contributed 70% of total detected C, with very little aryl C detected. The shale used in this study has also been previously characterized as low in aromaticity and high in alkyl biopolymers that constitute the cell walls of algae (Trewhella et al., 1986).

1.4.4. Methodological considerations

We relied heavily on TEY measurements for the interpretation of environmental matrices. BC measurements with FLY suffered from self-absorption, which caused distortions in the spectra and negatively impacted data quality. This was a result of the material characteristics; self-absorption phenomena occur when measuring highly concentrated particles and is due to particle size, which in this case was already quite small. We felt that it was important to present both detection methods here, since improvements to the FLY method in particular should be explored in future studies.

Additionally, interpretation of absorption values should be understood to reflect relative concentrations of functional groups. Absolute concentration based on peak intensity cannot be determined with NEXAFS, since absorption intensity is a function of the magnitude of the oscillator strength of the transition (Cody et al., 1995a). Deconvolution values used in the context of this study are meant to be a comparative tool for BC reference standards, and not an absolute quantification of functional groups, particularly where comparisons to values obtained by other instrumental methods (such as ^{13}C NMR) are made.

NEXAFS deconvolution values in the aromatic C regions were around 30-40% lower overall than in the comparable characterization study of these identical materials using CPMAS and DPMAS ^{13}C NMR by Hammes et al. (2008). The complexity of the C 1s NEXAFS spectra made it difficult to correctly identify poorly resolved species in complex samples. For example, we may have misinterpreted band structures in poorly resolved regions by assigning either too many or too few bands in a particular region. The chemical complexity of environmental samples makes the assignment of a set deconvolution scheme for a wide range of samples extremely challenging. In addition, fit problems may have occurred because of poorly resolved, overlapping bands. The limitations of DPMAS ^{13}C have been acknowledged, but are unlikely to be responsible for the problems observed with the fits to NEXAFS data in this paper, particularly in regards to the aliphatic, carboxylic and O-alkyl C peak assignments, and our attempts to quantify them. Innovative fitting approaches are needed to improve the quantification of C groups in environmental samples.

1.5. Conclusions

We successfully characterized a broad range of materials from a BC ring trial including BC reference materials, potentially interfering materials and environmental matrices using C 1s NEXAFS. We were able to identify total aromaticity of around 40% as a common feature for both environmental matrices and the BC reference materials. However, we encountered certain limitations, despite the sophisticated data capturing capabilities offered by NEXAFS. Establishing distinct differences between plant biomass derived BC (wood and grass chars) and fossil fuel derived BC (soot) was not possible from the results obtained here, due to the similarities between the spectral and deconvolution data for these samples. Advantages such as the ability to directly measure soil C *in-situ* were mitigated by the disparity between deconvolution data from the two different detection methods, which are expected to yield similar results but did not in our more detailed analyses of specific spectral regions.

While NEXAFS spectroscopy has the advantage of obtaining high resolution spectra for a wide range of environmental materials, including those encompassed in the BC combustion continuum, the quantitativeness of deconvolution methods will be limited until improved experimental techniques can be developed. It is also important to note that issues with FLY data may arise if the sample of interest is concentrated in particles (such as BC), regardless of concentration which may limit the resolution attainable for BC using NEXAFS. In the future, more extensive research into deconvolution techniques for environmental samples with known chemistries is warranted in order to maximize the potential of this advanced spectroscopy.

References

Akhter, M.S., Chughtai, A.R. and Smith, D.M., 1985a. Aromaticity of elemental carbon

(soot) by C-13 CP/MAS and FT-IR spectroscopy. Carbon 23, 593-594.

Akhter, M.S., Chughtai, A.R., Smith, D.M., 1985b. The structure of hexane soot-I. Spectroscopic studies. Applied Spectroscopy 39, 143-153.

Baldock, J.A., Masiello, C.A., Gelinas, Y., Hedges, J.I., 2004. Cycling and composition of organic matter in terrestrial and marine ecosystems. Marine Chemistry 92, 39-64.

Bernard, S., Beyssac, O., Benzerara, K., Findling, N., Tzvetkov, G., Brown Jr., G.E., 2010. XANES, Raman and XRD study of anthracene-based cokes and saccharose-based chars submitted to high temperature pyrolysis. *Carbon* 48, 2506-2516.

Bourke, J., Manley-Harris, M., Fushimi, C., Dowaki, K., Nunoura, T., Antal, M.J., 2007. Do all carbonized charcoals have the same chemical structure? 2. A model of the chemical structure of carbonized charcoal. Industrial and Engineering Chemistry Research, 46, 5954-5967.

Braun, A., 2005. Carbon speciation in airborne particulate matter with C (1s) NEXAFS spectroscopy. Journal of Environmental Monitoring 7, 1059-1065.

Brodowski, S., Amelung, W., Haumaier, L., Abetz, C., Zech, W., 2005. Morphological and chemical properties of black carbon in physical soil fractions as revealed by scanning electron microscopy and energy-dispersive X-ray spectroscopy. Geoderma 128, 116-129.

Carter, M.R., Skjemstad, J.O., MacEwan, R.J., 2002. Comparison of structural stability, carbon fractions and chemistry of krasnozem soils from adjacent forest and pasture areas in south-western Victoria. Australian Journal of Soil Research 40, 283-298.

Chughtai, A.R., Kim, J.M., Smith, D.M., 2002. The effect of air/fuel ratio on properties

and reactivity of combustion soots. Journal of Atmospheric Chemistry 43, 21-43.

Cody, G.D., Botto, R.E., Ade, H., Behal, S., Disko, M., Wirick, S., 1995a. Inner-Shell spectroscopy and imaging of a sub-bituminous coal - in-situ analysis of organic and inorganic microstructure using C(1s)-NEXAFS, Ca(2p)-NEXAFS, and C1(2s)-NEXAFS. Energy & Fuels 9, 525-533.

Cody, G.D., Botto, R.E., Ade, H., Behal, S., Disko, M., Wirick, S., 1995b. C-Nexafs microanalysis and scanning-X-Ray microscopy of microheterogeneities in a high-volatile bituminous coal. Energy and Fuels 9, 75-83.

Cody, G.D., Botto, R.E., Ade, H., Wirick, S. 1996. The application of soft X-ray microscopy to the in-situ analysis of sporinite in coal. International Journal of Coal Geology 32, 69-86.

Cody, G.D., Ade, H., Wirick, S., Mitchell, G.D., Davis, A., 1998. Determination of chemical-structural changes in vitrinite accompanying luminescence alteration using C-NEXAFS analysis. Organic Geochemistry 28, 441-455.

Coffey, T., Urquhart, S.G., Ade, H., 2002. Characterization of the effects of soft X-ray irradiation on polymers. Journal of Electron Spectroscopy and Related Phenomena 122, 65-78.

Cornelissen, G., Elmquist, M., Groth, I., Gustafsson, O., 2004. Effect of sorbate planarity on environmental black carbon sorption. Environmental Science and Technology 38, 3574-3580.

Currie, L.A., Benner, B.A., Kessler, J.D., Klinedinst, D.B., Klouda, G.A., Marolf, J.V., Slater, J.F., Wise, S.A., Cachier, H., Cary, R., Chow, J.C., Watson, J., Druffel, E.R.M., Masiello, C.A., Eglinton, T.I., Pearson, A., Reddy, C.M., Gustafsson, O., Quinn, J.G., Hartmann, P.C., Hedges, J.I., Prentice, K.M., Kirchstetter, T.W., Novakov, T., Puxbaum, H., Schmid, H., 2002. A critical evaluation of

interlaboratory data on total, elemental, and isotopic carbon in the carbonaceous particle reference material, NIST SRM 1649a. Journal of Research of the National Institute of Standards and Technology 107, 279-298.

Czimczik, C.I., Masiello, C.A., 2007. Controls on black carbon storage in soils. Global Biogeochemical Cycles 21, 1-8.

di Stasio, S., Braun, A., 2006. Comparative NEXAFS study on soot obtained from an ethylene/air flame, a diesel engine, and graphite. Energy and Fuels 20, 187-194.

Elmquist, M., Cornelissen, G., Kukulska, Z., Gustafsson, O., 2006. Distinct oxidative stabilities of char versus soot black carbon: Implications for quantification and environmental recalcitrance. Global Biogeochemical Cycles 20, 1-11.

Fernandes, M.B., Brooks, P., 2003. Characterization of carbonaceous combustion residues: II. Nonpolar organic compounds. Chemosphere 53, 447-458.

Freitas, J.C.C., Bonagamba, T.J., Emmerich, F.G., 1999. C-13 High-resolution solid-state NMR study of peat carbonization. Energy and Fuels 13, 53-59.

Freitas, J.C.C., Passamani, E.C., Orlando, M.T.D., Emmerich, F.G., Garcia, F., Sampaio, L.C., Bonagamba, T.J., 2002. Effects of ferromagnetic inclusions on C-13 MAS NMR spectra of heat-treated peat samples. Energy and Fuels 16, 1068-1075.

Haberstroh, P.R., Brandes, J.A., Gelinas, Y., Dickens, A.F., Wirick, S., Cody, G., 2006. Chemical composition of the graphitic black carbon fraction in riverine and marine sediments at sub-micron scales using carbon X-ray spectromicroscopy. Geochimica et Cosmochimica Acta 70, 1483-1494.

Hammes, K., Schmidt, M.W.I., Smernik, R.J., Currie, L.A., Ball, W.P., Nguyen, T.H., Louchouarn, P., Houel, S., Gustafsson, O., Elmquist, M., Cornelissen, G., Skjemstad, J.O., Masiello, C.A., Song, J., Peng, P., Mitra, S., Dunn, J.C., Hatcher, P.G., Hockaday, W.C., Smith, D.M., Hartkopf-Froeder, C., Boehmer, A., Luer,

B., Huebert, B.J., Amelung, W., Brodowski, S., Huang, L., Zhang, W., Gschwend, P.M., Flores-Cervantes, D.X., Largeau, C., Rouzaud, J.N., Rumpel, C., Guggenberger, G., Kaiser, K., Rodionov, A., Gonzalez-Vila, F.J., Gonzalez-Perez, J.A., de la Rosa, J.M., Manning, D.A.C., Lopez-Capel, E., Ding, L., 2007. Comparison of quantification methods to measure fire-derived (black/elemental) carbon in soils and sediments using reference materials from soil, water, sediment and the atmosphere. Global Biogeochemical Cycles 21, 1-18.

Hammes, K., Smernik, R.J., Skjemstad, J.O., Schmidt, M.W.I., 2008. Characterisation and evaluation of reference materials for black carbon analysis using elemental composition, colour, BET surface area and C-13 NMR spectroscopy. Applied Geochemistry 23, 2113-2122.

Hedges, J.I., Eglinton, G., Hatcher, P.G., Kirchman, D.L., Arnosti, C., Derenne, S., Evershed, R.P., Kögel-Knabner, I., de Leeuw, J.W., Littke, R., Michaelis, W., Rullkotter, J., 2000. The molecularly-uncharacterized component of nonliving organic matter in natural environments. Organic Geochemistry 31, 945-958.

Hockaday, W.C., Grannas, A.M., Kim, S., Hatcher, P.G., 2006. Direct molecular evidence for the degradation and mobility of black carbon in soils from ultrahigh-resolution mass spectral analysis of dissolved organic matter from a fire-impacted forest soil. Organic Geochemistry 37, 501-510.

Hopkins, R.J., Lewis, K., Desyaterik, Y., Wang, Z., Tivanski, A.V., Arnott, W.P., Laskin, A., Gilles, M.K., 2007. Correlations between optical, chemical and physical properties of biomass burn aerosols. Geophysical Research Letters 34, 573-591.

Jacobsen, C., Wirick, S., Flynn, G., Zimba, C., 2000. Soft X-ray spectroscopy from image sequences with sub-100 nm spatial resolution. Journal of Microscopy-Oxford 197, 173-184.

Jokic, A., Cutler, J.N., Ponomarenko, E., van der Kamp, G., Anderson, D.W., 2003. Organic carbon and sulphur compounds in wetland soils: Insights on structure and transformation processes using K-edge XANES and NMR spectroscopy. Geochimica et Cosmochimica Acta 67, 2585-2597.

Keiluweit, M., Nico, P.S., Johnson, M.G., Kleber, M., 2010. Dynamic Molecular Structure of Plant Biomass-Derived Black Carbon (Biochar). Environmental Science and Technology 44, 1247-1253.

Kinyangi, J., Solomon, D., Liang, B.I., Lerotic, M., Wirick, S., Lehmann, J., 2006. Nanoscale biogeocomplexity of the organomineral assemblage in soil: Application of STXM microscopy and C 1s-NEXAFS spectroscopy. Soil Science Society of America Journal 70, 1708-1718.

Kirz, J., Jacobsen, C., Howells, M., 1995. Soft X-ray microscopies and their biological applications. Quarterly Reviews of Biophysics 28, 33-130.

Knicker, H., Muffler, P., Hilscher, A., 2007. How useful is chemical oxidation with dichromate for the determination of "Black Carbon" in fire-affected soils? Geoderma 142, 178-196.

Kuhlbusch, T.A.J., 1998 Black carbon and the carbon cycle. Science 280, 1903-1904.

Lehmann, J., da Silva, J.P., Steiner, C., Nehls, T., Zech, W., Glaser, B., 2003. Nutrient availability and leaching in an archaeological Anthrosol and a Ferralsol of the Central Amazon basin: fertilizer, manure and charcoal amendments. Plant and Soil 249, 343-357.

Lehmann, J., Liang, B.Q., Solomon, D., Lerotic, M., Luizao, F., Kinyangi, J., Schäfer, T., Wirick, S., Jacobsen, C., 2005. Near-edge X-ray absorption fine structure (NEXAFS) spectroscopy for mapping nano-scale distribution of organic carbon forms in soil: Application to black carbon particles. Global Biogeochemical

Cycles 19, 1-12.

Lehmann, J., Brandes, J., Fleckenstein, H., Jacobsen, C., Solomon, D., Thieme, J., 2009. Synchrotron-based near-edge X-ray Spectroscopy of natural organic matter in soils and sediments. In: N. Senesi, Xing, P. Huang, P.M. (eds.), Biophysico-Chemical Processes Involving Natural Nonliving Organic Matter in Environmental Systems, 729-781. IUPAC Series on Biophysico-Chemical Processes in Environmental Systems. Wiley, NJ.

Lehmann, J., Solomon, D., 2010. Organic carbon chemistry in soils observed by synchrotron-based spectroscopy. In: B. Singh, Gräfe, M. (eds.), Synchrotron-based Techniques in Soils and Sediments, 289-312. Elsevier, Amsterdam.

Liang, B., Lehmann, J., Solomon, D., Kinyangi, J., Grossman, J., O'Neill, B., Skjemstad, J.O., Thies, J., Luizao, F.J., Petersen, J., Neves, E.G., 2006. Black carbon increases cation exchange capacity in soils. Soil Science Society of America Journal 70, 1719-1730.

Liang, B., Lehmann, J., Solomon, D., Sohi, S., Thies, J.E., Skjemstad, J.O., Luizao, F.J., Engelhard, M.H., Neves, E.G., Wirick, S., 2008. Stability of biomass-derived black carbon in soils. Geochimica et Cosmochimica Acta 72, 6069-6078.

Masiello, C.A., Druffel, E.R.M., 1998. Black carbon in deep-sea sediments. Science 280, 1911-1913.

Nguyen, B., Lehmann, J., Hockaday, W.C., Joseph, S., Masiello, C., 2010. Temperature sensitivity of black carbon decomposition and oxidation. Environmental Science and Technology 44, 3324-3331.

Pietikäinen, J., Kiikkila, O., Fritze, H., 2000. Charcoal as a habitat for microbes and its effect on the microbial community of the underlying humus. Oikos 89, 231-242.

Preston, C.M., Schmidt, M.W.I., 2006. Black (pyrogenic) carbon: a synthesis of current

knowledge and uncertainties with special consideration of boreal regions. Biogeosciences 3, 397-420.

Ravel, B., Newville, M., 2005. Athena, artemis, hephaestus. Journal of Synchrotron Radiation 12, 537-541.

Reeves, J.B., McCarty, G.W., Rutherford, D.W., Wershaw, R.L., 2007. Near infrared spectroscopic examination of charred pine wood, bark, cellulose and lignin: implications for the quantitative determination of charcoal in soils. Journal of Near Infrared Spectroscopy 15, 307-315.

Regier, T., Krochak, J., Sham, T.K., Hu, Y.F., Thompson, J., Blyth, R.I.R., 2007. Performance and capabilities of the Canadian Dragon: The SGM beamline at the Canadian Light Source. Nuclear Instruments & Methods in Physics Research Section a-Accelerators Spectrometers Detectors and Associated Equipment 582, 93-95.

Schäfer, T., Hertkorn, N., Artinger, R., Claret, F., Bauer, A., 2003. Functional group analysis of natural organic colloids and clay association kinetics using C(1s) spectromicroscopy. Journal De Physique IV 104, 409-412.

Scheinost, A.C., Kretzschmar, R., Christl, I., Jacobsen, C., 2001. Carbon group chemistry of humic and fulvic acid: a comparison of C 1s NEXAFS and ^{13}C NMR spectroscopies. In: E.A. Ghabbour, Davies, G. (Ed.), Humic Substances: Structures, Models and Functions, pp. 39-47. Royal Society of Chemistry, Cambridge, UK.

Schmidt, M.W.I., Masiello, C.A., Skjemstad, J.O., 2003. Final recommendations for reference materials in black carbon analysis. EOS 84, 582-583

Schmidt, M.W.I., Noack, A.G., 2000. Black carbon in soils and sediments: Analysis, distribution, implications, and current challenges. Global Biogeochemical Cycles

14, 777-793.

Schmidt, M.W.I., Skjemstad, J.O., Czimczik, C.I., Glaser, B., Prentice, K.M., Gelinas, Y., Kuhlbusch, T.A.J., 2001. Comparative analysis of black carbon in soils. Global Biogeochemical Cycles 15, 163-167.

Schmidt, M.W.I., Skjemstad, J.O., Gehrt, E., Kögel-Knabner, I., 1999. Charred organic carbon in German chernozemic soils. European Journal of Soil Science 50, 351-365.

Skjemstad, J.O., Taylor, J.A., Smernik, R.J., 1999 Estimation of charcoal (char) in soils. Communications in Soil Science and Plant Analysis 30, 2283-2298.

Solomon, D., Lehmann, J., Kinyangi, J., Liang, B.Q., Heymann, K., Dathe, L., Hanley, K., Wirick, S., Jacobsen, C., 2009. Carbon (1s) NEXAFS spectroscopy of biogeochemically relevant reference organic compounds. Soil Science Society of America Journal 73, 1817-1830.

Solomon, D., Lehmann, J., Kinyangi, J., Liang, B.Q., Schäfer, T., 2005. Carbon K-edge NEXAFS and FTIR-ATR spectroscopic investigation of organic carbon speciation in soils. Soil Science Society of America Journal 69, 107-119.

Solomon, D., Lehmann, J., Thies, J., Schäfer, T., Liang, B.Q., Kinyangi, J., Neves, E., Petersen, J., Luizão, F., Skjemstad, J., 2007. Molecular signature and sources of biochemical recalcitrance of organic C in Amazonian Dark Earths. Geochimica et Cosmochimica Acta 71, 2285-2298.

Stöhr, J., 1992. NEXAFS Spectroscopy. Springer Series in Surface Sciences. Vol 25. Springer, Berlin, Germany.

Trewhella, M.J., Poplett, I.J.F., Grint, A., 1986. Structure of green river oil-shale kerogen - determination using solid-state C-13 NMR-spectroscopy. Fuel 65, 541-546.

Urquhart, S.G., Ade, H., 2002. Trends in the carbonyl core (C 1s, O 1s) -> pi*c=o

transition in the near-edge X-ray absorption fine structure spectra of organic molecules. Journal of Physical Chemistry B 106, 8531-8538.

Watts, B., Thomsen, L., Dastoor, P.C., 2006. Methods in carbon K-edge NEXAFS: Experiment and analysis. Journal of Electron Spectroscopy and Related Phenomena 151, 105-120.

Xiao, B.H., Yu, Z.Q., Huang, W.L., Song, J.Z., Peng, P.A., 2004. Black carbon and kerogen in soils and sediments. 2. Their roles in equilibrium sorption of less-polar organic pollutants. Environmental Science and Technology 38, 5842-5852.

Yoon, T.H., Benzerara, K., Ahn, S., Luthy, R.G., Tyliszczak, T., Brown, G.E. 2006. Nanometer-scale chemical heterogeneities of black carbon materials and their impacts on PCB sorption propwerties:soft X-ray spectromicroscopy study. Environmental Science and Technology 40, 5923-5929.

2. ESTIMATING BLACK CARBON CONCENTRATION IN SOILS USING NEAR EDGE X-RAY FINE STRUCTURE SPECTROSCOPY

Abstract

We evaluated two mathematical modeling approaches to quantify black carbon (BC) in a BC-rich Anthrosol using carbon (C) near-edge X-ray absorption fine-edge structure (NEXAFS) spectroscopy. The first utilized spectra obtained from ecological fractions (e.g. plant, microbe, BC pieces) manually separated from the soil; the second utilized biomolecular endmembers (e.g. carbohydrate, lignin, lipid, protein, BC) to approximate total soil C. The molecular mixing model (MMM) using ecological fractions yielded an estimated concentration of 93% BC. In comparison, the mixing model with 5 biomolecular endmembers yielded an estimated concentration of only 31% BC, a lower concentration compared with a similarly modeled value of the same soil by ^{13}C NMR (51%). We used a sliding scale to explore the efficiency of the model quantifying different BC types along the combustion continuum. A corn BC temperature series ranging from 350º-600ºC was substituted for the BC component of the model. The best fit results (lowest error) were achieved using the BCs formed at 500ºC, 550ºC and 600ºC, which resulted in BC predictions between 58 and 64%, in good agreement with similarly modeled values of BC concentration from a previous study. Using BC produced at 350ºC, 400ºC and 450ºC resulted in much higher error values with BC predictions between 39 and 69%. BC produced at lower temperatures were characterized by lower aromaticity than those produced at higher temperatures. These differences suggest that assumptions about formation temperature of BC may affect the quantification of BC contained in soil for methods that rely on reference materials.

2.1. Introduction

Identifying the presence of pyrolytic residues of biomass and fossil fuels in terrestrial and marine environments, and the potential implications for defining organic carbon dynamics (Masiello, 2004; Czimczik and Masiello, 2007), has led to the development of a range of methodologies that attempt to quantify different BC forms in soils (Hammes et al., 2007). Black C is a product of the incomplete combustion of fossil fuel or plant biomass and describes a combustion continuum ranging from soot through to chars (Goldberg, 1985; Schmidt and Noack, 2000; Preston and Schmidt, 2006). Black C is known to be present in many soils accounting for up to 60% of soil organic C (Skjemstad et al. 1999; Schmidt et al., 1999). Based on the presence of condensed aromatic ring structures and the resultant stability to biological decomposition, BC represents a significant sink for atmospheric C in terrestrial ecosystems (Kuhlbusch, 1998; Masiello, 2004).

Both the physical and chemical composition of BC has rendered quantification by wet-chemical, thermal, or optical methods somewhat inconclusive. A comparative analysis of a common set of samples containing variable amounts of BC (Schmidt et al., 2001), measured BC contents varied by over two orders of magnitude for the same sample. This variability may have resulted from an inability of some methods to chemically or physically separate BC from sample matrices such as soil or sediment, prior to quantification with ^{13}C NMR, molecular markers, mass balance or elemental composition (Simpson and Hatcher, 2004). For example, while BC is known to be highly resistant to chemical oxidants, some portions of BC may be less recalcitrant, leading to the accidental removal of some portions of BC prior to analysis (Hammes et al., 2007). Another major limitation in quantifying BC is that it exists by definition as a continuum

ranging from char to soot (Goldberg, 1985). The chemistry of these materials varies with conditions such as formation temperature and source material. Chemical characteristics of soot and char often overlap, which can confound detection and quantification methods since methods may be optimized to detect specific BC forms. Such issues ultimately affect global C budgets, by either overestimating BC due to biases associated with false positives or kerogens, or by underestimating BC due to inadvertent bias towards a particular form of BC (Hammes et al., 2007; Lehmann et al., 2008).

^{13}C nuclear magnetic resonance (NMR) spectroscopy has been established as a structural characterization tool for soil C in environmental matrices (Preston, 2006); however, quantification of BC using ^{13}C NMR presents challenges for several reasons. ^{13}C NMR analysis is often considered semi-quantitative for obtaining detailed information about the chemistry of soil organic matter. The more routinely used cross polarization NMR experiment will not detect 100% of highly aromatic C because a lack of protons in close proximity to C reduces cross polarization efficiency and observability (Hedges et al., 2000). Direct polarization ^{13}C NMR analyses will provide enhanced observability of aromatic BC carbon, but sensitivity is low and long recycle delay times are required leading to long acquisition times (~24 hours per sample). C 1s NEXAFS may be useful for studies of BC in complex environmental matrices where destructive sample preparation is a limitation. NEXAFS spectroscopy uses the intense, tunable, polarized X-ray beams generated by a synchrotron light source to probe the electronic states of a sample (Watts et al., 2006). Resonance peaks in absorption spectra represent transitions from ground state to a core excited state (Stöhr, 1992). NEXAFS has an advantage over those spectroscopic techniques that require chemically or physically destructive pre-treatment (Lehmann and Solomon, 2010). Therefore, a range of environmental matrices including soils, sediments and BC may be measured.

Modeling NEXAFS spectra to derive estimates of C composition for polymers and polymer mixtures is based on schemes ranging from semi-quantitative to qualitative. The "building block model" is a semi-quantitative approach that uses the spectra of building block molecules to simulate the NEXAFS spectra of complex species or molecular mixtures and has been proposed for modeling complex organic molecules and polymers (Urquart et al., 2000). A qualitative approach called "functional group fingerprinting" uses the unique spectroscopic signatures of chemical units present in polymers (e.g. phenyl, carbonyl, amide, etc) to model sample C (Urquart et al., 2000). The "molecular modeling" approach uses the spectra of small molecules (spectral library) to establish qualitative fingerprints for polymers (Urquart et al., 2000).

Even though several investigations to characterize soil C (Scheinost et al., 2001; Kinyangi et al., 2006; Lehmann et al., 2007, 2008; Solomon et al., 2007) and BC (Lehmann et al., 2005; Liang et al., 2008; Keiluweit et al., 2010) have been conducted using NEXAFS, no studies have been published on using NEXAFS to quantify BC in soils. A mathematical modeling approach was previously developed for studying environmental matrices such as marine sediment and soil organic matter using ^{13}C NMR (Nelson et al., 1999, Baldock et al., 2004). This MMM has been successfully applied to soil organic matter to predict the individual contributions of major biomolecular components of SOM (carbohydrates, protein, lipids, lignin, and char). This method assumes that organic matter exists in the form of molecules produced by organisms (biomolecules) (Kelleher and Simpson, 2006), most of which can be classified into distinct types (proteins, carbohydrates, lipids, etc.), each having a characteristic spectrum. The mixing process estimates the proportion of organic C found in a sample of organic matter that can be attributed to each distinct type of biomolecule. Baldock et al. (2004) indicated that a high level of agreement between measured and modeled distributions of

^{13}C NMR signal intensity suggested that the organic matter in the samples might consist purely of chemically distinct biomolecules rather than humic molecules such as proposed by Schulten and Schnitzer (1993).

The objective of this study was to utilize NEXAFS as an alternative spectroscopic approach to ^{13}C NMR in conjunction with the MMM capable to estimate the composition of organic C in soil. We attempted to determine whether soil C could be modeled using ecological fractions (plant litter, microbial C and BC particles physically separated from the soil) or a combination of biochemical endmembers (carbohydrate, protein, lignin, lipid and BC). Additionally, we used a sliding scale to accommodate a broad range of physical and chemical properties encompassed by the BC combustion continuum.

2.2. Experimental Methods

2.2.1. Materials

A BC-rich Anthrosol was utilized to develop the method. This soil was sampled from the Lago Grande (LG) site near Manaus, Brazil (3°8´S, 59°52´W, 40-50 m above the sea level). This type of Anthrosol is referred to as 'Terra Preta de Indio' and is the result of pre-Columbian settlements, and is covered by old secondary forest. The period of occupation and therefore the age of the BC at this site has been estimated to range from 900-1100 years BP (Liang et al., 2006). The soil used in this study was collected from a depth of 0-0.16 m (A horizon), the litter layer (O horizon) was removed prior to sampling and retained as the Plant Litter sample used in this study. The organic C content of this soil has been reported as 31.5 mg g^{-1}. The sand-silt-clay distribution of this soil is 48-30-23.

Soil was sieved to 50 μm to remove sand and ball ground for analysis. Ecological fractions were obtained for the LG soil as described by Liang et al. (2006). Black C

particles (BCP) were manually picked from the collected 0-0.16 m LG soil using super tweezers (N5, Dumont, Montignez, Switzerland) under a light microscope (303; SMZ-10, Nikon, Japan). Plant litter (PL) was manually harvested from the O horizon of the LG soil. Microbial extract (ME) was made as follows: bacteria [gram (-) *alphaprotobacteria*] colonies were isolated from the LG soil, cultivated in broth (Bacto peptone 10g, yeast extract 5 g, NaCl 5g L^{-1}) and distributed into 5 mL volumes in screw top tubes and sterilized for 15 min at 121°C. One milliliter of the sterilized bacterial culture (after 24 h, 37°C) was transferred into Eppendorf tubes and centrifuged at 5000 rpm for 5 min, and sequentially washed with 0.05 *M* NaCl twice after discarding the supernatant. Samples were dried and stored under desiccant until measured (Liang et al., 2006).

We chose biomolecules similar to those used in Nelson and Baldock (2005), originally selected because they are produced in greatest abundance by plants (i.e. cellulose, protein, lignin, lipids) and microorganisms (chitin, lipid). These biomolecules were divided into specific categories of (A) carbohydrate, (B) protein (C) lignin and (D) a lipid or aliphatic component. All chemicals used in this study were obtained from Sigma-Aldrich corp., St. Louis, MO, USA). Powdered cellulose was used to represent the carbohydrate component, powdered lignin was used as the lignin component, stearic acid was used as the lipid component. A mixture of 16 amino acids was composed according to the molar ratios extracted from a soil by Beavis and Mott (1996).

The corn char temperature series was produced by carbonizing total corn crop residue (*Zea mays,* L.) using slow pyrolysis (Daisy Reactor, Best Energies Inc., Cashton, WI, USA) as described previously by Nguyen and Lehmann (2009). Chars were produced at 350º, 400º, 450º, 500º, 550º and 600ºC. Elemental analysis of these chars can be found in the Supplementary online material (Table S1). The corn char temperature series was used in the model to test a sliding scale approach, described below.

2.2.2. NEXAFS spectroscopy

C (1s) NEXAFS spectra were obtained with a Spherical Grating Monochromator (SGM) (Regier et al., 2007) on beamline 11ID-1 at the Canadian Light Source (CLS) located at the University of Saskatchewan, Saskatoon, Canada, as described by Heymann et al. (2011). In brief, total fluorescence yield (FLY) was measured using a chevron stacked Micro-Channel Pate (MCP) detector with a bias of -1600 V. The beamline was configured for resolving power of approximately 7500 at the C K edge (exit slit gap of 50 μm). The photon energy was scanned from 270 to 310 eV using a dwell time of 0.5 s. Background measurements were taken on an empty gold wafer for each sample plate loaded into the chamber. A normalization current was also measured during each scan by collecting the TEY from an Au mesh. The mesh was monitored for C contamination and was periodically refreshed using an in-situ Au evaporator that is incorporated into the beamline vacuum system. Duplicate measurements were taken for each sample at different spots on the sample. If differences were observed, additional measurements (up to five) were taken. The fine structures in the C (1s) NEXAFS region above 290 eV transitions tend to be broad and overlap with each other (Cody et al., 1998; Schäfer et al., 2003); therefore, only the main 1s-pi* transitions were used for interpretation of the NEXAFS results in this study. TEY and FLY were measured at the same time; however, for samples enriched in C only the TEY data were usable due to self-absorption (as described in Heymann et al. (2011)). For the soil only the signal captured by FLY was useful due to the relative low C content and the need for a higher sensitivity. FLY data was used for spectra of the biomolecular components. The cellulose spectra were obtained at the National Synchrotron Light Source at Brookhaven National Lab by methods detailed in Solomon et al. (2009). This was done to avoid any irradiation damage as documented by Cody et al. (2008) and observed in our preliminary

measurements at CLS due to the direct impact of the beam on the sample (at NSLS a defocused beam was used). The measurements taken at the two different locations were highly similar, with the exception of the features observed as a result of irradiation damage.

Spectra were corrected for background signals as follows:

$$I_{sub} = I_{(FLY,\ TEY)} - gold_{(FLY,\ TEY)}/I_o$$

where I_{sub} corresponded to the subtracted signal, $I_{(FLY,\ TEY)}$ to the sample current from either FLY or TEY, $gold_{(FLY,TEY)}$ to a blank and Io to the current from Au mesh-monitor located upstream from the sample. In order to correct for C contamination in the beamline optics, a linear transformation was applied to normalize the pre-edge region of the sample with the pre-edge region of clean Au measured at the beginning of the experimental run. Further details are described in Heymann et al. (2011). All data were normalized prior to curve fitting using ATHENA 0.8.052 software (Ravel and Newville, 2005). The photon energy was calibrated to the C 1s-> pi^* resonance in CO gas at 287.38 eV. The samples in this study were not expected to have any long range order since the C in the sample was randomly oriented and, therefore, there should be no polarization effects.

2.2.3 Analysis

Peak resonances were assigned based on the spectral signatures of pure chemical standards representative of specific functional groups as described by Solomon et al. (2009). In order to compare the chemistry of the different samples in a semi-quantitative way, a least-squares fitting scheme was applied to the normalized NEXAFS spectra in the range of 280 to 310 eV. The scheme was based on eight Gaussians (labeled “G-1”, etc.)

following the procedure suggested by Scheinost et al. (2001), with additional bands to account for substituted aryl C (G3) and an additional carbonyl group (G8) (Liang et al., 2008) (Table 1). An arctangent function was used to model the ionization step at 290 eV. The full width at half maximum of the bands was set at 0.4 ± 0.2 eV, while the amplitude was floated during the fit. Spectral regions represented by Gaussian curves were described as being generally attributed to the following functional groups: overall aromatic type C was represented by the sum of the [G1+G2+G3] peaks; aromatic C with side chain substituent (such as phenolic C) by the G4 peak; alkyl C by the G5 peak; carboxylic/carbonyl C by the G6 peak, and O-alkyl C by the sum of [G7+G8] peaks (Lehmann et al., 2009). The application of a Gaussian fitting procedure for the extraction of semi-quantitative information is validated by the diversity of C species in these samples. Absorption intensity and transition intensity values (percentages) reflect relative concentrations of functional groups, since absolute concentration based on peak intensity cannot be determined with NEXAFS. Deconvolution values used in the context of this study are meant to be a comparative tool. Further details on this fitting method have been described by Heymann et al. (2011).

2.2.4.Mixing model for inferring molecular structures from NEXAFS spectra

The MMM assumes that the organic matter in natural ecosystems exists in the form of molecules produced by organisms (biomolecules), with more than 90% of biomolecules being classified into distinct types (e.g. carbohydrates, proteins, lignin, lipids, etc.) (Kelleher and Simpson, 2006). Different classes of biomolecules can be characterized according to a unique NEXAFS spectral signature. Similarly, Baldock et al. (2004) and Nelson and Baldock (2005) were able to identify distinct spectra for individual biomolecules using ^{13}C NMR. The model proposes that if the MMM can

successfully account for the distribution of the signal from organic materials then the modeling process will allow the overall gross molecular composition of natural organic materials to be estimated. The previous mixing model developed for ^{13}C NMR data (Nelson and Baldock, 2005) used the signal intensity from a set of spectral regions chosen because they differed most widely across the model components. However; for NEXAFS data, deconvolution was used to determine the contributions of individual regions to the overall spectra.

The MMM has been previously described by Baldock et al. (2004); we used either three ecological (plant litter, microbe and char) or six biomolecular components (carbohydrate, protein, lipid, lignin, char, and pure carbonyl). to describe the molecular composition of samples. A set of components representative of soil ecosystems was derived. The MMM used five components to describe the molecular composition of samples (carbohydrate, protein, lipid, lignin, char). A set of components representative of soil ecosystems was derived. In the modeling process, the proportion of total sample signal intensity allocated to each of the five components was adjusted from an initial value of 1 using the Generalized Reduced Gradient nonlinear optimization code within the Solver add-in of Microsoft Excel. As these proportions varied, the predicted distribution of the ^{13}C NMR signal intensity in each of the delineated NMR spectral regions calculated by the MMM also varied. The optimization process continued until the sum of the squares of the differences between the predicted and measured distributions of ^{13}C NMR signal intensities was minimized. The model was constrained by forcing the sum of the proportion of C allocated to all model components to be equal to 1 and by ensuring that the contribution of each component was ≥ 0.

A sliding scale was introduced using the corn chars produced at different temperatures as the char component in the model, in order to measure differences in

predicted allocations of sample C to the different biomolecules.

2.3. Results

2.3.1 NEXAFS characterization of model components

The NEXAFS spectrum acquired for the LG soil was characterized by a broad, well resolved absorption band near 285 eV corresponding to the C 1s-$\pi^*_{C=C}$ transition related to protonated and alkylated to carbonyl substituted aryl-C (C=C) (Fig. 2.1). This transition comprised 36% of total C and was the major defining characteristic of the soil (Table 2.1).

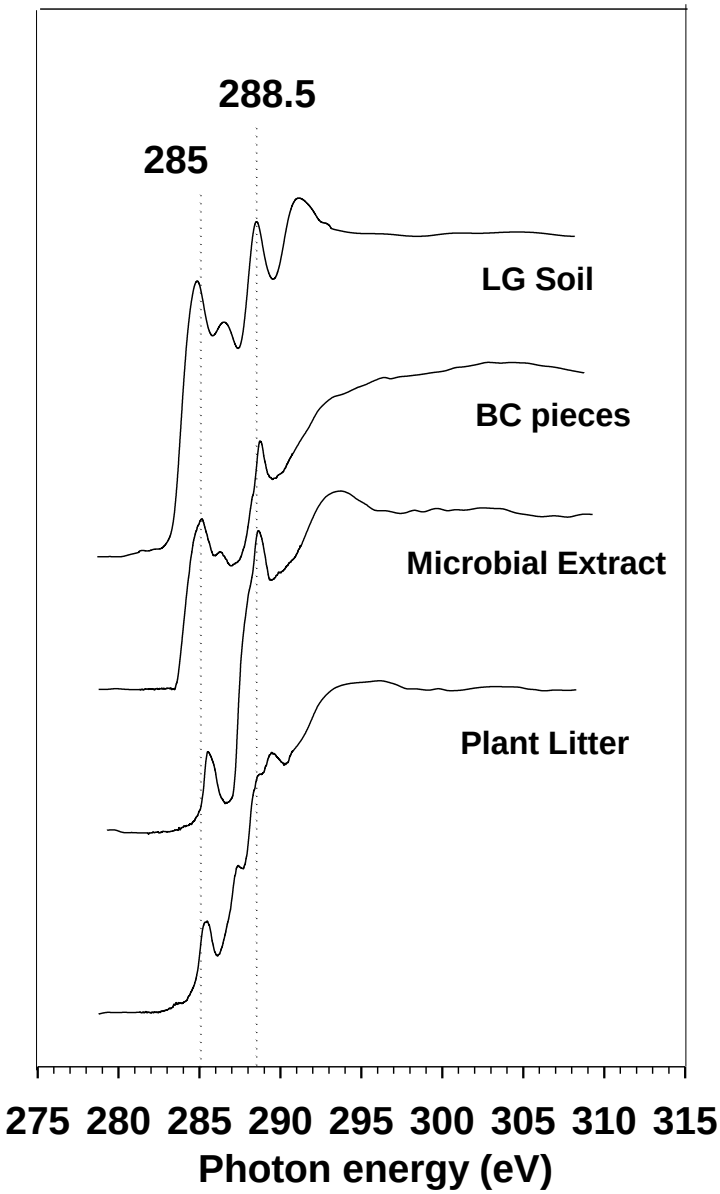

Figure 2.1. C 1s NEXAFS spectra of the *Terra preta* soil and ecological fractions that were physically separated from the same soil.

Table 2. 1 Proportion (%) of C species in *Terra preta* soil using a MMM with five components and biomolecular endmembers; model was applied using either BC particles isolated from the soil or corn char produced at different pyrolysis temperatures

	284.3	**285.1**	**286.1**	**286.7**	**287.6**	**288.4**	**289.2**	**289.9**
Soil	19	13	3	19	6	18	13	7
Ecological fractions								
Plant litter	2	12	1	13	13	25	24	10
Microbe	0	9	1	7	20	31	22	9
Black carbon	14	16	12	11	13	19	11	5
Biomolecular components								
Carbohydrate	0	0	0	1	3	27	31	39
Amino mix	25	0	12	8	3	30	15	8
Lignin	13	13	9	15	11	15	5	20
Lipid	8	7	3	18	11	24	18	11
Temperature series chars								
Corn 350	8	19	0	21	9	21	21	8
Corn 400	11	22	1	20	9	17	19	11
Corn 450	10	27	1	22	10	17	13	10
Corn 500	25	18	1	19	9	13	15	25
Corn 550	26	18	2	19	10	13	12	26
Corn 600	23	21	0	20	8	13	14	23

Secondary peaks were present at 286.4, 288.4 and 291 eV, indicating a heterogeneous composition. Phenolic type (aromatic ring C substituted with O), carboxylic/carbonyl type C and O-alkyl C each comprised approximately equal proportions (around 20% each) to total absorption intensity. The proportion of aliphatic type C was 7 %.

The BC NEXAFS spectrum contained a broad C 1s-$\pi^*_{C=C}$ transition at 285 eV (42% aromaticity), and a smaller C 1s-$\pi^*_{C=O}$ transition representing carboxylic/carbonyl-type C (19 % of total absorption intensity (Fig. 2.1).

Phenolic, aliphatic and O-alkyl type C transitions represented 11-16% of total absorption intensity. The spectrum acquired for the microbial extract was characterized by a small peak around 285.3 eV (10% aromaticity) and another narrow peak at 288.4 eV (31% of total absorption intensity; Table 2.2).

Table 2.2. Proportion (%) of C species in *Terra preta* soil using a MMM with five components and biomolecular endmembers; model was applied using either BC particles isolated from the soil or corn char produced at different pyrolysis temperatures

	Carbohydrate	Protein	Lignin	Lipid	BC	Sum of Squares
BC particles	0	18	28	23	31	200
Corn 350	0	18	28	7	48	190
Corn 400	0	0	3	28	69	108
Corn 450	0	18	13	31	38	182
Corn 500	0	18	0	18	64	42
Corn 550	3	18	0	21	58	51
Corn 600	0	19	0	23	59	54

The proportions of total signal intensity in the aliphatic (20%), carboxylic/carbonyl type C regions (31%) and the O-alkyl C region (31%) distinguished it from the BC particles.

The plant litter was heterogeneous as evidenced by multiple peaks present near 284.5, 285, 288 and 289 eV in the acquired NEXAFS spectrum. The aromatic, phenolic and aliphatic type C regions each comprised 13-15% of total absorption intensity. The proportion of absorption intensity present in the carboxylic type C transition was around 25%, while the O-alkyl region value was around 34%.

The cellulose spectra was characterized by one sharp peak at 289.4 eV (Fig. 2.2),

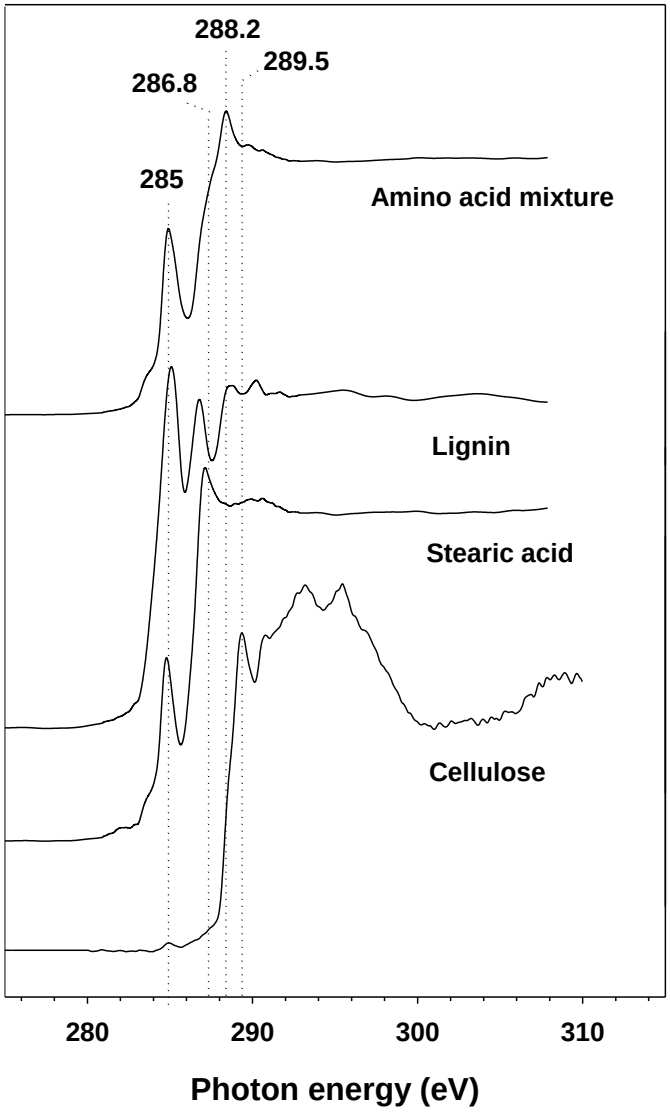

Figure 2.2. C 1s NEXAFS spectra of biomolecular components

which was attributed to the 1s-3p/σ^* transitions of O-alkyl (C-OH) moieties. Cellulose deconvolution results attributed the majority of signal intensity to the carboxylic/carbonyl C type (27%) and O-alkyl type C (60%). The amino mixture was characterized by a narrow and well resolved peak at 285 eV and another sharp peak at around 289 eV. The distribution of the amino mixture attributed 37% of total absorption intensity to the aromatic region, while the carboxylic/carbonyl C region comprised 30% and the O-alkyl C region comprised 23%. Lignin was characterized by a large aromatic C peak at 285 eV and an additional peak at 286.9 eV. 35% of total absorption intensity was present as aromatic type C, 8% as phenolic type, 15% as carboxylic/carbonyl C and 25% as O-alkyl. The lipid component (stearic acid) was characterized by peaks at 284.8 eV and 287.2 eV, whereby 18% of total absorption intensity was present in the aromatic region along with 18% in the phenolic C region, 24% in the carboxylic/carbonyl C region and 29% in the O-alkyl C region.

The temperature series of chars made from corn stover were characterized by a main aromatic transition at 285 eV and an additional main carboxylic/carbonyl region at 288.4 eV. The proportion of signal present in the aromatic C region increased with charring temperature, from 27% at 350ºC to 37% at 450ºC and then stabilized around 44% for the chars produced between 500º and 600ºC (Table 1). At the same time, the proportion of C present in the carboxylic/carbonyl type C region decreased from 21% to 13% and the proportion in the O-alkyl C region increased from 29% to 37%.

2.3.2. Mixing model results

The 3-component model, using the ecological fractions resulted in a high sum of squares (212) and calculated that BC comprised 94% of total absorption intensity, plant

litter 6%, and microbial C 0% (Tables 2.2 and 2.3).

Table 2.3. Measured versus predicted proportion (%) of total C for the 3-component mixing model using ecological fractions

	Measured signal	Predicted	Sum of Squares
284.5	13.8	14	0.1
285.4	15.9	15.6	0.1
286.1	12.3	11.8	0.2
286.7	12.7	11.2	2.1
287.6	12.3	12.8	0.2
288.4	16.0	18.3	5.1
289.2-289.9	17.1	17.4	0.1
Total	100	101.1	7.9

The 5-component MMM was run using the BC particles as the BC component, and resulted in distribution of 31% BC, 28% lignin, 28 % protein and 23% lipid composition with a sum of squares around 199.6.

The sliding scale results obtained using the 5-component mixing model attributed between 38% and 69% of total signal intensity to the temperature series chars used for the BC component in the mixing model. The proportion did increase with increasing formation temperature; however, not in a linear fashion (see Table 2.2). The sum of squares was considerably higher (108-189) for chars produced at 350º-450ºC compared with a sum of square range of between 42-54 for chars produced at 500º-600ºC. The

model result for the proportion of signal attributed to lignin depended more on the char deconvolution values than the other components. The model values for the corn char produced at 400ºC appeared to be inconsistent with the other low temperature char values.

The proportion of signal intensity attributed to protein was consistent (around 18%) regardless of the type of char used in the model. However, the lignin and lipid components varied and were highly dependent on char type. For example, the model attributed around 28% when BC particles were used, and between 3-28% when low temperature chars (350º-450°C) were used. The model runs using the higher temperature chars (500º-600°C) did not attribute any portion of the modeled result to lignin. The lipid values remained consistent (18% to 31% with the exception of the chars produced at 350°C with a value of 7%).

2.4. Discussion

2.4.1. Model components

Spectral characterization provided the necessary justification for the use of the different components we selected in the models. We were able to observe that the components used in each model as representative of classes of molecules present in soil organic matter were distinct in their spectral signatures. The need for chemically distinct components has been emphasized as imperative for obtaining good fits when utilizing the mixing model (Nelson and Baldock, 2005).

The spectra and characterization of the soil and ecological fractions were compared to previous studies of similar materials. The spectral characteristics of the soil were consistent with other soils measured by NEXAFS (Jokic et al., 2003; Heymann et

al., 2011). The characterization of the microbial extract corresponded to previous ^{13}C NMR analysis of microbial materials synthesized from glucose by soil microorganisms in a laboratory incubation (Golchin, 1996). Those microbial materials were characterized mostly by O-alkyl, alkyl and COOH structures, as was the case in this study (82% of total absorption intensity in this region). Plant litter also contained a high proportion of overall absorption intensity in this region (around 70%) with the highest proportion present as O-alkyl C. This corresponded to ^{13}C NMR characterizations of a variety of plant materials (Frund and Ludemann, 1989) which found that most C was present at O-alkyl type structures. We interpreted the broad feature in the 287-290 eV region of the plant litter as indicating the presence of multiple overlapping bands in regions of close proximity.

Spectra of biomolecular components were mostly consistent with other studies looking at similar materials. The spectral characteristics of lignin agreed with STXM XANES measurements of plant lamellar structure, where the main absorption features were positioned at 285 eV and 289.5 eV (propyl sidechains and methoxyl C) (Cody et al., 2008). Cellulose was also measured in the same study and characterized by a main absorption intensity at 289.5 eV. The spectrum acquired for the amino acid mixture was consistent with previous characterizations of amino acids by Solomon et al. (2009) who found that a peak at 288.7 eV appeared consistently for 6 amino acids measured with NEXAFS. Additionally, Kaznacheyev et al. (2002) measured 20 amino acids commonly found in nature and found that a peak consistently appeared at 288.6 (+/- 0.1 eV). The main transition for stearic acid at 288 eV has been previously documented by Risse et al. (1998); however, the peak at 285 eV was not documented in that study. It is possible that main transitions above 288 eV displayed some additional resonance in the 285 eV region due to the high sensitivity of NEXAFS.

The increasing aromaticity values obtained with increasing temperature used to

create the corn chars showed that the temperature series would be useful for the application of a sliding scale of char composition in the modeling the biochemical composition of organic C in soil. The changes in functional group distribution with temperature were consistent with those observed by Keiluweit et al. (2010) (increase in aromaticity, decrease in carboxylic and O-alkyl C with increasing temperature as measured by C NEXAFS). The main spectral difference between the chars produced at lower temperatures (350º-450° C) and those produced at higher temperatures (500º-600º C) was the proportion of signal intensity associated with the aromatic region. The relative increase in aromaticity with increasing temperature noted in this study was consistent with observations by Nguyen et al. (2010) using ^{13}C NMR; however, the percentage of C observed in the aromatic C regions was much higher in our study (83-86% for 350ºC corn char and 90-94% for 600ºC char).

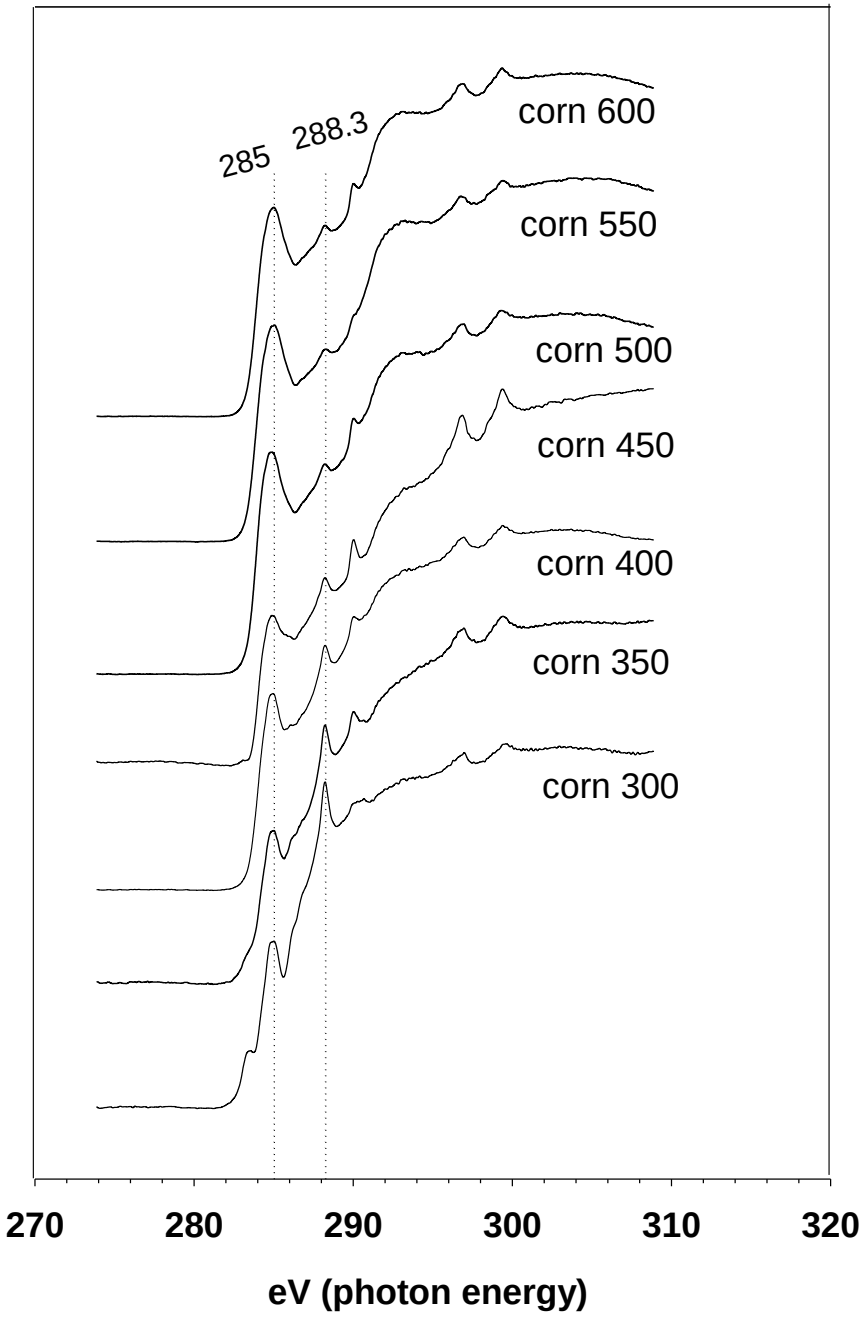

Figure 2.3. C 1s NEXAFS spectra of corn charred at different temperatures

2.4.2. Goodness of Fit

Despite the clear spectral differentiation between the ecological fractions, the 3-component mixing model produced an unacceptably high sum of squares value. Minimization of the sum of squares has been emphasized as a condition for confidence in mathematical mixing model results (Nelson and Baldock, 2005; Nelson et al., 2002). Possible explanations for the poor fit are that either too few components were used to fit the model (the model was too simplistic for such complex material); or that the ecological fractions obtained do not accurately represent the actual components for this soil. It is very likely that significant amounts of non-BC were adsorbed to the BC particles (Lehmann et al., 2005) that were isolated as a proxy for BC. In addition, the final value for the BC component did not agree with conclusions of others attempting to quantify the concentration of BC in the *Terra Preta* soil used in this study (Liang et al., 2006). Liang et al. (2006) attributed 51% of total C to BC using the mathematical mixing model method.

The 5-component mixing model produced variable fits depending on char type used in the model. The lower temperature chars (350º-450°C) and BC particles produced poor fits while the higher temperature chars (500º-600ºC) improved the model fits estimated by the sum of squares values. This may suggest that the studied soil contained BC that is better characterized by chars made at higher temperature. This is in contrast to assumptions that chars in *Terra Preta* soils originate from low temperature in-field burning (Hecht, 2003), which may have temperatures near the soil surface of less than 400°C as shown for slash-and-burn in Indonesia (Ketterings et al., 2000). Further analysis of the 5-component model revealed that iterations with the lowest error values attribute the remainder of C to protein and lipid components.

Table 2.4. Measured versus predicted proportion (%) of total C for a 5-component model using biomolecular endmembers including BC particles

	Measured signal	Predicted	Sum of Squares
284.5	19	15	19
285.4	14	16	6
286.1	3	5	3
286.7	19	13	34
287.6	6	9	8
288.4	19	20	3
289.2-289.9	20	21	2
Total	100	100	75

2.4.3. Pitfalls of black carbon quantification using NEXAFS data

C NEXAFS spectra of environmental matrices may be highly complex due to the multitude of possible electronic bonding environments of C (e.g. sp^2 vs. sp^3). Therefore many different absorption coefficients are produced which may lead to overlapping absorption bands from different functional groups (Stöhr, 1992, Solomon et al., 2010). Furthermore, NEXAFS is quantitative for an element only under certain circumstances such as when measuring in transmission mode with scanning transmission X-ray microscopy. Using STXM one can extract the total attenuation coefficient with units of

1/length and the magnitude of the edge-step can then be related to the partial density of the excited element in the sample. However, under bulk measurement conditions variable sample thickness will limit this ability, and deconvolution values cannot be related to absolute concentrations of an element of interest (Cody et al., 1995). However, the relative proportions of functional groups are in theory quantitative, albeit its quantification challenged by the ability to mathematically separate functional groups and edge step. Even in a case where little overlap occurred and unique spectral features could be attributed to specific functional group types (e.g. phenolic or carboxylic type C), it may not be possible to determine what percentage of a particular type of molecule is present in a specific region.

In addition, the demonstrated high sensitivity of the estimates to the BC standard used in the mixing model questions the applicability in those situations where the form of BC present in soil is not known. Black C properties may vary significantly as shown for different formation temperatures in this study, but also with different biomass types (Keiluweit et al., 2010; Nguyen et al., 2010).

2.5. Conclusions

NEXAFS has been demonstrated as a highly useful tool for the qualitative and semi-quantitative characterization of BC characterization. Concerns related to the quantitative data analysis of NEXAFS results for BC content remain and additional research into modeling the BC component of soils is warranted. Modeled composition of the soil strongly depended on the composition of the components included in the analyses. For some selection of BC reference material, particularly the high-temperature chars using the 5-component model, the results obtained were in line with previous estimates of BC content in this soil. However, a-priori information about the nature of the

BC component of a soil is typically not available. The results of the mixing model approach applied in this study demonstrate that NEXAFS is a promising tool for estimating the char component of soils in a non-invasive manner. Since it is not possible to pre-determine the extent of heating that char in soils has been exposed to, a new and exciting approach would be to develop a modeling approach with a sliding scale approach as shown in this study. Future research may need to demonstrate how robust the proposed approach is to other soils and to a range of BC made from different forms of biomass.

References

1. Beavis, J., Mott, C.J.B., 1996. Effects of land use on the amino acid composition of soils: 1. Manured and unmanured soils from the Broadbalk continuous wheat experiment, Rothamsted, England. Geoderma 72, 259– 270.
2. Cody G.D., Botto, R.E., Ade, H., 1995. Inner-Shell Spectroscopy and Imaging of Subbituminous Coal: In Situ Analysis of Organic and Inorganic Microstructure Using C (1s)-, Ca (2p)- and Cl (2s)- NEXAFS. Energy and Fuels 9, 525-533.
3. Cody, G.D., Ade, H., Wirick, S., Mitchell, G.D., Davis, A., 1998. Determination of chemical-structural changes in vitrinite accompanying luminescence alteration using C-NEXAFS analysis. Organic Geochemistry 28, 441-455.

4. Cody, G.D., Brandes, J., Jacobsen, C., Wirick, S., 2009. Soft X-ray induced chemical modification of polysaccharides in vascular plant cell walls. Journal of Electron Spectroscopy and Related Phenomena 170, 57-64.
5. Coffey, T., Urquhart, S.G., Ade, H., 2001. Characterization of the effects of soft X-ray irradiation on polymers. Journal of Electron Spectroscopy and Related Phenomena 122, 65-78.
6. Czimczik, C.I., Masiello, C.A., 2007. Controls on black carbon storage in soils. Global Biogeochemical Cycles 21, 1-8.
7. Glaser, B., Haumaier, L., Guggenberger, G., Zech, W., 2001. The Terra Preta phenomenon: a model for sustainable agriculture in the humid tropics. Naturwissenschaften 88, 37-41.
8. Goldberg, E.D., 1985. Black Carbon in the Environment. John Wiley and Sons, New York.
9. Hammes, K., Schmidt, M.W.I., Smernik, R.J., Currie, L.A., Ball, W.P., Nguyen, T.H., Louchouarn, P., Houel, S., Gustafsson, O., Elmquist, M., Cornelissen, G., Skjemstad, J.O., Masiello, C.A., Song, J., Peng, P., Mitra, S., Dunn, J.C., Hatcher, P.G., Hockaday, W.C., Smith, D.M., Hartkopf-Froeder, C., Boehmer, A., Luer, B., Huebert, B.J., Amelung, W., Brodowski, S., Huang, L., Zhang, W., Gschwend, P.M., Flores-Cervantes, D.X., Largeau, C., Rouzaud, J.N., Rumpel, C., Guggenberger, G., Kaiser, K., Rodionov, A., Gonzalez-Vila, F.J., Gonzalez-Perez, J.A., de la Rosa, J.M., Manning, D.A.C., Lopez-Capel, E., Ding, L., 2007. Comparison of quantification methods to measure fire-derived (black/elemental) carbon in soils and sediments using reference materials from soil, water, sediment and the atmosphere. Global Biogeochemical Cycles 21, 1-18.

10. Hecht, S.B., 2003. Indigenous soil management and the creation of Amazonian Dark Earths: implications of Kayapó practices. In: Lehmann, J., Kern, D.C., Glaser, B., Woods, W.I. (Eds.), Amazonian Dark Earths: Origin, Properties, Management, Springer Science and Business Media, Inc., pp. 355-372.
11. Hedges, J.I., Eglinton, G., Hatcher, P.G., Kirchman, D.L., Arnosti, C., Derenne, S., Evershed, R.P., Kogel-Knabner, I., de Leeuw, J.W., Littke, R., Michaelis, W., Rullkotter, J., 2000. The molecularly-uncharacterized component of nonliving organic matter in natural environments. Organic Geochemistry 31, 945-958.
12. Heymann, K., Lehmann, J., Solomon, D., Schmidt, M., Regier, T., 2011. C 1s K-edge near-edge X-ray fine structure (NEXAFS) spectroscopy for characterizing the functional group chemistry of black carbon. Organic Geochemistry 42, 1055-1064.
13. Kaznacheyev, K., Osanna, A., Jacobsen, C., Plashkevych, O., Vahtras, O., Agren, H., Carravetta, V., Hitchcock, A.P., 2002. Innershell Absorption Spectroscopy of Amino Acids. Journal of Physical Chemistry 106, 3153-3168.
14. Keiluweit, M., Nico, P.S., Johnson, M.G., Kleber, M., 2010. Dynamic molecular structure of plant biomass-derived black carbon (biochar). Environmental Science and Technology 44, 1247-1253.
15. Kelleher, B.P., Simpson, A.J., 2006. Humic substances in soils: are they really chemically distinct? Environmental Science and Technology 40, 4605-4611.
16. Ketterings, Q. M., Bigham, J.M., Laperche, V., 2000. Changes in soil mineralogy and texture caused by slash-and-burn fires in Sumatra, Indonesia. Soil Science Society of America Journal 64, 1108-1117.
17. Kinyangi, J., Solomon, D., Liang, B.I., Lerotic, M., Wirick, S., Lehmann, J., 2006. Nanoscale biogeocomplexity of the organomineral assemblage in soil:

Application of STXM microscopy and C 1s-NEXAFS spectroscopy. Soil Science Society of America Journal 70, 1708-1718.

18. Kramer, R.W., Kujawinski, E.B., Hatcher, P.G., 2004. Identification of black carbon derived structures in a volcanic ash soil humic acid by Fourier transform ion cyclotron resonance mass spectrometry. Environmental Science and Technology 38, 3387-3395.
19. Kuhlbusch, T.A.J., 1998. Black carbon and the carbon cycle. Science 280, 1903-1904.
20. Lehmann, J., Liang, B.Q., Solomon, D., Lerotic, M., Luizao, F., Kinyangi, J., Schafer, T., Wirick, S., Jacobsen, C., 2005. Near-edge X-ray absorption fine structure (NEXAFS) spectroscopy for mapping nano-scale distribution of organic carbon forms in soil: Application to black carbon particles. Global Biogeochemical Cycles, 19.
21. Lehmann J., Kinyangi, J. and Solomon, D., 2007. Organic matter stabilization in soil microaggregates: implications from spatial heterogeneity of organic carbon contents and carbon forms. Biogeochemistry 85, 45-57.
22. Lehmann J, Skjemstad J.O., Sohi, S., Carter, J., Barson, M., Falloon, P., Coleman, K., Woodbury, P., and Krull, E., 2008. Australian climate-carbon cycle feedback reduced by soil black carbon. Nature Geoscience 1, 832–835.
23. Lehmann, J., Brandes, J., Fleckenstein, H., Jacobsen, C., Solomon, D., Thieme, J., 2009. Synchrotron-based near-edge X-ray Spectroscopy of natural organic matter in soils and sediments. In: N. Senesi, Xing, P. Huang, P.M. (eds.), Biophysico-Chemical Processes Involving Natural Nonliving Organic Matter in Environmental Systems, IUPAC Series on Biophysico-Chemical Processes in Environmental Systems. Wiley, New Jersey, 729-781.

24. Lehmann, J. and Solomon, D., 2010. Organic carbon chemistry in soils observed by synchrotron-based spectroscopy. In: B Singh and M Gräfe (Eds.) Synchroton-based Techniques in Soils and Sediment. Elsevier, Amsterdam, pp. 289-312.
25. Liang, B., Lehmann, J., Solomon, D., Kinyangi, J., Grossman, J., O'Neill, B., Skjemstad, J.O., Thies, J., Luizao, F.J., Petersen, J., Neves, E.G., 2006. Black carbon increases cation exchange capacity in soils. Soil Science Society of America Journal 70, 1719-1730.
26. Liang, B., Lehmann, J., Solomon, D., Sohi, S., Thies, J.E., Skjemstad, J.O., Luizao, F.J., Engelhard, M.H., Neves, E.G., Wirick, S., 2008. Stability of biomass-derived black carbon in soils. Geochimica et Cosmochimica Acta 72, 6069-6078.
27. Masiello, C.A., 2004. New directions in black carbon organic geochemistry. Marine Chemistry 92, 201−213.
28. Nelson P.N., Baldock J.A., Clarke P., Oades J.M. and Churchman G.J., 1999. Dispersed clay and organic matter in soil: their nature and associations. Australian Journal of Soil Research 37, 289–315.
29. Nelson, P.N., Baldock, J.A., 2005. Estimating the molecular composition of a diverse range of natural organic materials from solid-state C-13 NMR and elemental analyses. Biogeochemistry 72, 1-34.
30. Nguyen, B., Lehmann, J., 2009. Black carbon decomposition under varying water regimes. Organic Geochemistry 40, 846-853.
31. Nguyen, B., Lehmann, J., Hockaday W.C., Joseph S., Masiello C., 2010. Temperature sensitivity of black carbon decomposition and oxidation. Environmental Science and Technology 44, 3324-3331.

32. Novotny, E.H., Hayes, M.H.B., Madari, B.E., Bonagamba, T.J., deAzevedo, E.R., de Souza, A.A., Song, G.X., Nogueira, C.M., Mangrich, A.S., 2009. Lessons from the Terra Preta de Indios of the Amazon Region for the Utilization of Charcoal for Soil Amendment. Journal of the Brazilian Chemical Society 20, 1003-1010.

33. Preston, C.M., 2006. Applications of NMR to soil organic matter analysis: history and prospects. Soil Science 161, 133-166.

34. Preston, C.M., Schmidt, M.W.I., 2006. Black (pyrogenic) carbon: a synthesis of current knowledge and uncertainties with special consideration of boreal regions. Biogeosciences 3, 397-420.

35. Ravel and Newville, 2005. Athena, artemis, hephaestus. Journal of Synchrotron Radiation 12, 537-541.

36. Regier, T., Krochak, J., Sham, T.K., Hu, Y.F., Thompson, J., Blyth, R.I.R., 2007. Performance and capabilities of the Canadian Dragon: The SGM beamline at the Canadian Light Source. Nuclear Instruments & Methods in Physics Research Section -Accelerators Spectrometers Detectors and Associated Equipment 582, 93-9.

37. Risse T., Hill, T., Schmidt, J., Abend, G., Hamann, H., Freund, H.J., 1998. Investigation of the molecular motion of self-assembled fatty acid films. Journal of Physical Chemistry B 102, 2668-2676.

38. Schäfer, T., Hertkorn, N., Artinger, R., Claret, F., Bauer, A., 2003. Functional group analysis of natural organic colloids and clay association kinetics using C (1s) spectromicroscopy. Journal De Physique IV 104, 409-412.

39. Scheinost, A.C., Kretzschmar, R., Christl, I., Jacobsen, C., 2001. Carbon group chemistry of humic and fulvic acid: a comparison of C 1s NEXAFS and ^{13}C NMR

spectroscopies. In: E.A. Ghabbour, Davies, G. (Eds.), Humic Substances: Structures, Models and Functions, Royal Society of Chemistry. Cambridge, UK, pp. 39-47.

40. Schmidt, M.W.I., Skjemstad, J.O., Gehrt, E., Kogel-Knabner, I., 1999. Charred organic carbon in German chernozemic soils. European Journal of Soil Science 50, 351-365.
41. Schmidt, M.W.I., Noack, A.G., 2000. Black carbon in soils and sediments: Analysis, distribution, implications, and current challenges. Global Biogeochemical Cycles 14, 777-793.
42. Schmidt, M.W.I., Skjemstad, J.O., Czimczik, C.I., Glaser, B., Prentice, K.M., Gelinas, Y., Kuhlbusch, T.A.J., 2001. Comparative analysis of black carbon in soils. Global Biogeochemical Cycles 15, 163-167.
43. Schulten and Schnitzer, H., Schnitzer, M., 1993. A state of the art structural concept for humic substances. Naturwissenschaften 80, 29-30.
44. Simpson, M.J. and Hatcher, P.G., 2004. Overestimates of black carbon in soils and sediments. Naturwissenschaften 91, 436-440.
45. Smith, N.J.H., 1980. Anthrosols and human carrying capacity in Amazonia. Annals of the Association of American Geographers 70, 553-566.
46. Solomon, D., Lehmann, J., Kinyangi, J., Liang, B., Hanley, K., Heymann, K., Wirick, S. and Jacobsen, C., 2009. Carbon (1s) NEXAFS spectroscopy of biogeochemically relevant organic reference compounds. Soil Science Society of America Journal 73, :1817-1830.
47. Solomon, D., Lehmann, J., Thies, J., Schafer, T., Liang, B.Q., Kinyangi, J., Neves, E., Petersen, J., Luizao, F., Skjemstad, J., 2007. Molecular signature and

sources of biochemical recalcitrance of organic C in Amazonian Dark Earths. Geochimica et Cosmochimica Acta 71, 2285-2298.

48. Spokas, K.A., 2010. Review of the stability of biochar in soils: predictability of O:C molar ratios. Carbon Management 1, 289-303.
49. Stöhr, J., 1992. NEXAFS Spectroscopy. Springer series in surface sciences. Vol 25. Springer, Berlin, Germany.
50. Urquhart, S.G., Ade, H., 2000. Trends in the carbonyl core (C 1s, O 1s) -> pi*c=o transition in the near-edge X-ray absorption fine structure spectra of organic molecules. Journal of Physical Chemistry 106, 8531-8538.
51. Watts, B., Thomsen, L., Dastoor, P.C., 2006. Methods in carbon K-edge NEXAFS: Experiment and analysis. Journal of Electron Spectroscopy and Related Phenomena 151, 105-120.

3. DO BLACK HUMIC SUBSTANCES EXIST?

Abstract

Humic substances (HS) are operationally defined and may not necessarily correlate to the existence of a distinct molecular type. In black carbon (BC) rich soils the existence of specific HS originating from black carbon has been suggested. While it is clear that oxidation of BC occurs in soils it is not proven that a chemically distinct class of BC HS exclusive of plant and microbial monomers exists in soils. We attempted to verify the existence of BC HS using Scanning Transmission X-ray Microscopy (STXM) coupled with near-edge X-ray absorption fine-edge spectroscopy (NEXAFS) spectroscopy to analyze the spatial composition of a BC rich soil microaggregate at a scale of < 50 µm. The soil was analyzed from 3 depths (0-0.16 m, 0.16-0.43 m, 0.43-0.67 m) along with their respective HA and FA extracts. NEXAFS was used to validate the spectral signature of HS extracts. Using principal component analysis we identified distinct spectra within the spectral map as characteristic of previously measured ecological fractions (microbial extracts, black carbon, plant litter). However, we were unable to obtain a good fit (RMS = <0.01) for the HS extracts within the spatial map. Our results did not verify the existence of a distinct HS component with the soil organic matter matrix. Our results suggest that HS do not exist in soil as a distinct component class but rather reflect the extraction of various materials at different stages of decomposition.

3.1. Introduction

The severe consequences of potentially large carbon (C) losses from rapidly warming terrestrial ecosystems (Schuur and Abbott 2011) highlight the importance of biogeochemical processes that are essential to building concise global C and climate models. Soils rich in black carbon (BC), such as the *Terra Preta de Indio* soils of the

Brazilian Amazon have provided insight into the capacity for soils to serve as long-term sinks for atmospheric C (Liang et al. 2008). However, little is understood about the precise mechanisms and chemical properties that control the longevity of BC in soils (Keiluweit et al. 2010, Kleber et al. 2010; Schmidt et al. 2010) and there remains some uncertainty about the use of biochar as a C sequestration tool (Lehmann et al. 2009). At the core of improving the ability to model and predict the behavior of SOM is it'schemical structure. Researchers have long relied on the extraction of an operationally defined class of humic substances to model and predict the behavior of organic matter (Schulten and Schnitzer 1993). However, contemporary analyses of soil organic matter or the "new view" (Sutton and Sposito 2005; Kelleher and Simpson 2006; Lehmann et al. 2008) that rely on *in-situ* observations of macromolecular components of soil organic matter, have not directly identified a distinct class of humic substances (HS) within the soil matrix. By extension, the existence of a distinct class of HS derived from BC in soils (Kumada 1983; Shindo et al. 1986 a-c; Shindo 1992; Shindo et al. 1998; Hiradate et al. 2004; Shindo et al. 2001; Shindo et al. 2004; Shindo et al. 2005; Nishimura et al. 2006; Song et al. 2008) is also brought into question but to our knowledge, has not yet been verified. The ongoing and persistent strategy of HS extraction as a means to explain various soil phenomena (Mao et al. 2010; Richard et al. 2011; Yang et al. 2011) justifies the need to validate their existence or at the very least to quantify the relationship between extracts and intact soil organic matter (SOM) components. A growing body of research (Kleber 2010; Schmidt et al. 2011) suggests that the mechanisms of stabilization of microbial metabolites in soils does not necessarily hinge on the recalcitrance of organic matter input to soil. Therefore, scrutinizing the decomposition products of BC should improve our understanding of C stabilization processes and the mechanics of climate-carbon feedbacks in terrestrial systems.

Humic substances are described by the International Humic Substances Society (IHSS) as complex, heterogeneous mixtures formed during the decay and transformation

of plant and microbial remains (humification) are characterized as both chemically reactive yet recalcitrant to biodegradation (www.humicsubstances.org/whatarehs.html). Humic substances formed from BC have been the subject of numerous studies (Kumada 1983; Shindo 1986a-c; Shindo 1991; Nishimura 2009). Black C is the product of incomplete combustion of plant biomass and fossil fuels, and comprises a fairly substantial portion of molecularly uncharacterized natural organic matter (Hedges et al. 2000). Black C has been characterized as intrinsically refractory (Cheng et al. 2008; Liang et al. 2008); however, various degradation pathways of BC have been described (Baldock and Smernik 2002; Hockaday et al. 2006; Hammes et al. 2008). Black C humic acids (HA) have been suggested to play an important role in the overall humification processes in soil (Kumada 1965; Kumada 1983; Shindo 1986a; Shindo 1986b; Shindo 1986c; Shindo 1991; Nishimura 2009), and the contribution of BC to the operationally defined alkali-soluble fraction (i.e. HA) of organic matter has been recognized (Masiello and Druffel 1998). However, humified BC has not been observed directly on a fine-scale and has not been implicitly distinguished from other types of microbial exudates. Since BC may potentially be a driver for various soil processes (Joseph et al. 2010) it is imperative to gain a more sophisticated comprehension of its role in the soil organic matter.

The term “humic acid” is operationally defined and does not correlate to the existence of a distinct molecular type (Schmidt et al. 2011). However, the formation of dark HAs has been attributed to the presence of charred plant materials commonly present in Japanese Andisols (Kumada 1983; Shindo 1986a-c; Shindo 1991; Hiradate et al. 2004; Shindo et al. 2005; Nishimura et al. 2006). Charcoal produced by the incomplete combustion of plants was suggested to be either weathered under natural conditions or subjected to oxidative depolymerization under the influence of oxygen and moisture. This process was thought to result in the formation of dark colored HAs and fulvic acids (FAs). Other studies observed nitric-acid oxidation of furnace carbon blacks

and charcoals produced extracts with condensed, substituted aromatic structures bearing carboxylic, phenolic and carbonyl functional groups with molecular weights in the range of 400-1200 Da, similar to HS (Haumaier and Zech 1995; Kamegawa et al. 2002; Trompowsky et al. 2005). While it is clear that oxidation of BC particles does occur naturally, it is not proven that oxidation of BC results in the formation of a chemically distinct class of BC-HS in soils.

The main objective of our study was to examine whether we could detect HA and FA in BC-rich soils that bear functional group chemistry resembling BC using STXM coupled with NEXAFS spectroscopy. The existence of BC HS or lack thereof would also provide input into the discussion of whether quality of organic matter input to soil has a bearing on stabilization pathways.

3.2. Methods

3.2.1. Study site

Black C rich Anthrosols were obtained from an archaeological site, Lago Grande (LG), near Manaus, Brazil (3º8’ S, 59º52’ W, 40-50 m above sea level). Details concerning soil formation conditions and local climate and vegetation have been described elsewhere (Liang et al. 2006, Fig. A 3.1) (Table 3.1).

Table 3.1. Profile characteristics of the studied Amazonian Dark Earth soil (Liang et al., 2006)

Depth	Sand	Silt	Clay	Total C	BC	BC	CEC
(m)	----------(%)----------			(mg g^{-1})	(mg g^{-1})	(% of C)	($mmol_C$ kg^{-1})
0-0.16	46.7	28.0	25.3	29.0	18.0	62.2	292
0.16-0.43	43.4	26.0	30.5	21.3	16.4	77.0	264
0.43-0.67	44.3	25.3	30.4	19.1	14.6	76.2	258

A depth profile of the soil from 0-0.67 m was obtained from 0-0.16 m, 0.16-0.43 m, and 0.43-0.67 m. Spectra from plant litter, BC materials and microorganisms were obtained from previously published research by Liang et al. (2008). Spectra of these materials are provided in the Supplementary Online Material.

Microaggregates were isolated from all three horizons as described by Kinyangi et al. (2006). Free stable aggregates between 20-200 μm from each soil were prepared for spectroscopic measurement as follows: aggregates were misted, shock-frozen and sectioned using a cryo-microtome (Ultracut UTC, Leica Microsystems Inc., Bannockburn, IL). Sections 100-200 nm thick were cut at -55ºC using a diamond knife (MS9859 Ultra 458, Diatome Ltd., Biel, Switzerland) at a cutting speed of 0.3 to 1.2 mm s^1 (angle of 6º) and transferred to copper (Cu) grids (carbon free, 200 mesh, silicon monoxide No. 53002, Ladd Research, Williston, VT). After sectioning, the microaggregate thin sections were mounted on Cu grids impregnated with silicon monoxide (SiO) substrate. Each grid was mounted onto the center pinhole of stainless steel sample stage plates (46-mm diam.).

Soil humic extracts were obtained using the methods recommended by the IHSS (Swift 1996). Soils were extracted with 0.5 M NaOH at a soil:solution ratio of 1:10 (mass:volume) under an N_2 atmosphere (Stevenson 1984). The extracted HS were separated into HA and FA fractions by acidifying the extract to pH 2 using 6 M HCl. Humic substance extracts were mounted on 100-nm thick silicon nitride (Si_3Ni_4) windows (Silson Ltd., Northampton, UK) by dissolving 1 mg of sample in 400 μL of pure trifluoroacetic acid (TFA, Sigma-Aldrich Corp. St. Louis, MO) and transferring 1 μL of solution onto the window (Boese 1996; Boese 1997; Solomon et al. 2009).

3.2.2. STXM and C NEXAFS Data Acquisition

Spectroscopic measurements were performed at beamline X1A1 of the National Synchrotron Light Source, Brookhaven National Laboratory, which is equipped with a STXM endstation. The STXM consists of a tunable undulator inserted into the electron storage ring (2.8 GeV); a spherical grating monochromator (tunable over 250-800 eV), and a 160-µm Fresnel zone plate (45 nm spatial resolution).

To map the microaggregates, the z-stage was adjusted to focus the X-rays through the microaggregate sample section. Slit openings were set at 40/25/25 mm to give an energy resolution of 0.1 eV. The slit settings and zone plate together provided a scanning spatial resolution of 50 nm. The monochromator energy was increased from 280 to 282.5 eV in 0.3 eV increments (scan time 1 msec), from 282.5 to 292 eV in 0.1 eV steps (scan time 3 msec), and from 292 to 310 eV in 0.3 eV steps (scan time 3 msec). Smaller energy steps of 0.1 eV were chosen in the main spectroscopic regions where C 1s core electron excitation is indicative of sharp 1s 2p*, and broad 1s, 3p 1s* transitions. The dwell time was increased to reduce error and improve data. Single images were recorded at each photon energy level and built into a stack using the program Stack Analyze 2.6.1 (Jacobsen et al. 2000). Alignment was performed using cross-correlation. Stack image processing software and data analyses instructional manuals can be accessed on the website at http://xray1.physics.sunysb.edu/data/software.php.

To obtain NEXAFS spectra of humic extracts, the beamline slit width was set to 45/25/25 (Plaschke et al. 2004). Monochromator calibration was performed as described by Solomon et al. (2009). Background spectra (I_o) were collected for each sample from sample-free region of the Si_3N_4 windows. Samples were measured under Helium (He) atmosphere in triplicate. Measurements were taken by adjusting the grating from 280-310 eV with 0.1 eV energy step, 120 ms dwell time. The three spectra were confirmed to be

in agreement with each other and averaged. WinXas 3.1 (WinXAS Software, Hamburg, Germany) was used to baseline correct and normalize the data.

3.2.3. Data analysis

For NEXAFS data, peak resonances with specific bonding environments were assigned based on the spectral signatures of pure chemical standards representative of specific functional groups (Solomon et al. 2009), and a least-squares fitting scheme was applied to the normalized NEXAFS spectra in the range of 280 to 310 eV. We used a scheme based on eight Gaussians curves (labeled "G-1", etc.) following the procedure suggested by Scheinost et al. (2001), with additional bands for substituted aryl C (G3) and an additional carbonyl group (G8) (Liang et al. 2008). Specific positions for the Gaussian bands have been published previously (Heymann et al. 2011). An arctangent function was used to model the ionization step and was fixed at 290 eV. The full width at half maximum of the bands was set at 0.4 ± 0.2 eV, while the amplitude was floated during the fit. Deconvolution was performed by resolving spectra into individual arctangent and Gaussian curve components (G) using the ATHENA software (ATHENA 0.8.052; Ravel and Newville 2005). Spectral regions represented by Gaussian curves were described as being generally attributed to the following functional groups: overall aromatic type C was represented by the sum of the [G1+G2+G3] peaks; aromatic C with side chain substituent (such as phenolic C) by the G4 peak; alkyl C by the G5 peak; carboxylic/carbonyl C by the G6 peak, and O-alkyl C by the sum of [G7+G8] peaks (Lehmann et al. 2009).

For the maps obtained using STXM, the program PCA_GUI 1.1.1 was used to orthogonalize and noise-filter the data, as well as to identify the number of significant components (s = 1, 2, 3…..10) in the microaggregate as well as group spectrally distinct

pixels into clusters. Different numbers of components and clusters were used to identify the combination of components and clusters which yielded the lowest errors. Singular value decomposition (SVD) was calculated to obtain target maps and associated target spectra (Lehmann et al. 2005). Target spectra were used from the HA and FA extracts to identify whether they would explain a significant portion of a region in the maps, similar to the method used for total humic extracts (Lehmann et al. 2008).

3.3. Results

3.3.1. Characterization of components

The three HA extracts appeared highly similar to one another (Fig. 3.1).

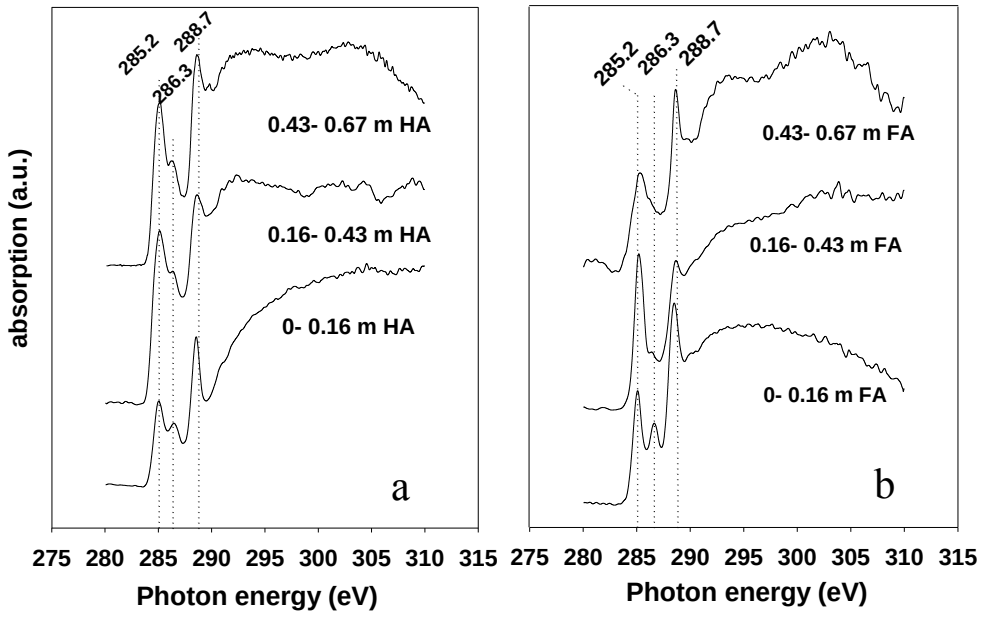

Figure 3.1. Carbon 1s NEXAFS spectra of (a) HA and (b) FA extracts from an Amazonian Dark Earth

The peak positions between HA and FA extracts were not systematically different, appearing at 285.2, 286.3 and 288.7 eV. The well resolved absorption band near 285 eV corresponds to the C 1s-$\pi^*_{C=C}$ transition related to the protonated and alkylated to carbonyl substituted aryl-C (C=C) (Cody et al. 1998). A second, well resolved, less intense absorption band was present around 286.2 eV for all HA and FA extracts, representing phenolic type C. A third absorption band present around 288.7 eV for all HA and FA extracts and was very clearly resolved and indicates the presence of carboxyl/carbonyl type C.

We used spectral deconvolution results to compare the functional group distribution for the HS extracts (Table 3.2).

Table 3.2. Proportion (%) of functional group distribution of humic acid (HA) extracts and fulvic acid (FA) extracts obtained using deconvolution of C NEXAFS spectra

	Depth (m)	Aromatic (G1+G2+G3)	Phenolic (G4)	Alkyl (G5)	Carboxylic (G6)	O-alkyl (G7+G8)
HA	0-0.16	29	11	5	29	26
	0.16-0.43	33	8	0	18	32
	0.43-0.67	45	9	1	27	40
FA	0-0.16	25	13	4	30	29
	0.16-0.43	42	7	5	18	27
	0.43-0.67	35	10	5	32	18

The proportion of total C present in the aromatic C region (G1-G3) of the HA extracts increased with increasing depth, from 29% at 0-0.16 m depth to 45% at 0.43-0.67 m depth (Table 3.2.). The phenolic and aliphatic type C regions (G4 and G5) did not exhibit distinct differences between the three HA extracts over the depth profile. The carboxylic/carbonyl C absorption region (G6) showed that at a depth of 0-0.16 m and 0.43-0.67 m the proportion of total absorption intensity present in this region was very similar (27-29%) but was lower in HA extracts from 0.16-0.43 m (18%). The proportion of the O-alkyl C region (G7 + G8) in HA extracts increased with depth, from 26% at a depth of 0-0.16 m to 40% at 0.43-0.67 m

Black C particles were characterized by a broad C 1s-$\pi^*_{C=C}$ transition at 285 eV (40% aromaticity) (Table 3-3), and a smaller C 1s-$\pi^*_{C=O}$ transition representing carboxylic-type C (9% of total absorption intensity).

Table 3.3. Proportion (%) of functional group distribution of plant litter, microbial extracts and black carbon obtained using deconvolution of C NEXAFS spectra

	Aromatic (G1+G2+G3)	Phenolic (G4)	Alkyl (G5)	Carboxylic (G6)	O-alkyl (G7+G8)
Plant litter	15	13	13	25	34
Microbial extract	10	7	20	31	31
Black carbon	42	11	13	19	16

In contrast, the microbial extract was characterized by only a small peak around 285.3 eV (10% aromaticity) (Table 3.3). The proportions of total signal intensity in the aliphatic (20%), carboxylic (31%) and the O-alkyl C region (31%) defined the material and distinguished it from the BC particles (Table 3.3). Plant litter was fairly heterogeneous with multiple peaks present near 284.5, 285, 288 and 289 eV. The aromatic, phenolic and aliphatic C regions each comprised 17-21% of total absorption intensity. The proportion of C present in the carboxylic type C transition was around 14%, and the O-alkyl region value was around 30%.

3.3.2. Principal component and cluster analysis

Cluster analysis and principal component analyses were performed by systematically testing combinations of components and clusters for each sample (Fig. 3.4, Fig. 3.5, Fig. 3.6).

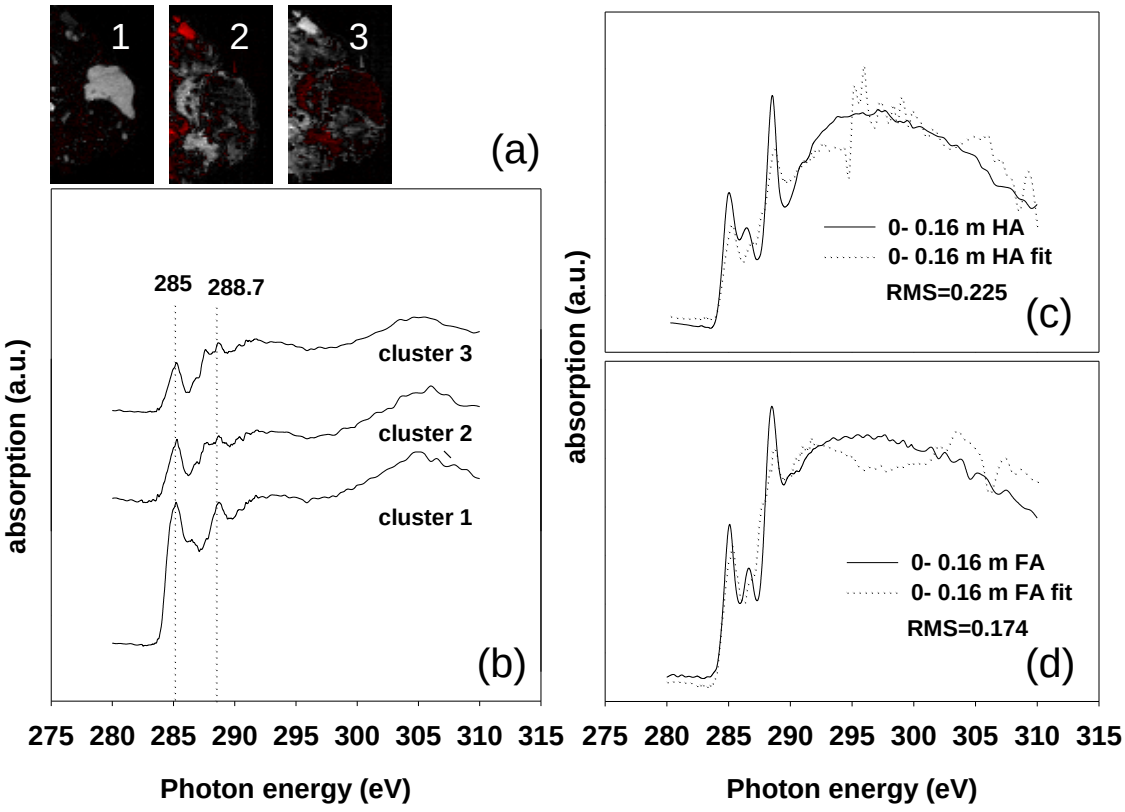

Figure 3.2. Carbon 1s NEXAFS analysis of a microaggregate from an Amazonian Dark Earth at a depth of 0-0.16 m; (a) target maps, (b) cluster spectra, (c) HA spectra and fit, (d) FA spectra and fit

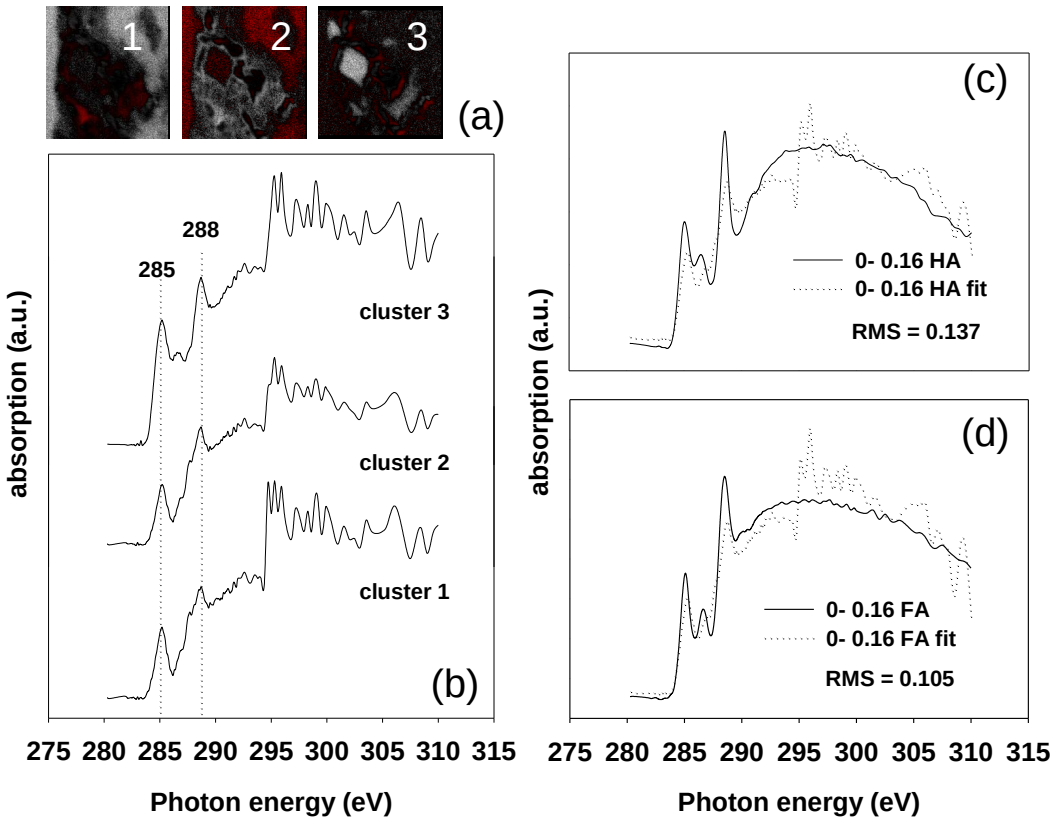

Figure 3.3. Carbon 1s NEXAFS analysis of a portion of a microaggregate (from Fig. 2) from an Amazonian Dark Earth sampled at a depth of 0-0.16 m: (a) target maps, (b) cluster spectra, (c) HA spectra and fit, (d) FA spectra and fit

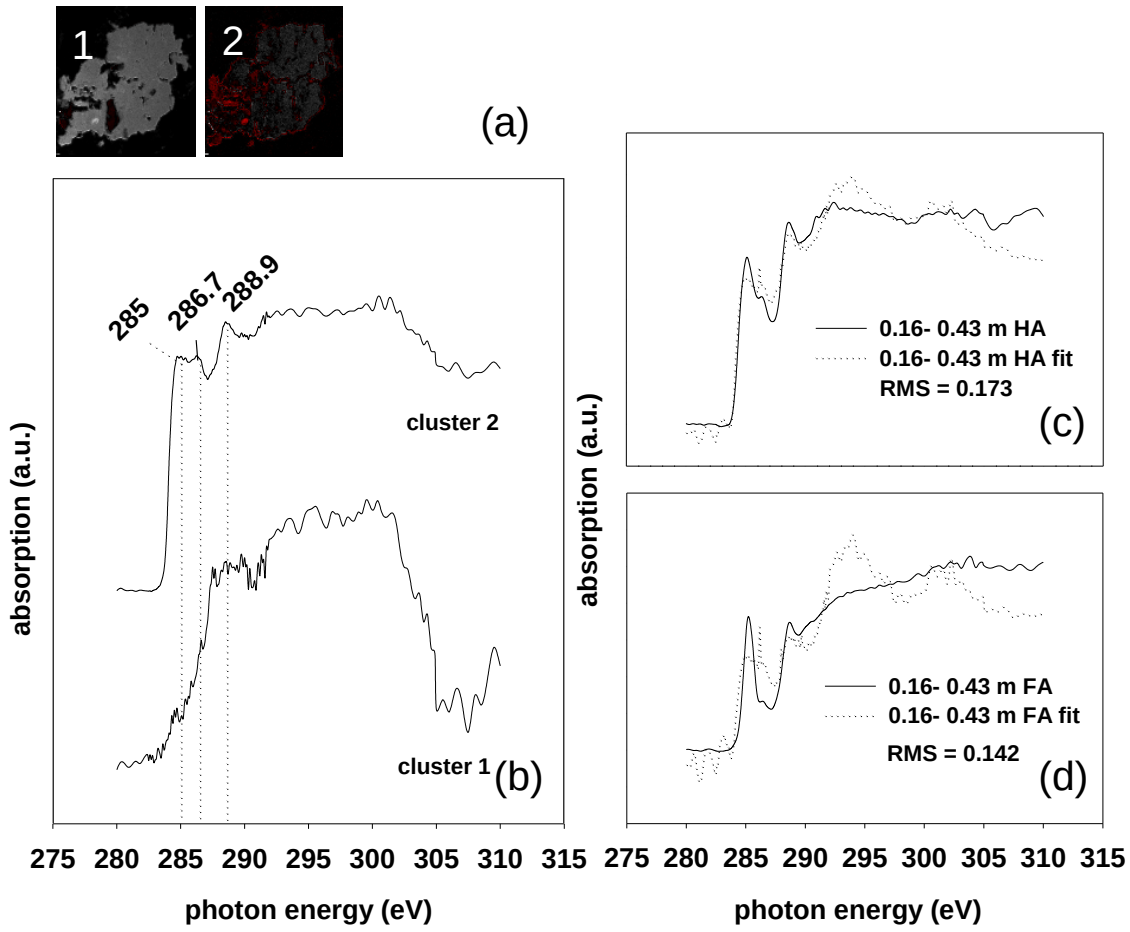

Figure 3.4. Carbon 1s NEXAFS analysis of a microaggregate from an Amazonian Dark Earth sampled at a depth of 0.16-0.43 m; (a) target maps, (b) cluster spectra, (c) HA spectra and fit, (d) FA spectra and fit

This was done in order to determine whether the spatial distribution of the clusters was significantly affected by changing the number of principal components and to determine which combination would be the most representative of the sample.

For the 0-0.16 m soil depth we mapped an overview of the entire microaggregate as well as a close-up area of interest within the microaggregate (Fig. 3.3). Principal component analysis was performed and target maps were constructed from cluster spectra for all analyzed combinations of principal component and cluster analyses. For example, for each sample we tested combinations of 2-8 components and 2-10 clusters. For the overview of the microaggregate from the 0-0.16 m depth increasing the number of principal components to 6 or 7 improved the RMS error (to < 0.01) of the first three components for 6/2 through 6/7 and 7/2 through 7/4 compared with lower component/cluster combinations. Increases beyond these combinations did not result in improved fits. However, increasing the number of clusters changed the distribution of C forms. For this reason a combination of 6 components and 5 clusters was chosen as the most robust. An analysis of a specific region within the microaggregate from 0-0.16 m sample, however, revealed that a combination of 5 principal components and 8 clusters yielded the most clusters (the first 4) with RMS values < 0.01. Decreasing the number of clusters reduced the number of significant RMS values for target maps. For this reason, the 5/8 component/cluster combination was chosen for these high-resolution observations in an area of the micro-aggregate.

For the analysis of an entire microaggregate from 0.16-0.43 m depth (Fig. 3.4), 5 principal components combined with 5 clusters gave the best fit for the first 3 clusters (lowest RMS values, <0.01). Five components with 4-10 clusters or 4 principal components with 4-10 clusters also resulted in good fits; however, the resulting RMS values were higher than when using 5 components. The number of significant clusters (3)

was the same for both the 4 and 5 components fits and did not change by changing the number of clusters. The number of significant components decreased with less than 4 or more than 5 principal components. The best fit for the microaggregates from the depth 0.43-0.67 m was found for 5 components with 4 clusters where the first 3 components were significant (Fig. 3.5).

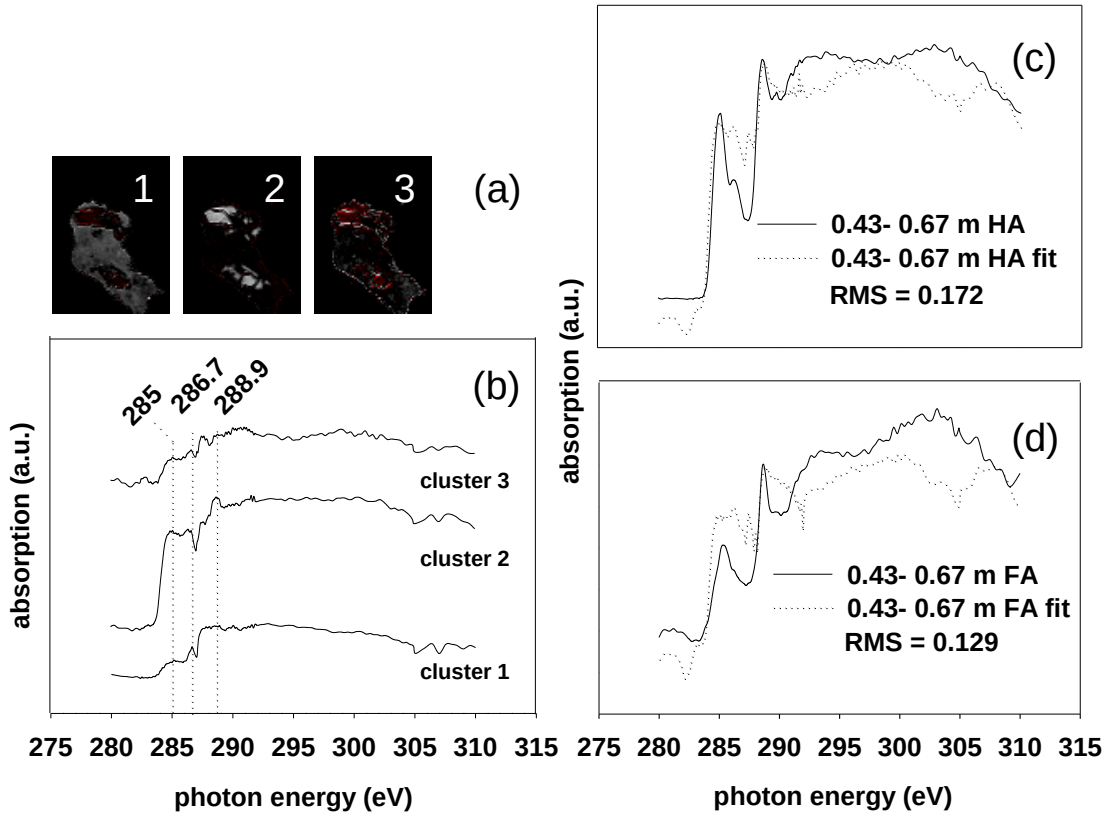

Figure 3.5. Carbon 1s NEXAFS analysis of a microaggregate from an Amazonian Dark Earth sampled at a depth of 0.43-0.67 m; (a) target maps, (b) cluster spectra, (c) HA spectra and fit, (d) FA spectra and fit

All other component/cluster combinations only resulted in significant fits for the first one or two clusters.

Humic extract spectra from each soil were searched for in the respective component/cluster combination representing the best fit for each map. No significant fits (RMS < 0.01) were found for any of the soil HA or FA extracts in their respective maps and RMS were 0.11 to 0.23 (Fig. 3.2; Fig. 3.3; Fig. 3.4; Fig. 3.5).

3.4. Discussion

3.4.1. Functional group composition of humic and fulvic acid extracts

Humic substance extract spectra were characteristic for *Terra Preta de Indio* soils according to comparisons with previously published work (Liang et al. 2006; Lehmann et al. 2008; Solomon et al. 2006, 2007; Scheinost et al. 2001). Solomon et al. (2007) observed differences between humic extracts from similar BC-rich soils used in this study and BC-poor adjacent soils. In addition, Liang et al. (2006) measured a HS extract from a similar *Terra Preta de Indio* soil with NEXAFS and produced a spectrum comparable to those observed in this study. The major changes in functional group composition of the HA and FA extracts with depth were an increase in the proportion of aromatic type C and O-alkyl type C for the HA extracts. This may be explained by the greater proportion of BC as a fraction of total organic C with depth (Liang 2008). Together with a lack of a systematic difference between HA and FA extracts, these results suggest that according to our NEXAFS analyses, HS extracts do not provide useful information for the studied soils.

3.4.2. Black humic substances in soils?

The C functional group composition of the studied microaggregates resemble the results of earlier work on Amazonian Dark Earths (Lehmann et al. 2005; Liang et al. 2006). The poor fit of the NEXAFS spectra obtained from HA and FA extracts to the spectra found at a high spatial resolution in microaggregates using STXM suggests that neither HA or FA exist as distinct chemical compounds as highlighted for HS in general by Lehmann et al. (2008). These findings support a growing body of research which indicates that HS do not represent a distinct component class in soils or sediments and are merely operationally defined. Such observations are not new (Waksman 1936), and perhaps the most convincing argument has been made by Kleber (2010), who applies the second law of thermodynamics to soil organic matter degradation whereby the process of breaking down complex, high energy forms of matter commands that energy spontaneously flows in one direction, and that organisms must continuously move energy from highly ordered, high energy molecules to disordered, free energy forms in order to survive. There is no direct observational evidence to support existence of humic fractions as thermodynamic anamolies, while the hard evidence to support development of new language and methods by which to study soil organic matter is growing (Kelleher and Simpson 2006; Lehmann et al. 2008).

While differences are observed between HS extracts from BC rich and BC poor soils (Solomon et al., 2007), these may simply be attributed to the experimental procedure where unaltered or weakly altered BC particles are partially extracted in addition to varying proportions of SOM in BC rich soil extracts. This likely gives the impression of the existence of decomposition products of BC with a distinct chemical signature reminiscent of the original BC. That said, the HS extracts may still give an adequate picture of the proportion of BC and its degree of oxidation in soil as also seen

from the increase in aromaticity with depth coinciding with greater BC contents in our study, but do not appear to represent a distinct compound class. However, studies that implicate a unique compound class of BCHS as responsible for increased soil fertility may need to be reevaluated; and a more extensive look at the BC-mineral interactions unique to that particular soil may be more relevant.

3.4.3. Implications for our understanding of C stabilization in soil

The lack of fit of HS spectra to direct observations of total C at a fine spatial scale of less than 100 nm suggest that the decomposition products of BC do not bear functional group characteristics of BC. Similar conclusions can be drawn from the lack of BC-type spectral characteristics in close proximity of micrometers to BC surfaces (Lehmann et al. 2008; Liang 2008; Lehmann and Solomon 2010). These observations lend support to recent suggestions (Kleber 2010; Schmidt et al. 2011) that the recalcitrance of organic matter entering soils does not affect the way C is stabilized. Microbial metabolites may ultimately have the same chemical composition whether they are generated from leaf litter or from BC, and hence undergo the same stabilization processes such as interactions with mineral surfaces and entrapment in pores inaccessible to decomposers. The chief difference between the rate at which this stabilization will occur and that of BC is then the rate of decomposition of BC by the microbial community, which is at least one order of magnitude slower for BC than uncharred organic matter (Baldock and Smernik 2002; Kuzyakov et al. 2009; Lehmann et al. 2009). Black C may be viewed as a stage of plant litter decomposition, its decomposition products undergoing similar processes as those of other forms of organic matter. Forms that appear more “recalcitrant” may be avoided by decomposers because, for example, it is energetically less expensive to choose non-BC and therefore preferable. Differences in the stabilization of metabolites from leaf litter or

BC may arise by the concomitant presence of BC and adsorption reactions on BC surfaces, which may decrease or increase availability to microorganisms (Lehmann et al. 2011). In addition, BC particle surfaces themselves may be oxidized and react with minerals in soils (Brodowski et al. 2006; Chia et al. 2010; Joseph et al. 2010). These processes may lead to their stabilization in soils (Liang et al. 2008) which are different processes than those acting on metabolites.

3.5. Conclusions

Principal component analysis of BC-rich soil microaggregates showed that the major components of soil organic matter were well resolved, spatially distinct and identifiable bio-molecules, such as BC and microbial exudates. We were not able to identify the spectral signature of HS extracts within spatial maps of soil organic matter in microaggregates using NEXAFS and STXM at a spatial resolution of 50 nm. These results agree with more recent data which question HS as an abundant and highly complex component of SOM. Our data also show that the stabilization of microbial metabolites originating from BC may not be fundamentally different from those of other organic additions to soil. As recently suggested, HS extractions should be increasingly scrutinized for their biogeochemical information value. Future research should include stable isotope studies in combination with high-resolution mapping using Nano-SIMS and with compound-specific analyses using GC that unequivocally demonstrate the nature and reactions of decomposition products of BC in soils.

References

Baldock JA, Smernik RJ (2002) Chemical composition and bioavailability of thermally, altered *Pinus resinosa* (Red Pine) wood. Org Geochem 33:1093-1109

Boese J, Osanna A, Jacobsen C, Kirz J (1997) Carbon edge XANES spectroscopy of amino acids and peptides. J Electron Spectros Relat Phenomena 85:9-15

Brodowski S, Rodionov A, Haumaier L, Glaser B, Amelung W (2005) Revised black carbon assessment using benzene polycarboxylic acids. Org Geochem 36:1299-1310

Cheng C, Lehmann J, Engelhard MH (2008) Natural oxidation of black carbon in soils: Changes in molecular form and surface charge along a climosequence. Geochim Cosmochim Acta 72:1598-1610

Cody GD, Ade H, Wirick S, Mitchell GD, Davis A (1998) Determination of chemical-structural changes in vitrinite accompanying luminescence alteration using C-NEXAFS analysis. Org Geochem 28:441-455

Cunha TJF, Novotny EH, Madari BE, Martin-Neto L, Rezende MO d O, Canellas LP, Benites V de M (2009) Spectroscopy characterization of humic acids isolated from Amazonian Dark Earth Soils. In: Woods WI, Teixeira WG, Lehmann J, Steiner C, Winkler-Prins AMGA, Rebellato L (eds) Amazonian Dark Earths, Wim Sombroek's Vision. Springer Science and Business Media, BV, pp 363-372

Glaser B, Haumaier L, Guggenberger G, Zech W (1998) Black carbon in soils: the use of benzenecarboxylic acids as specific markers. Org Geochem 29:811-819

Hammes K, Torn MS, Lapenas AG, Schmidt MWI (2008) Centennial black carbon turnover observed in a Russian steppe soil. Biogeosciences 5:1339-1350

Haumaier L, Zech W (1995) Black carbon-possible source of highly aromatic components of soil humic acids. Org Geochem 23:191-196

Hedges JI, Eglinton G, Hatcher PG, Kirchman DL, Arnosti C, Derenne S, Evershed RP, Kögel-Knabner I, de Leeuw JW, Littke R, Michaelis W, Rullkötter J (2000) The molecularly-uncharacterized component of nonliving organic matter in natural environments. Org Geochem 31:945-958

Heymann K, Lehmann J, Solomon D, Schmidt MWI, Regier T (2011) C 1s K-edge near edge X-ray absorption fine structure (NEXAFS) spectroscopy for characterizing functional group chemistry of black carbon. Org Geochem 42:1055-1064

Hockaday WC, Grannas AM, Kim S, Hatcher PG (2006) Direct molecular evidence for the degradation and mobility of black carbon in soils from ultra high-resolution mass spectral analysis of dissolved organic matter from a fire-impacted forest soil. Org Geochem 37:501-510

Joseph SD, Camps-Arbestain M, Lin Y, Munroe P, Chia CH, Hook J, van Zwieten L, Kimber S, Cowie A, Singh BP, Lehmann J, Foidl N, Smernik RJ, Amonette JE (2010) An investigation into the reactions of biochar in soil. Aust J Soil Res 48:501-515

Kamegawa K, Nishikubo K, Kodama M, Adachi Y, Yoshida H (2002) Oxidative degradation of carbon blacks with nitric acid-II. Formation of water-soluble polynuclear aromatic compounds. Carbon 40:1447-1455

Keiluweit M, Nico PS, Johnson MG, Kleber M (2010) Dynamic molecular structure of plant biomass-derived black carbon. Environ Sci Technol 44:1247-1253

Kelleher BP, Simpson AJ (2006) Humic substances in soils: Are they really chemically distinct? Environ Sci Technol 40:4605-4611

Kinyangi J, Solomon D, Liang B, Lerotic M, Wirick S, Lehmann J (2006) Nanoscale biogeocomplexity of the organo-mineral assemblage in soil: application of STXM microscopy and C 1s-NEXAFS spectroscopy. Soil Sci Soc Am J 70:1708-1718

Kleber M (2010) What is recalcitrant soil organic matter? Environ Chem 7:320-332

Kleber M, Nico PS, Plante A, Filley T, Kramer M, Swanston C, Sollins P (2011) Old and stable soil organic matter is not necessarily chemically recalcitrant: Implications for modeling concepts and temperature sensitivity. Global Change Biol 17:1097-1107

Kumada K (1983) Carbonaceous materials as a possible source of soil humus. Soil Sci Plant Nutr 29:383-386

Kumada K (1985) Elementary composition and adsorption spectra of humic and fulvic acids. Soil Sci Plant Nutr 31:437-448

Kuzyakov Y, Subbotina I, Chen H, Bogomolova I, Xu X (2009) Black carbon decomposition and incorporation into soil microbial biomass estimated by ^{14}C labeling. Soil Biol Biochem 41:210-219

Lehmann J, Brandes J, Fleckenstein H, Jacobsen C, Solomon D, Thieme J (2009) Synchrotron-based near-edge X-ray Spectroscopy of natural organic matter in soils and sediments. In: Senesi N, Xing, B, Huang, PM (eds) Biophysical-Chemical Processes Involving Natural Nonliving Organic Matter in Environmental Systems, IUPAC Series on Biophysico-Chemical Processes in Environmental Systems, Wiley, New Jersey, pp 729-781

Lehmann J, Liang BQ, Solomon D, Lerotic M, Luizão F, Kinyangi J, Schäfer T, Wirick S, Jacobsen C (2005) Near-edge X-ray absorption fine structure (NEXAFS) spectroscopy for mapping nano-scale distribution of organic carbon forms in soil: Application to black carbon particles. Global Biogeochem Cycles 19: GB1013

Lehmann J, Solomon D, Kinyangi J, Dathe L, Wirick S, Jacobsen C (2008) Spatial complexity of soil organic matter forms at nanometer scales. Nature Geosci 1:238-242

Liang B, Lehmann J, Solomon D, Kinyangi J, Grossman J, O'Neill B, Skjemstad JO, Thies J, Luizão FJ, Petersen J, Neves EG (2006) Black Carbon increases cation exchange capacity in soils. Soil Sci Soc Am J 70:1719-1730

Liang B, Lehmann J, Solomon D, Sohi S, Thies JE, Skjemstad JO, Luizão FJ, Engelhard MH, Neves EG, Wirick S (2008) Stability of biomass-derived black carbon in soils.

Geochim Cosmochim Acta 72:6069-6078

Mao JD, Chen N, Cao XY (2010) Characterization of humic substances by advanced solid state NMR spectroscopy: Demonstration of a systematic approach. Org Geochem 42:891-902

Masiello CA, Druffel ERM (1998) Black carbon in deep-sea sediments. Science 280:1911-1913

Nishimura S, Tani M, Fujitake N, Shindo H (2006) Relationship between distribution of charred plant residues and humus composition in chernozemic soils. Pedologist 53:86-93

Plaschke M, Rothe J, Denecke MA, Fanghänel T (2004) Soft X-ray spectromicroscopy of humic acid euporium (III) complication by comparison to model substances. J Elec Spec Rel Pheno 135:53-62

Ravel B, Newville M (2005) Athena, artemis, hephaestus. J Synchr Rad 12:537-541

Richard C, Coelho C, Guyot, G, Shaloiko L, Trubetskoj O, Trubetskaya O (2011) Fluorescence properties of the < 5 kDa molecular size fractions of a soil humic acid. Geoderma 163:24-29

Scheinost AC, Kietzschmar R, Christl I, Jacobsen C (2001) Carbon group chemistry of humic and fulvic acid: a comparison of C 1s NEXAFS and ^{13}C NMR spectroscopies. In: Ghabbour EA, Davies G (eds) Humic Substances: Structures, Models and Functions. Royal Society of Chemistry, Cambridge, UK, pp 39-47

Schmidt MWI, Torn MS, Abiven S, Dittmar T, Guggenberger G, Janssens IA, Kleber M, Kögel-Knabner I, Lehmann J, Manning DAC, Nannipieri P, Rasse DP, Weiner S, Trumbore SE (2011) Persistence of soil organic matter as an ecosystem property. Nature 478:49-56

Schulten HR, Schnitzer M (1993) A state of the art structural concept for humic

substances. Naturwissenschaften 28:311-312

Shindo H (1992) Elemental composition, humus composition and decomposition in soil of charred grassland plants. Soil Sci Plant Nutr 37:651-657

Shindo H (2004) Contribution of charred plant fragments to soil organic carbon in Japanese volcanic ash soils containing black humic acids. Org Geochem 35: 235-241

Shindo H, Higashi T, Matsui Y (1986b) Comparison of humic acids from charred residues of Susuki (Eulalia, *Miscanthus sinensis* A.) and from the A horizons of volcanic ash soils. Soil Sci Plant Nutr 32: 579-586

Shindo H, Honma H (1998) Comparison of humus composition of charred Susuki (Eulalia *Miscanthus sinensis*) plants before and after HNO_3 treatment. Soil Sci Plant Nutr 44:675-678

Shindo H, Honma H (2001) Significance of burning vegetation in the formation of black humic acids in Japanese volcanic ash soils. In: Ghabbour EA, Davies G (eds), Humic Substances: Structures, Models and Functions. Royal Society of Chemistry, Cambridge, pp 297-306

Shindo H, Matsui Y, Higashi T (1986a) A possible source of humic acids in volcanic ash soils in Japan - charred residue of *Miscanthus-sinensis*. Soil Sci 141:84-87

Shindo H, Matsui Y, Higashi T (1986c) Humus composition of charred plant residues. Soil Sci Plant Nutr 32: 475-478

Shindo, H, Miho, Y, Yamamoto, A, Honma, H, Syuntaro, H (2005) $\delta^{[delta]\ 13}C$ values of organic constituents and possible source of humic substances in Japanese volcanic ash soils. Soil Sci 170: 175-182

Shoji S, Nanzyo M, Dahlgren R (1993) Volcanic ash soils: genesis, properties, and utilization. Elsevier Science Publishers BV Amsterdam, The Netherlands.

Shoji T, Jurebayashi T, Yamada I (1990) Growth and chemical composition of Japanese

pampas grass (*Miscanthus sinensis*) with special reference to the formation of dark colored Andisols in Northeastern Japan. Soil Sci Plant Nutr 36:105-120

Solomon D, Lehmann J, Kinyangi J, Amelung W, Lobe I, Ngoze S, Riha S, Pell A, Verchot L, Mbugua D, Skjemstad J, Schäfer T (2007) Long-term impacts of anthropogenic perturbations on dynamics and speciation of organic carbon in tropical forest and subtropical grassland ecosystems. Global Change Biol 13:511-530

Solomon D, Lehmann J, Thies J, Schafer T, Liang B, Kinyangi J, Neves E, Petersen J, Luizão, Skjemstad, J (2007) Molecular signature and sources of biochemical recalcitrance of organic C in Amazonian Dark Earths. Geochimica et Cosmochimica Acta 71: 2285-2298

Solomon D, Lehmann J, Kinyangi J, Liang BQ, Heymann K, Dathe L, Hanley K, Wirick S, Jacobsen C (2009) Carbon (1s) NEXAFS spectroscopy of biogeochemically relevant reference organic compounds. Soil Sci Soc Am J 73:1817-1830

Song G, Novotony E, Hayes MHB, Azevedo E, Bonagambab T (2008) Charcoal and humin fractions in Amazonian Dark Earths. 14th International Conference of International Humic Substance Society, Moscow, Russia

Stevenson FJ (1994) Humus Chemistry: Genesis, Composition Reactions, 2nd ed. John Wiley and Sons, Inc. New York

Sutton R, Sposito G (2005) Molecular structure in soil humic substances: The new view. Environ Sci Technol 39:9009-9015

Swift RS (1996) Organic matter characterization. In: Sparks DL, Bartels JM, Bigham JM (eds) Methods of Soil Analysis. Chemical Methods. Part 3. Agron Monogr 5 ASA, SSSA, Madison, WI, pp 1018-1020

Trompowsky PM, Benites VD, Madari BE, Pimenta AS, Hockaday WC, Hatcher, PG (2005) Characterization of humic like substances obtained by chemical oxidation of

eucalyptus charcoal. Org Geochem 36:1480-1489

Wada (1986) Ando soils in Japan. Kyushu University Press, Fukuoka, Japan

Wada K, Higashi T (1976) The categories of aluminium- and iron-humus complexes in Ando soils determined by selective dissolution. J Soil Sci 27:357-368

Yang Y, Shu L, Wang, X, Xing B, Tao S (2011) Impact of de-ashing humic acid and humin on organic matter structural properties and sorption mechanisms of phenanthrene. Environ Sci Technol 45:3996-4002

4. BLACK CARBON AND MINERAL INTERACTIONS IN SOIL

Abstract

The mechanisms by which black carbon (BC) is chemically stabilized in soils are not well understood. Several studies have found evidence of BC and clay mineral interactions in soils; however, these results are highly complex and may involve numerous mechanisms occurring together. Near-edge X-ray absorption fine-edge spectroscopy (NEXAFS), scanning electron microscopy (SEM) and scanning transmission electron microscopy (STEM) were used to compare BC exposed to water, nitric acid (HNO_3), kaolinite, pyrophyllite, vermiculite and goethite. Nitric acid pretreatment resulted in a highly oxidized surface of BC with a doubling of the proportion of absorption intensity in the carboxylic/carbonyl C region and of the ratio of carboxyl/carbonyl-to-aromatic C of NEXAFS spectra. NEXAFS also indicated that both goethite with hydroxylated, amphoteric surfaces and vermiculite with permanently negative-charged siloxane surfaces caused a 30% increase in the proportion of total absorption intensity in the carboxylic/carbonyl C region, stressing the amphoteric character of BC surfaces. This effect was twice as pronounced for BC that had been pre-treated with HNO_3 (BCO) and strongest for interactions with goethite. Therefore, it is likely that multiple mechanisms such as electrostatic interactions, ligand exchange, electron donor or acid-base reactions play a role in the interaction between BC and clay minerals. High-resolution microscopy revealed 100-nm thick BCO-pyrophyllite interfaces with accumulation of Aluminum (Al) over Silicon (Si) suggesting the importance of small-scale variation in mineral distribution. The reactions in this study took place over a short period of time, demonstrating that BC-mineral interactions can commence quickly and

result in chemical changes to BC.

4.1. Introduction

Soils contain the largest pool of organic carbon (OC) in terrestrial ecosystems and can have a multitude of effects on global carbon (C) budgets and related environmental impacts (IPCC, 2007). The residues of biomass burning, collectively termed black carbon (BC), play an important role in soil biogeochemistry and represent the most stable C pool in soils (Skjemstad et al., 2004; Lehmann et al., 2008). BC stability has been attributed to several proposed mechanisms, including inherent chemical recalcitrance, physical protection and chemical protection within the organo-mineral fraction of soils (Baldock, 2000; Czimczik and Masiello, 2007). Due to the complex nature of BC the abiotic interactions with mineral surfaces are not well understood. Numerous studies have explored associations between organic matter (OM) and minerals in soils (Brodowski et al., 2005; Kleber et al., 2007; Mikutta et al., 2007; Kögel-Knabner et al., 2008), but only a few studies have focused on BC-mineral interactions with respect to their behavior in soils (Brodowski et al., 2005; Brodowski et al., 2006; Chia et al., 2010; Joseph et al., 2010).

BC is often an intrinsic component of highly heterogeneous soil organic matter (SOM) and as such may undergo similar reactions and interactions with mineral pools in soils. Soil organic C (SOC) for example, may be chemically stabilized by the adsorption of C compounds onto clay-mineral surfaces, or by organo-mineral bonds within the clay mineral matrix (Hedges and Oades, 1997; Baldock, 2000; Kaiser and Zech, 2000; Eusterhues et al., 2003; Mikutta et al., 2007; Kögel-Knabner et al., 2008). This strong association of OC with mineral surfaces renders it less susceptible to desorption (Kaiser et al., 2007) and more resistant to biological mineralization (Keil et al., 1994). Since BC

is characterized along a continuum of chemical properties including reactivity (Schmidt and Noack, 2000), soil BC can be significantly oxidized (Brodowski et al., 2005; Cheng et al., 2006a; Cheng et al., 2008a) and may therefore favor chemical interaction with the soil mineral phase. BC surface properties are often in flux according to changes in soil solution chemistry and temperature (Cheng et al., 2008b). Such changes may occur rapidly (Cheng et al., 2006b) or over extended time scales (Cheng et al., 2008a; Nguyen et al., 2009). For these reasons the mechanisms by which BC is chemically stabilized in soils may change over time or with different environmental properties, which has been insufficiently studied to date.

Several studies have found evidence of BC and mineral interactions in soils. Lehmann et al. (2005) detected a large proportion of oxidized (carboxylic and phenolic) C forms as well as adsorbed non-BC on the surface of aged *Terra preta di Indio* BC particles using scanning transmission X-ray microscopy. Brodowski et al. (2005) even found evidence that partially oxidized BC chemically interacted with the mineral phase using scanning electron microscopy (SEM). Joseph et al. (2010) detected numerous interactions between biochar and mineral phases in soils amended with biochar in field trials, and Nguyen et al. (2009) showed presence of Al, Si, and Iron (Fe) on BC surfaces within short periods of time. Chia et al. (2010) were also able to discern interactions between the organic and inorganic phases of torrefied biomass and soil minerals. However, Liang et al. (2008) studied the mineralization rates of *Terra preta di Indio* BC particles from different textured soils and concluded that chemical recalcitrance was a major contributor to BC stability. Also Glaser et al. (2000) found most of the BC in *Terra preta di Indio* soil to be located in the free light fraction which was not contained inside stable aggregates. Therefore, it is not clear what effect interactions between BC surfaces and soil minerals may have on BC stability and what the nature of those interactions may

be. The objective of this study was to investigate changes to BC chemistry upon interaction with common soil minerals under abiotic conditions. We investigated changes at the BC-mineral interface on the micron and sub-micron scale after short-term abiotic mineral interactions.

4.2. Materials and Methods

4.2.1. Sample preparation

Oak shavings (*Quercus* spp.) were carbonized at a temperature of 550ºC using slow pyrolysis (Daisy Reactor, Best Energies, Inc, Cashton, WI, USA). Details of this process have been described elsewhere (Nguyen et al., 2010). The resulting char was ground manually and passed through an 850-µm sieve. The char has a volatile matter of 39%, ash of 0.6%, fixed carbon of 61% (all w/w), total C of 87.9%, no measureable inorganic C, total O of 9%, total H f 2.4%, a molar H/C ratio of 0.32 and a molar O/C ratio of 0.08, a pH (1M KCl) of 8, potential CEC (at pH 7) 126-147 mmolv kg^{-1} (Enders et al., 2012). A portion of the char was refluxed with a 50% nitric acid solution for 2 hours, cooled, rinsed 10 times with deionized water and air-dried. The starting material char will be referred to as BC and the acid treated char will be referred to as BCO for the purposes of this manuscript.

Three common soil phyllosilicates (vermiculite, kaolinite and pyrophyllite) and an iron oxide (goethite) were used in order to compare mineral surfaces with different surface characteristics. Three major types of functional surface sites may be distinguished among these minerals, offering different bonding possibilities to BC: (1) surfaces inhabited by single coordinated hydroxyl groups (goethite); (2) siloxane surfaces with permanent negative layer charge due to isomorphic substitution (vermiculite); and (3)

siloxane surfaces without layer charge (~neutral) which occurs in both 2:1 layer type (pyrophyllite) and in 1:1 mineral (kaolinite) (Kleber et al., 2007). Goethite has therefore highly reactive surfaces with positive charges at low pH, vermiculite is characterized by a permanent negative charge, kaolinite by a dual hydroxyl and siloxane surface and pyrophyllite by a neutral siloxane surface and therefore the least reactive (Mikutta et al., 2007). The minerals were prepared as follows: geothite (α-FeOOH) was prepared by adjusting 0.5 M $FeCl_3$ to pH 12 by addition of 5 M NaOH (Atkinson, 1967). The suspension was aged for 48 hours at 328 K, washed with deionized water, and dialyzed (Sigma Aldrich D9527 cellulose dialysis tubing M.W. 12,400) until the electric conductivity was <40 μS cm^{-1}. The goethite was then lyophilized and sieved to a particle size of <200 μm. X-ray diffraction (Scintag Theta-Theta X-ray diffractometer, Scintag Inc., Cupertino, CA (currently Thermo Scientific)) was used to confirm the structure of goethite. Pyrophyllite and vermiculite were obtained as raw minerals (Wards Natural Science, Rochester, NY) and kaolinite was purchased as Kaolin powder (Fischer Scientific, Pittsburgh, PA). To remove carbonates and organic matter the minerals were treated with dilute HCl (pH 5), followed by 2 wt % NaOCl. After rinsing three times with deionized water, the Stoke's equivalent <2 μm fraction was obtained by sedimentation. The minerals were then converted to the Na form by washing with 1 M NaCl (1/5 w/v), rinsed three times with deionized water and dialyzed until the electrical conductivity was <40μS cm^{-1}. The minerals were lyophilized and sieved to a particle size of <200 μm.

Mineral solutions were made at a concentration of 100 mg L^{-1} in a stock solution of 4 μM mercury chloride ($HgCl_2$) to inhibit the growth of bacteria during mixing. Mineral solutions were adjusted to pH 4 using 0.1 M HCl, dropwise until the pH was stable for 10 minutes. Mineral solutions were stirred constantly until added to vials. BC-mineral mixtures were made by weighing 100 mg BC into 8-mL glass vials and adding

mineral solution so as to leave minimal headspace in the vial, with two replicates included for each sample. The mixtures were then shaken at 60ºC in a rotary shaker (Orbit Environ, Lab-Line Instrument Inc., IL, U.S.) for 14 days. Prior studies measuring sorption of dissolved organic matter to minerals indicated an equilibrium time of at least 24 hours (Mikutta et al., 2007; Ohno et al., 2007). Other studies indicated an appropriate equilibrium time for sorption of phenanthrene to BC at 5 d (Pan, 2011). In preliminary experiments, samples were equilibrated for 48 hours, 7 days and 14 days. Only samples shaken for 14 d showed measurable changes in NEXAFS spectra, and the samples shaken for 24 hours or 7 d did not. After shaking, vials were opened and placed in a 60ºC oven to dry until constant weight.

In preparation for NEXAFS analysis, all samples were mixed with C-free nanopure water (1 mg per 2 mL water) in 5-mL Eppendorf vials. The vials were lowered briefly into an ultrasound bath in order to achieve homogeneous wetting of the samples. Using a pipette, approximately 1 mL of the sample solution was deposited onto gold coated silicon wafers and air-dried. The wafers were prepared by thermally evaporating an optically opaque layer of pure gold onto the unpolished side of commercially available Si wafers. The thermal evaporation used a 0.25-mm thick W filament that was wetted with Au (Lesker, 99.9% pure). The deposition was done at 10^{-5} Torr and once prepared, the substrates were left under vacuum until shortly before the sample preparation and subsequent NEXAFS measurements.

For scanning electron microscope (SEM) and scanning transmission electron microscope analysis (STEM), approximately 20 particles of each sample were randomly isolated. The particles were mounted in Spurr's resin (10 g vinylcyclohexane dioxide, 6 g diglycidyl ether of polypropylene glycol, 26 g nonenyl succinic anhydride, and 0.3 g diamethylamine ethanol). The resin mixture was placed in an oven at 60ºC to cure for 2

days. Cross-sections of only the BCO-mineral samples (due to constraints on instrument availability) were prepared by grinding the mounted samples with a grade 800 grinding paper for 5 min followed by a grade 1200 grinding paper for 5 min. The ground samples were then polished with a 3-µm diamond polish followed by 1-µm polishing. A 25-nm C coating was applied to the resin [Edwards Auto 306 evaporator (Edwards, Tewksbury, MA)] to make it electronically conductive so that the sample did not affect the beam charging.

4.2.2. Sample measurements

C (1s) NEXAFS spectra were obtained on beamline 11ID-1 at the Canadian Light Source (CLS) located at the University of Saskatchewan, Saskatoon, Canada. The beamline is equipped with a Spherical Grating Monochromator (SGM) designed for high resolution soft X-ray spectroscopy (Regier et al., 2007). Details of this methodology have been described previously in great detail (Heymann et al., 2011). All samples were measured in duplicate to ensure consistency.

SEM microprobe analysis was used to examine each polished BCO-mineral mixture. The polished mounts containing the cross-sectioned samples were fastened to the SEM sample holder using carbon tape. The particles were examined using a JEOL 8900 microprobe (JEOL Ltd., Tokyo Japan) fitted with an energy X-ray dispersive spectrometry (EDS) detector. Distinctive phases were identified and analysis of the relative concentration of different elements was recorded using EDS.

The mounted and polished sample of pyrophyllite (only one treatment due to limited instrument availability) was placed into a FEI Strata 400 STEM focused ion beam (FIB) microscope (FEI Company, Hillsboro, OR, USA). A layer of platinum was

deposited on the region of interest (ROI) to protect it from damage by the ion beam. The area around the ROI was then milled away using a 30 kV ion beam. A high current beam (6500 pA) was used to mill away the outer region and the beam current was slowly decreased from 6500 pA to a final current of 70 pA as the milled region became closer to the electron transparent section. The final TEM specimen had an approximate thickness of 100-150 nm. The TEM specimen was freed from the bulk sample and a micromanipulator was used to 'lift-out' the specimen from the trench created by milling. The final TEM specimen was placed on a carbon-coated copper mesh TEM grid (Giannuzzi and Stevie, 1999) and placed into a Philips (Amsterdam, The Netherlands) CM200 field emission gun TEM. This specimen was then examined using a FEI T12 Spirit TEM STEM (FEI Company, Hillsboro, OR, USA) to which an electron energy loss spectroscopy (EELS) detector was attached. Given the heterogeneous nature of the sample, STEM examination of the cross section was performed for over 20 different regions.

4.2.3. Analysis

For NEXAFS data, peak resonances with specific bonding environments were assigned based on the spectral signatures of pure chemical standards representative of specific functional groups (Solomon et al., 2009). In order to compare the chemistry of the different samples in a semi-quantitative way, a least-squares fitting scheme was applied to the normalized NEXAFS spectra in the range of 280 to 310 eV. The scheme was based on eight Gaussians curves (labeled "G-1", etc.) following the procedure suggested by Scheinost et al. (2001), with additional bands to account for substituted aryl C (G3) and an additional carbonyl group (G8) (Liang et al., 2008). Further detail of the peak assignments used in this study can be found in Heymann et al. (2011). An

arctangent function at 290 eV was used to model the ionization step. The full width at half maximum of the bands was set at 0.4 ± 0.2 eV, while the amplitude was floated during the fit. Deconvolution was performed by resolving spectra into individual arctangent and Gaussian curve components (G) using the ATHENA 0.8.052 software (Ravel and Newville, 2005). software. Spectral regions represented by Gaussian curves were described as being generally attributed to the following functional groups: overall aromatic type C was represented by the sum of the [G1+G2+G3] peaks; aromatic C with side chain substituent (such as phenolic C) by the G4 peak; alkyl C by the G5 peak; carboxylic/carbonyl C by the G6 peak, and O-alkyl C by the sum of [G7+G8] peaks (Lehmann et al., 2009). The application of a Gaussian fitting procedure for the extraction of semi-quantitative information is validated by the diversity of C species in these samples. Further details of the curve fitting procedure can be found in Heymann et al. (2011). Absorption intensity and transition intensity values (percentages) reflect relative concentrations of functional groups, since absolute concentration based on peak intensity cannot be determined with NEXAFS according to our methods. In order to compare the changes in relative concentrations of aromatic and carboxylic C for the various treatments, we used a ratio of aromatic C/ carboxylic C peak heights at maximum. These values were used to compare the change which each sample underwent as a result of treatment, since the aromatic regions tended to decrease as the carboxylic regions increased.

4.3. Results

4.3.1. NEXAFS

NEXAFS spectra of all BC and BCO treatments revealed a broad, well resolved C

1s-$\pi^*_{C=C}$ transition at 285 eV and a small C 1s-$\pi^*_{C=C}$ (carboxylic type C) transition near 288.5 eV (Fig. 4.1).

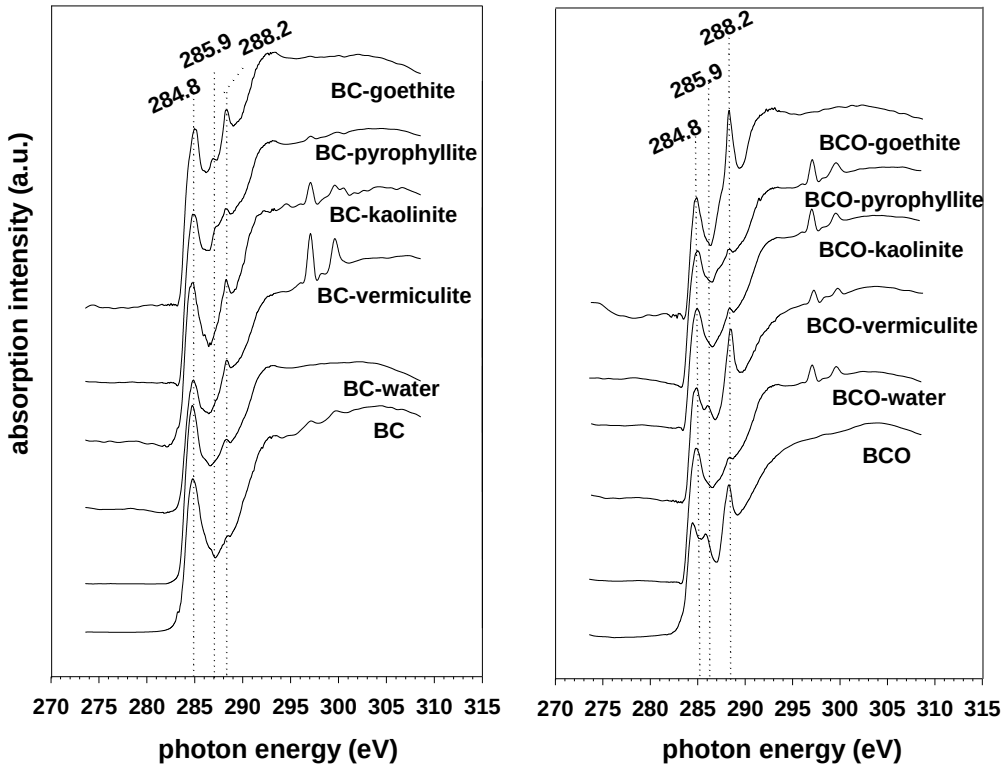

Figure 4.1. NEXAFS spectra of (a) BC mixed with water and minerals (BC), and (b) acid treated char (BCO) mixed with water and mineral mixtures.

A small shoulder was observed at 285.9 eV for BCO and BCO-Vermiculite. NEXAFS deconvolution values indicated that 62% of total absorption intensity was present in the aromatic C region for BC, and that water and mineral treatments decreased this relative proportion by around 35% to 40-42% (Table 1).

Table 4.1. Functional group distribution of unoxidized (BC) and oxidized (BCO) BC and mixtures with water or water together with different clay minerals using NEXAFS.

	Aromatic	Phenolic	Aliphatic	Carboxylic	O-alkyl
			(%)		
BC	62	10	9	10	9
BC water	42	18	10	13	17
BC vermiculite	40	18	11	17	15
BC kaolinite	41	17	10	13	19
BC pyrophyllite	40	20	7	15	19
BC goethite	40	11	12	16	20
BCO	49	5	13	21	12
BCO water	41	19	10	14	15
BCO vermiculite	39	12	13	23	14
BCO kaolinite	40	18	10	13	19
BCO pyrophyllite	44	11	13	14	17
BCO goethite	33	8	13	25	21

The acid treatment decreased the proportion of total absorption intensity in the aromatic C region by around 20% and more than doubled the proportion in the carboxylic C region from 10% to 21% of total absorption intensity. BC-water and BC-mineral

treatments increased the amount of absorption intensity in the phenolic C region of BC by 80-100% with the exception of goethite which did not show any change. The proportion of total intensity present in the aliphatic C region did not change more than 30% for any treatment. The carboxylic/carbonyl type C region increased by 70% (BC-vermiculite) and 60% (BC-goethite) compared with BC, but only by 23-25% when compared with BC-water. Other transition regions showed little change compared with the starting material.

For the oxidized BCs, the largest decrease in the aromatic C region was observed for BCO-goethite by 32% compared to BCO alone (from 49% to 33%) or by 20% compared to BCO-water (from 41% to 33%) (Table 4-1). The transition representing phenolic type C increased 1.6 to 4-fold with the largest increases observed for BCO-water and BCO-kaolinite compared with BCO. There were few observable changes (less than 30% change) in the aliphatic type C transitions according to the spectral deconvolution. Differences in the carboxylic type C region were observed for BCO-kaolinite (38% decrease), BCO-water and BCO-pyrophyllite (both 29% decrease), compared with the starting material. Goethite and vermiculite did not reveal any notable changes in this region compared with the starting material. However, compared with BCO-water they showed an increase by 64-79% from 14% to 23-25% of total absorbance. When compared with the BCO-water, pyrophyllite and kaolinite were highly similar with regard to the proportion of overall absorption intensity present in the carboxylic/carbonyl C region. Within the transition representing O-alkyl type C, the largest change was between BCO-water (15%) and BCO-goethite (21%) with a 40% increase in overall absorption intensity.

The carboxylic/carbonyl-to-aromatic C peak height ratios were highest for BCO-goethite (1.73) and BCO-vermiculite (1.54) (Table 4.2).

Table 4.2.

Ratio of peak heights of COOH-to-aromatic C obtained by NEXAFS of BC with (BCO) or without (BC) oxidation by nitric acid, and incubation with water or water together with different clay minerals.

	No treatment	Water	Vermiculite	Kaolinite	Pyrophyllite	Goethite
BC	0.63	0.81	1.15	1.02	1.03	1.15
BCO	1.41	0.93	1.54	1.00	1.02	1.73

The lowest values were observed for BC (0.63) and BC-water (0.81). Oxidation (BCO 1.41) caused more than a doubling compared to the starting material (BC 0.63). The values for kaolinite and pyrophyllite were around 1, only a slight increase from BC-water alone (0.8). BCO-kaolinite and BCO-pyrophyllite values were also around 1.0, similar to BCO-water (0.93). BC-vermiculite and BC-goethite showed a 42% increase compared to CR-water. Addition of vermiculite and especially goethite to oxidized BCO-water (0.93) caused a pronounced increase by 66% and 86%, respectively.

Changes in peak position were observed among BC-mixtures only, with the peak representing carboxylic/carbonyl shifting approximately - 0.3 eV, from 288.6 eV (BC) to 288.38 eV for BC mixed with kaolinite, goethite and pyrophyllite (Table 4-3).

Table 4.3. Peak positions of aromatic and carboxyl/carbonyl C in unoxidized (BC) and oxidized (BCO) BC and mixtures with water or water together with different clay minerals using NEXAFS.

	Aromatic (eV)	Carboxyl/carbonyl (eV)
BC	284.8	288.6
BC water	284.8	288.3
BC vermiculite	284.9	288.4
BC kaolinite	284.8	288.3
BC pyrophyllite	284.8	288.3
BC goethite	284.8	288.3
BCO	284.8	288.3
BCO water	284.9	288.4
BCO vermiculite	284.7	288.3
BCO kaolinite	284.9	288.4
BCO pyrophyllite	284.8	288.4
BCO goethite	284.9	288.3

4.3.2. SEM

SEM analyses of the BC-mineral mixtures focused on capturing distinct interfaces between BC and mineral phases based on a preliminary analysis of observed regions. Whiter regions indicated mineral phases and darker regions indicated C-rich phases (Fig. 4.2).

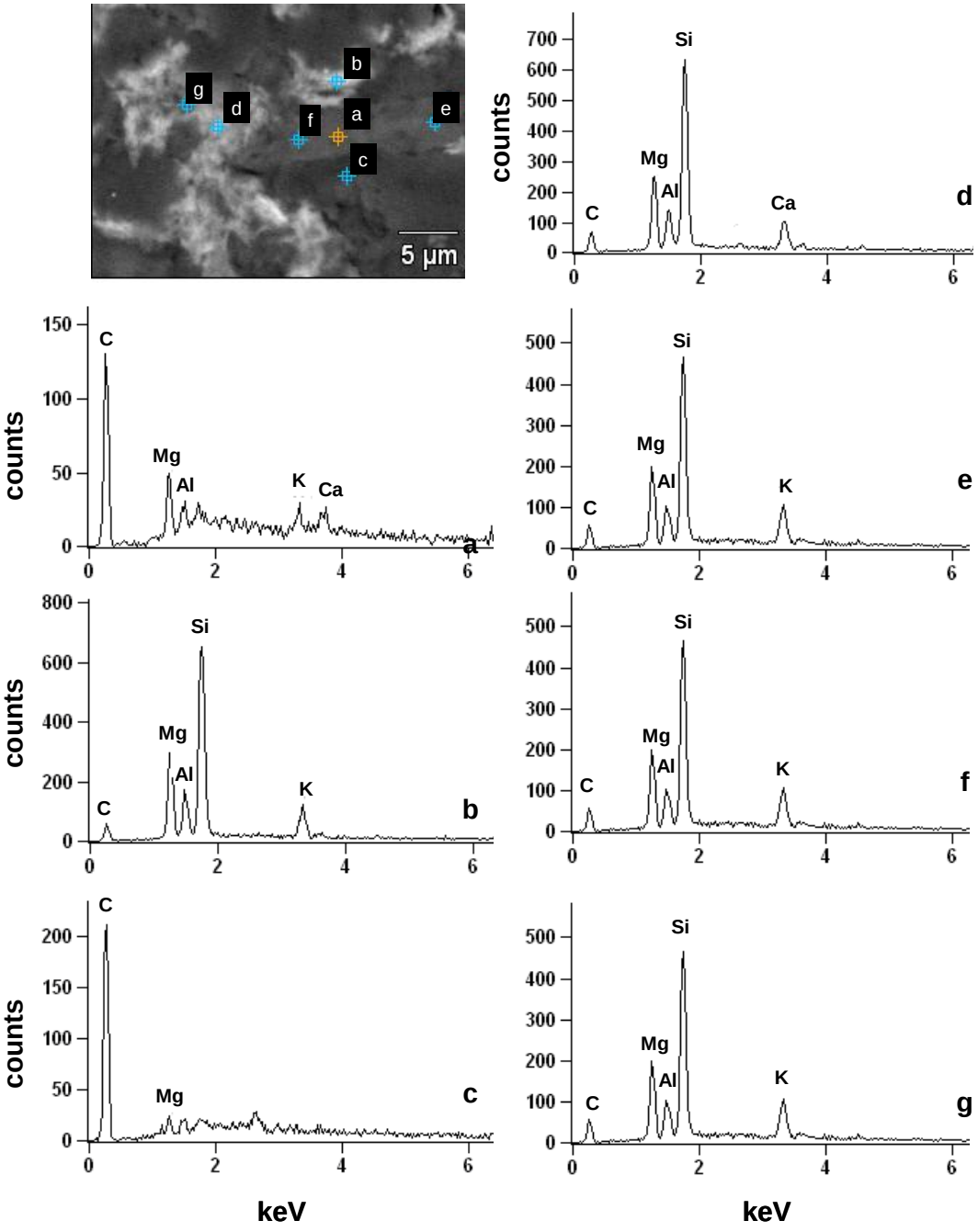

Figure 4.2. SEM image and point spectra of acid treated BCO mixed with vermiculite.

For most samples we observed three distinct regions, the third being a gray region between the predominantly white mineral and dark C regions.

We examined BCO-vermiculite at 4000x magnification (Fig. 4.2) and took seven different point spectra due to the heterogeneity of the region. Points (a) and (c) were rich in C and poor in mineral elements. Points (b), (d) and (f) were rich in mineral elements but poor in C. Point (b), however, revealed similar proportions of C and the mineral elements Mg and Si.

SEM analysis of BCO-kaolinite at 5000x magnification revealed the simultaneous presence of Al, Si and C both at multiple measured points (Fig. 4.3).

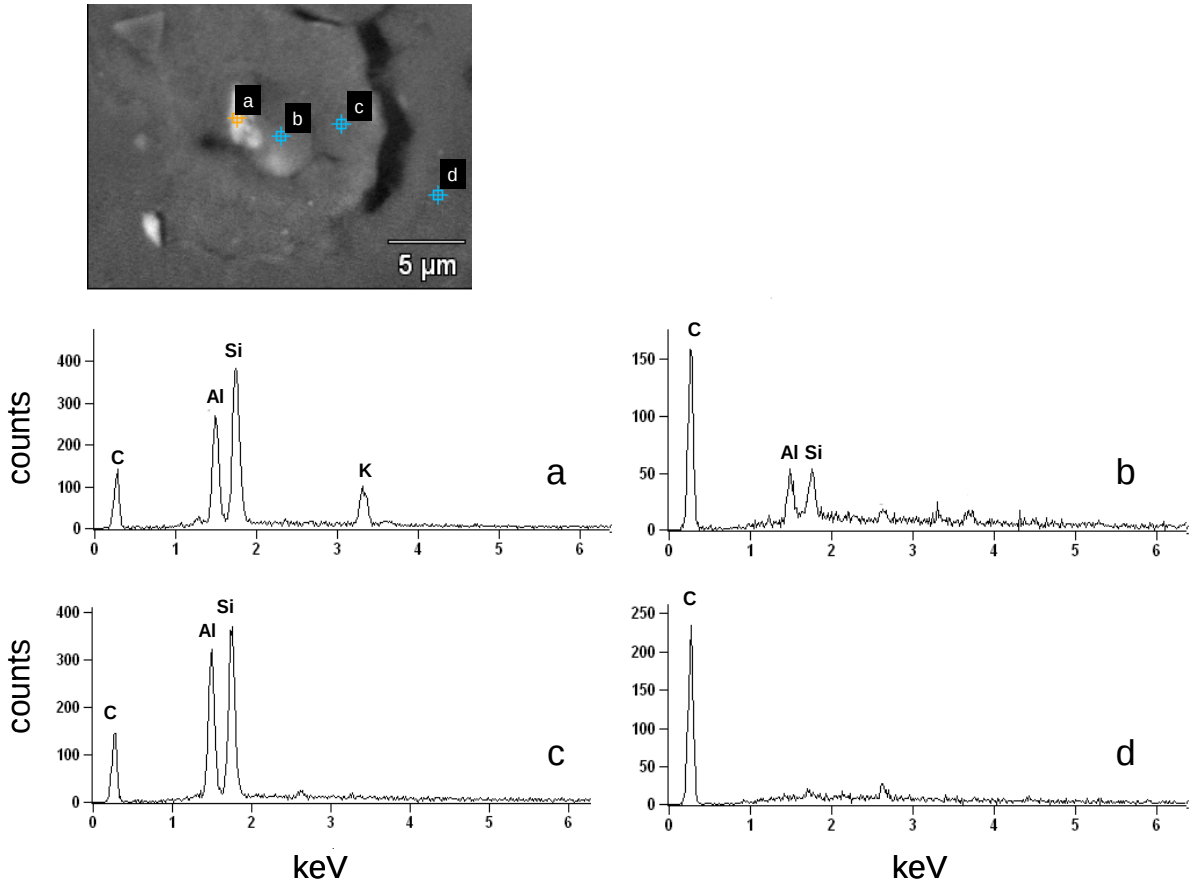

Figure 4.3. SEM image and point spectra of acid treated BCO mixed with kaolinite.

We observed that the lightest and grey areas were mixtures of Al, Si and C. Lighter areas contained mostly Al and Si with some C (points a to c), and the darkest area (d) contained only C. Pyrophyllite was examined at 4000 times magnification (Fig. 4.4).

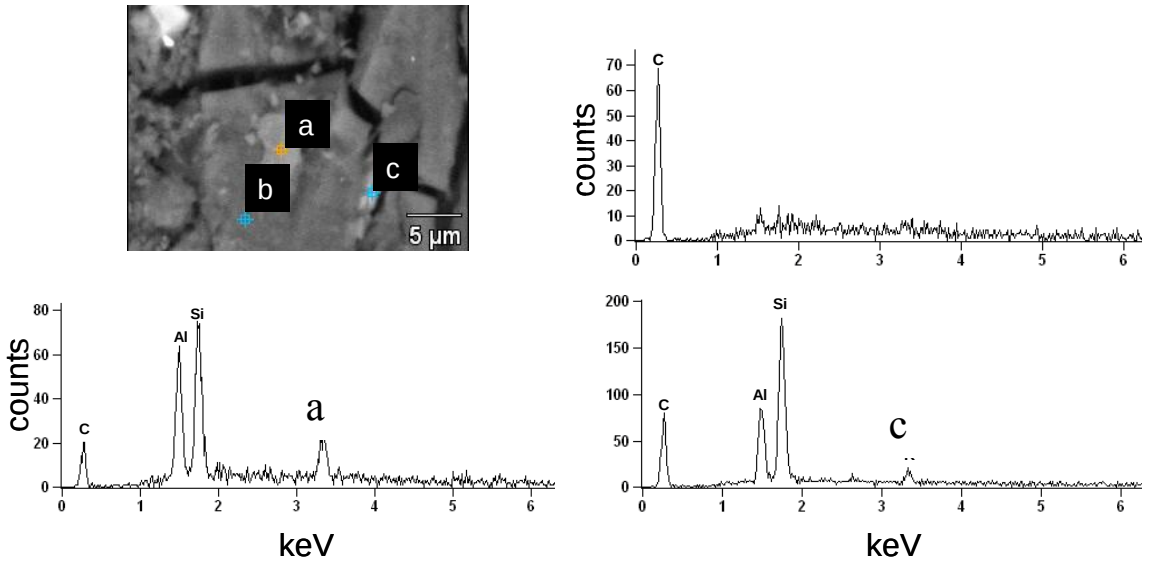

Figure 4.4. SEM image and point spectra of acid treated BCO mixed with pyrophyllite.

Point (a) was rich in both Al and Si, detected along with the presence of C and potassium (K). Point (b) was rich in C, with no other elements detected. Point (c) was rich in Si, with Al and C also being detected simultaneously.

We took three point spectra across a 5-μm region of the BCO-goethite sample at 5000x magnification (Fig. 4.5).

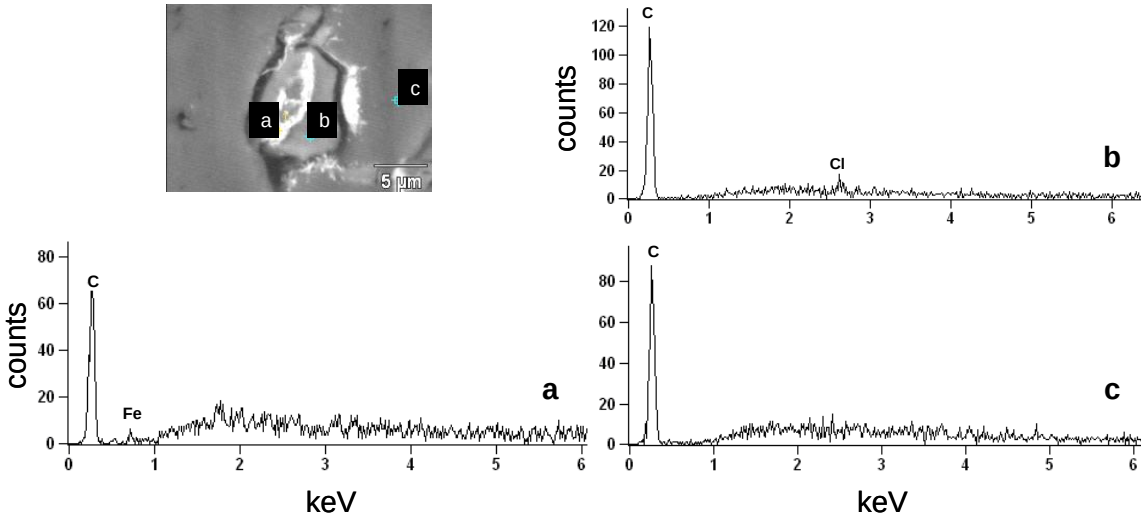

Figure 4.5. SEM image and point spectra of acid treated BCO mixed with goethite.

Some Fe was detected at points (a) and (b) along with high counts of C, but we were not able to find a region with a high concentration of Fe.

4.3.3. STEM

STEM analysis of four organo-mineral interfaces (Fig. 4.6) of BCO-pyrophyllite produced consistent distribution of C, Si, O and Al across the transition from ACR to the mineral.

Figure 4.6. Scanning transmission electron microscopy image of four interfaces of acid treated BC (BCO) mixed with pyrophyllite. The red boxes indicate a region on the BCO surface where Al contents increased in relation to Si.

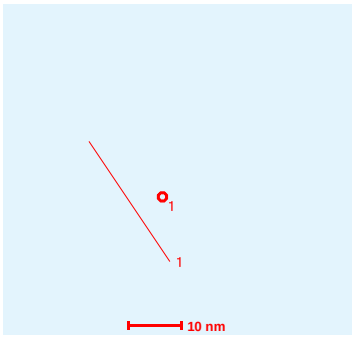
1
1
10 nm

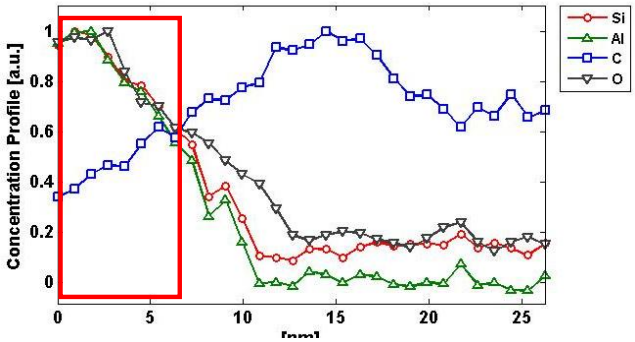
Concentration Profile [a.u.]
[nm]
Si
Al
C
O

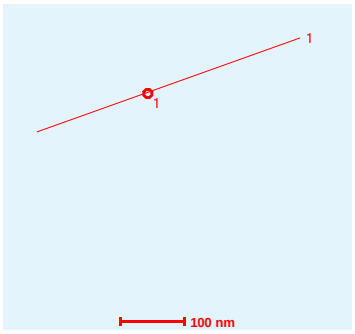
1
1
100 nm

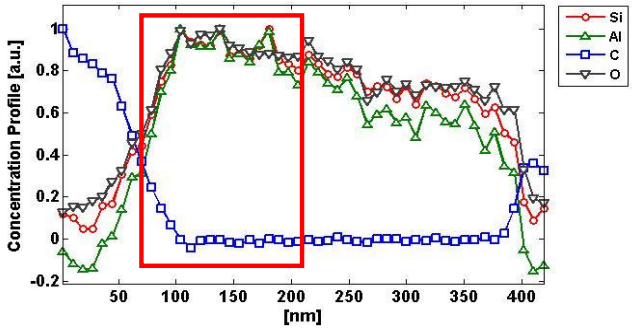
Concentration Profile [a.u.]
[nm]
Si
Al
C
O

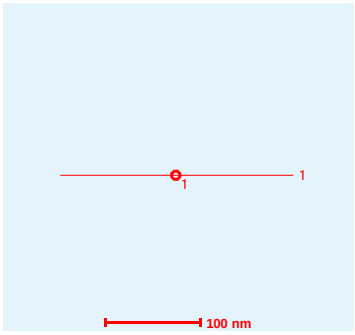
1
1
100 nm

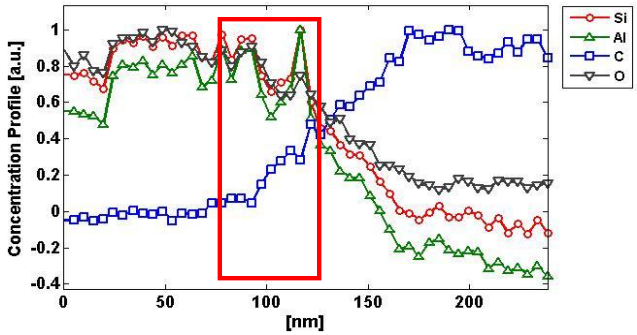
Concentration Profile [a.u.]
[nm]
Si
Al
C
O

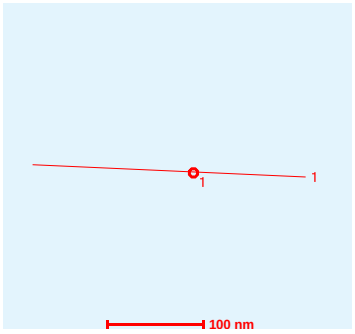
1
1
100 nm

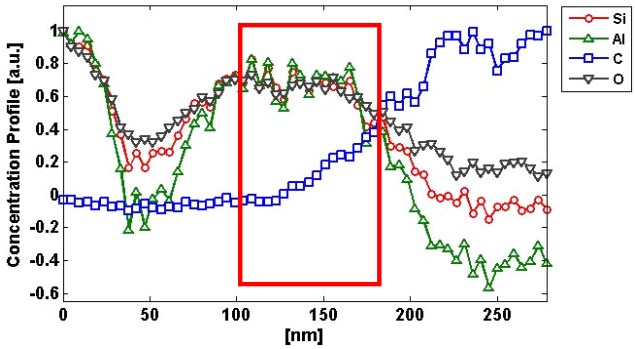
Concentration Profile [a.u.]
[nm]
Si
Al
C
O

The transition between C and mineral was gradual rather than sharp, which suggested that elements formed a highly heterogeneous mixture. In the organic phase as well at a distance from the BCO, Si dominated over Al. However, 50-100 nm from the BCO surface (approximately where C contents were 50% of maximum amounts within the BCO), Al concentrations increased in comparison to Si. Oxygen contents were greater in the mineral phase, but increased in comparison to Si and Al within the BCO.

4.4. Discussion

4.4.1. Oxidation of black carbon

BC produced at 550°C possesses a range of acid and base surface functional groups, and exhibits high surface area with high pH (Joseph, 2010). Nitric acid oxidation (BC compared with BCO) increased the proportion of absorption intensity in the region representing O-containing functional groups such as carboxylic/carbonyl type C. Proportionally, transitions representing aromatic and phenolic type C decreased as a result of oxidation. Our observations are in agreement with a previous study (Moreno-Castilla, 2000) which observed an increase in the concentration of O-containing functional groups on the surfaces of activated carbon particles as a result of nitric acid oxidation. The characteristics of oxidized BC in soils have also been documented by Cheng et al. (2008a) who observed that aged BC (130 years) was higher in O and lower in C than fresh BC, and that aged BC was higher in carboxylic and phenolic functional groups. The additional peak at 285.9 eV in BCO resembled NEXAFS spectra of well oxidized (aged) BC particles separated from anthropogenic soils in previous studies (Lehmann et al., 2005; Liang et al., 2006).

We observed that water alone had an oxidizing effect on BC, regardless of

minerals also present in solution. Shaking the BC with water resulted in an increase in the proportion of total spectral absorption intensity for oxygen substituted C regions such as the phenolic, carboxylic and O-alkyl regions. The oxidizing properties of water may be important to understanding the pathways for organic and mineral phase transactions in soils. Similar to mineral weathering, water plays a major role in BC chemistry and may initiate abiotic oxidation processes (Cheng et al., 2006a; Joseph et al., 2010). Interaction of BCO surfaces with water neutralized or reversed the effects of nitric acid oxidation. This was expected, since nitric acid likely increased the proportion of total adsorption intensity in the carboxylic region; therefore we would expect interaction with water to result in the dissociation of those acid groups in water (since water acts as a base). Soil solution would likely have more complex interactions due to the number of ions present in solution.

4.4.2 Interaction of black carbon with minerals

Goethite and vermiculite had profound effects on the functional group distribution of the oxidized BC, increasing the proportion of total absorption intensity in the carboxylic/carbonyl C region. In the case of unoxidized BC, the lack of significant interaction can be explained by the characteristics of new BC, which possessed low CEC and likely some positive surface charge at the low pH used in this study (Cheng et al., 2008a). For BC, the lack of interaction with pyrophyllite may have been caused by repulsion forces between the surface of BC and the neutral planes of pyrophyllite. For BC-kaolinite, the surface charge of the BC may have been too low while that of the mineral is understood to be heterogeneous (Ma and Eggleton, 1999) so it is possible that the repulsion forces between the BC and mineral were too great to result in any measureable change to the BC. BC interactions with vermiculite may be explained by

possible electrostatic interactions between the functional groups of BC and surface charge sites of the clay mineral, or by electron donor-acceptor reactions where the aromatic groups of BC act as electron acceptors and clay siloxane oxygen acts as an electron donor. The mineral surface is dominated by negatively charged sites arising from isomorphic substitution, but has a few variably charged sites which could be positive or negative (Zhang et al., 2010).

Other researchers such as Brodowski et al. (2005) observed that BC particles spatially associate with mineral matter and that small BC particles bind to minerals and small mineral particles bind to large BC particles. Analyses of the density fractionation of *Terra Preta* soils by Glaser et al. (2000) showed that BC was present mostly in the light fractions, indicating that its refractory nature and not chemical stabilization determined its longevity. However, BC was also found in Fe and Al oxide plaques on mineral surfaces, and Liang et al. (2008) found BC mostly in the heavy soil fraction of these same soils, trapped in Fe and Al plaques but not necessarily chemically associated. We can now show that changes to BC are linked to organo-mineral interactions in soils.

Strong protection of organic matter has been correlated with the presence of hydroxylated mineral phases in acidic soil environments. For example, chemically stable OM has been positively correlated with the Fe oxides and/or clay concentration in soils (Eusterhues et al., 2003), while Kaiser and Guggenberger (2003) demonstrated that goethite interacts strongly with the carboxyl and aromatic functional groups of organic C. At low pH where goethite carries a positive charge (such as in our experiment) it has been shown that for fulvic acid extracts, carboxylic groups in solution can be deprotonated and thus bound as anions to goethite (Gu et al., 1995; Evanko and Dzombak, 1998). Kleber et al. (2007) hypothesized interactions between BC and organic matter and/or minerals in soil as surface hydrophobic and hydrophilic interactions

involving direct electrostatic interactions, H bonding, cation bridging and ligand exchange reactions (Yariv and Cross, 2002). It is therefore not surprising that goethite was found to induce the greatest changes in BC functional group composition among the different minerals studied here. Mikutta et al. (2007) showed that goethite sorbed OM by innersphere complexation (ligand exchange), and observed that in acidic conditions goethite exhibited larger affinity and capacity to sorb OM and larger selectivity for aromatic moieties compared with phyllosilicates. This agrees with our finding that goethite had the strongest effect on BC functional group composition.

The peak position changes were only observed for BC, not for BCO. This indicates that interactions with minerals likely involved ligand exchange or H bonding rather than electrostatic adsorption that would not result in a pronounced shift in energy positions. The demonstrated interactions between mineral surfaces and BC therefore go beyond spatial association, and may indicate stabilization of BC through chemical reactions or adsorption. Whether this mechanism is similarly or more important in reducing mineralization of BC as is known for non-BC materials (Schmidt et al., 2011), is unclear.

4.4.3. Chemical changes over time

The short duration of the experiment and the low temperature at which the reactions occurred demonstrates that changes to BC can occur quickly upon interaction with minerals. In comparison, Chia et al. (2010) observed the formation of an organo-mineral phase in a mixture of BC and mineral matter exposed to high temperatures. It was hypothesized that higher temperatures may have catalyzed the breakdown of biomass to form liquid and gas, which then recondensed on or in interplanar spaces of clay particles. Rather than use heat or pressure to initiate reactions which normally occur on

longer geological time scales, we altered the surface of the BC to mimic an aged, well oxidized surface. Our results suggest that the chemical reactions between BC and mineral fraction happen relatively quickly on a geological time scale, and confirm observations that BC undergoes fairly rapid chemical changes upon deposition as shown by Nguyen et al. (2009).

4.4.4. Thickness of the BC-mineral interface

The SEM and STEM analyses may indicate a gradual change from pure BC material to pure mineral. According to the STEM data, the thickness of the BC-pyrophyllite interface is about 100 nm, estimated from maximum to minimum C contents. This could accommodate dozens of phyllosilicate layers which have an approximate spacing of 1 nm (Barton and Karathanasis, 2002). However, at the periphery of the BCO, the ratio of Al to Si is greater than at points close to the interface, suggesting that more Al accumulated relative to Si near BC surfaces. Such a finding may indicate that free Al may preferentially interact with BC surfaces compared to pyrophyllite which may be electrostatically sorbed to BC and did not appear to change the functional group distribution according to the NEXAFS data. The association of Al with the acidic aromatic components of Australian podzols has been observed by Skjemstad (1992), as well as by Wada (1985) in Japanese Andisols, and has been invoked as an explanation of their ability to stabilize large amounts of OC. NEXAFS studies of SOC-mineral associations are limited; however, Wan et al. (2007) observed that SOC coatings on mineral grains had C NEXAFS with peaks at 286.7 eV (phenolic) and 288.2-288.5 eV (peptidic, carboxylic C), similar to what we observed in this study. No information is available for the other studied minerals.

A confounding factor of the STEM analysis may be the inevitable thickness of the

thin section which was in our case about 100-150 nm. If the interface was not positioned exactly perpendicular to the cut surface, the interface would appear to be thicker than it actually is. This artifact is more likely to occur than not, and could lead to considerable overestimation of the interface dimension. The observed interface thickness of about 100 nm is therefore a conservative upper limit and is likely to be much smaller. Three-dimensional observation may help to arrive at a more precise estimate.

4.5. Conclusions

The stabilization of organic matter by interaction with mineral matrices is a crucial factor in its preservation. Short term changes to BC functional group chemistry as a result of oxidation were already known, but significant changes upon interaction with minerals were only suspected. In this study we were able to demonstrate that the previously known spatial associations of minerals with BC are actually chemical interactions. It is likely that multiple mechanisms such as electrostatic interactions, ligand exchange, electron donor or acid-base reactions play a role in the interaction between BC and clay minerals. Future research should focus on short-term interactions, as well as the impact of aging on BC-mineral associations since surface changes may penetrate BC over time. In addition, three-dimensional mapping of the organo-mineral interface is needed to quantify its thickness.

References

Atkinson, R.J., Posner, A.M. and Quirk, J.P., 1967. Adsorption of potential-determining ions at the ferric oxide-aqueous electrolyte interface. J. Phys. Chem. 71, 550-558.

Baldock, J.A., Skjemstad, J.O., 2000. Role of the soil matrix and minerals in protecting

natural organic materials against biological attack. Org. Geochem. 31, 697-710.
Barton CD and Karathanasis AD, 2002. Clay minerals. In: Lal R (ed.) Encyclopedia of Soil Science. Marcel Dekker, NY, pp 187-192.
Brodowski, S., Amelung, W., Haumaier, L., Abetz, C., Zech, W., 2005. Morphological and chemical properties of black carbon in physical soil fractions as revealed by scanning electron microscopy and energy-dispersive X-ray spectroscopy. Geoderma 128, 116-129.
Brodowski, S., John, B., Flessa, H., Amelung, W., 2006. Aggregate-occluded black carbon in soil. Eur. J. Soil Sci. 57, 539-546.
Cheng, C.H., Lehmann, J., Thies, J.E., Burton, S.D., Engelhard, M.H., 2006a. Oxidation of black carbon by biotic and abiotic processes. Org. Geochem. 37, 1477-1488.
Cheng, Y., Lee, S.C., Ho, K.F., Wang, Y.Q., Cao, J.J., Chow, J.C., Watson, J.G., 2006b. Black carbon measurement in a coastal area of south China. J. Geophys. Res.-Atmospheres 111, D12310.
Cheng, C.H., Lehmann, J., Engelhard, M.H., 2008a. Natural oxidation of black carbon in soils: Changes in molecular form and surface charge along a climosequence. Geochim. Cosmochim. Acta 72, 1598-1610.
Cheng, C.H., Lehmann, J., Thies, J.E., Burton, S.D., 2008b. Stability of black carbon in soils across a climatic gradient. J. Geophys. Res.-Biogeosciences 113, G02027.
Chia, C.H., Munroe, P., Joseph, S., Lina, Y., 2010. Microscopic characterisation of synthetic *Terra Preta*. Austr. J. Soil Res. 48, 593-605.
Czimczik, C.I., Masiello, C.A., 2007. Controls on black carbon storage in soils. Global Biogeochem. Cycles 21, GB3005.
Enders, A., Lehmann, J., 2012. Comparison of Wet-Digestion and Dry-Ashing Methods for Total Elemental Analysis of Biochar. Comm. Soil Sci. Plant Anal., 43, 1042-1052.
Enders, 2012 Comparison of Wet-Digestion and Dry-Ashing Methods for Total

Evanko, C.R. and Dzombak, D.A., 1998. Surface Complexation Modeling of Organic Acid Sorption to Goethite. J. Coll. Interface Sci., 214, 189-206.

Eusterhues, K., Rumpel, C., Kleber, M., Kogel-Knabner, I., 2003. Stabilisation of soil organic matter by interactions with minerals as revealed by mineral dissolution and oxidative degradation. Org. Geochem. 34, 1591-1600.

Giannuzzi, L.A., Stevie, F.A., 1999. A review of focused ion beam milling techniques for TEM specimen preparation. Micron 30, 197–204.

Glaser B., Balashov, E., Haumaier, L., Guggenberger G., Zech, W., 2000. Black carbon in density fractions of anthropogenic soils of the Brazilian Amazon region. Org. Geochem., 31, 669– 678.

Gu, B., Schmitt, J., Chen, Z., Liang, L., McCarthy, J.F. 2000. Adsorption and desorption of different organic matter fractions on iron oxide. Geochim. Cosmochim. Acta, 59, 219-229.

Hedges, J.I., Oades, J.M., 1997. Comparative organic geochemistries of soils and marine sediments. Org. Geochem. 27, 319-361.

Heymann, K., Lehmann, J., Solomon, D., Schmidt, M., Regier, T., 2011. C 1s K-edge near-edge X-ray fine structure (NEXAFS) spectroscopy for characterizing the functional group chemistry of black carbon. Org. Geochem. 42, 1055-1064.

Joseph, S.D., Camps-Arbestain, M., Lin, Y., Munroe, P., Chia, C.H., Hook, J., van Zwieten, L., Kimber, S., Cowie, A., Singh, B.P., Lehmann, J., Foidl, N., Smernik, R.J., Amonette, J.E., 2010. An investigation into the reactions of biochar in soil. Austr. J. Soil Res. 48, 501-515.

IPCC, 2007. Climate Change 2007: Synthesis Report. Contribution of Working Groups I, II and III to the Fourth Assessment Report of the Intergovernmental Panel on Climate Change [Core Writing Team, Pachauri, R.K and Reisinger, A. (eds.)]. IPCC, Geneva,

Switzerland, 104 pp.

Kaiser, K., Mikutta, R., Guggenberger, G., 2007. Increased stability of organic matter sorbed to ferrihydrite and goethite on aging. Soil Sci. Soc. Am. J. 71, 711-719.

Kaiser, K. and G. Guggenberger, 2003. Mineral surfaces and soil organic matter. Eur. J. Soil Sci. 54, 219-236.

Kaiser, K., Zech, W., 2000. Dissolved organic matter sorption by mineral constituents of subsoil clay fractions. J. Plant Nutr. Soil Sci. 163, 531-535.

Keil, R.G., Tsamakis, E., Fuh, C.B., Giddings, J.C., Hedges, J.I., 1994. Mineralogical and textural controls on the organic composition of coastal marine-sediments - hydrodynamic separation using split-fractionation. Geochim. et Cosmochim. Acta 58, 879-893.

Kleber, M., Sollins, P., Sutton, R., 2007. A conceptual model of organo-mineral interactions in soils: self-assembly of organic molecular fragments into zonal structures on mineral surfaces. Biogeochemistry 85, 9-24.

Kögel-Knabner, I., Guggenberger, G., Kleber, M., Kandeler, E., Kalbitz, K., Scheu, S., Eusterhues, K., Leinweber, P., 2008. Organo-mineral associations in temperate soils: Integrating biology, mineralogy, and organic matter chemistry. J. Plant Nutr. Soil Sci. 171, 61-82.

Lehmann, J., Liang, B.Q., Solomon, D., Lerotic, M., Luizao, F., Kinyangi, J., Schäfer, T., Wirick, S., Jacobsen, C., 2005. Near-edge X-ray absorption fine structure (NEXAFS) spectroscopy for mapping nano-scale distribution of organic carbon forms in soil: Application to black carbon particles. Global Biogeochem. Cycles 19, GB1013.

Lehmann J, Skjemstad J.O., Sohi, S., Carter, J., Barson, M., Falloon, P., Coleman, K., Woodbury, P., and Krull, E., 2008. Australian climate-carbon cycle feedback reduced by soil black carbon. Nature Geoscience 1, 832–835.

Lehmann, J., Brandes, J., Fleckenstein, H., Jacobsen, C., Solomon, D., Thieme, J., 2009.

Synchrotron-based near-edge X-ray Spectroscopy of natural organic matter in soils and sediments. In: N. Senesi, Xing, P. Huang, P.M. (eds.), Biophysico-Chemical Processes Involving Natural Nonliving Organic Matter in Environmental Systems, 729-781. IUPAC Series on Biophysico-Chemical Processes in Environmental Systems. Wiley, NJ.

Liang, B., Lehmann, J., Solomon, D., Kinyangi, J., Grossman, J., O'Neill, B., Skjemstad, J.O., Thies, J., Luizao, F.J., Petersen, J., Neves, E.G., 2006. Black Carbon increases cation exchange capacity in soils. Soil Sci. Soc. Am. J. 70, 1719-1730.

Liang, B., Lehmann, J., Solomon, D., Sohi, S., Thies, J.E., Skjemstad, J.O., Luizao, F.J., Engelhard, M.H., Neves, E.G., Wirick, S., 2008. Stability of biomass-derived black carbon in soils. Geochim. Cosmochim. Acta 72, 6069-6078.

Ma, C., Eggleton, R., 1999. Cation exchange capacity of kaolinite. Clays Clay Min. 47, 174-180.

Mikutta, R., Mikutta, C., Kalbitz, K., Scheel, T., Kaiser, K., Jahn, R., 2007. Biodegradation of forest floor organic matter bound to minerals via different binding mechanisms. Geochim. Cosmochim. Acta 71, 2569-2590.

Moreno-Castilla, C., M.V. Lopez-Ramon and F. Carrasco-Marin, 2000. Changes in surface chemistry of activated carbons by wet oxidation. Carbon, 38, 1995-2001.

Nguyen, B., Lehmann, J., 2009. Black carbon decomposition under varying water regimes. Org. Geochem. 40, 846-853.

Nguyen, B., Lehmann, J., Hockaday, W.C., Joseph, S., Masiello, C., 2010. Temperaure sensitivity of black carbon decomposition and oxidation. Environ. Sci. Technol. 44, 3324-3331.

Ohno, T., I.J. Fernandez, S. Hiradate, and J.F. Sherman. 2007. Effects of soil acidification and forest type on water-soluble soil organic matter properties. Geoderma 140,176-187.

Pan, B., Tao., S., Wu, D., Zhang, D., Peng, H., Xing, B. 2011. Phenanthrene sorption/desorption sequences provide new insight to explain high sorption coefficients in field studies. Chemosphere. 84, 1578-83.

Regier, T., Krochak, J., Sham, T.K., Hu, Y.F., Thompson, J., Blyth, R.I.R., 2007. Performance and capabilities of the Canadian Dragon: The SGM beamline at the Canadian Light Source. Nuclear Instr. Methods Physics Res. Section A-Accelerators Spectrometers Detectors and Associated Equipment 582, 93-9.

Scheinost, A.C., Kretzschmar, R., Christl, I., Jacobsen, C., 2001. Carbon group chemistry of humic and fulvic acid: a comparison of C 1s NEXAFS and ^{13}C NMR spectroscopies. In: E.A. Ghabbour, Davies, G. (Eds.), Humic Substances: Structures, Models and Functions, Royal Society of Chemistry. Cambridge, UK, pp. 39-47.

Schmidt, M.W.I., Noack, A.G., 2000. Black carbon in soils and sediments: Analysis, distribution, implications, and current challenges. Global Biogeochem. Cycles 14, 777-793.

Schmidt, M.W.I., Abiven, S., Dittmar, T., Guggenberger, G., Janssens, I.A., Kleber, M., Kogel-Knabner, I., Lehmann, J., Manning, D.A.C., Nannipieri, P, Rasse, D.P., Weiner, S., Trumbore, S.E., 2011. Persistence of soil organic matter as an ecosystem property. Nature 478, 49-56.

Skjemstad, J.O., Spouncer, L.R., Cowie, B., Swift, R.S., 2004. Calibration of the Rothamsted organic carbon turnover model (rothc ver. 26.3) using measurable soil organic carbon pools. Austr. J. Soil Res. 42, 79–88.

Skjemstad, J.O. 1992. Genesis of podzols on coastal dunes in southern Queensland. III. The role of aluminium-ogranic complexes in profile development. Aust. J. Soil Res. 30, 645-665.

Solomon, D., Lehmann, J., Kinyangi, J., Liang, B., Hanley, K., Heymann, K., Wirick, S.

and Jacobsen, C., 2009. Carbon (1s) NEXAFS spectroscopy of biogeochemically relevant organic reference compounds. Soil Sci. Soc. Am. J. 73, 1817-1830.

Wada, 1985

Wan, J., Tyliszczack, T., Tokunaga, T.K., 2007. Organic carbon distribution, speciation, and elemental correlation within soil microaggregates: Applications of STXM and NEXAFS Spectroscopy. Geochim. Cosmochim. Acta 71, 5439-5449.

Yariv, S.. Cross, H., 2002. Organo-clay complexes and interactions, Marcel Dekker: New York.

Zhang, L., Lio, L., Zhang, S., 2011. Absorption of phenanthrene and 1,3-dinitrobenzene on cation modification of clay minerals. Colloid Surface A 377, 278-283.

5. DISCOURSE ON CONTENTIOUS ENVIRONMENTAL ISSUES AND THE BIOCHAR DEBATE

5.1. Introduction

In the discourse on possible solutions to the multitude of environmental issues facing society, a contentious debate over the use of biochar technology as a climate mitigation tool and soil amendment has arisen within the scientific community and in the public domain. Biochar, a technology still in the research phase, has both been lauded as a key technology able to help mitigate the effects of climate change, and vilified as 'junk science' and a false-solution that endangers the world's forests and the global poor. This public debate involved well-known scientists, such as James Lovelock and Jim Hansen, who responded publicly to the harsh critiques by *The Guardian's* George Monbiot[1] and environmental activists against biochar and against the scientists supporting it. Even Vice-President Al Gore issued a statement: "One of the most exciting new strategies for restoring carbon to depleted soils, and sequestering significant amounts of CO_2 for 1,000 years and more, is the use of biochar." The debate ramped up in early 2009, prior to the United Nations (UN) climate talks in Bonn, Germany. Over 150 environmental groups signed an anti-biochar declaration[2], while others spammed biochar scientists[3] and publicly criticized biochar advocates in a highly personal manner more often reserved for political elections.

The most notable aspects of the biochar debate were that it appeared to mimic and be embedded in earlier debates at the nexus of science and technology, particularly those

[1] Monbiot, G. 24 March 2009. "Woodchips with everything. It's the Atkins plan of the low-carbon world." The Guardian.
[2] //www.rainforest-rescue.org/news/1150/declaration-biochar-a-new-big-threat-to-people-land-and-ecosystems
[3] http://www.carboncommentary.com/2009/04/07/539

related to genetically modified crops, biofuels and globalization. The tactics employed by environmental groups against biochar accused scientists and advocates of working at the behest of industry, and frequently referred to their "false claims", "blindness" and "false assumptions." One of the most prominent activists, Vandana Shiva, initially stated that "biochar proponents are proposing a solution based on killing and burning trees and turning living carbon into dead carbon."[4] Regardless of their disagreement with some of the more generous scenarios laid out by biochar promoters, those opposed to biochar were not as interested in the facts as they were in preventing what they perceived as a real threat to society, regardless of the potential of biochar to serve as a multi-purpose, multi-scale climate mitigation tool; or, at the very least a clean cook-stove option in developing countries where the mortality rate from indoor smoke is among the leading causes of death among children[5].

Contentious debates in the agriculture and environmental policy arenas often arise due to conflicting normative views about the environment, sustainability and the best way to address society's most pressing problems. The role of science, and of scientists, within political and social movements has become more complex with the increasing severity of environmental problems. Stakeholders must learn to successfully navigate an increasingly polarized world where science becomes entangled in a web of social movements and political issues (Shurman and Munro 2010). The objective of this paper is to investigate the way in which information was spread by anti-biochar groups, and how the communication strategy fits into broader discourse on environmental policies,

[4] Shiva, V. 10 April 2009. "Soils need carbon as a living humus." The Tribune. <http://www.tribuneindia.com/2009/20090410/science.htm#1>.
[5] Tielch, J.M., Katz, J., Thulasiraj, R.D., Coles, C.L., Sheeladevi, S., Yanik, E.L., Rahmathullah, L. 2009. Exposure to indoor biomass fuel and tobacco smoke and risk of adverse reproductive outcomes, mortality and respiratory morbidity and growth among newborn infants in south India. International Journal of Epidemiology, 38, 1351-1363.

particularly at the agriculture-technology nexus.

5.2. An Overview of the Biochar Debate

5.2.1. Biochar Defined

Biochar is defined as a soil amendment made by heating biomass feedstock in the absence of oxygen[6], a process known as pyrolysis. In addition to biochar, pyrolysis produces gases and liquids which can be used as forms of renewable energy, thus reducing the need for fossil fuel-based energy, soil inputs such as chemical fertilizers, or other valuable products such as food flavoring, insecticides and other bioproducts. The excitement over biochar systems as portrayed in the public domain is due to their potential to provide carbon-negative energy[7]. Estimating the total effect of biochar systems on climate is highly complex, but models have placed the upper technical potential to reduce carbon emissions with biochar systems in a sustainable way between 0.25 Gt (most conservative estimate) and 1 Gt by 2040[8].

Enthusiasm for biochar in the scientific community stemmed from the discovery of the Terra Preta de Indio, highly fertile anthropogenic soils found in the Amazon Basin and notable for their enhanced soil properties compared to surrounding highly weathered, nutrient poor soils typical of this region. Also known as Amazonian Dark Earths, these soils have been highlighted for their ability to store high concentrations of biochar-type substances (also called black carbon (C) in the relevant literature), as well as a remarkably high cation exchange capacity, and high phosphorus (P), and calcium (Ca)

[6] Lehmann, J. and Joseph, S. eds. Biochar for Environmental Management: Science and Technology. London: Earthscan, 2009.
[7] Marris, E. 2006. Putting the carbon back: Black is the new green. Nature, 442, 624-626.
[8] Woolf, D., Amonette, J.E., Street-Perrott, F.A., Lehmann, J., Joseph, S. 2010 Sustainable biochar to mitigate global climate change. Nature Communications, DOI: 10.1038/ncomms1053

contents[9]. Wim Sombroek, former Secretary General of the International Union of Soil Sciences (IUSS), studied the Terra Preta soils and highlighted the role they might someday play in increasing the capacity of soils to hold large quantities of carbon[10].

5.2.2. The Biochar Debate

In the lead-up to the 2009 UN climate talks in Bonn, Germany, Vandana Shiva, a highly regarded anti-globalization activist argued against any market-based solution to climate change, including biochar, that neglected to address long term sustainable solutions to soil management and health[11]. Subsequently, 156 international environmental groups issued a declaration entitled "Declaration Biochar: A new big threat to people, land and ecosystems"[12]. This declaration was issued in reaction to a proposal by 11 African countries and biochar proponents to have the UN consider biochar as an eligible and official means to offset their emissions under international regulations. Anti-biochar activists argued that the market for biochar would encourage the destruction of tropical forests, much as the market for biofuels had encouraged forest destruction for palm-oil plantations. A series of press releases and reports were issued by the groups EcoNexus and Biofuelwatch[13],[14]; these materials were not peer-reviewed scientific papers and, although many useful questions were raised, their objective was to prove that biochar was

---

[9] Liang, B., Lehmann, J., Solomon, D., Kinyangi, J., Grossman, J., O'Neill, B., Skjemstad, J.O., Thies, J., Luizao, F.J., Petersen, J., Neves, E.G., 2006. Black carbon increases cation exchange capacity in soils. Soil Science Society of America Journal 70, 1719-1730.

[10] Sombroek, W., Nachtergaele, F.O. and Hebel, A. 1993. Amounts, dynamics and sequestering of carbon in tropical and subtropical soils, Ambio 22, 417-426.

[11] Shiva, V. 10 April 2009. "Soils need carbon as a living humus." The Tribune. http://www.tribuneindia.com/2009/20090410/science.htm#1>

[12] http://www.rainforest-rescue.org/news/1150/declaration-biochar-a-new-big-threat-to-people-land-and-ecosystems

[13] Ernsting, A., Smolker, R. 2009. Biochar for Climate Change Mitigation: Fact or Fiction? http://www.biofuelwatch.org.uk/wp-content/uploads/biocharbriefing.pdf

[14] NOAH (Friends of the Earth Denmark), Grupo de Reglexion Rural, Econexus and Biofuelwatch. 2009. Agriculture and Climate Change: Real Problems, False Solutions. http://www.econexus.info/publication/agriculture-and-climate-change-real-problems-false-solutions

'junk-science' and to derail any inclusion of biochar in a portfolio of solutions to address climate change.

Leading biochar proponents, mainly scientists and the International Biochar Initiative (IBI) sought to provide a rebuttal to the anti-biochar groups[15]. The IBI, a member-based organization serving as a clearinghouse for biochar science and information, works to develop guidelines for sustainable biochar production and use, and to evaluate biochar projects and systems against these guidelines[16]. IBI issued a response paper refuting many of the claims by anti-biofuels groups, citing numerous scientific studies. The high profile debate that ensued between Monbiot[17,18] and scientists James Lovelock[19], Jim Hansen[20], and Peter Read[21] and entrepreneur Chris Goodall[22] over Monbiot's harsh portrayal of biochar as a technology with potentially disastrous consequences, and of biochar scientists as misguided and ignorant was a turning point. Regardless of their original intentions and attempts to set the record straight or generate a dialogue, scientists found their inboxes flooded with petitions from the website 'Climate Ark'[23], and the "debate" continued. The questions raised about what dangers biochar might pose to the environment were valid, but the consensus among scientists was that it was questionable to vilify biochar approaches, pre-emptively, or to draw conclusions without proper inquiry. Casting biochar as 'a big new threat to people, land and ecosystems' prior to much of the work which remained to be done (life-cycle analyses, field trials, etc.) in the scientific community also appeared biased. The entire debate

[15] Biochar Misconceptions and Science, International Biochar Initiative. October 29, 2009.
[16] http://www.biochar-international.org/about
[17] http://www.guardian.co.uk/environment/2009/mar/24/george-monbiot-climate-change-biochar
[18] http://www.guardian.co.uk/environment/georgemonbiot/2009/mar/27/biochar-monbiot-global-warming
[19] http://www.guardian.co.uk/environment/2009/mar/24/biochar-earth-c02
[20] http://www.guardian.co.uk/environment/2009/mar/25/hansen-biochar-monbiot-response
[21] http://www.guardian.co.uk/commentisfree/2009/mar/27/biochar
[22] http://www.guardian.co.uk/environment/cif-green/2009/mar/24/response-biochar-chris-goodall
[23] http://www.carboncommentary.com/2009/04/07/539

raised interesting questions about the role of scientists in public debates and the best way to approach misguided accusations against emerging technologies (Table 5.1).

Table 5.1. Fact or Fiction?

CLAIMS	REFUTATIONS
Only around 11 peer-reviewed field trials have been published, their results very greatly, even within individual studies and only 3 of them lasted longer than two years	11 peer-reviewed field trials is substantial
Wardle et al. (2009)24 study is proof that biochar cannot be relied upon to sequester carbon	There was a response from the scientific community that because they did not measure C leaving litter bags that the data did not justify the conclusion
Use of the term laboratory studies	Uses the term "laboratory study' as a negative, implying that nothing practical can be learned
Cite numerous studies where, for example biochar increased C in one plot and not in another as proof that biochar is unreliable	Misconstrues the scientific process
Claims about the negative impacts of airborne black carbon.	Smallest particles of biochar are larger than soot, unable to be transported long distances. Best practice techniques can be used to apply biochar, to minimize dust.
IBI promotes large monoculture tree plantations that will decimate native forests and displace indigenous people	IBI promotes sustainable biochar (Mission Statement), using residues and waste to produce biochar

[24] Wardle, D.A., Nilsson, M., Zackrisson, O. 2008. Fire-derived charcoal causes loss of forest humus. Science, 320, p. 629.

5.3. Narratives in the biochar debate

5.3.1. Framing the biochar debate

Numerous social science studies have been conducted in order to frame and analyze environmental discourses. Normative frames are useful to political and social movements because they help to construct arguments to support one side of a contentious debate. According to Scandizzo[25], two dominant and conflicting narratives characterize the debate on world agriculture. These narratives can be identified within the biochar debate discourse; for example, a conservative narrative – which describes scientific progress in a positive light and discounts the unrealized goals of biotechnology as yet unrealized but anticipated in the future – was used by the biochar industry to promote its value. The radical discourse, as adopted by the anti-biochar activists describes science and technology as being ineffective and profit driven, thus threatening the environment and livelihoods of the global poor.

Opposition to biochar technology not only represents a highly polarized position, it appears to be based in an overall narrative of the anti-globalization movement, which objects to market-based solution to global problems. For example, the anti-biochar declaration claimed that "given that successful strategies for combining charcoal with diverse biomass in soils were developed by indigenous peoples, 'biochar' patenting raises serious concerns over biopiracy."[26] Biopiracy concerns have been continuously raised in the anti-globalization debate over transgenic crops and land conversion for biofuel crops.[27] Anti-globalization activists have been accused of an "assert-don't-analyze"

[25] Scandizzo, P.L., 2009 Science and Technology in World Agriculture: Narratives and Discourses. AgBioForum, 12(1): 23-33

[26] //www.rainforest-rescue.org/news/1150/declaration-biochar-a-new-big-threat-to-people-land-and-ecosystems

[27] Shiva, V. 1999. Biopiracy: The Plunder of Nature and Knowledge. South End Press, Boston, Massachusetts.

approach, whereby simplistic untruths are asserted repeatedly, often by those who have little expertise in the matter at hand[28]. In 'Fighting the Wrong Enemy', David Graham highlights how misinformation spread by NGO's can have far-reaching effects, often counterproductive to the very goals of those protesting globalization.[29] For example, he writes that the assertion that the anti-globalization narrative describing transnational corporations that prey on the world's most vulnerable workers is contradicted by studies that have found that low labor and environmental standards were more likely to be a deterrent for foreign investment, rather than an incentive. This is not to say that the poor are not marginalized, or that large corporations do not use loopholes to evade regulation. This analysis is, however, meant to illustrate the power that narratives have in making it easier to differentiate between "good" and "evil", particularly when an overwhelming stream of information makes it increasingly difficult to do so.

A cultural lexicon has developed that is almost universal among environmentalists, and terms such as biodiversity, sustainable development, defense of indigenous claims to land, intellectual property rights[30] are meaningful and represent a master narrative organizing environmentalists to take action in order to protect the environment. This master narrative serves as a rallying cry and as a unifier for many activists and NGO's. Hannah Paul from EcoNexus states that "by using terms like 'agroforestry' or 'silvo-pastoral systems', the biochar advocates mask large plantation plans which in no way resemble the 'sustainable practices used by small farmers and pastoralists around the world" in reference to a Nature Communications article[31] which

[28] Dale, R. Thinking ahead/commentary: exposing anti-globalization myths

[30]Brosius, J.P. 1997. Endangered forests, endangered people: Environmentalist representations of indigenous knowledge. Human Ecology 25(1): 47-69

[31] Woolf, D., Amonette, J.E., Street-Perrott, F.A., Lehmann, J., Joseph, S. 2010 Sustainable biochar to mitigate global climate change. Nature Communications, DOI: 10.1038/ncomms1053

outlined potential carbon savings achievable with biochar. Deepak Rughahni of Biofuelwatch likened the use of biochar as a soil amendment to the release of a new pharmaceutical product without clinical testing[32]. He stated that biochar cookstoves would actually require higher fuel loads, cause more deforestion, and send loud clouds of smoke into the atmosphere. These narratives may, in a rational discourse, be framed as questions leading to inquiry but are typically stated as facts, particularly since Rughani's remarks were given at the anti-biochar side event at the climate conference in Copenhagen, Denmark in 2009.

5.3.2. The Golden Age of Misinformation

Anti-GMO (genetically modified organisms) activists have long accused biotechnology companies, such as Monsanto, with patenting genes found in local varieties of plants grown by traditional farmers[33]. The battles over genetic plant breeding may be the most inflammatory debate at the agriculture-technology nexus. Agricultural biotechnologies are being examined at the international level in order to address the undernourishment of an estimated 925 million people around the world in 2010[34]. The scope of the debate spans many countries, with activists around the globe mobilizing to stop the spread of GMO technology across Europe and in developing countries such as India, Indonesia and Thailand. The United Nation's Food and Agricultural Organization (FAO) along with other international organizations have agreed to increase their efforts in

[32] http://peaksurfer.blogspot.com/search?updated-max=2009-12-14T16%3A34%3A00-06%3A00&max-results=7

[33] http://www.occupymonsanto360.org/Occupy,Monsanto,GMO,Genetic,Engineering,Modified,Organism,Food,Sustainable,Local,Locavore,Organic,RoundUp/gene-patent/

[34] Ruane, J., Sonnino, A. 2011. Agricultural biotechnologies in developing countries and their possible contribution to food security. Journal of Biotechnogy 156, 356-363

the development and use of pro-poor agricultural biotechnologies[35]. Despite continued concern over transgenic crops, governing and scientific bodies have found no evidence to justify banning them or limiting their use, although many countries require labeling of products containing GMO's. As the debate continues, its adoption has become widespread, and like biochar, interest in its practical applications has not abated. For example, a simple Google search of the term 'biochar' (Fig. 5.1) showed a consistent increase in results over the past decade, with the most dramatic increase occurring after many of the debate "events" discussed in this paper (Table 5.2).

[35] Ruane, J., Sonnino, A. 2011. Agricultural biotechnologies in developing countries and their possible c tribution to food security. Journal of Biotechnogy 156, 356-363

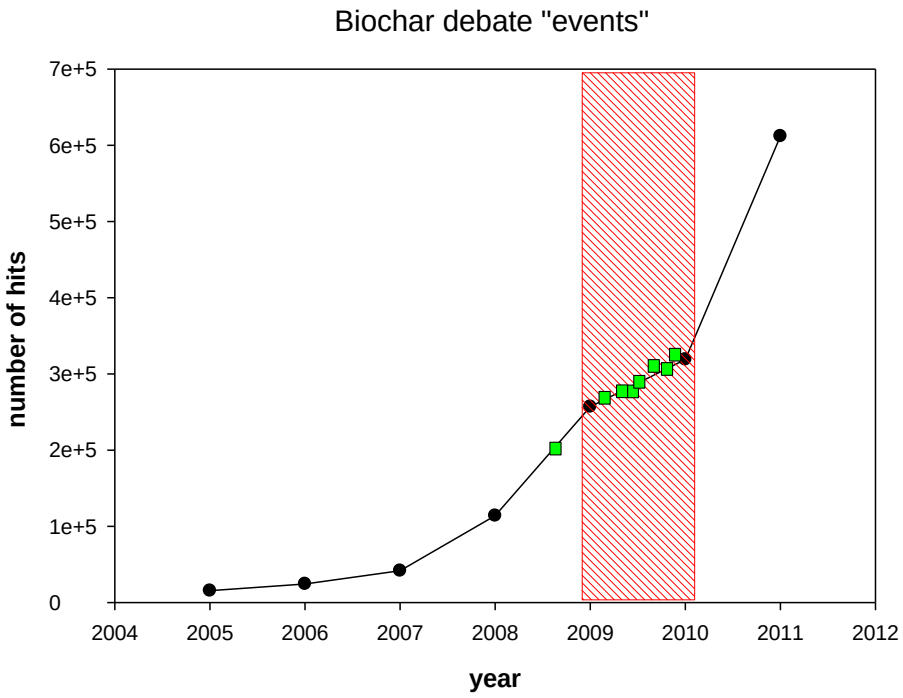

Figure 5.1. Cluster of biochar debate "events" (see Table 5.2) versus Google hits for the term 'biochar' between the years of 2005 – 2011.

Table 5.2. Timeline of selected biochar controversy events highlighted in this paper

DATE	EVENT
08/09/2006	Emma Marris, Black is the New Green, Nature News Feature[36]
05/10/2007	Lehmann, J. A Handful of Carbon, Nature Commentary[37]
02/13/2009	Ernsting, A., Smolker, R., Biochar for Climate Change Mitigation: Fact of Fiction[38]
03/2009	Biochar Declaration: A Big New Threat to People, Land and Ecosystems (issued by Econexus and BFW, 156 signatories)[39]
03/31/2009	Monbiot, G. Woodchips with everything. It's the Atkins plan of the low-carbon world (blog post)[40]
04/10/2009	Shiva, V. Soils need living carbon as humus[41]
12/2009	COP 15, Copenhagen, Denmark – Biochar side event, Anti-biochar side event hosted by EcoNexus

[36] Marris, E. 2006. Putting the carbon back: Black is the new green. Nature, 442, 624-626.
[37] Lehmann, J. A Handful of Carbon, Nature Communications
[38] Ernsting, A., Smolker, R. 2009. Biochar for Climate Change Mitigation: Fact or Fiction? http://www.biofuelwatch.org.uk/wp-content/uploads/biocharbriefing.pdf
[39] //www.rainforest-rescue.org/news/1150/declaration-biochar-a-new-big-threat-to-people-land-and-ecosystems
[40] Monbiot, G. 24 March 2009. "Woodchips with everything. It's the Atkins plan of the low-carbon world." The Guardian.
[41] Shiva, V. 10 April 2009. "Soils need carbon as a living humus." The Tribune. <http://www.tribuneindia.com/2009/20090410/science.htm#1>.

Stone[42] highlights the battle over genetic modification of crops as central in the 'Golden Age of Misinformation'. Stone implicates both industry and the green lobby as guilty of perpetuating misinformation, either by capitalizing on fears of overpopulation, or intentionally blocking any reasoning whereby global hunger can be addressed by GMO crops. Anti-GMO activists have conducted violent protests against the biotechnology used in growing papayas, and such demonstrations are widespread, from Thailand to Hawaiian Islands. In 2011, thousands of transgenic papaya trees in Hawaii were chopped down by environmental activists[43]. The environmental group Greenpeace has protested transgenic papaya extensively in Thailand, going so far as to dump 11 tons of transgenic papaya in front of the Thai Agriculture and Cooperatives Ministry only to have local citizens rush in to take the "poison" papayas home to eat with fear of hunger outweighing fear of poison papayas[44]. These incidents are not restricted to papaya; activists have cut down test crops of drought-resistant wheat in Australia and destroyed plots of biotech eggplants in the Philippines. The protests against transgenic crops are clearly more widespread than those over biochar, but they highlight the increasing difficulty in discerning which side of a debate is "correct" or truthful. This difficulty is compounded by the lack of real-world interaction in these debates, and the reliance on the internet and social media to derive information.[45] For example, comparing Greenpeace (millions of members, global campaigns) to Biofuelwatch (no members, few core activists) provides quite a stark contrast. However, their influence with regard to the biochar debate has outsized their organization, and the number of signee organizations

[42] Stone, G.D. 2002. Both Sides Now: Fallacies in the Genetic-Modification Wars, Implications for Developing Countries, and Anthropological Perpectives. Current Anthropology, 43, 611-630
[43] http://hilo.hawaiitribune-herald.com/sections/news/local-news/papaya-fields-destroyed.html
[44] http://www.salon.com/2007/08/29/gm_papaya/
[45] O'Neil, M & Ackland, R 2006, 'The Structural Role of Nanotechnology-Opposition in Online Environmental Activist Networks', *In*: International Sunbelt Social Network Conference 2006, ed. International Network for Social Network Analysis, pp. 1-32

gathered for the anti-biochar declaration was clearly remarkable.

5.3.3. Scientists in the Middle

According to Sarewitz[46], science lies at the center of environmental debates; scientific justification is used by the proponents of some action, while those opposing the action cite scientific uncertainty or competing scientific results to support their position. Controversies at the nexus of technology and agriculture are abundant, and illustrate the complex relationship between science and real-world decision making. Skills aimed at navigating the interface between science and public policy are not traditionally taught in academia, and as Lackey[47] notes, although scientists should be engaged in the public policy process to explain underlying science, personal policy preferences can and often do come into play. However, according to Altieri[48], researchers who attempt to remain neutral must realize that technical and political choices often go together, and that research will largely tend to serve those in a position to dictate the research agenda. In the case of biochar, advocates justify their positions using the severe consequences of climate change and soil degradation as the result of inaction.

5.4. Conclusion

Increasing scientific evidence suggests that biochar has the promise to be a powerful tool to combat climate change, provide carbon negative energy and improve global soil health. To avoid the pitfalls noted by those warning against the use of biochar,

---

[46] Sarewitz, D. 2004 How science makes environmental controversies worse. Environmental Science & Policy 7, 385-40

[47] Lackey, R.T. 2007. Science, scientists, and policy advocacy. Conservation Biology, 21, 12-17

[48] Stone, G.D. 2002. Both sides now: Fallacies in the genetic-modification wars, implications for developing countries, and anthropological perspectives. Current Anthropology, 43, 611-630

biochar technology must be linked with stringent sustainability guidelines such as those proposed by the IBI. Scientists can stand behind those guidelines without overstepping their role in the policy-sphere since without advocacy for stringent guidelines for any new technology, the outcome might be different from that predicted or intended – if the technology were not used as recommended. It may seem impossible to anticipate all unintended outcomes, negative or positive, and past experience has shown those to emanate from many innovations. The discourse, therefore, is important; yet, debate events have not decreased the interest in biochar as judged from internet searches of ongoing projects and research. A key seems to be that the debate leads to dissemination of verifiable information and to improvement of inquiry with the goal of developing advances in those areas that are beneficial for the global good.

Appendix A

Supplementary information

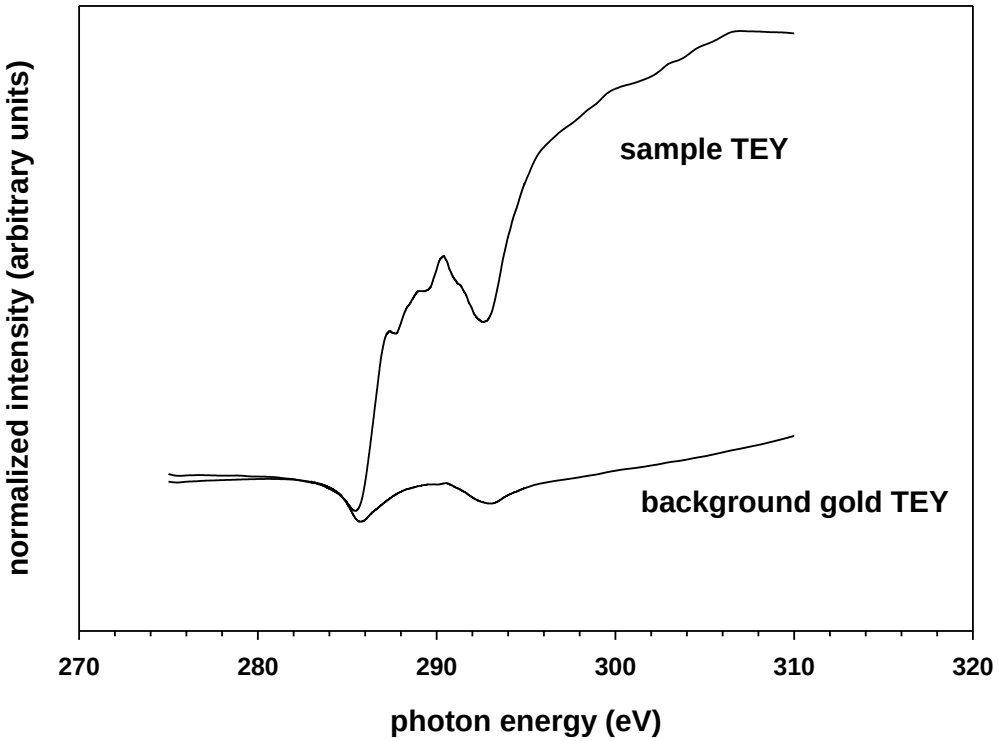

Fig. 1.S1. Under optimal conditions, the clean gold pre-edge region (background) is scaled to match the sample pre-edge region to eliminate the spectral dip, which is due to second-order oxygen effects

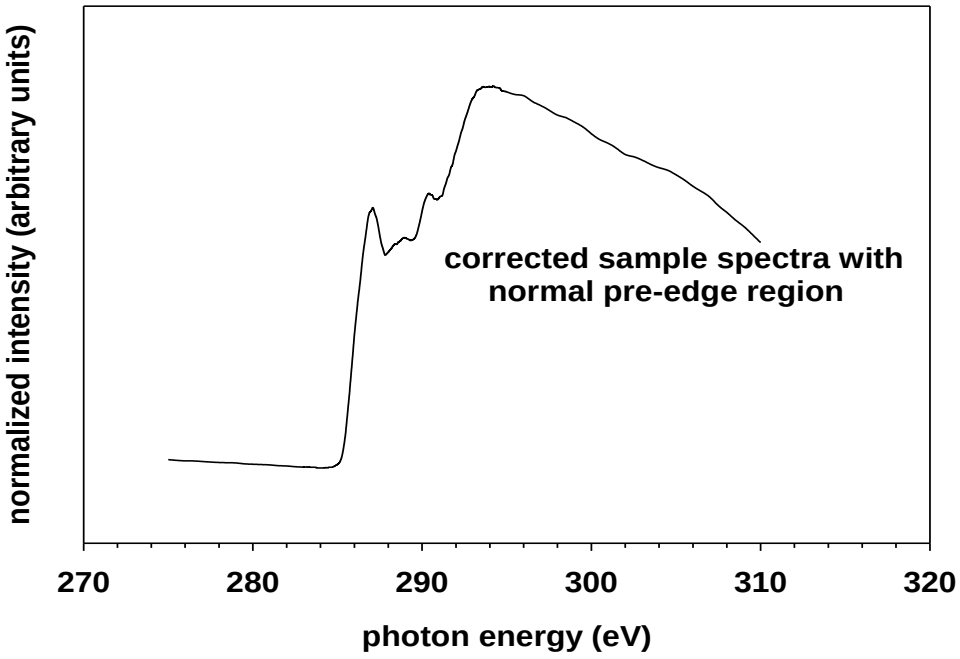

Fig. 1.S2. Sample spectrum after successful subtraction of clean gold and normalization

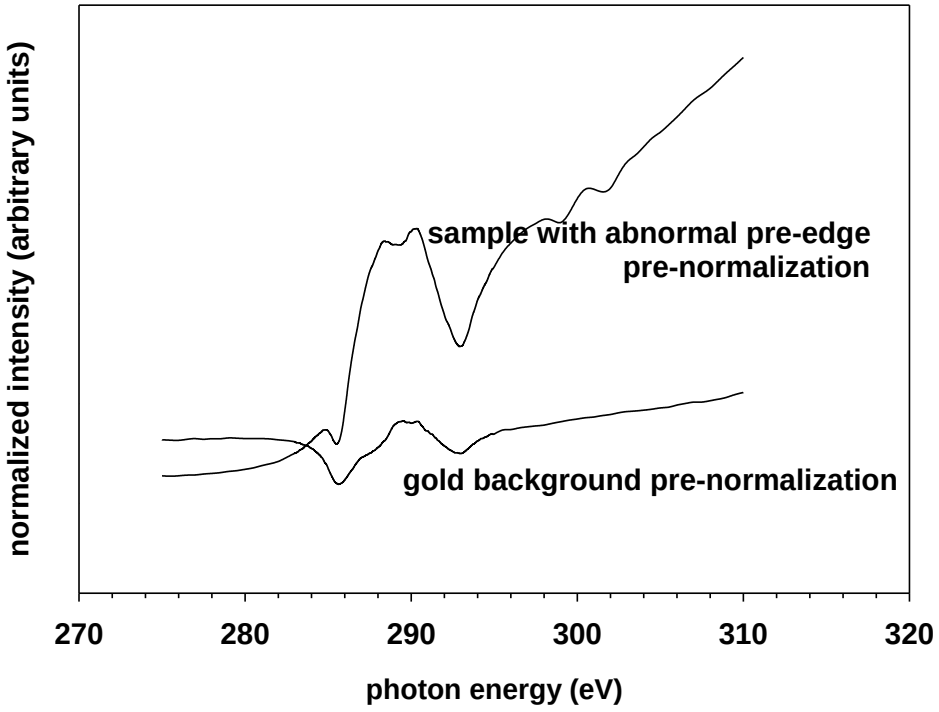

Fig. 1.S3. Example of abnormal sample pre-edge region possibly due to self-absorption effects, which makes it impossible to subtract the clean pre-edge region as the background

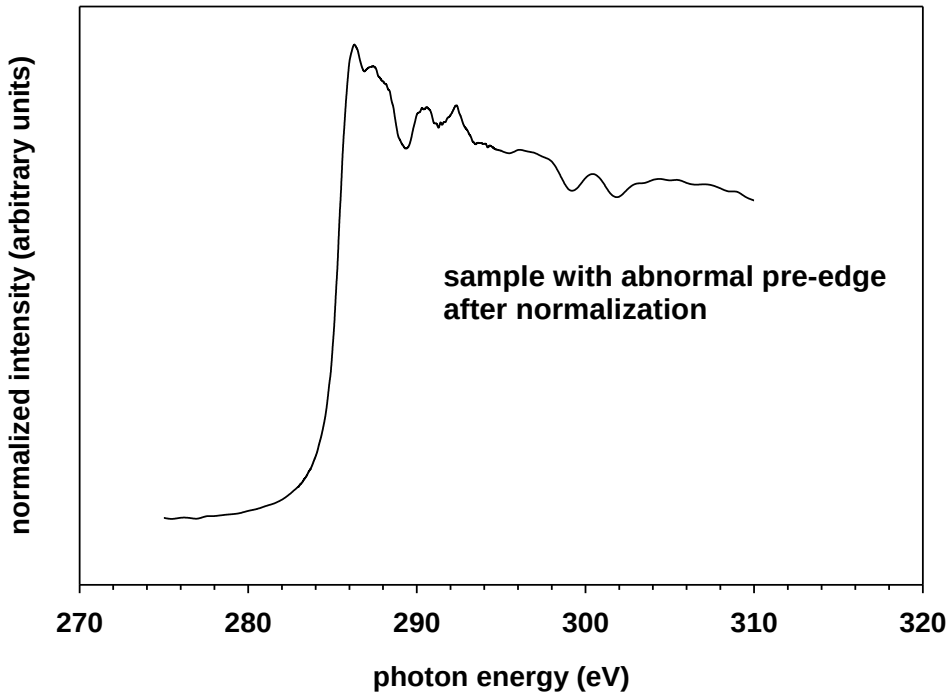

Fig. 1.S4. Result of subtracting clean background from sample with abnormal pre-edge region; artifacts are created in the spectra

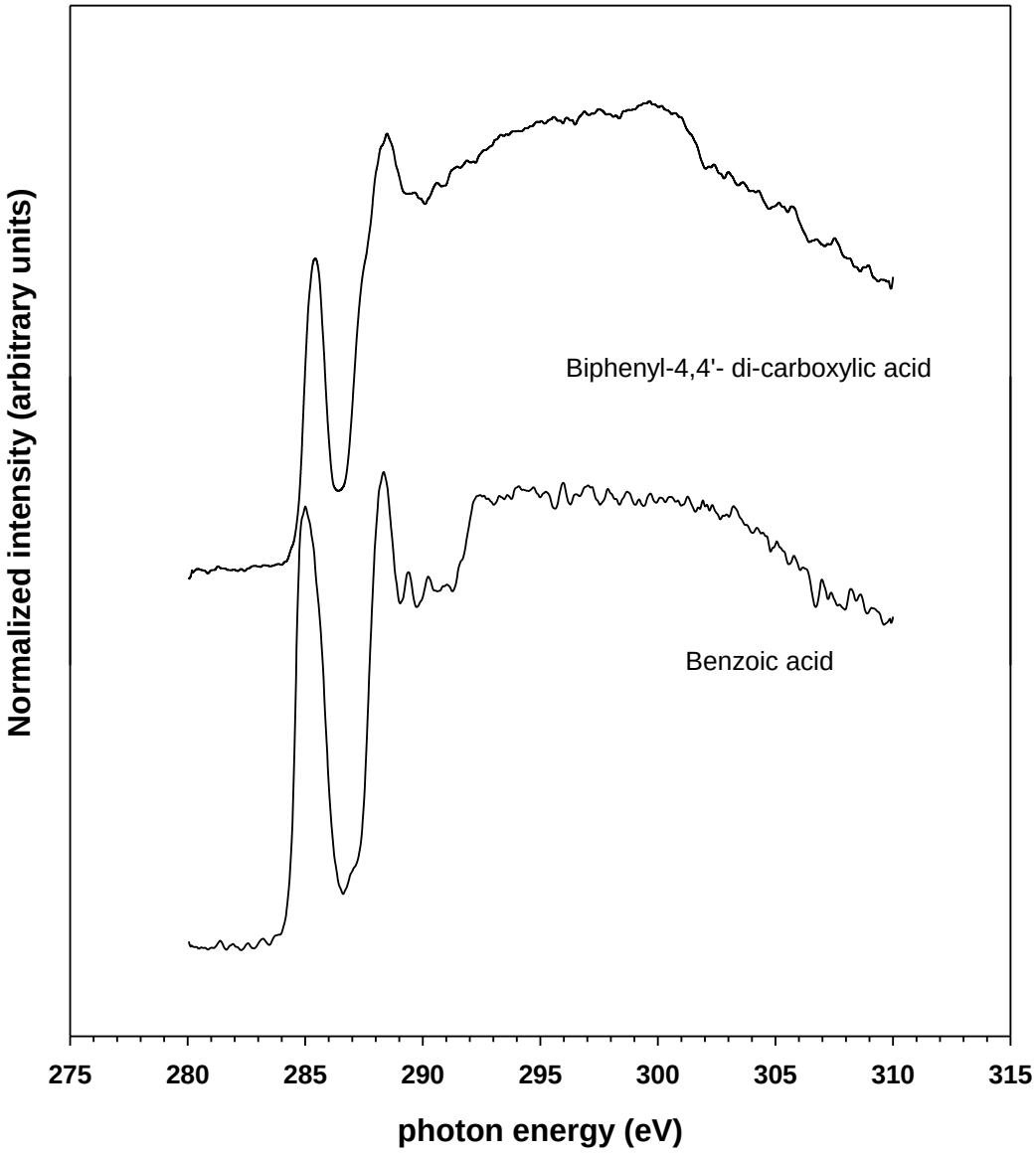

Fig. 1.S5. Carbon K-edge NEXAFS spectra of benzenecarboxylic acids (redrawn from data of Solomon et al., 2009)

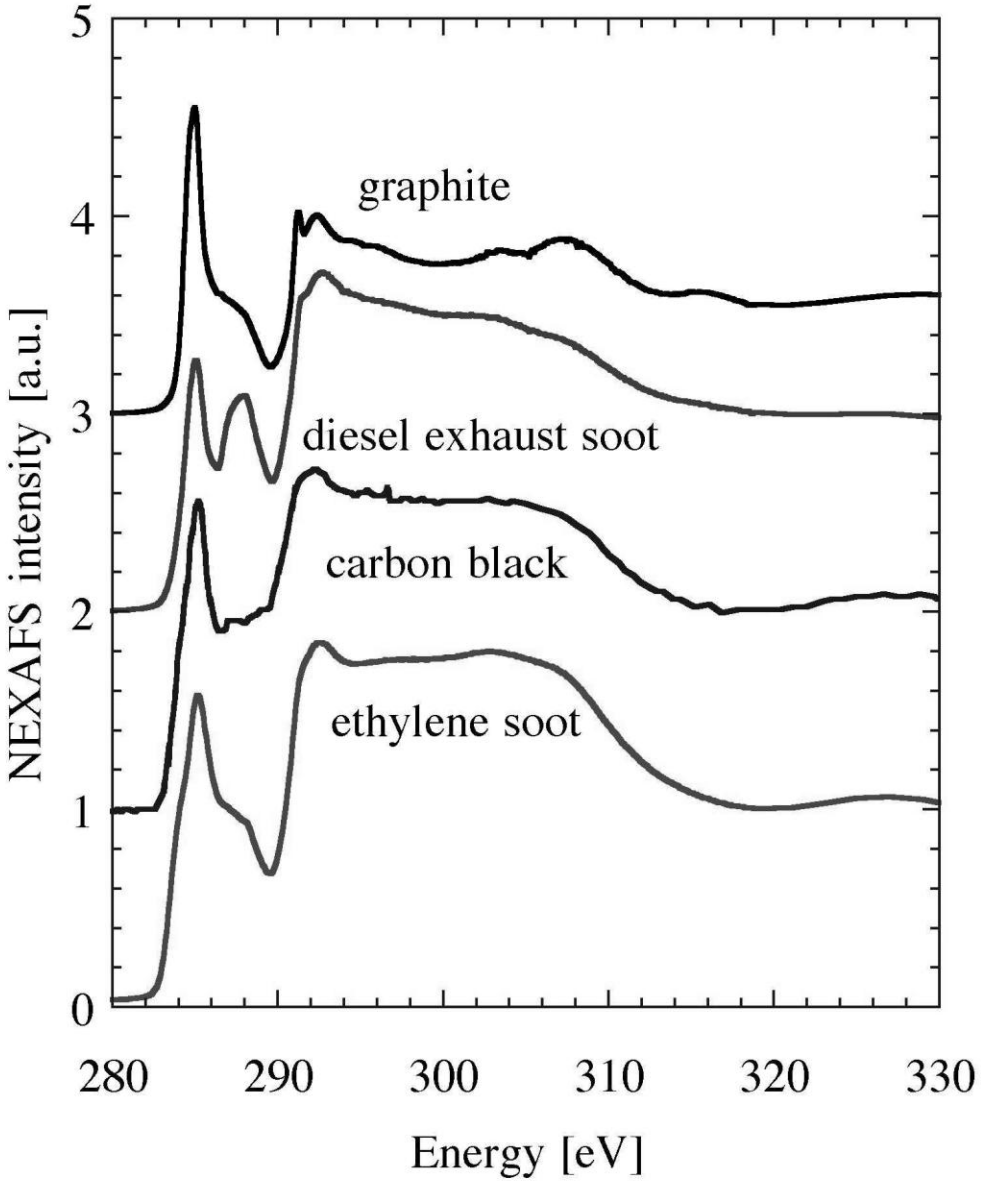

Fig. 1.S6. Carbon K-edge NEXAFS spectra of soots and graphite from di Stasio and Braun (2006). Reprinted with permission from *Energy and Fuels*, 2006 American Chemical Society

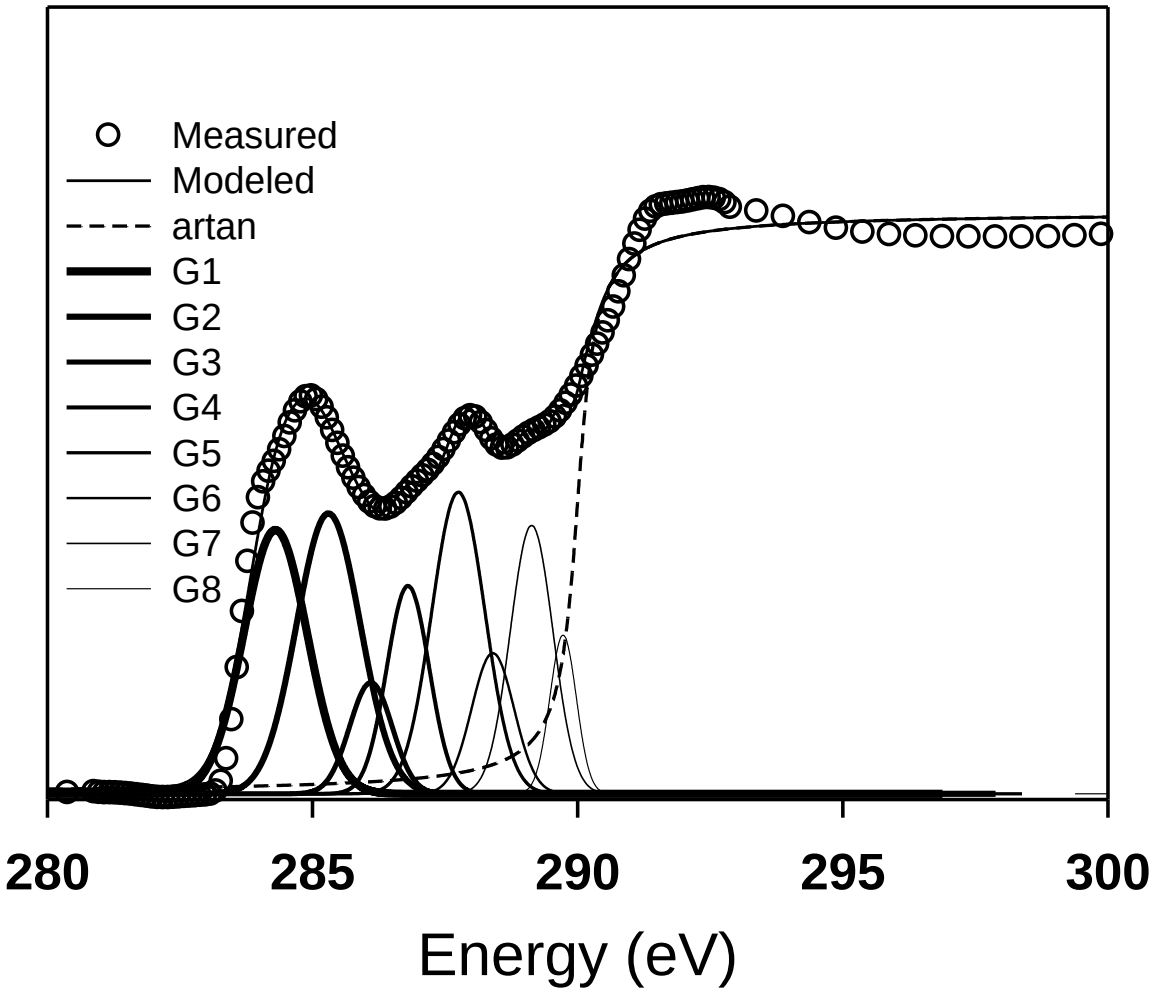
Measured
Modeled
artan
G1
G2
G3
G4
G5
G6
G7
G8
280
285
290
295
300
Energy (eV)

Fig. 1.S7. Deconvolution of soot spectra using eight Gaussian curves and an arctangent step function

Supplementary Table 2.S1. Elemental analysis of corn char temperature series.

Char Temperature	C	N	O	H	K	Ca	Fe	Si
	(%)							
300	59.8	1.15	24.8	4.55	1.71	0.65	0.01	.009
350	60.4	1.18	23.2	3.82	2.15	0.61	0.06	.021
400	63.6	1.2	20.1	3.26	2.02	0.73	0.09	.036
450	67.3	1.2	16.4	2.71	2.57	0.73	0.08	.025
500	68.7	1.09	10.7	1.88	2.48	1.11	0.11	.024
550	70.5	1.01	12.3	2.28	2.39	0.98	0.85	.033
600	70.6	1.07	9.26	2.30	2.46	0.94	0.14	.032

Supplementary data
Fig. 1.1.a

	GRASSCHAR	WOODCHAR	SOOT
272.88	-0.00399	-0.00034	-0.0037
273.38	-0.00287	-0.00042	-0.00227
273.88	-0.00222	-0.00039	-0.00194
274.38	-0.00157	-5.3E-05	-0.00184
274.88	-0.0013	-3.6E-06	-0.00156
275.38	-0.00052	-0.0001	-0.00085
275.88	0.00123	1.47E-05	0.000285
276.38	0.002694	0.000361	0.001349
276.88	0.002183	0.00047	0.001705
277.38	0.000221	0.000135	0.001305
277.88	-0.0008	-6.3E-05	0.000716
278.38	-0.00096	8.29E-05	0.00041
278.88	-0.00067	0.000101	0.000413
279.38	-0.0005	-0.00015	0.000654
279.88	-0.00108	-0.00041	0.001223
280.38	-0.00091	-0.00062	0.002179
280.88	-7.3E-05	-0.00055	0.003465
280.98	-0.00042	-0.00073	0.00243
281.08	-0.00082	-0.00045	0.001879
281.18	-0.0006	-0.0003	0.001655
281.28	-0.00066	-0.00047	0.001391
281.38	-0.0002	-0.00051	0.000882
281.48	0.000744	-0.00046	0.000152
281.58	0.001821	-0.0007	-0.00076
281.68	0.003181	-0.00119	-0.00185
281.78	0.004526	-0.00143	-0.00311
281.88	0.005509	-0.00143	-0.00446
281.98	0.006365	-0.00139	-0.00573
282.08	0.008422	-0.00114	-0.00664
282.18	0.010806	-0.00086	-0.00699
282.28	0.01229	-0.00073	-0.00681
282.38	0.015397	-0.0005	-0.0063
282.48	0.019883	-0.00043	-0.00566
282.58	0.023541	-0.00026	-0.00499
282.68	0.028194	0.000594	-0.00431
282.78	0.035555	0.001898	-0.00364
282.88	0.046038	0.003401	-0.00296
282.98	0.060118	0.005946	-0.00222
283.08	0.081666	0.011954	-0.0007
283.18	0.118264	0.024354	0.004765
283.28	0.172248	0.044821	0.022029

283.38	0.2396	0.073665	0.062131
283.48	0.311108	0.109098	0.131544
283.58	0.380086	0.148005	0.224407
283.68	0.448862	0.189229	0.32414
283.78	0.51874	0.231993	0.413249
283.88	0.58448	0.273245	0.481338
283.98	0.61781	0.309996	0.526508
284.08	0.663674	0.345042	0.554781
284.18	0.70911	0.378087	0.57363
284.28	0.755005	0.412011	0.591119
284.38	0.796524	0.445551	0.611726
284.48	0.827034	0.475283	0.635504
284.58	0.845045	0.502538	0.659699
284.68	0.852326	0.52688	0.681058
284.78	0.847432	0.543089	0.697075
284.88	0.83302	0.551928	0.706161
284.98	0.811393	0.555059	0.707535
285.08	0.78223	0.550573	0.70114
285.18	0.748423	0.540916	0.687666
285.28	0.712347	0.527312	0.66866
285.38	0.675469	0.510764	0.646363
285.48	0.641847	0.496147	0.623098
285.58	0.614738	0.485304	0.600607
285.68	0.595592	0.479382	0.579824
285.78	0.585636	0.480475	0.561096
285.88	0.58088	0.485834	0.54453
285.98	0.578335	0.492029	0.530274
286.08	0.580251	0.498568	0.518782
286.18	0.58377	0.504916	0.510759
286.28	0.585152	0.509692	0.506698
286.38	0.584728	0.513496	0.506564
286.48	0.583914	0.518123	0.510011
286.58	0.585062	0.523246	0.516574
286.68	0.587691	0.52852	0.525485
286.78	0.589971	0.532989	0.535638
286.88	0.593934	0.535266	0.545971
286.98	0.598915	0.536013	0.555886
287.08	0.602201	0.536271	0.565436
287.18	0.607938	0.536981	0.575208
287.28	0.618071	0.53925	0.585966
287.38	0.630733	0.543317	0.59829
287.48	0.647482	0.549943	0.612244
287.58	0.667989	0.560713	0.627227
287.68	0.689867	0.575372	0.642276
287.78	0.710456	0.592268	0.656234

287.88	0.729183	0.610089	0.667207
287.98	0.746352	0.62637	0.672478
288.08	0.759932	0.638993	0.670026
288.18	0.770734	0.648087	0.66028
288.28	0.777402	0.65299	0.646103
288.38	0.779496	0.654103	0.631464
288.48	0.779296	0.653016	0.620164
288.58	0.776179	0.651171	0.614668
288.68	0.772096	0.651064	0.615234
288.78	0.769886	0.653387	0.620219
288.88	0.771398	0.658018	0.627302
288.98	0.776177	0.663529	0.634536
289.08	0.783812	0.671097	0.640879
289.18	0.795837	0.68308	0.646224
289.28	0.812548	0.696449	0.650964
289.38	0.831879	0.708588	0.655766
289.48	0.853383	0.720612	0.661749
289.58	0.879144	0.733129	0.670113
289.68	0.910065	0.746329	0.681229
289.78	0.944362	0.761211	0.69452
289.88	0.979073	0.775644	0.709266
289.98	1.015133	0.789082	0.725212
290.08	1.050894	0.803448	0.74246
290.18	1.084471	0.818076	0.760964
290.28	1.116574	0.832276	0.78021
290.38	1.144058	0.846425	0.799685
290.48	1.16567	0.859702	0.819724
290.58	1.184721	0.872333	0.841471
290.68	1.20354	0.885127	0.86586
290.78	1.217518	0.896636	0.892845
290.88	1.22208	0.90586	0.921482
290.98	1.222957	0.914583	0.950341
291.08	1.223254	0.923592	0.977807
291.18	1.216178	0.930438	1.002254
291.28	1.20213	0.935059	1.022085
291.38	1.188206	0.939592	1.036026
291.48	1.171846	0.943518	1.044023
291.58	1.152082	0.945817	1.047705
291.68	1.135624	0.947996	1.049332
291.78	1.122467	0.950776	1.050402
291.88	1.109916	0.953025	1.051477
291.98	1.098818	0.955298	1.052783
292.08	1.088226	0.957838	1.054479
292.18	1.077889	0.959337	1.056549
292.28	1.069233	0.960512	1.058673

292.38	1.06096	0.961994	1.060239
292.48	1.051273	0.962275	1.060619
292.58	1.040713	0.961616	1.059499
292.68	1.031813	0.962112	1.056705
292.78	1.025621	0.963526	1.051655
292.88	1.016755	0.963708	1.0433
293.38	1.00192	0.971038	1.036808
293.88	0.988304	0.976481	1.026983
294.38	0.981802	0.978945	1.015962
294.88	0.980331	0.980375	1.006241
295.38	0.98288	0.981837	0.999227
295.88	0.9904	0.98397	0.994848
296.38	1.003654	0.987398	0.992363
296.88	1.013479	0.989946	0.991127
297.38	1.004413	0.990147	0.990622
297.88	0.98515	0.988563	0.990385
298.38	0.98	0.987983	0.990346
298.88	0.992633	0.989301	0.990967
299.38	1.008355	0.9899	0.99262
299.88	1.013015	0.990863	0.99505
300.38	1.005039	0.994533	0.997766
300.88	0.99646	0.998545	1.000601
301.38	0.994112	1.001627	1.003453
301.88	0.995036	1.005538	1.005872
302.38	0.99708	1.009684	1.00731
302.88	0.998402	1.011856	1.007503
303.38	0.997565	1.01182	1.006533
303.88	0.996504	1.010986	1.004905
304.38	0.998022	1.010397	1.003466
304.88	0.999788	1.008403	1.002678
305.38	0.998915	1.00424	1.001966
305.88	0.999073	1.000001	1.000247
306.38	1.001692	0.996313	0.997222
306.88	1.003285	0.992486	0.994022
307.38	1.002994	0.987593	0.992686
307.88	1.002029	0.985915	0.995135

Fig. 1.1.b.

	BITUMINOUS COAL	LIGNITE COAL	MELANOIDIN	SHALE
272.88	-0.00083	-1.7E-05	0.000265	-0.00148

273.38	-0.00101	-0.00064	0.000153	-0.00077
273.88	-0.00077	-0.00111	0.000282	-0.00123
274.38	-0.00025	0.00061	0.000535	-0.00072
274.88	-0.00022	-0.00098	0.000305	-0.0005
275.38	-0.00018	-0.00073	-1E-05	0.000256
275.88	0.000375	0.001185	-0.00018	0.002462
276.38	0.000832	0.000274	-0.00027	0.003103
276.88	0.000658	0.00082	-0.00037	0.001737
277.38	0.000224	0.000738	-0.00055	0.000696
277.88	0.000106	-0.00064	-0.00049	0.000301
278.38	0.000243	-0.00095	-6.4E-05	-0.00017
278.88	0.000305	-0.00016	0.000499	-0.00034
279.38	0.000103	-0.00014	0.000591	-0.00041
279.88	-0.00018	-0.00195	0.000449	-0.00037
280.38	-0.00014	0.000826	0.000852	0.000779
280.88	-9.9E-05	0.001231	0.001259	0.001434
280.98	-0.00042	-0.00052	0.001397	-0.00146
281.08	-0.00042	-0.00054	0.001774	-0.0019
281.18	-0.00024	0.001053	0.002072	-0.0013
281.28	-0.00047	-0.00086	0.001855	-0.0018
281.38	-0.00073	-0.00022	0.001717	-0.00188
281.48	-0.00077	-0.00027	0.00181	-0.0016
281.58	-0.00062	-8.3E-05	0.001739	-0.0016
281.68	-0.00023	-0.00065	0.001905	-0.00065
281.78	0.000398	0.000636	0.002558	0.001354
281.88	0.001018	0.00101	0.003081	0.002608
281.98	0.001478	0.000258	0.003398	0.003439
282.08	0.002064	0.001054	0.004144	0.005225
282.18	0.002868	0.003335	0.004857	0.006499
282.28	0.003292	0.000858	0.005115	0.006326
282.38	0.00328	0.000552	0.005574	0.006174
282.48	0.003773	-0.00059	0.00637	0.005754
282.58	0.004955	-0.00198	0.007574	0.004894
282.68	0.00651	-0.00209	0.009301	0.004562
282.78	0.008398	-0.00327	0.011622	0.005582
282.88	0.010037	-0.00168	0.015189	0.008417
282.98	0.011366	-0.00213	0.020739	0.012014
283.08	0.014677	0.001539	0.030384	0.020673
283.18	0.024257	0.020218	0.047193	0.043969
283.28	0.042284	0.058407	0.071219	0.083248
283.38	0.068067	0.10727	0.099268	0.133096
283.48	0.102634	0.160766	0.126484	0.181405
283.58	0.148821	0.20156	0.147352	0.212967
283.68	0.20885	0.233106	0.160646	0.229301
283.78	0.282865	0.257963	0.17024	0.24067

283.88	0.366248	0.277211	0.178414	0.248361
283.98	0.454463	0.291045	0.174407	0.252182
284.08	0.54359	0.30233	0.185064	0.259674
284.18	0.631341	0.321334	0.200042	0.277243
284.28	0.714591	0.348255	0.219527	0.308408
284.38	0.7885	0.380893	0.241973	0.354609
284.48	0.847765	0.418883	0.263052	0.414356
284.58	0.893518	0.456233	0.281663	0.478666
284.68	0.9229	0.48504	0.298262	0.53784
284.78	0.934373	0.510373	0.311193	0.584208
284.88	0.9334	0.520941	0.321065	0.611644
284.98	0.920243	0.521733	0.330634	0.619205
285.08	0.895335	0.512838	0.340587	0.607008
285.18	0.860599	0.493779	0.35157	0.577205
285.28	0.815003	0.471508	0.363409	0.535797
285.38	0.763157	0.447482	0.375846	0.488811
285.48	0.712368	0.421459	0.390677	0.442776
285.58	0.665353	0.405162	0.407745	0.404713
285.68	0.623714	0.395618	0.426975	0.376311
285.78	0.590469	0.389808	0.45065	0.357725
285.88	0.56556	0.395359	0.477132	0.350577
285.98	0.546729	0.401704	0.502184	0.352065
286.08	0.533435	0.41582	0.525173	0.361054
286.18	0.525105	0.429749	0.544838	0.379542
286.28	0.522387	0.445594	0.556535	0.409291
286.38	0.525621	0.462753	0.558231	0.452556
286.48	0.533444	0.477025	0.551514	0.512091
286.58	0.545698	0.493399	0.538222	0.591393
286.68	0.560659	0.509106	0.521536	0.682482
286.78	0.575967	0.519993	0.504842	0.765799
286.88	0.589898	0.529875	0.490214	0.830498
286.98	0.601227	0.537833	0.480242	0.873003
287.08	0.610106	0.543466	0.476922	0.893675
287.18	0.616569	0.549013	0.480308	0.902522
287.28	0.621355	0.561176	0.489764	0.906436
287.38	0.625117	0.570118	0.504793	0.907027
287.48	0.628126	0.584504	0.523775	0.907841
287.58	0.630983	0.601996	0.545259	0.906975
287.68	0.635103	0.615522	0.568731	0.902462
287.78	0.640753	0.63561	0.592453	0.898813
287.88	0.646272	0.653224	0.615381	0.899289
287.98	0.650387	0.678587	0.637539	0.903082
288.08	0.655415	0.694473	0.658588	0.905522
288.18	0.662269	0.70921	0.677634	0.905225
288.28	0.668545	0.717201	0.692064	0.9038

288.38	0.674188	0.718394	0.701649	0.90039
288.48	0.680699	0.708764	0.70857	0.895793
288.58	0.688778	0.698412	0.713644	0.891789
288.68	0.697039	0.693437	0.71874	0.889534
288.78	0.705012	0.687881	0.726263	0.888435
288.88	0.71397	0.687977	0.73718	0.889412
288.98	0.724237	0.691438	0.74973	0.89389
289.08	0.734783	0.696515	0.763555	0.900042
289.18	0.746336	0.702965	0.778936	0.908283
289.28	0.760003	0.71476	0.793244	0.918514
289.38	0.774175	0.724642	0.804852	0.927464
289.48	0.788856	0.734115	0.813681	0.937358
289.58	0.806409	0.750502	0.821253	0.951358
289.68	0.826666	0.764528	0.829492	0.971395
289.78	0.847319	0.780494	0.838729	0.999589
289.88	0.868848	0.794417	0.847817	1.031666
289.98	0.890602	0.808144	0.856836	1.06479
290.08	0.910723	0.822577	0.865927	1.094922
290.18	0.931448	0.839933	0.874096	1.116982
290.28	0.951462	0.852162	0.882454	1.13018
290.38	0.968315	0.863833	0.892252	1.134787
290.48	0.984514	0.875871	0.901069	1.136165
290.58	1.000962	0.884441	0.908682	1.140723
290.68	1.017877	0.896661	0.917106	1.148913
290.78	1.036249	0.909266	0.924677	1.156652
290.88	1.055074	0.919308	0.930166	1.163497
290.98	1.071848	0.933755	0.935741	1.170634
291.08	1.085442	0.943919	0.942813	1.175831
291.18	1.095083	0.950994	0.947744	1.175736
291.28	1.100539	0.957702	0.949547	1.169419
291.38	1.10297	0.962416	0.952085	1.162256
291.48	1.101781	0.96568	0.954433	1.155737
291.58	1.098362	0.963994	0.954716	1.145788
291.68	1.094924	0.964435	0.955136	1.134642
291.78	1.09156	0.964747	0.956779	1.128646
291.88	1.088895	0.96441	0.958902	1.127796
291.98	1.086692	0.963782	0.961319	1.126975
292.08	1.08377	0.967592	0.963386	1.120506
292.18	1.080152	0.966248	0.964713	1.108469
292.28	1.077706	0.968578	0.966665	1.099232
292.38	1.076863	0.969803	0.969036	1.094732
292.48	1.074732	0.969394	0.97008	1.089593
292.58	1.070862	0.96986	0.970087	1.082532
292.68	1.066557	0.97081	0.970247	1.075529
292.78	1.062909	0.97134	0.970673	1.070141

292.88	1.056408	0.972036	0.972173	1.061601
293.38	1.042622	0.971988	0.975238	1.050425
293.88	1.027684	0.97254	0.977888	1.036234
294.38	1.016392	0.972275	0.979572	1.024731
294.88	1.00729	0.974301	0.979985	1.014036
295.38	0.999635	0.974369	0.979424	1.00276
295.88	0.993964	0.976671	0.980165	0.995458
296.38	0.990789	0.982053	0.982106	0.997444
296.88	0.988251	0.984407	0.983203	1.002289
297.38	0.985163	0.985011	0.983698	0.998819
297.88	0.983745	0.984734	0.984096	0.991423
298.38	0.985906	0.98601	0.985492	0.98946
298.88	0.990455	0.987596	0.988854	0.992498
299.38	0.994801	0.991483	0.991335	0.998679
299.88	0.997459	0.997044	0.993116	1.001757
300.38	0.998	0.997166	0.997135	1.000089
300.88	0.998593	0.999077	1.001256	1.000828
301.38	1.001595	1.004429	1.003711	1.002647
301.88	1.004767	1.006211	1.006002	1.003401
302.38	1.006343	1.008379	1.008737	1.004747
302.88	1.006653	1.009513	1.010309	1.00429
303.38	1.006117	1.007557	1.009327	1.001098
303.88	1.005122	1.006981	1.007361	0.998025
304.38	1.003713	1.004323	1.006105	0.997491
304.88	1.002465	1.003204	1.003775	0.997332
305.38	1.002036	1.00154	1.000025	0.997116
305.88	1.001326	0.999203	0.997159	0.999078
306.38	0.999056	0.997358	0.995203	0.999797
306.88	0.996506	0.994507	0.993977	0.999074
307.38	0.993813	0.992458	0.993462	0.998444
307.88	0.991179	0.991973	0.993152	0.998442

Fig. 1.1.c.

	AEROSOL	DISSOLVED ORGANIC MATTER	VERTISOL	CHERNOZEM		MARINE SEDIMENT
272.88	0.000237	0.000383	0.001745	0.001615	272.88	7.78E-05
273.38	-0.00015	0.00056	0.011169	0.006336	272.98	-0.00119
273.88	-0.0003	0.00053	0.004176	0.006472	273.08	-0.0016
274.38	-0.00025	0.00042	0.006642	0.002606	273.18	-0.00119
274.88	-0.0004	0.000203	0.000392	-0.00019	273.28	-0.00034
275.38	-0.00067	-9.3E-05	-0.00205	-0.00154	273.38	0.000224

275.88	-0.0005	-0.00038	-0.01477	-0.00179	273.48	-0.00039
276.38	0.000211	-0.00031	0.003044	-0.00038	273.58	-0.00274
276.88	0.000489	-9.9E-05	-0.00158	-0.00145	273.68	-0.00651
277.38	0.00031	-0.0003	-0.00944	-0.00606	273.78	-0.01047
277.88	0.000358	-0.0005	0.004033	-0.00776	273.88	-0.01308
278.38	0.00049	-0.00055	0.009532	-0.00374	273.98	-0.01332
278.88	0.000604	-0.00054	0.009417	0.00164	274.08	-0.01119
279.38	0.000529	-0.00064	0.013784	0.004519	274.18	-0.00767
279.88	0.000387	-0.00087	0.021077	0.007692	274.28	-0.00407
280.38	0.00072	-0.0007	0.016002	0.014132	274.38	-0.00147
280.88	0.000833	-0.00037	0.034478	0.018525	274.48	-0.0003
280.98	0.000233	-0.00035	0.050541	0.015247	274.58	-0.00041
281.08	3.81E-06	-0.00026	0.050638	0.013087	274.68	-0.00138
281.18	4.74E-05	-5.1E-05	0.052618	0.013213	274.78	-0.00277
281.28	-0.00022	-1.2E-05	0.0616	0.012948	274.88	-0.00424
281.38	-0.00032	7.62E-05	0.062457	0.013966	274.98	-0.00557
281.48	-0.00032	0.000211	0.070281	0.017722	275.08	-0.00671
281.58	-0.00042	0.000308	0.073101	0.022908	275.18	-0.00773
281.68	-0.00047	0.000487	0.075143	0.02828	275.28	-0.00877
281.78	-0.00045	0.000707	0.086264	0.032771	275.38	-0.00985
281.88	-0.00048	0.000912	0.090277	0.034629	275.48	-0.01082
281.98	-0.00051	0.001221	0.100603	0.035235	275.58	-0.01136
282.08	-0.00032	0.001732	0.107463	0.039325	275.68	-0.01116
282.18	-0.00052	0.002114	0.12555	0.044877	275.78	-0.01009
282.28	-0.00142	0.002129	0.133974	0.046951	275.88	-0.00834
282.38	-0.00216	0.002293	0.158312	0.049118	275.98	-0.00628
282.48	-0.00286	0.002522	0.182675	0.05653	276.08	-0.00429
282.58	-0.0038	0.002757	0.213324	0.070701	276.18	-0.00262
282.68	-0.00471	0.003516	0.252292	0.092298	276.28	-0.00136
282.78	-0.00558	0.004718	0.304025	0.118939	276.38	-0.00045
282.88	-0.00641	0.00621	0.360531	0.146545	276.48	0.000237
282.98	-0.00693	0.008258	0.437857	0.176342	276.58	0.000831
283.08	-0.00469	0.01196	0.516031	0.217719	276.68	0.001277
283.18	0.004698	0.018539	0.663115	0.277541	276.78	0.001324
283.28	0.022877	0.027523	0.58339	0.347035	276.88	0.000703
283.38	0.046855	0.038188	0.516677	0.411575	276.98	-0.00059
283.48	0.071334	0.049351	0.427218	0.465089	277.08	-0.00221
283.58	0.092088	0.059114	0.363795	0.497447	277.18	-0.00361
283.68	0.108165	0.068307	0.322009	0.494245	277.28	-0.0044
283.78	0.121386	0.079109	0.30182	0.463933	277.38	-0.00451
283.88	0.132715	0.091821	0.265126	0.427943	277.48	-0.00415
283.98	0.139659	0.087893	0.259319	0.392427	277.58	-0.00369
284.08	0.151377	0.106151	0.253062	0.360036	277.68	-0.00345
284.18	0.167235	0.128801	0.257811	0.329548	277.78	-0.00355
284.28	0.190095	0.155695	0.260217	0.307177	277.88	-0.00388

284.38	0.221245	0.186462	0.264488	0.299583	277.98	-0.0041
284.48	0.257758	0.21926	0.252122	0.303849	278.08	-0.00383
284.58	0.295576	0.252586	0.26869	0.313324	278.18	-0.00279
284.68	0.329699	0.283777	0.264493	0.32988	278.28	-0.00099
284.78	0.355063	0.306727	0.268455	0.352537	278.38	0.00127
284.88	0.367996	0.31835	0.273	0.368082	278.48	0.003479
284.98	0.367185	0.31865	0.276936	0.36861	278.58	0.00509
285.08	0.353716	0.308784	0.286944	0.358276	278.68	0.005733
285.18	0.330178	0.293243	0.302956	0.341866	278.78	0.005398
285.28	0.301188	0.275744	0.313397	0.322352	278.88	0.004481
285.38	0.271529	0.259013	0.324962	0.301321	278.98	0.003651
285.48	0.245562	0.245937	0.348487	0.280508	279.08	0.003562
285.58	0.227054	0.238745	0.362421	0.26478	279.18	0.004539
285.68	0.216714	0.2398	0.373155	0.257616	279.28	0.006392
285.78	0.213984	0.251581	0.40712	0.257748	279.38	0.008495
285.88	0.218203	0.274209	0.427649	0.263205	279.48	0.010084
285.98	0.227785	0.305654	0.447249	0.273121	279.58	0.010614
286.08	0.241386	0.344565	0.460511	0.28329	279.68	0.009972
286.18	0.258306	0.387631	0.467479	0.290189	279.78	0.008473
286.28	0.277873	0.426986	0.479883	0.298228	279.88	0.006671
286.38	0.300309	0.455822	0.488239	0.307872	279.98	0.005119
286.48	0.328026	0.472348	0.501545	0.312849	280.08	0.004174
286.58	0.363365	0.477167	0.517574	0.314224	280.18	0.003896
286.68	0.404994	0.473672	0.540896	0.313715	280.28	0.004062
286.78	0.448503	0.465552	0.556147	0.309527	280.38	0.004279
286.88	0.490395	0.455347	0.586435	0.304594	280.48	0.004207
286.98	0.528049	0.446554	0.615008	0.3001	280.58	0.003781
287.08	0.559898	0.441182	0.644227	0.295646	280.68	0.003277
287.18	0.587734	0.440334	0.690684	0.295986	280.78	0.003102
287.28	0.614026	0.445867	0.735859	0.304372	280.88	0.00346
287.38	0.639024	0.459193	0.782705	0.322286	280.98	0.004141
287.48	0.663165	0.480777	0.83359	0.353929	281.08	0.004627
287.58	0.686235	0.510596	0.879614	0.399192	281.18	0.004415
287.68	0.706415	0.548643	0.916568	0.45546	281.28	0.003329
287.78	0.723664	0.595365	0.945778	0.525272	281.38	0.001604
287.88	0.738627	0.651591	0.967084	0.606536	281.48	-0.00026
287.98	0.749885	0.713733	0.960031	0.679495	281.58	-0.00177
288.08	0.755979	0.775328	0.969783	0.719537	281.68	-0.00265
288.18	0.758878	0.828703	0.946226	0.725718	281.78	-0.00281
288.28	0.760402	0.863076	0.9302	0.713289	281.88	-0.00227
288.38	0.759665	0.872856	0.905113	0.690565	281.98	-0.00104
288.48	0.757602	0.859137	0.894436	0.664754	282.08	0.000856
288.58	0.758726	0.829038	0.886454	0.64337	282.18	0.003288
288.68	0.765894	0.794991	0.877156	0.627442	282.28	0.006051
288.78	0.778298	0.766291	0.89658	0.617794	282.38	0.009014

288.88	0.795044	0.746632	0.910319	0.617635	282.48	0.012237
288.98	0.813679	0.735309	0.931484	0.627079	282.58	0.015931
289.08	0.831841	0.732099	0.929028	0.641826	282.68	0.020326
289.18	0.848643	0.736809	0.958379	0.655619	282.78	0.025572
289.28	0.862549	0.745541	0.948842	0.664275	282.88	0.031749
289.38	0.870374	0.755395	0.986255	0.67061	282.98	0.038918
289.48	0.872333	0.766706	0.995689	0.680589	283.08	0.04713
289.58	0.875124	0.778956	1.017323	0.694591	283.18	0.056341
289.68	0.88043	0.791502	1.034537	0.711082	283.28	0.066241
289.78	0.885756	0.804305	1.060104	0.729564	283.38	0.076125
289.88	0.893187	0.815927	1.065542	0.746512	283.48	0.084937
289.98	0.903114	0.8274	1.088104	0.762859	283.58	0.09156
290.08	0.91285	0.838973	1.086497	0.784024	283.68	0.095285
290.18	0.923089	0.848566	1.090503	0.807352	283.78	0.096218
290.28	0.934346	0.857363	1.086562	0.825758	283.88	0.095391
290.38	0.945231	0.866736	1.091019	0.835533	283.98	0.094426
290.48	0.954909	0.874695	1.071837	0.83631	284.08	0.094886
290.58	0.964067	0.881475	1.048686	0.834341	284.18	0.097653
290.68	0.975021	0.888046	1.048697	0.837884	284.28	0.102658
290.78	0.985457	0.89291	1.03161	0.845701	284.38	0.109046
290.88	0.993396	0.895664	1.007478	0.850747	284.48	0.115513
290.98	1.002406	0.898628	0.988756	0.850037	284.58	0.12055
291.08	1.012024	0.903148	0.992868	0.84406	284.68	0.12256
291.18	1.019337	0.906979	0.978982	0.835047	284.78	0.120068
291.28	1.025964	0.909968	0.968375	0.827236	284.88	0.112195
291.38	1.032173	0.913807	0.960067	0.822736	284.98	0.099177
291.48	1.033951	0.917883	0.958848	0.81918	285.08	0.082569
291.58	1.033339	0.920766	0.947738	0.81531	285.18	0.064895
291.68	1.034235	0.923322	0.943019	0.813048	285.28	0.04889
291.78	1.035502	0.926676	0.935762	0.81157	285.38	0.036733
291.88	1.036533	0.930039	0.923158	0.809648	285.48	0.029602
291.98	1.037634	0.933044	0.927031	0.809393	285.58	0.027669
292.08	1.038377	0.935634	0.917309	0.811518	285.68	0.030419
292.18	1.03821	0.937604	0.907851	0.814368	285.78	0.037077
292.28	1.03839	0.93986	0.899578	0.816438	285.88	0.046947
292.38	1.039086	0.942611	0.900172	0.818302	285.98	0.059569
292.48	1.038108	0.944245	0.893782	0.821268	286.08	0.074683
292.58	1.035447	0.945015	0.891226	0.824464	286.18	0.092116
292.68	1.033396	0.946649	0.889599	0.826886	286.28	0.111759
292.78	1.032317	0.948837	0.887149	0.829636	286.38	0.133677
292.88	1.030629	0.95345	0.877512	0.834005	286.48	0.158242
293.38	1.028248	0.963109	0.879217	0.852086	286.58	0.18611
293.88	1.023446	0.972785	0.902537	0.866669	286.68	0.217968
294.38	1.015105	0.979369	0.941061	0.877265	286.78	0.254165
294.88	1.007061	0.984222	1.111703	0.887052	286.88	0.294401

295.38	1.002107	0.987672	1.108131	0.897963	286.98	0.337619
295.88	0.999733	0.99078	0.916421	0.910786	287.08	0.382181
296.38	0.998769	0.994492	0.909312	0.935242	287.18	0.426365
296.88	0.998385	0.997571	0.953804	0.972487	287.28	0.469011
297.38	0.99682	0.9986	1.050851	0.985655	287.38	0.510032
297.88	0.994357	0.997922	1.180836	0.955994	287.48	0.550475
298.38	0.993023	0.997527	1.011917	0.929791	287.58	0.592034
298.88	0.993864	0.997875	0.98894	0.950631	287.68	0.636216
299.38	0.997066	0.996731	0.988868	1.006973	287.78	0.683526
299.88	0.99977	0.995708	0.975863	1.045056	287.88	0.733017
300.38	1.000252	0.997605	0.990643	1.030876	287.98	0.783319
300.88	1.000828	0.999429	0.991552	0.997948	288.08	0.829858
301.38	1.002889	1.000341	0.99408	0.985395	288.18	0.868371
301.88	1.004514	1.002848	0.979094	0.989089	288.28	0.894626
302.38	1.004701	1.005825	0.979677	0.995133	288.38	0.905631
302.88	1.004131	1.007131	0.987871	0.998961	288.48	0.900963
303.38	1.002607	1.006274	0.975007	1.000014	288.58	0.883421
303.88	1.000343	1.003995	0.97894	0.999925	288.68	0.858347
304.38	0.998117	1.001993	0.999033	1.000847	288.78	0.831844
304.88	0.996275	0.99924	1.010613	1.003252	288.88	0.808889
305.38	0.994644	0.99459	1.021061	1.007129	288.98	0.79234
305.88	0.993614	0.990415	1.032039	1.013322	289.08	0.783047
306.38	0.993058	0.988156	1.010613	1.022285	289.18	0.780491
306.88	0.992944	0.987165	1.021061	1.033959	289.28	0.783259
307.38	0.994507	0.985974	1.032039	1.046909	289.38	0.789261
307.88	0.996572	0.984514	1.032039	1.060585	289.48	0.796074
					289.58	0.801616
					289.68	0.804871
					289.78	0.806181
					289.88	0.806932
					289.98	0.808805
					290.08	0.812994
					290.18	0.81974
					290.28	0.828322
					290.38	0.837373
					290.48	0.845288
					290.58	0.850663
					290.68	0.852828
					290.78	0.852335
					290.88	0.850975
					290.98	0.851081
					291.08	0.85446
					291.18	0.861683
					291.28	0.872129
					291.38	0.884641

					291.48	0.898271
					291.58	0.912724
					291.68	0.928352
					291.78	0.945764
					291.88	0.965289
					291.98	0.986571
					292.08	1.008558
					292.18	1.029972
					292.28	1.049993
					292.38	1.068673
					292.48	1.086692
					292.58	1.104672
					292.68	1.12263
					292.78	1.139992
					292.88	1.156011
					292.98	1.170094
					293.08	1.181786
					293.18	1.19061
					293.28	1.196078
					293.38	1.197944
					293.48	1.196503
					293.58	1.192644
					293.68	1.187582
					293.78	1.182331
					293.88	1.177165
					293.98	1.171395
					294.08	1.163723
					294.18	1.153125
					294.28	1.139754
					294.38	1.125255
					294.48	1.112197
					294.58	1.102932
					294.68	1.098535
					294.78	1.098394
					294.88	1.100623
					294.98	1.103065
					295.08	1.104334
					295.18	1.104311
					295.28	1.103828
					295.38	1.103812
					295.48	1.104544
					295.58	1.105498
					295.68	1.10572
					295.78	1.104343
					295.88	1.100924

					295.98	1.095547
					296.08	1.088751
					296.18	1.081335
					296.28	1.074108
					296.38	1.067733
					296.48	1.062793
					296.58	1.059946
					296.68	1.05985
					296.78	1.062699
					296.88	1.067661
					296.98	1.072848
					297.08	1.076159
					297.18	1.076557
					297.28	1.074781
					297.38	1.072835
					297.48	1.072603
					297.58	1.074668
					297.68	1.078175
					297.78	1.081632
					297.88	1.083826
					297.98	1.084182
					298.08	1.08255
					298.18	1.078906
					298.28	1.07332
					298.38	1.066162
					298.48	1.058259
					298.58	1.050861
					298.68	1.045382
					298.78	1.042992
					298.88	1.044182
					298.98	1.048571
					299.08	1.055134
					299.18	1.062703
					299.28	1.070376
					299.38	1.077517
					299.48	1.083491
					299.58	1.087528
					299.68	1.088952
					299.78	1.087582
					299.88	1.083893
					299.98	1.078774
					300.08	1.073128
					300.18	1.067637
					300.28	1.062787
					300.38	1.058943

					300.48	1.056239
					300.58	1.054369
					300.68	1.052563
					300.78	1.049962
					300.88	1.046204
					300.98	1.041758
					301.08	1.037681
					301.18	1.03499
					301.28	1.034105
					301.38	1.034728
					301.48	1.036119
					301.58	1.037506
					301.68	1.038374
					301.78	1.038524
					301.88	1.037983
					301.98	1.036883
					302.08	1.035419
					302.18	1.033855
					302.28	1.032451
					302.38	1.031336
					302.48	1.030387
					302.58	1.029266
					302.68	1.027576
					302.78	1.025067
					302.88	1.021764
					302.98	1.017989
					303.08	1.014258
					303.18	1.011082
					303.28	1.008741
					303.38	1.007143
					303.48	1.005866
					303.58	1.004375
					303.68	1.002308
					303.78	0.999635
					303.88	0.996629
					303.98	0.993702
					304.08	0.991224
					304.18	0.989414
					304.28	0.988333
					304.38	0.987948
					304.48	0.988222
					304.58	0.989194
					304.68	0.990949
					304.78	0.993474
					304.88	0.996479

					304.98	0.999351
					305.08	1.001343
					305.18	1.001896
					305.28	1.000854
					305.38	0.998452
					305.48	0.995149
					305.58	0.991535
					305.68	0.988374
					305.78	0.986576
					305.88	0.986901
					305.98	0.989516
					306.08	0.993787
					306.18	0.998504
					306.28	1.002392
					306.38	1.004552
					306.48	1.004686
					306.58	1.00311
					306.68	1.000614
					306.78	0.9982
					306.88	0.996764
					306.98	0.996821
					307.08	0.998354
					307.18	1.000845
					307.28	1.003517
					307.38	1.005727
					307.48	1.007306
					307.58	1.008594
					307.68	1.010136
					307.78	1.0123
					307.88	1.015116

Fig. 1.2.

	AEROSOL	VERTISOL	CHERNOZEM	MARINE SEDIMENT	DISSOLVED ORGANIC MATTER
272.88	0.007673	0.017697	0.01004	0.013374	0.002793
273.38	0.00443	0.00725	0.00481	0.003446	0.002237
273.88	0.002326	-0.00277	0.00249	-3.7E-05	0.001252
274.38	0.001056	-0.00727	-0.0063	-0.0071	0.00019
274.88	6.17E-05	-0.00841	-0.01129	-0.01188	-0.00078
275.38	-0.00072	-0.0104	-0.00591	-0.00643	-0.00082
275.88	-0.0016	-0.01173	-0.0024	-0.00151	-0.00043
276.38	-0.00187	-0.00864	-0.00307	-0.00115	-6.7E-05
276.88	-0.00172	-0.00112	-0.00323	-0.0022	-0.00015

277.38	-0.00122	0.008375	0.003018	0.002597	-0.00036
277.88	1.79E-05	0.017013	0.011838	0.010896	0.001163
278.38	0.001257	0.022881	0.016592	0.016944	0.003104
278.88	0.002415	0.0284	0.022264	0.020985	0.004273
279.38	0.003833	0.038134	0.029086	0.025821	0.006689
279.88	0.005059	0.051732	0.030989	0.032834	0.010506
280.38	0.006289	0.06423	0.033088	0.035855	0.014982
280.88	0.007821	0.07038	0.040614	0.036181	0.019378
280.98	0.009637	0.071027	0.044814	0.038167	0.021555
281.08	0.010702	0.065816	0.043676	0.038371	0.022531
281.18	0.012141	0.063185	0.046923	0.040361	0.024296
281.28	0.013832	0.066271	0.052929	0.046279	0.02617
281.38	0.015212	0.070686	0.057158	0.04809	0.027142
281.48	0.015549	0.072543	0.056709	0.047235	0.028413
281.58	0.016022	0.071689	0.054466	0.04576	0.031026
281.68	0.017849	0.069766	0.059945	0.044226	0.033829
281.78	0.020127	0.070172	0.067679	0.0486	0.035669
281.88	0.022143	0.076171	0.071817	0.055074	0.037114
281.98	0.024754	0.085987	0.077185	0.060395	0.039358
282.08	0.02806	0.094079	0.086155	0.065618	0.042314
282.18	0.030872	0.098528	0.092054	0.068675	0.046598
282.28	0.032899	0.101672	0.092502	0.067122	0.051505
282.38	0.035213	0.104913	0.094953	0.067817	0.05549
282.48	0.038506	0.108966	0.095209	0.070355	0.059124
282.58	0.042694	0.115351	0.101046	0.0735	0.063361
282.68	0.047411	0.12383	0.113201	0.080437	0.06975
282.78	0.053121	0.132136	0.11378	0.084355	0.078119
282.88	0.061081	0.136926	0.122099	0.099108	0.085907
282.98	0.070321	0.137651	0.13977	0.123243	0.093673
283.08	0.079739	0.144806	0.14792	0.145007	0.106086
283.18	0.092392	0.168057	0.165067	0.183389	0.127655
283.28	0.11232	0.217902	0.192991	0.239831	0.158507
283.38	0.142919	0.289524	0.229383	0.296328	0.196515
283.48	0.189313	0.379526	0.282721	0.34642	0.241104
283.58	0.250539	0.471947	0.341451	0.39214	0.291819
283.68	0.320134	0.555457	0.410577	0.43233	0.348531
283.78	0.392573	0.615965	0.495411	0.45679	0.408782
283.88	0.461565	0.656365	0.577396	0.472458	0.466873
283.98	0.522072	0.689841	0.631228	0.498018	0.523086
284.08	0.575769	0.722771	0.657644	0.526201	0.576763
284.18	0.621811	0.743917	0.672391	0.550361	0.625369
284.28	0.66311	0.745535	0.683776	0.566313	0.67236
284.38	0.702265	0.733758	0.693298	0.579561	0.722691
284.48	0.741623	0.713895	0.691819	0.587602	0.767615
284.58	0.780063	0.689438	0.682328	0.581911	0.802825

284.68	0.810561	0.667056	0.665793	0.566777	0.826683
284.78	0.833327	0.65045	0.646273	0.551214	0.826693
284.88	0.849976	0.639029	0.63929	0.536098	0.811536
284.98	0.85807	0.633446	0.640064	0.521526	0.797244
285.08	0.856265	0.638854	0.634074	0.504195	0.781023
285.18	0.842266	0.659262	0.633243	0.484622	0.763367
285.28	0.820254	0.688492	0.644048	0.472326	0.745418
285.38	0.797208	0.716514	0.661714	0.46939	0.729917
285.48	0.771511	0.740364	0.685988	0.473319	0.720359
285.58	0.745074	0.760151	0.706713	0.477211	0.719824
285.68	0.724522	0.775166	0.72375	0.48478	0.732449
285.78	0.71107	0.784539	0.745551	0.503194	0.759834
285.88	0.704245	0.781342	0.773952	0.527301	0.806051
285.98	0.702699	0.756107	0.792959	0.548638	0.868316
286.08	0.704497	0.710995	0.791193	0.560188	0.940434
286.18	0.708808	0.657853	0.780282	0.569498	1.010584
286.28	0.713897	0.607083	0.764023	0.577084	1.063417
286.38	0.716181	0.566612	0.727673	0.564272	1.089463
286.48	0.717892	0.539998	0.664909	0.528164	1.089289
286.58	0.724419	0.523499	0.586291	0.477668	1.073786
286.68	0.735514	0.515567	0.504282	0.422809	1.045948
286.78	0.749144	0.522244	0.436703	0.37454	1.006044
286.88	0.765708	0.546166	0.39886	0.342619	0.960521
286.98	0.783554	0.583696	0.38344	0.329362	0.917108
287.08	0.79849	0.635059	0.381273	0.330078	0.883702
287.18	0.810272	0.704094	0.398231	0.343958	0.86484
287.28	0.823735	0.78997	0.431342	0.365183	0.855364
287.38	0.840516	0.886167	0.479262	0.39714	0.85433
287.48	0.860374	0.982676	0.556463	0.456026	0.873782
287.58	0.8835	1.067333	0.65155	0.535029	0.911718
287.68	0.903964	1.131477	0.741784	0.608955	0.959993
287.78	0.920797	1.173664	0.837987	0.679714	1.019855
287.88	0.936784	1.194041	0.941997	0.757814	1.086322
287.98	0.948106	1.191214	1.027459	0.824382	1.155397
288.08	0.954375	1.166259	1.077199	0.855508	1.220534
288.18	0.956564	1.12414	1.096428	0.85434	1.266708
288.28	0.954761	1.072705	1.093304	0.83626	1.293343
288.38	0.951059	1.020635	1.072379	0.811815	1.298176
288.48	0.94541	0.973103	1.038839	0.781929	1.271571
288.58	0.941989	0.930777	0.989864	0.743521	1.218962
288.68	0.943722	0.895456	0.932101	0.71121	1.160475
288.78	0.9489	0.873927	0.875752	0.676041	1.108331
288.88	0.958405	0.86932	0.834154	0.637517	1.065124
288.98	0.971098	0.87293	0.81827	0.626964	1.036518
289.08	0.984155	0.872983	0.800727	0.624735	1.019824

289.18	0.997383	0.865215	0.773582	0.622124	1.005006
289.28	1.00808	0.854559	0.755601	0.62796	0.99001
289.38	1.009112	0.851712	0.744929	0.632388	0.97737
289.48	1.002687	0.861496	0.735617	0.639887	0.97215
289.58	0.999422	0.874512	0.727996	0.644784	0.968494
289.68	0.999293	0.878815	0.731516	0.651916	0.964955
289.78	0.996663	0.877012	0.743873	0.66625	0.970902
289.88	0.996485	0.880233	0.757978	0.680515	0.978678
289.98	1.001142	0.890695	0.781822	0.70273	0.982893
290.08	1.005499	0.902178	0.817968	0.737677	0.985539
290.18	1.014089	0.907297	0.845627	0.771886	0.986568
290.28	1.025986	0.902749	0.846348	0.796051	0.98828
290.38	1.032637	0.896055	0.834482	0.817974	0.984668
290.48	1.037199	0.895342	0.824629	0.838432	0.979829
290.58	1.041384	0.896588	0.810694	0.84134	0.983266
290.68	1.046552	0.895223	0.796512	0.832083	0.985872
290.78	1.052547	0.894	0.794005	0.833197	0.984853
290.88	1.053757	0.892559	0.79258	0.84161	0.987012
290.98	1.053682	0.887365	0.782501	0.84106	0.990419
291.08	1.054049	0.880903	0.776977	0.826147	0.996263
291.18	1.053661	0.877016	0.77421	0.802399	1.008613
291.28	1.055184	0.873456	0.765653	0.782878	1.019322
291.38	1.055356	0.868887	0.759994	0.77381	1.01775
291.48	1.05096	0.867641	0.759231	0.768434	1.009479
291.58	1.048462	0.871149	0.765206	0.76571	1.007605
291.68	1.048013	0.874546	0.770998	0.764633	1.007541
291.78	1.04333	0.875484	0.763655	0.757863	1.008212
291.88	1.038742	0.878878	0.75887	0.749793	1.013617
291.98	1.037357	0.889134	0.759307	0.741657	1.014978
292.08	1.036816	0.901763	0.757905	0.736068	1.011223
292.18	1.037009	0.9075	0.760139	0.741517	1.006005
292.28	1.036033	0.904065	0.763327	0.745018	1.003822
292.38	1.034207	0.897326	0.766002	0.744017	1.006728
292.48	1.032551	0.888536	0.767233	0.745924	1.006631
292.58	1.029483	0.887174	0.766898	0.742277	1.001476
292.68	1.025561	0.881419	0.768598	0.738828	0.997028
292.78	1.022812	0.879079	0.779984	0.748373	0.99339
292.88	1.019396	0.878507	0.79216	0.752651	0.991499
293.38	1.018814	0.876485	0.794988	0.749539	0.990591
293.88	1.016213	0.889925	0.800132	0.758156	0.992978
294.38	1.010699	0.945057	0.811027	0.767727	1.000077
294.88	1.005302	1.025057	0.819305	0.777026	1.004091
295.38	1.003559	1.062138	0.823845	0.797286	1.005816
295.88	1.003128	1.022173	0.834355	0.82713	1.005489
296.38	1.002911	0.955926	0.915348	0.934028	1.005149

296.88	1.005005	0.936003	1.06629	1.094881	1.008559
297.38	1.00551	0.977895	1.086187	1.086053	1.0059
297.88	1.002513	1.031996	0.950739	0.933622	1.001391
298.38	0.998655	1.04756	0.871395	0.865559	1.001503
298.88	0.995221	1.03113	0.896256	0.90406	1.000841
299.38	0.997494	1.016467	1.003003	1.021516	1.001143
299.88	1.001862	1.011081	1.097697	1.109663	1.001985
300.38	1.000295	1.005256	1.062065	1.053133	1.001316
300.88	0.998349	0.997451	0.999828	0.98135	1.000125
301.38	1.000299	0.99118	0.984408	0.967777	0.99809
301.88	1.002509	0.987228	0.982715	0.96851	0.996147
302.38	1.003472	0.984926	0.986698	0.97965	0.996221
302.88	1.004573	0.984158	0.991568	0.992926	0.99881
303.38	1.004888	0.985159	0.997955	1.002189	1.00004
303.88	1.001984	0.988182	0.99913	1.007732	0.998379
304.38	0.997864	0.993473	0.998677	1.011494	1.000872
304.88	0.996569	1.000602	1.005868	1.020139	1.007145
305.38	0.996791	1.009179	1.015927	1.037425	1.004802
305.88	0.99783	1.021074	1.02408	1.055175	0.994083
		0.978414			0.98645
		0.98355			0.983319
		0.987271			0.980852
		0.987271			0.978036

Fig. 1.3.a.

	NMR ARYL	NEXAFS ARYL C
wood char	76.9	39.24883
grass char	73.9	41.44028
soot	75.9	45.87258
marine sediment	49.2	6
aerosol	37.6	19.42597
chernozem	54.9	40.42993
vertisol	53	38.07379
dissolved OM	24	22.38562
shale	18.8	26.13279
melanoidin	36.3	6.772908
lignite coal	61.8	33.47147
bituminous coal	85.3	46.10559

Fig. 1.3.b.

	NMR ARYL/O-ALKYL	NEXAFS ARYL/ALKYL-C
wood char	6.355372	1.73444
grass char	8.903614	1.777983
soot	5.540146	2.512898
marine sediment	2.226244	0.2
aerosol	1.446154	0.544118
chernozem	2.786802	1.624585
vertisol	2.304348	1.351866
dissolved OM	0.625	0.853051
shale	1.27027	0.854106
melanoidin	1.103343	0.268139
lignite coal	3.791411	1.310861
bituminous coal	16.72549	2.172414

Fig. 2.1.

	LG 18 SOIL		BC PIECES		MICROBE		PLANT LITTER
279	0.007806	278.63	-0.00519	278.63	-0.00046	278.68	0.016803
279.5	0.008569	279.13	-0.00012	279.13	-0.00046	279.18	0.016803
280	0.000909	279.63	-0.00079	279.63	0.001587	279.68	0.016803
280.5	0.000743	280.13	-1.3E-05	280.13	0.000287	280.18	0.016803
281	-0.0004	280.63	-0.00031	280.63	-0.00109	280.68	0.023031
281.5	-0.00068	281.13	0.0002	281.13	-0.00127	281.18	0.028802
281.55	-0.00409	281.18	0.000639	281.18	-0.00074	281.28	0.032897
281.6	-0.00176	281.23	-0.00012	281.23	-0.00164	281.38	0.035303
281.65	-0.00045	281.28	-0.00106	281.28	-0.00011	281.48	0.035997
281.7	-4.2E-05	281.33	-0.00039	281.33	0.000328	281.58	0.035456
281.75	-0.00012	281.38	0.000761	281.38	-0.00226	281.68	0.034528
281.8	0.000552	281.43	-0.0012	281.43	-0.00096	281.78	0.034098
281.85	0.002214	281.48	-0.00026	281.48	0.00086	281.88	0.034678
281.9	0.000737	281.53	0.002583	281.53	0.000333	281.98	0.036138
281.95	0.000813	281.58	0.000792	281.58	0.001032	282.08	0.037841
282	0.001578	281.63	-0.001	281.63	0.000885	282.18	0.039104
282.05	0.001668	281.68	0.001135	281.68	0.000576	282.28	0.039658
282.1	0.001909	281.73	-0.00019	281.73	-0.00013	282.38	0.039766
282.15	0.002881	281.78	-5.8E-05	281.78	0.001631	282.48	0.040006
282.2	0.000586	281.83	-0.00089	281.83	0.000752	282.58	0.040994
282.25	-0.00059	281.88	-0.00158	281.88	-4.1E-05	282.68	0.043243

282.3	0.001781	281.93	0.001039	281.93	0.001707	282.78	0.047091
282.35	0.000805	281.98	-0.0001	281.98	-0.00033	282.88	0.052575
282.4	0.002419	282.03	-0.0011	282.03	-4.1E-05	282.98	0.059471
282.45	0.004661	282.08	0.001693	282.08	-0.00196	283.08	0.067846
282.5	0.004287	282.13	0.001316	282.13	0.001	283.18	0.079028
282.55	0.003866	282.18	-0.00059	282.18	0.000791	283.28	0.096129
282.6	0.003689	282.23	0.001307	282.23	0.002473	283.38	0.123312
282.65	0.003696	282.28	-0.00017	282.28	0.001423	283.48	0.163945
282.7	0.002724	282.33	-0.00074	282.33	-0.00019	283.58	0.21887
282.75	0.003895	282.38	0.001897	282.38	0.002226	283.68	0.285949
282.8	0.003202	282.43	-0.00012	282.43	0.001082	283.78	0.360951
282.85	0.003356	282.48	0.003174	282.48	0.001224	283.88	0.438803
282.9	0.003974	282.53	0.004307	282.53	0.002996	283.98	0.515146
282.95	0.004491	282.58	0.003193	282.58	0.000469	284.08	0.586345
283	0.004697	282.63	0.003668	282.63	0.002379	284.18	0.64987
283.05	0.005535	282.68	0.006097	282.68	0.002379	284.28	0.704441
283.1	0.006132	282.73	0.005501	282.73	0.000512	284.38	0.75002
283.15	0.006857	282.78	0.007145	282.78	0.001249	284.48	0.787396
283.2	0.008772	282.83	0.006618	282.83	0.003382	284.58	0.817314
283.25	0.008616	282.88	0.008785	282.88	0.002294	284.68	0.839607
283.3	0.008889	282.93	0.009026	282.93	0.003245	284.78	0.852982
283.35	0.009408	282.98	0.012026	282.98	0.003021	284.88	0.85581
283.4	0.00798	283.03	0.013211	283.03	0.001463	284.98	0.84744
283.45	0.01615	283.08	0.010897	283.08	0.003753	285.08	0.829133
283.5	0.009534	283.13	0.014478	283.13	-0.00056	285.18	0.803977
283.55	0.012518	283.18	0.014351	283.18	1.94E-05	285.28	0.775953
283.6	0.01608	283.23	0.018818	283.23	0.001545	285.38	0.748811
283.65	0.016348	283.28	0.025595	283.28	0.000509	285.48	0.725345
283.7	0.017233	283.33	0.023462	283.33	-0.00068	285.58	0.707268
283.75	0.020915	283.38	0.024034	283.38	0.007807	285.68	0.695443
283.8	0.019886	283.43	0.030197	283.43	0.017	285.78	0.690092
283.85	0.019296	283.48	0.024996	283.48	0.024873	285.88	0.690774
283.9	0.022242	283.53	0.027014	283.53	0.041345	285.98	0.69629
283.95	0.021933	283.58	0.030093	283.58	0.059983	286.08	0.704771
284	0.022077	283.63	0.027464	283.63	0.081758	286.18	0.714069
284.05	0.023671	283.68	0.029823	283.68	0.10462	286.28	0.722262
284.1	0.025891	283.73	0.028075	283.73	0.129715	286.38	0.728024
284.15	0.028048	283.78	0.027916	283.78	0.153442	286.48	0.730704
284.2	0.025567	283.83	0.028205	283.83	0.177872	286.58	0.730116
284.25	0.029412	283.88	0.031775	283.88	0.204131	286.68	0.72622
284.3	0.033234	283.93	0.032427	283.93	0.229055	286.78	0.718952
284.35	0.035872	283.98	0.033952	283.98	0.254192	286.88	0.708367
284.4	0.036862	284.03	0.035206	284.03	0.279417	286.98	0.694994
284.45	0.042814	284.08	0.037426	284.08	0.302072	287.08	0.680153
284.5	0.047412	284.13	0.043807	284.13	0.326561	287.18	0.665996

284.55	0.051276	284.18	0.049954	284.18	0.34637	287.28	0.655261
284.6	0.05315	284.23	0.051785	284.23	0.364772	287.38	0.650853
284.65	0.061352	284.28	0.056742	284.28	0.389969	287.48	0.655386
284.7	0.066983	284.33	0.062846	284.33	0.408852	287.58	0.670777
284.75	0.071039	284.38	0.0672	284.38	0.424366	287.68	0.697902
284.8	0.079842	284.43	0.073144	284.43	0.441908	287.78	0.736351
284.85	0.09446	284.48	0.078031	284.48	0.457294	287.88	0.784286
284.9	0.11269	284.53	0.084178	284.53	0.46828	287.98	0.838431
284.95	0.130916	284.58	0.09271	284.58	0.478492	288.08	0.894272
285	0.159094	284.63	0.101807	284.63	0.488547	288.18	0.946538
285.05	0.190168	284.68	0.113668	284.68	0.494113	288.28	0.990009
285.1	0.21791	284.73	0.125214	284.73	0.503588	288.38	1.020469
285.15	0.23632	284.78	0.141844	284.78	0.508602	288.48	1.035512
285.2	0.249679	284.83	0.163597	284.83	0.51279	288.58	1.034993
285.25	0.249839	284.88	0.186246	284.88	0.521477	288.68	1.021044
285.3	0.248372	284.93	0.208687	284.93	0.524358	288.78	0.997658
285.35	0.243001	284.98	0.230658	284.98	0.528174	288.88	0.969743
285.4	0.237835	285.03	0.250341	285.03	0.527887	288.98	0.941828
285.45	0.232346	285.08	0.264122	285.08	0.52127	289.08	0.916975
285.5	0.22515	285.13	0.272003	285.13	0.513623	289.18	0.89651
285.55	0.218346	285.18	0.277659	285.18	0.504132	289.28	0.880644
285.6	0.210388	285.23	0.278652	285.23	0.494295	289.38	0.869369
285.65	0.199278	285.28	0.278593	285.28	0.485298	289.48	0.862953
285.7	0.188017	285.33	0.282382	285.33	0.477755	289.58	0.861843
285.75	0.171797	285.38	0.278333	285.38	0.465827	289.68	0.866355
285.8	0.156339	285.43	0.271883	285.43	0.45866	289.78	0.876502
285.85	0.144072	285.48	0.266254	285.48	0.451326	289.88	0.892037
285.9	0.13319	285.53	0.25329	285.53	0.440956	289.98	0.912486
285.95	0.12278	285.58	0.24111	285.58	0.431233	290.08	0.937041
286	0.115871	285.63	0.223562	285.63	0.42541	290.18	0.964375
286.05	0.109484	285.68	0.212796	285.68	0.417463	290.28	0.992598
286.1	0.105713	285.73	0.20076	285.73	0.414505	290.38	1.01957
286.15	0.102914	285.78	0.189705	285.78	0.416141	290.48	1.043522
286.2	0.097853	285.83	0.184749	285.83	0.413815	290.58	1.063543
286.25	0.094668	285.88	0.178774	285.88	0.415884	290.68	1.079549
286.3	0.090017	285.93	0.176475	285.93	0.41809	290.78	1.091817
286.35	0.094786	285.98	0.174469	285.98	0.421218	290.88	1.10057
286.4	0.091938	286.03	0.179122	286.03	0.422337	290.98	1.105998
286.45	0.09346	286.08	0.179133	286.08	0.425142	291.08	1.108489
286.5	0.095147	286.13	0.184864	286.13	0.426445	291.18	1.108663
286.55	0.096424	286.18	0.192366	286.18	0.424922	291.28	1.107162
286.6	0.099294	286.23	0.199734	286.23	0.424097	291.38	1.104435
286.65	0.102633	286.28	0.206751	286.28	0.420883	291.48	1.100742
286.7	0.106466	286.33	0.218211	286.33	0.414271	291.58	1.096271
286.75	0.112075	286.38	0.227815	286.38	0.413517	291.68	1.091205

286.8	0.122447	286.43	0.238812	286.43	0.408602	291.78	1.085651
286.85	0.143931	286.48	0.249302	286.48	0.403359	291.88	1.079559
286.9	0.172188	286.53	0.261878	286.53	0.402472	291.98	1.072764
286.95	0.20736	286.58	0.274037	286.58	0.394844	292.08	1.065172
287	0.257749	286.63	0.28298	286.63	0.390489	292.18	1.057011
287.05	0.309344	286.68	0.295513	286.68	0.38735	292.28	1.048971
287.1	0.366305	286.73	0.308788	286.73	0.384535	292.38	1.042058
287.15	0.423175	286.78	0.319928	286.78	0.382879	292.48	1.037154
287.2	0.466129	286.83	0.341483	286.83	0.382614	292.58	1.034478
287.25	0.514434	286.88	0.359421	286.88	0.383552	292.68	1.033349
287.3	0.548864	286.93	0.382097	286.93	0.3863	292.78	1.032473
287.35	0.577928	286.98	0.399805	286.98	0.387922	292.88	1.03057
287.4	0.605377	287.03	0.419472	287.03	0.387862	292.98	1.026927
287.45	0.62743	287.08	0.427694	287.08	0.39166	293.08	1.02162
287.5	0.649067	287.13	0.444399	287.13	0.392218	293.18	1.015424
287.55	0.666638	287.18	0.449025	287.18	0.393431	293.68	1.009303
287.6	0.687625	287.23	0.45355	287.23	0.395899	294.18	1.004537
287.65	0.705879	287.28	0.45282	287.28	0.398618	294.68	1.001686
287.7	0.724655	287.33	0.448776	287.33	0.401328	295.18	1.000547
287.75	0.741109	287.38	0.449054	287.38	0.406922	295.68	1.000297
287.8	0.752477	287.43	0.446093	287.43	0.412279	296.18	0.999918
287.85	0.763172	287.48	0.445261	287.48	0.42011	296.68	0.998695
287.9	0.776199	287.53	0.444925	287.53	0.428887	297.18	0.996551
287.95	0.789316	287.58	0.444953	287.58	0.436757	297.68	0.994101
288	0.803996	287.63	0.453361	287.63	0.442735	298.18	0.992379
288.05	0.825215	287.68	0.458964	287.68	0.454852	298.68	0.992303
288.1	0.850848	287.73	0.474303	287.73	0.46753	299.18	0.994101
288.15	0.879109	287.78	0.486154	287.78	0.480593	299.68	0.997088
288.2	0.901186	287.83	0.505708	287.83	0.497361	300.18	1.00001
288.25	0.919218	287.88	0.529216	287.88	0.512599	300.68	1.0018
288.3	0.930699	287.93	0.556544	287.93	0.53113	301.18	1.002191
288.35	0.934123	287.98	0.58575	287.98	0.551348	301.68	1.00177
288.4	0.9316	288.03	0.618232	288.03	0.567565	302.18	1.001453
288.45	0.928063	288.08	0.64174	288.08	0.584428	302.68	1.001844
288.5	0.919471	288.13	0.660345	288.13	0.597619	303.18	1.002933
288.55	0.91209	288.18	0.675498	288.18	0.605246	303.68	1.004247
288.6	0.901159	288.23	0.687326	288.23	0.62068	304.18	1.005236
288.65	0.889545	288.28	0.692065	288.28	0.641776	304.68	1.005546
288.7	0.87364	288.33	0.708706	288.33	0.664635	305.18	1.005032
288.75	0.860497	288.38	0.718347	288.38	0.689974	305.68	1.003659
288.8	0.845978	288.43	0.729312	288.43	0.718801	306.18	1.001472
288.85	0.828497	288.48	0.731911	288.48	0.74213	306.68	0.998683
288.9	0.817295	288.53	0.734627	288.53	0.759773	307.18	0.995735
288.95	0.800931	288.58	0.736126	288.58	0.769229	307.68	0.993219
289	0.788738	288.63	0.736196	288.63	0.768951	308.18	0.991678

289.05	0.781464	288.68	0.735332	288.68	0.764814		
289.1	0.783552	288.73	0.736709	288.73	0.755362		
289.15	0.781443	288.78	0.740674	288.78	0.741396		
289.2	0.781229	288.83	0.741667	288.83	0.723809		
289.25	0.783926	288.88	0.749686	288.88	0.710156		
289.3	0.783999	288.93	0.759205	288.93	0.699302		
289.35	0.788586	288.98	0.762753	288.98	0.686785		
289.4	0.789417	289.03	0.771498	289.03	0.676463		
289.45	0.795666	289.08	0.78218	289.08	0.667129		
289.5	0.796056	289.13	0.788407	289.13	0.664432		
289.55	0.799974	289.18	0.795578	289.18	0.657688		
289.6	0.806225	289.23	0.796218	289.23	0.657362		
289.65	0.803849	289.28	0.801805	289.28	0.655981		
289.7	0.805503	289.33	0.803251	289.33	0.652324		
289.75	0.804297	289.38	0.799378	289.38	0.650678		
289.8	0.808155	289.43	0.800776	289.43	0.653369		
289.85	0.808797	289.48	0.798616	289.48	0.654093		
289.9	0.811694	289.53	0.796979	289.53	0.654475		
289.95	0.814379	289.58	0.79342	289.58	0.654686		
290	0.816414	289.63	0.789851	289.63	0.657429		
290.05	0.821482	289.68	0.787264	289.68	0.662053		
290.1	0.825398	289.73	0.78552	289.73	0.663875		
290.15	0.825821	289.78	0.781577	289.78	0.666053		
290.2	0.830095	289.83	0.77938	289.83	0.667309		
290.25	0.834296	289.88	0.775955	289.88	0.668931		
290.3	0.836193	289.93	0.772466	289.93	0.670092		
290.35	0.837679	289.98	0.772141	289.98	0.673258		
290.4	0.841385	290.03	0.769255	290.03	0.674557		
290.45	0.843605	290.08	0.763723	290.08	0.67998		
290.5	0.845742	290.13	0.769667	290.13	0.684224		
290.55	0.848091	290.18	0.765842	290.18	0.687471		
290.6	0.851487	290.23	0.7705	290.23	0.694414		
290.65	0.854788	290.28	0.770868	290.28	0.699386		
290.7	0.86103	290.33	0.773552	290.33	0.703849		
290.75	0.864469	290.38	0.779544	290.38	0.709086		
290.8	0.871589	290.43	0.790162	290.43	0.714414		
290.85	0.877087	290.48	0.794858	290.48	0.718796		
290.9	0.879742	290.53	0.800876	290.53	0.722965		
290.95	0.887774	290.58	0.806378	290.58	0.728986		
291	0.889525	290.63	0.808011	290.63	0.730903		
291.5	0.949582	291.13	0.840379	291.13	0.774204		
292	1.003436	291.63	0.887259	291.63	0.813841		
292.5	1.038026	292.13	0.943359	292.13	0.859945		
293	1.053102	292.63	0.978129	292.63	0.88779		
293.5	1.056796	293.13	0.999762	293.13	0.906557		

294	1.047505	293.63	1.010795	293.63	0.913859		
294.5	1.029631	294.13	1.016225	294.13	0.924158		
295	1.015153	294.63	1.019222	294.63	0.936088		
295.5	0.998157	295.13	1.020976	295.13	0.945062		
296	0.996385	295.63	1.023696	296.13	0.965729		
296.5	0.993358	296.13	1.024543	296.63	0.962954		
297	0.987971	296.63	1.018945	297.13	0.968303		
297.5	0.990315	297.13	1.010498	297.63	0.97092		
298	0.997272	297.63	1.000333	298.13	0.973809		
298.5	0.992279	298.13	1.000023	298.63	0.976868		
299	0.999239	298.63	0.997498	299.13	0.981181		
299.5	1.002278	299.13	0.996414	299.63	0.984198		
300	0.996176	299.63	1.000329	300.13	0.988787		
300.5	0.99903	300.13	0.995142	300.63	0.996916		
301	0.997779	300.63	0.994516	301.13	0.9996		
301.5	1.00025	301.13	0.996479	301.63	1.003638		
302	1.004382	301.63	1.000474	302.13	1.008612		
302.5	1.004181	302.13	1.003903	302.63	1.013761		
303	1.00268	302.63	1.006084	303.13	1.012383		
303.5	1.001142	303.13	1.007283	303.63	1.011784		
304	0.992864	303.63	1.006413	304.13	1.01376		
304.5	0.986731	304.13	1.005942	304.63	1.012311		
305	0.983256	304.63	1.004655	305.13	1.011151		
305.5	0.978941	305.13	0.9995	305.63	1.006642		
306	0.977712	305.63	0.997253	306.13	1.002537		
306.5	0.979896	306.13	0.993666	306.63	0.999881		
307	0.978551	306.63	0.995842	307.13	0.995685		
307.5	0.976295	307.13	0.996107	307.63	0.990401		
308	0.981361	307.63	0.995146	308.13	0.985588		
308.5	0.985536	308.13	0.997108	308.63	0.981184		
309	0.984304						

Fig. 2.2.

	cellulose	stearic acid	amino mix	lignin
280.06	0.002219	0.003429	-0.00015	-0.02482
280.1	0.000996	0.001251	0.000135	-0.02492
280.14	-0.00014	-0.00111	0.000215	-0.02647
280.18	-0.00111	-0.00251	-0.0005	-0.02914
280.22	-0.00197	-0.00298	-0.00049	-0.03215
280.26	-0.00261	-0.00288	-0.00041	-0.0345
280.3	-0.003	-0.00244	-0.00031	-0.03517
280.34	-0.00293	-0.00185	-0.00042	-0.03347
280.38	-0.00249	-0.00148	-0.00053	-0.02935
280.42	-0.00189	-0.0018	-0.00062	-0.02336

280.46	-0.0017	-0.00272	-0.00051	-0.01635
280.49	-0.00172	-0.00372	-0.00043	-0.00922
280.53	-0.00181	-0.00441	-0.00038	-0.00284
280.57	-0.00129	-0.00468	-0.0003	0.001924
280.61	-0.00055	-0.00436	5.99E-05	0.004448
280.65	0.000314	-0.00332	0.000545	0.004634
280.69	0.001016	-0.00162	0.000938	0.003024
280.73	0.002092	0.000381	0.00105	0.000523
280.77	0.003324	0.002469	0.000958	-0.00202
280.81	0.004562	0.004606	0.000789	-0.00407
280.85	0.005057	0.00657	0.000566	-0.00539
280.89	0.00495	0.008291	0.000325	-0.0059
280.93	0.004284	0.009739	8.46E-05	-0.00551
280.97	0.003554	0.010559	-2.7E-05	-0.0042
281.01	0.002817	0.010297	-4.4E-05	-0.0021
281.05	0.002218	0.008947	-3.2E-05	0.000376
281.09	0.001631	0.007113	-5.6E-05	0.002616
281.13	0.001062	0.005424	-7.9E-05	0.004
281.16	0.000497	0.004027	5.18E-05	0.004214
281.2	3.17E-05	0.00266	0.000252	0.003445
281.24	-0.0003	0.000851	0.000507	0.002295
281.28	-0.00046	-0.00146	0.000741	0.001506
281.32	-0.00065	-0.00341	0.000947	0.001742
281.36	-0.00088	-0.00397	0.001076	0.003512
281.4	-0.00126	-0.0031	0.000979	0.007064
281.44	-0.00165	-0.00212	0.000603	0.012143
281.48	-0.00201	-0.00241	5.68E-05	0.017867
281.52	-0.00228	-0.00408	-0.00044	0.023008
281.56	-0.00252	-0.00615	-0.0008	0.026564
281.6	-0.00269	-0.00784	-0.00104	0.028124
281.64	-0.00262	-0.009	-0.00119	0.027849
281.68	-0.00219	-0.00936	-0.00115	0.026242
281.72	-0.00153	-0.00841	-0.00095	0.02399
281.76	-0.00088	-0.00607	-0.00064	0.021827
281.8	-0.00035	-0.003	-0.00038	0.020291
281.83	0.000124	0.000329	-0.00015	0.019501
281.87	0.000587	0.003723	1.35E-05	0.019168
281.91	0.000949	0.00649	0.000198	0.018856
281.95	0.001154	0.007767	0.000388	0.018247
281.99	0.001082	0.007341	0.000519	0.017226
282.03	0.000885	0.005926	0.000552	0.015811
282.07	0.000608	0.004211	0.0005	0.01409
282.11	0.000255	0.002395	0.000394	0.012239
282.15	-0.00031	0.000692	0.000241	0.010555
282.19	-0.00106	-0.00059	6.05E-05	0.009405

282.23	-0.00191	-0.00132	-0.00011	0.009087
282.27	-0.00264	-0.00173	-0.00021	0.009702
282.31	-0.00315	-0.00218	-0.00027	0.011145
282.35	-0.00335	-0.00282	-0.00034	0.013199
282.39	-0.00326	-0.00356	-0.00046	0.015602
282.43	-0.00299	-0.00423	-0.00064	0.018045
282.47	-0.00268	-0.00478	-0.00088	0.02017
282.5	-0.00233	-0.00527	-0.00115	0.021657
282.54	-0.00203	-0.00572	-0.00154	0.022355
282.58	-0.00163	-0.00605	-0.00201	0.022311
282.62	-0.00122	-0.00643	-0.00254	0.021648
282.66	-0.00093	-0.00749	-0.00303	0.020416
282.7	-0.00094	-0.0097	-0.00339	0.018585
282.74	-0.00128	-0.01207	-0.00355	0.016179
282.78	-0.00172	-0.01251	-0.00353	0.013384
282.82	-0.00207	-0.00971	-0.00334	0.010499
282.86	-0.00222	-0.00496	-0.00299	0.007779
282.9	-0.00229	-0.00115	-0.00248	0.005351
282.94	-0.0022	2.55E-05	-0.00192	0.003242
282.98	-0.00173	-0.00102	-0.00147	0.001435
283.02	-0.00079	-0.00301	-0.00118	-0.00015
283.06	0.000407	-0.00532	-0.00102	-0.00169
283.1	0.001568	-0.00764	-0.00092	-0.0034
283.13	0.002451	-0.00935	-0.00084	-0.00542
283.17	0.00292	-0.01001	-0.00082	-0.00763
283.21	0.002861	-0.00974	-0.00077	-0.00969
283.25	0.002434	-0.00915	-0.00065	-0.01119
283.29	0.00183	-0.0087	-0.00049	-0.01177
283.33	0.001506	-0.00852	-0.00027	-0.01126
283.37	0.001361	-0.00854	-8.5E-05	-0.00975
283.41	0.00129	-0.00861	4.16E-05	-0.00754
283.45	0.00096	-0.00875	-6.2E-05	-0.00507
283.49	0.000638	-0.00933	-0.00032	-0.00285
283.53	0.000285	-0.01087	-0.00064	-0.00148
283.57	-8.7E-05	-0.01331	-0.00077	-0.00146
283.61	-0.00085	-0.01576	-0.00078	-0.00306
283.65	-0.00182	-0.01752	-0.00069	-0.00621
283.69	-0.00277	-0.01846	-0.00065	-0.01059
283.73	-0.00331	-0.01842	-0.00049	-0.01578
283.77	-0.00352	-0.01694	-0.00026	-0.02131
283.8	-0.00354	-0.01395	1.33E-05	-0.02672
283.84	-0.0036	-0.01027	3.86E-05	-0.03156
283.88	-0.00364	-0.00638	-6.7E-05	-0.0354
283.92	-0.00356	-0.00245	-0.00015	-0.03807
283.96	-0.0034	0.000332	2.22E-06	-0.03966

284	-0.00317	0.001689	0.00038	-0.04057
284.04	-0.00199	-0.00128	0.002288	-0.04277
284.08	-0.00066	-0.00556	0.004353	-0.04454
284.12	0.000746	-0.00881	0.006547	-0.04556
284.16	0.00201	-0.01006	0.008867	-0.04524
284.2	0.002952	-0.00977	0.011234	-0.04287
284.24	0.00367	-0.00863	0.013582	-0.0376
284.28	0.00445	-0.00695	0.015791	-0.02861
284.32	0.005489	-0.00501	0.0178	-0.01543
284.36	0.006736	-0.00333	0.019713	0.001672
284.4	0.008048	-0.0022	0.021678	0.021702
284.44	0.009399	-0.00151	0.023821	0.04328
284.47	0.010838	-0.00084	0.02585	0.065116
284.51	0.012853	0.000119	0.028431	0.086289
284.55	0.015426	0.001544	0.031417	0.106399
284.59	0.018186	0.003683	0.034872	0.125654
284.63	0.020987	0.006842	0.038606	0.144822
284.67	0.023606	0.010831	0.04199	0.164926
284.71	0.026265	0.014819	0.045375	0.186844
284.75	0.028824	0.018059	0.049307	0.21112
284.79	0.03119	0.020739	0.055326	0.238068
284.83	0.032822	0.024159	0.06337	0.267957
284.87	0.033767	0.030044	0.073349	0.301021
284.91	0.033966	0.038207	0.08552	0.337313
284.95	0.033837	0.045542	0.099862	0.376602
284.99	0.033399	0.049119	0.115121	0.418404
285.03	0.032726	0.048574	0.129156	0.461999
285.07	0.031633	0.045391	0.140038	0.506332
285.11	0.030231	0.040612	0.147745	0.549951
285.14	0.028401	0.034741	0.151981	0.591229
285.18	0.026804	0.029204	0.153201	0.628798
285.22	0.02534	0.025454	0.151655	0.661838
285.26	0.024157	0.023691	0.148186	0.68994
285.3	0.023175	0.022837	0.144393	0.712741
285.34	0.022288	0.021403	0.140615	0.729701
285.38	0.021273	0.018846	0.136992	0.740124
285.42	0.02013	0.016144	0.13361	0.743216
285.46	0.018989	0.014872	0.130287	0.738103
285.5	0.017978	0.015712	0.126753	0.723975
285.54	0.017075	0.017623	0.122763	0.70046
285.58	0.016267	0.018665	0.118361	0.667996
285.62	0.015647	0.017785	0.11359	0.627918
285.66	0.015431	0.01607	0.108358	0.582241
285.7	0.015764	0.015961	0.102857	0.53333
285.74	0.016568	0.019015	0.097397	0.483552

285.78	0.017815	0.02445	0.09231	0.434918
285.81	0.019096	0.030026	0.08757	0.388816
285.85	0.020672	0.03451	0.08382	0.345999
285.89	0.022193	0.037841	0.080894	0.306842
285.93	0.023731	0.040085	0.078849	0.271614
285.97	0.02527	0.041016	0.077548	0.240557
286.01	0.026832	0.040738	0.076908	0.213825
286.05	0.02825	0.040334	0.076826	0.191456
286.09	0.029591	0.040761	0.077185	0.173469
286.13	0.030922	0.042168	0.077896	0.159971
286.17	0.032429	0.044213	0.078809	0.151142
286.21	0.03406	0.046614	0.079871	0.147061
286.25	0.035747	0.049268	0.080971	0.147502
286.29	0.037382	0.052067	0.082057	0.151856
286.33	0.03897	0.05484	0.083188	0.159241
286.37	0.04058	0.057468	0.084508	0.168751
286.41	0.042235	0.059985	0.086079	0.179633
286.45	0.043858	0.062484	0.087847	0.191308
286.48	0.045117	0.06508	0.089385	0.2033
286.52	0.046215	0.067714	0.091236	0.215266
286.56	0.047108	0.069935	0.093232	0.227156
286.6	0.047918	0.071336	0.095465	0.239346
286.64	0.048732	0.072462	0.098002	0.252623
286.68	0.049623	0.074447	0.100816	0.267981
286.72	0.050764	0.077733	0.104017	0.286305
286.76	0.052659	0.082755	0.107849	0.308035
286.8	0.055311	0.090749	0.112451	0.33299
286.84	0.058444	0.10295	0.117693	0.360434
286.88	0.061597	0.11957	0.123538	0.389269
286.92	0.064611	0.139553	0.129711	0.418122
286.96	0.067431	0.161512	0.13607	0.445333
287	0.069947	0.185777	0.142366	0.469033
287.04	0.071886	0.215756	0.148442	0.487462
287.08	0.073496	0.25595	0.154297	0.499373
287.12	0.075096	0.308512	0.159871	0.50431
287.15	0.076927	0.372369	0.164758	0.502661
287.19	0.079339	0.447971	0.169703	0.495493
287.23	0.08222	0.53719	0.174673	0.48429
287.27	0.085611	0.636231	0.179989	0.470724
287.31	0.089296	0.736891	0.18566	0.456513
287.35	0.092914	0.832809	0.191595	0.443264
287.39	0.095992	0.920745	0.197735	0.432162
287.43	0.098603	0.997522	0.204152	0.423646
287.47	0.100911	1.058468	0.210883	0.417425
287.51	0.103078	1.103376	0.218015	0.412875

287.55	0.105142	1.137861	0.225398	0.409525
287.59	0.107314	1.164827	0.233039	0.407247
287.63	0.110025	1.185572	0.240835	0.40615
287.67	0.113559	1.204878	0.248961	0.406436
287.71	0.11773	1.226573	0.257416	0.408393
287.75	0.121602	1.251685	0.26599	0.412427
287.79	0.125338	1.281317	0.274652	0.41899
287.82	0.129478	1.318665	0.283488	0.42848
287.86	0.135407	1.364863	0.293804	0.441298
287.9	0.143561	1.413611	0.305964	0.458133
287.94	0.154509	1.456654	0.320232	0.480213
287.98	0.169177	1.489924	0.337155	0.509288
288.02	0.189187	1.512965	0.357546	0.547366
288.06	0.214596	1.525753	0.381656	0.596365
288.1	0.245502	1.527881	0.409878	0.657727
288.14	0.282041	1.521578	0.442719	0.73194
288.18	0.323437	1.510158	0.480449	0.818155
288.22	0.368943	1.494667	0.523193	0.914187
288.26	0.416885	1.477565	0.567981	1.016865
288.3	0.466169	1.464935	0.614314	1.122394
288.34	0.515931	1.462729	0.661647	1.226543
288.38	0.563918	1.469809	0.706828	1.324819
288.42	0.60869	1.476965	0.748242	1.412837
288.45	0.649971	1.478328	0.78453	1.486811
288.49	0.687754	1.472671	0.81552	1.543913
288.53	0.722559	1.456471	0.842483	1.582385
288.57	0.754752	1.425702	0.864159	1.601488
288.61	0.784698	1.381379	0.878856	1.601409
288.65	0.813968	1.330882	0.888115	1.583203
288.69	0.843212	1.280328	0.892412	1.548743
288.73	0.873331	1.231366	0.892646	1.500601
288.77	0.90572	1.185862	0.889448	1.441785
288.81	0.940652	1.146193	0.882447	1.375405
288.85	0.978322	1.112956	0.871865	1.304451
288.89	1.019494	1.084773	0.859031	1.231808
288.93	1.063631	1.059456	0.844243	1.160359
288.97	1.109751	1.035492	0.827184	1.092888
289.01	1.156137	1.012993	0.805489	1.031646
289.05	1.201133	0.993281	0.780602	0.9779
289.09	1.243562	0.977323	0.754903	0.931869
289.12	1.280704	0.964989	0.730595	0.893092
289.16	1.311452	0.955504	0.708905	0.860858
289.2	1.335763	0.94868	0.689917	0.834379
289.24	1.354554	0.94445	0.673382	0.81283
289.28	1.368377	0.941478	0.661069	0.795466

289.32	1.376921	0.93791	0.651603	0.781818
289.36	1.379455	0.932969	0.644221	0.771718
289.4	1.376923	0.928077	0.637612	0.765062
289.44	1.370395	0.925393	0.631559	0.761505
289.48	1.360422	0.925816	0.626182	0.760329
289.52	1.346931	0.928546	0.621864	0.760551
289.56	1.330484	0.931931	0.618771	0.761127
289.6	1.312366	0.935319	0.61667	0.761151
289.64	1.29431	0.938831	0.615579	0.759975
289.68	1.277858	0.94254	0.614961	0.757264
289.72	1.262908	0.946117	0.614635	0.752927
289.76	1.249844	0.949435	0.614002	0.746985
289.79	1.238137	0.953679	0.612987	0.739466
289.83	1.227648	0.960409	0.612345	0.730434
289.87	1.217014	0.969814	0.61223	0.720136
289.91	1.206111	0.979924	0.612412	0.709111
289.95	1.195509	0.988732	0.612914	0.698166
289.99	1.185852	0.995649	0.613681	0.688179
290.03	1.177306	1.00041	0.615114	0.679892
290.07	1.17037	1.002413	0.617255	0.673822
290.11	1.165817	1.001073	0.619953	0.670265
290.15	1.165247	0.997319	0.623062	0.669242
290.19	1.169255	0.993401	0.626098	0.67037
290.23	1.177542	0.990647	0.628968	0.672844
290.27	1.191158	0.989231	0.631259	0.675724
290.31	1.209026	0.989255	0.633303	0.678384
290.35	1.230016	0.991186	0.635163	0.680777
290.39	1.252124	0.994982	0.637023	0.683394
290.43	1.274063	0.999123	0.638548	0.687045
290.46	1.295007	1.001874	0.639638	0.6926
290.5	1.314582	1.002841	0.641178	0.700656
290.54	1.330463	1.003207	0.643544	0.711104
290.58	1.342634	1.004819	0.646518	0.722882
290.62	1.351565	1.008644	0.649705	0.734244
290.66	1.358593	1.013419	0.652427	0.74341
290.7	1.364118	1.016331	0.65468	0.749128
290.74	1.368004	1.015169	0.656593	0.750808
290.78	1.369488	1.010818	0.658317	0.748413
290.82	1.369013	1.007127	0.659886	0.742434
290.86	1.367089	1.007019	0.661474	0.733909
290.9	1.364095	1.010731	0.663648	0.724228
290.94	1.360545	1.016992	0.666621	0.714671
290.98	1.357149	1.02564	0.669945	0.705994
291.02	1.355168	1.036753	0.672746	0.698395
291.06	1.355991	1.047611	0.674495	0.691816

291.1	1.358934	1.054618	0.675482	0.686268
291.13	1.362813	1.05634	0.675762	0.681944
291.17	1.366869	1.054347	0.676026	0.67914
291.21	1.370928	1.051139	0.676158	0.678121
291.25	1.374924	1.047684	0.676556	0.679008
291.29	1.378883	1.044134	0.678538	0.681691
291.33	1.382144	1.040689	0.682082	0.685769
291.37	1.384897	1.037639	0.686468	0.690643
291.41	1.387188	1.035187	0.690295	0.695812
291.45	1.389933	1.033312	0.693094	0.701183
291.49	1.393009	1.032271	0.695079	0.7071
291.53	1.396239	1.032025	0.696742	0.713974
291.57	1.398862	1.031667	0.69778	0.721797
291.61	1.401395	1.030307	0.698337	0.729955
291.65	1.404773	1.027695	0.698475	0.737487
291.69	1.410656	1.023484	0.698796	0.743505
291.73	1.418273	1.016608	0.6995	0.747407
291.77	1.426575	1.005779	0.700481	0.748857
291.8	1.432689	0.99276	0.701113	0.747814
291.84	1.437364	0.982759	0.701845	0.744734
291.88	1.440794	0.97982	0.702681	0.740689
291.92	1.443508	0.983886	0.704222	0.737038
291.96	1.444856	0.99122	0.706899	0.734771
292	1.445636	0.99934	0.710463	0.734021
292.04	1.446996	1.007921	0.714649	0.734163
292.08	1.451546	1.015589	0.719141	0.734305
292.12	1.458232	1.020539	0.723787	0.733759
292.16	1.465645	1.022076	0.728372	0.732225
292.2	1.471417	1.021328	0.732422	0.729824
292.24	1.475807	1.020116	0.736086	0.727068
292.28	1.479387	1.019167	0.739617	0.724726
292.32	1.483067	1.018712	0.743755	0.723516
292.36	1.486898	1.019369	0.748418	0.723797
292.4	1.491349	1.02202	0.753415	0.725545
292.44	1.497803	1.02665	0.758113	0.728705
292.47	1.507083	1.031739	0.762354	0.733634
292.51	1.518277	1.036194	0.766879	0.741206
292.55	1.529465	1.039771	0.771836	0.752418
292.59	1.538526	1.042118	0.777076	0.767831
292.63	1.54549	1.042522	0.782571	0.787264
292.67	1.550413	1.040431	0.788276	0.809889
292.71	1.552549	1.036769	0.794311	0.834404
292.75	1.552461	1.033343	0.800889	0.859081
292.79	1.551201	1.03121	0.807858	0.881846
292.83	1.550928	1.030523	0.815059	0.900741

292.87	1.552544	1.031174	0.822002	0.914643
292.91	1.555717	1.033187	0.828787	0.923673
292.95	1.560184	1.036499	0.835675	0.928894
292.99	1.565846	1.040775	0.843171	0.931547
293.03	1.572047	1.046169	0.850889	0.932458
293.07	1.578147	1.052934	0.858246	0.931943
293.11	1.582906	1.059665	0.864291	0.930024
293.14	1.585874	1.064228	0.86889	0.926639
293.18	1.587315	1.065495	0.872903	0.921752
293.22	1.586348	1.063922	0.877051	0.915487
293.26	1.583453	1.061074	0.880963	0.908277
293.3	1.579176	1.058084	0.884296	0.900844
293.34	1.574282	1.05499	0.886001	0.893857
293.38	1.569167	1.05077	0.886502	0.887472
293.42	1.564105	1.044148	0.886101	0.881162
293.46	1.559658	1.035078	0.885211	0.874074
293.5	1.556809	1.025651	0.883289	0.86567
293.54	1.554747	1.018375	0.88092	0.856113
293.58	1.552517	1.014127	0.878884	0.84614
293.62	1.548182	1.012072	0.879533	0.836666
293.66	1.542165	1.01071	0.882225	0.828502
293.7	1.534997	1.009337	0.885733	0.82229
293.74	1.527271	1.007727	0.887218	0.818403
293.78	1.51909	1.0051	0.886656	0.816697
293.81	1.510881	1.00048	0.884495	0.816338
293.85	1.503779	0.994013	0.882511	0.816062
293.89	1.499086	0.987515	0.880254	0.814806
293.93	1.496167	0.982625	0.878214	0.812232
293.97	1.494454	0.97974	0.876762	0.808779
294.01	1.493051	0.979085	0.877543	0.805323
294.05	1.491638	0.981221	0.88037	0.80281
294.09	1.490053	0.986867	0.884644	0.802032
294.13	1.48729	0.995412	0.88961	0.80351
294.17	1.483782	1.004557	0.894549	0.807401
294.21	1.4802	1.012854	0.899608	0.813514
294.25	1.477983	1.020103	0.905172	0.82146
294.29	1.477586	1.026049	0.911752	0.830837
294.33	1.478689	1.030323	0.918902	0.841346
294.37	1.480665	1.032835	0.925963	0.852819
294.41	1.483527	1.034074	0.931794	0.86526
294.44	1.486942	1.034732	0.936387	0.878893
294.48	1.490959	1.03514	0.940722	0.894118
294.52	1.495148	1.035418	0.94539	0.911332
294.56	1.49876	1.035786	0.950426	0.930717
294.6	1.501812	1.035981	0.95588	0.952151

294.64	1.503601	1.035945	0.962058	0.97525
294.68	1.504927	1.03683	0.96926	0.999453
294.72	1.506267	1.040043	0.976894	1.024078
294.76	1.508664	1.045926	0.98412	1.048405
294.8	1.512423	1.052992	0.989514	1.071793
294.84	1.51736	1.059364	0.993352	1.093777
294.88	1.52335	1.064338	0.995986	1.11404
294.92	1.530804	1.067888	0.998041	1.13225
294.96	1.539558	1.069921	0.999677	1.147913
295	1.548608	1.069565	1.001106	1.160386
295.04	1.555771	1.067	1.002937	1.16911
295.08	1.559639	1.065075	1.005564	1.173859
295.11	1.561058	1.066674	1.008208	1.174828
295.15	1.561814	1.07248	1.010865	1.172546
295.19	1.563642	1.080928	1.012355	1.167785
295.23	1.566444	1.090411	1.012791	1.161533
295.27	1.570091	1.100746	1.012298	1.154908
295.31	1.575567	1.110788	1.01118	1.148913
295.35	1.582084	1.117863	1.009318	1.144151
295.39	1.58833	1.119142	1.006723	1.140705
295.43	1.591608	1.114505	1.003183	1.13826
295.47	1.590729	1.107979	0.999029	1.136305
295.51	1.586506	1.102883	0.994451	1.134298
295.55	1.579925	1.099714	0.989632	1.131791
295.59	1.571438	1.097853	0.984395	1.128537
295.63	1.561713	1.09668	0.979138	1.124569
295.67	1.551462	1.096161	0.974254	1.120178
295.71	1.542935	1.096026	0.970702	1.115871
295.75	1.535937	1.095534	0.968472	1.11233
295.78	1.529291	1.093987	0.966953	1.110308
295.82	1.520912	1.091434	0.966281	1.110316
295.86	1.510056	1.0888	0.965942	1.112207
295.9	1.49792	1.086855	0.965933	1.115017
295.94	1.486126	1.085701	0.966336	1.117346
295.98	1.475947	1.084983	0.967055	1.118085
296.02	1.467409	1.084129	0.968079	1.116941
296.06	1.460539	1.082742	0.969409	1.114417
296.1	1.456119	1.081101	0.971217	1.111437
296.14	1.453988	1.079999	0.973444	1.109038
296.18	1.453001	1.080034	0.975886	1.108252
296.22	1.451558	1.081388	0.978018	1.109931
296.26	1.447907	1.084038	0.97957	1.114373
296.3	1.442537	1.088272	0.980852	1.12103
296.34	1.435867	1.094248	0.982327	1.128666
296.38	1.428696	1.101165	0.984713	1.135973

296.42	1.42143	1.107969	0.987833	1.142167
296.45	1.414204	1.114478	0.991186	1.147165
296.49	1.40789	1.120414	0.994999	1.151346
296.53	1.402457	1.124435	0.998957	1.155231
296.57	1.397949	1.124908	1.002895	1.159304
296.61	1.394649	1.121656	1.006496	1.164015
296.65	1.392819	1.116903	1.009197	1.169851
296.69	1.391986	1.112708	1.011322	1.177374
296.73	1.39167	1.109549	1.013298	1.187124
296.77	1.391071	1.107337	1.016398	1.199397
296.81	1.390038	1.105993	1.02026	1.214041
296.85	1.388484	1.105702	1.024369	1.230447
296.89	1.386249	1.106273	1.027443	1.247663
296.93	1.383192	1.106796	1.029378	1.264502
296.97	1.37939	1.10628	1.030452	1.279609
297.01	1.374873	1.104557	1.0311	1.291642
297.05	1.369827	1.102571	1.031232	1.299588
297.09	1.364341	1.10165	1.031079	1.303021
297.12	1.358328	1.102607	1.030601	1.302101
297.16	1.352115	1.104679	1.031284	1.297345
297.2	1.345646	1.105733	1.032779	1.289386
297.24	1.339068	1.103138	1.034669	1.278864
297.28	1.332704	1.096847	1.036173	1.266406
297.32	1.326708	1.09142	1.03678	1.25264
297.36	1.320945	1.091774	1.036753	1.238186
297.4	1.315375	1.099119	1.036421	1.223634
297.44	1.310052	1.109625	1.036317	1.209534
297.48	1.304613	1.117967	1.036404	1.196397
297.52	1.298709	1.121568	1.036636	1.184656
297.56	1.290705	1.12071	1.037047	1.174533
297.6	1.281121	1.117077	1.037583	1.165884
297.64	1.270871	1.11079	1.038092	1.158188
297.68	1.261619	1.10194	1.038384	1.150772
297.72	1.254239	1.093672	1.038191	1.143135
297.76	1.248441	1.089763	1.037534	1.135146
297.79	1.243671	1.091699	1.036121	1.127043
297.83	1.240065	1.09707	1.034303	1.119367
297.87	1.237307	1.101216	1.032087	1.112935
297.91	1.234932	1.100666	1.029744	1.108708
297.95	1.232074	1.095412	1.027771	1.107414
297.99	1.227949	1.089041	1.026329	1.109053
298.03	1.223014	1.084881	1.02542	1.112686
298.07	1.217805	1.083558	1.025054	1.116755
298.11	1.21386	1.083129	1.025539	1.119688
298.15	1.210637	1.080908	1.026583	1.120353

298.19	1.20762	1.075318	1.027906	1.118163
298.23	1.203582	1.067289	1.028994	1.113017
298.27	1.198407	1.059865	1.029673	1.105285
298.31	1.192374	1.055492	1.02996	1.095758
298.35	1.185849	1.054461	1.029958	1.085408
298.39	1.179107	1.054864	1.029708	1.074975
298.43	1.172267	1.054906	1.02909	1.064673
298.46	1.165261	1.054174	1.027663	1.054235
298.5	1.158559	1.052925	1.025354	1.043245
298.54	1.152143	1.051538	1.022318	1.031465
298.58	1.146091	1.050261	1.018965	1.018954
298.62	1.140928	1.049054	1.016105	1.006007
298.66	1.136546	1.047354	1.01395	0.993058
298.7	1.132551	1.044677	1.01242	0.980627
298.74	1.128325	1.040982	1.011265	0.969252
298.78	1.123298	1.036491	1.010598	0.959408
298.82	1.117567	1.031247	1.010311	0.951429
298.86	1.111221	1.024905	1.010324	0.94549
298.9	1.103754	1.01807	1.01076	0.941597
298.94	1.095456	1.012759	1.011326	0.939593
298.98	1.087066	1.010652	1.011882	0.939165
299.02	1.080135	1.01184	1.01212	0.939881
299.06	1.076099	1.014929	1.012121	0.94121
299.1	1.073946	1.018703	1.011831	0.942545
299.13	1.072506	1.02306	1.010887	0.943251
299.17	1.069568	1.027399	1.009255	0.942776
299.21	1.065293	1.03025	1.006841	0.940757
299.25	1.06006	1.030282	1.004107	0.937054
299.29	1.054276	1.027472	1.002189	0.931725
299.33	1.04795	1.023643	1.001655	0.924995
299.37	1.041617	1.02014	1.001939	0.91724
299.41	1.035845	1.017068	1.002382	0.908905
299.45	1.032951	1.014721	1.001708	0.900348
299.49	1.031964	1.013571	1.000246	0.891706
299.53	1.031852	1.013932	0.998289	0.882884
299.57	1.030164	1.015682	0.996348	0.873664
299.61	1.026351	1.018169	0.994502	0.863817
299.65	1.021153	1.021329	0.99283	0.85317
299.69	1.015607	1.025397	0.991389	0.841656
299.73	1.01084	1.029451	0.990666	0.829419
299.76	1.00663	1.032599	0.990071	0.816903
299.8	1.003253	1.034617	0.989944	0.804785
299.84	1.000613	1.03523	0.989421	0.793732
299.88	0.998676	1.033871	0.988341	0.784139
299.92	0.997111	1.029179	0.986847	0.776039

299.96	0.995381	1.020986	0.985098	0.76921
300	0.992677	1.01201	0.983387	0.763327
300.04	0.989395	1.005268	0.981724	0.758058
300.08	0.98594	1.001952	0.98012	0.753137
300.12	0.983173	1.001441	0.978279	0.748513
300.16	0.981259	1.002437	0.976414	0.744516
300.2	0.980163	1.00456	0.974828	0.741844
300.24	0.980205	1.007601	0.974205	0.741229
300.28	0.981348	1.010226	0.974957	0.742948
300.32	0.983116	1.010903	0.976794	0.746539
300.36	0.984998	1.009098	0.979422	0.750942
300.4	0.9856	1.005632	0.9826	0.754923
300.43	0.985045	1.001945	0.985683	0.75745
300.47	0.983925	0.998875	0.988916	0.757833
300.51	0.982467	0.996514	0.991182	0.755754
300.55	0.980764	0.994754	0.992123	0.751344
300.59	0.978987	0.993568	0.991987	0.745235
300.63	0.977282	0.992962	0.991014	0.738401
300.67	0.976693	0.992907	0.989408	0.731808
300.71	0.976714	0.993474	0.987505	0.726091
300.75	0.976844	0.995186	0.985639	0.721467
300.79	0.975508	0.997869	0.984678	0.717871
300.83	0.972465	0.999878	0.98481	0.715122
300.87	0.968467	0.999247	0.985752	0.713018
300.91	0.964489	0.995395	0.987104	0.711387
300.95	0.961989	0.990494	0.988349	0.710139
300.99	0.96092	0.98732	0.989535	0.709294
301.03	0.961231	0.987402	0.990707	0.708965
301.07	0.963303	0.99036	0.991832	0.709287
301.1	0.966753	0.994071	0.992643	0.710342
301.14	0.971383	0.997281	0.993893	0.712132
301.18	0.976429	0.999834	0.995649	0.714603
301.22	0.981089	1.001783	0.998516	0.717674
301.26	0.985074	1.003223	1.002028	0.72126
301.3	0.988087	1.004178	1.005716	0.72527
301.34	0.988966	1.004527	1.008184	0.729602
301.38	0.987926	1.003883	1.009458	0.734149
301.42	0.985506	1.001775	1.009942	0.738792
301.46	0.982449	0.998125	1.010396	0.74337
301.5	0.979438	0.993677	1.011581	0.747589
301.54	0.976632	0.98905	1.013198	0.750953
301.58	0.974188	0.984235	1.0149	0.752837
301.62	0.972362	0.979478	1.015659	0.75271
301.66	0.971272	0.975361	1.01563	0.750394
301.7	0.97094	0.972262	1.015053	0.746142

301.74	0.971562	0.97025	1.014144	0.740538
301.77	0.973061	0.96933	1.012661	0.734353
301.81	0.97563	0.969909	1.011472	0.728464
301.85	0.978934	0.9724	1.01058	0.723733
301.89	0.983281	0.976163	1.011179	0.720747
301.93	0.988203	0.979872	1.012951	0.719545
301.97	0.993061	0.982774	1.015356	0.719575
302.01	0.996479	0.984676	1.017417	0.72
302.05	0.997301	0.985289	1.018286	0.720149
302.09	0.996155	0.983871	1.018339	0.719801
302.13	0.9937	0.979825	1.017982	0.719166
302.17	0.991273	0.974257	1.018375	0.718654
302.21	0.989142	0.96951	1.019477	0.718667
302.25	0.987435	0.96743	1.021081	0.719503
302.29	0.986528	0.968349	1.022995	0.721307
302.33	0.986687	0.9711	1.025016	0.724017
302.37	0.98762	0.974928	1.026903	0.727311
302.41	0.989028	0.979759	1.02841	0.730708
302.44	0.989974	0.984792	1.028452	0.733839
302.48	0.990802	0.98838	1.027742	0.736736
302.52	0.991435	0.988582	1.026202	0.739884
302.56	0.992021	0.985225	1.024044	0.743932
302.6	0.992683	0.981028	1.021496	0.749253
302.64	0.99344	0.979292	1.018807	0.755662
302.68	0.994307	0.981548	1.016222	0.762484
302.72	0.995551	0.986156	1.014276	0.768866
302.76	0.997026	0.989444	1.013008	0.774074
302.8	0.998535	0.987834	1.012407	0.777633
302.84	0.999537	0.980828	1.012687	0.779408
302.88	0.999654	0.972736	1.013965	0.779755
302.92	0.999243	0.96774	1.015861	0.779624
302.96	0.998659	0.967129	1.017987	0.780374
303	0.999033	0.970173	1.019473	0.783216
303.04	1.000263	0.975349	1.020255	0.78865
303.08	1.002061	0.98291	1.020362	0.796302
303.11	1.003905	0.992866	1.019277	0.805219
303.15	1.005752	1.00204	1.017475	0.814319
303.19	1.00722	1.006331	1.015069	0.822669
303.23	1.008094	1.003606	1.012488	0.82958
303.27	1.007584	0.996077	1.011074	0.834674
303.31	1.005824	0.989069	1.010684	0.837969
303.35	1.003069	0.986821	1.010941	0.839866
303.39	0.999646	0.989924	1.011245	0.840968
303.43	0.995813	0.994874	1.011035	0.84182
303.47	0.991818	0.99798	1.010383	0.842753

303.51	0.987902	0.997927	1.009346	0.843888
303.55	0.984221	0.995203	1.007778	0.845253
303.59	0.981104	0.991051	1.005843	0.84688
303.63	0.978898	0.985244	1.003746	0.848848
303.67	0.978472	0.977725	1.001867	0.851256
303.71	0.980751	0.971524	1.00052	0.854183
303.75	0.984968	0.970784	0.999627	0.857666
303.78	0.990182	0.97826	0.998821	0.861714
303.82	0.995299	0.991945	0.998823	0.866344
303.86	0.999665	1.005109	0.999217	0.871621
303.9	1.003069	1.012056	0.999746	0.877651
303.94	1.004996	1.011651	1.000078	0.884481
303.98	1.004762	1.007404	0.999731	0.891897
304.02	1.002892	1.003244	0.998693	0.899266
304.06	0.99993	1.000773	0.996954	0.905641
304.1	0.996538	0.999907	0.994056	0.910195
304.14	0.993203	0.999461	0.990188	0.912755
304.18	0.990426	0.99818	0.985771	0.914026
304.22	0.98908	0.995734	0.981399	0.915298
304.26	0.991202	0.993657	0.977883	0.917855
304.3	0.995845	0.994262	0.975114	0.922479
304.34	1.001971	0.99972	0.972984	0.929306
304.38	1.007365	1.009319	0.971293	0.93789
304.42	1.011076	1.017844	0.969968	0.947271
304.45	1.013096	1.020227	0.968723	0.956053
304.49	1.013661	1.01527	0.968163	0.962713
304.53	1.012392	1.006389	0.967907	0.966162
304.57	1.009885	0.998382	0.968084	0.966222
304.61	1.006804	0.993727	0.968829	0.963655
304.65	1.005159	0.992591	0.970688	0.959784
304.69	1.005383	0.993906	0.973847	0.956073
304.73	1.006736	0.99753	0.977958	0.953934
304.77	1.008433	1.003885	0.982645	0.954571
304.81	1.007742	1.011129	0.987166	0.95863
304.85	1.005445	1.016009	0.991334	0.965786
304.89	1.002442	1.015599	0.994996	0.974719
304.93	1.000497	1.00957	0.997625	0.983664
304.97	1.000993	1.001623	0.998987	0.991204
305.01	1.003591	0.995049	0.999404	0.996775
305.05	1.007921	0.990606	0.999223	1.000657
305.08	1.013789	0.988102	0.99911	1.003692
305.12	1.020759	0.987182	0.999657	1.007027
305.16	1.02796	0.988028	1.000452	1.011889
305.2	1.033962	0.990582	1.001371	1.019181
305.24	1.037631	0.993688	1.002249	1.028857

305.28	1.039345	0.995909	1.002995	1.039524
305.32	1.039517	0.99643	1.003518	1.048767
305.36	1.038859	0.99567	1.003335	1.054269
305.4	1.03763	0.995114	1.002548	1.055017
305.44	1.03612	0.996511	1.001432	1.051765
305.48	1.03474	1.000402	1.00037	1.046488
305.52	1.034364	1.004758	0.999971	1.04137
305.56	1.034722	1.006723	1.000155	1.038033
305.6	1.03554	1.003899	1.000841	1.037268
305.64	1.036389	0.996948	1.002204	1.03902
305.68	1.036915	0.990873	1.004075	1.042328
305.72	1.037075	0.990569	1.006086	1.04538
305.75	1.036512	0.997502	1.007512	1.046023
305.79	1.035034	1.007957	1.007478	1.042736
305.83	1.032929	1.016062	1.006259	1.035507
305.87	1.030663	1.017071	1.004416	1.025884
305.91	1.029305	1.01049	1.002938	1.016155
305.95	1.029337	1.002179	1.002667	1.008276
305.99	1.030488	0.99715	1.003472	1.003259
306.03	1.03248	0.996511	1.005162	1.001215
306.07	1.034445	0.99926	1.007797	1.001758
306.11	1.036455	1.003341	1.01079	1.004388
306.15	1.038734	1.008066	1.013744	1.008724
306.19	1.041584	1.013397	1.015696	1.014588
306.23	1.045545	1.018481	1.015874	1.021997
306.27	1.050536	1.022304	1.014819	1.031074
306.31	1.056479	1.02409	1.013121	1.041884
306.35	1.063958	1.024108	1.012323	1.054239
306.39	1.072575	1.023586	1.012635	1.067541
306.42	1.081455	1.023042	1.013512	1.080803
306.46	1.089939	1.022659	1.015332	1.092902
306.5	1.095852	1.023045	1.017271	1.102941
306.54	1.099713	1.025447	1.019239	1.110475
306.58	1.102029	1.031909	1.021155	1.115477
306.62	1.10371	1.042047	1.022782	1.118085
306.66	1.105468	1.05118	1.024177	1.118317
306.7	1.10721	1.054288	1.025333	1.115931
306.74	1.108898	1.049621	1.026278	1.110562
306.78	1.110437	1.040356	1.027065	1.102089
306.82	1.111554	1.032314	1.027612	1.091006
306.86	1.11216	1.029416	1.027903	1.078465
306.9	1.111377	1.031922	1.027657	1.065932
306.94	1.108659	1.036884	1.026728	1.054674
306.98	1.105096	1.041254	1.025457	1.045433
307.02	1.101826	1.044222	1.024198	1.03842

307.06	1.102054	1.046238	1.023843	1.03349
307.09	1.105836	1.048255	1.024142	1.030329
307.13	1.112705	1.051554	1.025529	1.02859
307.17	1.121853	1.056355	1.027603	1.027983
307.21	1.132727	1.06143	1.030474	1.028316
307.25	1.1441	1.065179	1.033756	1.029473
307.29	1.154734	1.066333	1.037055	1.031332
307.33	1.161164	1.064855	1.039587	1.033659
307.37	1.162276	1.061973	1.040999	1.035989
307.41	1.159609	1.058483	1.041412	1.037599
307.45	1.154658	1.054515	1.04093	1.037651
307.49	1.15007	1.050519	1.039364	1.035555
307.53	1.146704	1.047261	1.037045	1.031318
307.57	1.145048	1.044968	1.034332	1.025608
307.61	1.1468	1.043561	1.031756	1.019421
307.65	1.153052	1.043658	1.029706	1.013575
307.69	1.162122	1.046189	1.02823	1.008357
307.73	1.17239	1.05219	1.027384	1.003527
307.76	1.17983	1.060873	1.027213	0.998606
307.8	1.18401	1.068766	1.028299	0.993192
307.84	1.185427	1.072665	1.03011	0.987151
307.88	1.184562	1.071729	1.03241	0.980657
307.92	1.182253	1.06838	1.034729	0.974161
307.96	1.179282	1.066148	1.037011	0.968349
308	1.176402	1.067069	1.039222	0.96401
308.04	1.175712	1.071201	1.041289	0.9618
308.08	1.177982	1.076754	1.043313	0.961971
308.12	1.182218	1.082472	1.045188	0.964261
308.16	1.187453	1.088557	1.046821	0.96801
308.2	1.191692	1.094223	1.047896	0.972374
308.24	1.194577	1.097367	1.048344	0.976431
308.28	1.196074	1.095787	1.048358	0.979197
308.32	1.195883	1.088943	1.048016	0.979737
308.36	1.19342	1.079875	1.047841	0.977526
308.4	1.189483	1.07213	1.047903	0.972829
308.43	1.184669	1.067472	1.047966	0.966712
308.47	1.180671	1.065979	1.049054	0.960552
308.51	1.177958	1.06575	1.050714	0.955317
308.55	1.176586	1.06546	1.052685	0.951108
308.59	1.176635	1.065188	1.054674	0.947217
308.63	1.178941	1.064721	1.055697	0.942625
308.67	1.183004	1.063661	1.05603	0.936562
308.71	1.18817	1.061661	1.056054	0.928847
308.75	1.193591	1.058518	1.056318	0.919976
308.79	1.198419	1.05471	1.057598	0.911075

308.83	1.202405	1.050383	1.059802	0.903734
308.87	1.205303	1.045065	1.062826	0.899608
308.91	1.206334	1.038993	1.066939	0.899725
308.95	1.205465	1.033368	1.071892	0.903788
308.99	1.202988	1.029936	1.077174	0.910006
309.03	1.199228	1.029636	1.082191	0.915732
309.07	1.194262	1.030453	1.085362	0.918566
309.1	1.188249	1.028787	1.086617	0.917208
309.14	1.181973	1.020866	1.086993	0.911606
309.18	1.175721	1.006106	1.086684	0.90254
309.22	1.169702	0.990684	1.086597	0.891141
309.26	1.164499	0.98152	1.086752	0.878642
309.3	1.160675	0.98261	1.087181	0.866248
309.34	1.160241	0.992095	1.088167	0.854982
309.38	1.163748	1.001166	1.089327	0.845521
309.42	1.170203	1.002279	1.090641	0.838167
309.46	1.178592	0.99352	1.09193	0.832953
309.5	1.186764	0.979155	1.093552	0.829762
309.54	1.193993	0.965972	1.095611	0.828384
309.58	1.199883	0.958537	1.097963	0.828538
309.62	1.20303	0.957337	1.100718	0.829894
309.66	1.203081	0.958033	1.103274	0.832094
309.7	1.200601	0.956118	1.10544	0.834758
309.74	1.196256	0.949721	1.10702	0.837514
309.77	1.191839	0.939647	1.106657	0.840058
309.81	1.187707	0.92897	1.105195	0.842189
309.85	1.183414	0.919771	1.102816	0.843745
309.89	1.180615	0.91235	1.098837	0.844573
309.93	1.174733	0.906565	1.096969	0.844672
309.97	1.167888	0.902961	1.095741	0.844331

Fig. 2.3.

	300	350	400	450	500	550	600
273.88	0.000697	0.002551	0.000471	0.002238	0.001134	0.000573	0.000497
273.98	-0.00183	0.001408	0.000308	-0.00038	0.000503	0.000513	0.000104
274.08	-0.0032	-0.00125	-0.00068	-0.00075	0.000154	0.000556	-0.0002
274.18	-0.00278	-0.00178	-0.00067	-0.00197	-0.00026	0.000339	-0.00041
274.28	-0.00225	-0.00129	-0.0011	-0.00092	-0.00047	0.000298	-0.00047
274.38	-0.0013	-0.0005	-0.00054	-0.00208	-0.00011	0.000371	-0.00023
274.48	-0.00117	-0.00086	-0.00043	-0.00212	-0.00016	0.000211	-0.00026
274.58	-0.00015	0.001499	0.000313	-0.00082	0.000901	0.000263	0.000303
274.68	0.000283	0.000989	0.000344	-0.00086	0.000743	7.63E-05	0.000236
274.78	0.000736	-0.0011	-0.00011	-0.00107	0.000236	-0.0003	-0.00019
274.88	-0.00162	-0.00271	-0.00087	-0.00193	-0.00055	-0.00065	-0.00068
274.98	-0.00091	-0.00237	-0.00061	-0.00107	-0.00051	-0.00022	-0.00041
275.08	-0.00055	-0.00235	-0.00055	-0.00146	-0.00102	-0.00042	-0.00034
275.18	-0.00035	-0.00233	-0.00043	-0.00133	-0.00105	-0.00043	-0.0004
275.28	0.001149	-0.00024	0.000443	0.000125	-0.00023	6.38E-06	0.000178
275.38	0.002592	6.38E-05	0.000577	0.000241	0.000107	-0.00082	0.000184
275.48	0.000916	-0.00161	-0.0003	-0.00021	-0.00053	-0.0006	-0.00037
275.58	0.001002	-0.00223	-0.00026	-0.00096	-0.00049	-0.00066	-0.00029
275.68	0.001074	-0.00245	-0.00033	5.57E-05	-0.00054	-0.0001	-0.00023
275.78	0.000902	-0.00261	-0.00041	-0.00048	-0.00038	-0.00066	-0.00026
275.88	0.001133	0.000172	-0.00028	-1.1E-05	-0.00012	-0.00056	-8.8E-05
275.98	0.001751	0.002203	0.000665	0.001964	0.000496	9.36E-05	0.000492
276.08	0.000691	0.002288	0.00064	0.001436	0.000631	0.000182	0.000436
276.18	-0.00153	0.000991	0.000251	0.000843	-0.00013	3.41E-05	9.81E-05
276.28	0.002828	0.002401	0.001023	0.001369	0.000512	0.000324	0.000621
276.38	0.000867	0.000492	0.000139	0.00048	-0.00011	0.000197	0.000137
276.48	0.001174	0.002756	0.000852	0.001803	0.000559	0.000531	0.000586
276.58	0.000571	0.002892	0.000887	0.001734	0.000428	0.00022	0.000522
276.68	-7E-05	0.000914	0.000164	0.001	-8.9E-05	0.000293	4.27E-05
276.78	0.000605	0.000938	0.000176	0.000347	0.000131	-0.00016	4.91E-05
276.88	0.001365	0.002019	0.000224	0.001181	-8.8E-05	-2E-05	0.000141
276.98	0.000734	0.001102	0.000142	0.001326	7.84E-05	-0.00026	9.34E-05
277.08	-0.00119	0.003862	9.11E-05	0.001783	0.000563	0.000245	0.000135
277.18	-0.00102	0.000338	-6.6E-05	0.000557	-0.00011	-0.00015	2.66E-05
277.28	0.000304	0.00254	0.000698	0.002102	0.000523	0.000304	0.000684
277.38	0.000151	0.001672	0.000293	0.001533	9.99E-05	-8.2E-05	0.00028
277.48	-0.0002	0.001604	0.000328	0.001402	1.47E-05	-0.00024	0.000214
277.58	0.000851	0.001536	0.000613	0.002799	-4.2E-05	4.27E-05	0.000152
277.68	8.6E-05	0.001585	0.000449	0.002094	0.000118	-3.3E-05	0.000202
277.78	0.000342	0.00201	0.000623	0.002333	0.000325	0.000171	0.000326
277.88	0.002188	0.001188	0.000475	0.002808	0.000419	7.17E-05	0.000303

277.98	0.000335	0.00073	0.00026	0.002091	0.000127	7.46E-05	0.000262
278.08	0.00075	-2.3E-05	-2.6E-05	0.002066	0.000224	0.000369	0.000123
278.18	0.001371	-0.00015	-0.00014	-4.7E-05	0.00012	0.000134	0.000222
278.28	0.001535	-0.00043	2.45E-05	0.000161	0.000132	1.81E-05	0.000314
278.38	0.001903	0.00102	0.001258	0.000801	0.000793	0.000282	0.000115
278.48	0.001842	-0.00076	0.000379	0.001776	0.000328	0.000459	0.000238
278.58	0.001898	0.000556	0.00114	0.001562	0.000586	0.000349	0.000585
278.68	0.001438	-0.0008	0.000254	0.001076	6.9E-05	0.000329	4.45E-05
278.78	0.001498	0.000383	0.000488	0.000785	0.000535	0.000403	0.000246
278.88	0.000355	-0.00078	-0.00082	-0.00016	-0.00022	0.000293	-0.00022
278.98	-0.00033	-0.00098	-0.00072	-0.00274	-0.00037	-0.00015	-0.00025
279.08	-0.00062	-0.00144	-0.00064	-0.00228	-0.00057	0.000269	-0.0003
279.18	-0.00155	-0.00169	-0.00049	-0.00277	-0.00026	-0.0002	-0.00037
279.28	-0.00207	-0.00134	-0.00057	-0.00232	-0.00024	-0.00028	-0.00032
279.38	-0.00174	0.000472	-0.00011	-0.00127	0.000168	0.000112	0.00016
279.48	-0.00208	0.000575	0.000154	-0.00135	0.000156	5.67E-05	-0.00039
279.58	-0.00171	0.000449	0.000141	-0.00135	0.000163	-5.4E-05	0.0001
279.68	-0.00124	-0.00145	-0.00065	-0.00156	-0.00049	-9.1E-05	-0.00042
279.78	-0.00186	-0.00252	-0.0009	-0.00219	-0.00049	-0.00021	-0.00062
279.88	-0.00189	-0.00261	-0.00095	-0.00189	-0.00083	-0.00056	-0.00061
279.98	-0.00209	-0.00282	-0.00117	-0.00335	-0.00048	-0.00058	-0.00064
280.08	-0.00185	-0.00308	-0.00099	-0.00408	-0.00053	-0.00113	-0.00069
280.18	-0.00368	-0.00429	-0.00135	-0.00524	-0.00096	-0.00133	-0.00089
280.28	-0.00304	-0.00357	-0.0011	-0.00505	-0.00084	-0.00081	-0.00074
280.38	-0.00217	-0.00278	-0.00084	-0.0033	-0.00062	-0.00035	-0.00057
280.48	-0.0027	-0.00346	-0.00126	-0.00346	-0.00073	-0.00035	-0.00075
280.58	-0.00277	-0.00368	-0.00075	-0.00387	-9.2E-05	-0.00031	-0.00083
280.68	-0.00334	-0.00415	-0.0015	-0.00585	-0.00048	-0.00072	-0.00088
280.78	-0.00287	-0.00339	-0.00134	-0.00626	-0.00012	-0.0006	-0.00076
280.88	-0.00234	-0.00154	-0.00051	-0.0055	0.000409	1.9E-05	-0.00028
280.98	-0.00294	-0.00413	-0.00149	-0.00592	-0.00026	-0.0001	-0.00079
281.08	-0.00294	-0.00259	-0.00088	-0.00627	2.97E-05	0.000273	-0.00025
281.18	-0.00368	-0.00492	-0.00172	-0.0081	-0.00025	-0.00017	-0.00079
281.28	-0.00362	-0.00421	-0.00154	-0.00863	6.1E-05	-6.5E-05	-0.00068
281.38	-0.00226	-0.00451	-0.0016	-0.00818	0.000118	0.000392	-0.00059
281.48	-0.0016	-0.00388	-0.00126	-0.008	0.000464	0.000295	-0.00034
281.58	-0.00119	-0.00216	-0.00118	-0.00886	0.000363	0.000423	-0.00026
281.68	-0.00094	-0.00292	-0.00086	-0.01008	0.000927	0.000396	-6.3E-05
281.78	0.001024	-0.00085	0.000139	-0.00917	0.001421	0.000656	0.000675
281.88	0.002673	-0.00147	-1E-05	-0.00984	0.001706	0.000474	0.00065
281.98	0.005254	0.00118	0.001012	-0.00912	0.002852	0.001486	0.001306
282.08	0.007845	0.001891	0.001611	-0.00934	0.003648	0.002226	0.00188
282.18	0.010914	0.001656	0.001627	-0.00968	0.003907	0.002791	0.001985
282.28	0.012471	0.002386	0.002528	-0.01075	0.004557	0.003249	0.00282
282.38	0.018027	0.005039	0.003731	-0.00969	0.006334	0.004515	0.004061

282.48	0.023364	0.010078	0.005379	-0.00798	0.008458	0.006542	0.006014
282.58	0.029142	0.015051	0.007486	-0.00665	0.011524	0.009256	0.008541
282.68	0.038136	0.019099	0.009359	-0.00575	0.014485	0.012348	0.01171
282.78	0.049572	0.025386	0.011875	-0.00454	0.019193	0.016394	0.015809
282.88	0.063866	0.033293	0.015668	-0.00047	0.024999	0.022329	0.021573
282.98	0.084005	0.041446	0.020227	0.001434	0.032004	0.029419	0.028424
283.08	0.108955	0.055617	0.026868	0.005662	0.042637	0.039917	0.039102
283.18	0.129601	0.065601	0.034321	0.003649	0.054466	0.052477	0.051038
283.28	0.146955	0.075447	0.04433	0.004829	0.070991	0.070656	0.068232
283.38	0.154478	0.082845	0.057699	0.00561	0.09182	0.092429	0.09038
283.48	0.1567	0.091686	0.078181	0.010984	0.122592	0.123406	0.120653
283.58	0.157004	0.099771	0.104106	0.024713	0.160493	0.159258	0.156739
283.68	0.152973	0.110217	0.136529	0.047224	0.204816	0.202083	0.199148
283.78	0.152874	0.126143	0.174481	0.078067	0.258082	0.249714	0.248466
283.88	0.159987	0.144754	0.215816	0.116854	0.312415	0.298719	0.299632
283.98	0.182935	0.171269	0.261472	0.162153	0.371656	0.349749	0.352671
284.08	0.215146	0.205908	0.310054	0.210888	0.426935	0.398345	0.402824
284.18	0.252428	0.243363	0.357875	0.256604	0.477563	0.444638	0.450924
284.28	0.28737	0.276166	0.398277	0.295293	0.516616	0.483496	0.489839
284.38	0.322771	0.308594	0.435811	0.325554	0.550779	0.513852	0.522401
284.48	0.357421	0.337263	0.465976	0.350166	0.572165	0.534772	0.544637
284.58	0.398404	0.372372	0.500774	0.376039	0.59349	0.561207	0.569639
284.68	0.435115	0.399025	0.52746	0.391802	0.61139	0.578058	0.588828
284.78	0.456244	0.415486	0.541201	0.40192	0.617438	0.591494	0.600938
284.88	0.459708	0.42114	0.545134	0.408366	0.618369	0.599548	0.607813
284.98	0.462141	0.423096	0.54627	0.406735	0.616063	0.600254	0.612091
285.08	0.460572	0.421257	0.540443	0.404413	0.607743	0.602806	0.610355
285.18	0.446684	0.405538	0.521567	0.393444	0.593038	0.594366	0.601173
285.28	0.423605	0.391216	0.502865	0.38442	0.576325	0.583594	0.589039
285.38	0.397738	0.369576	0.480049	0.37264	0.553752	0.567051	0.5697
285.48	0.374865	0.356005	0.463512	0.364889	0.535316	0.548224	0.551869
285.58	0.36295	0.348125	0.450309	0.35974	0.519435	0.530091	0.531798
285.68	0.364711	0.345307	0.445749	0.354865	0.505103	0.510851	0.515466
285.78	0.380147	0.354413	0.447542	0.354796	0.49427	0.496876	0.502792
285.88	0.405266	0.363479	0.448915	0.35092	0.482646	0.482408	0.485952
285.98	0.436075	0.378546	0.455031	0.350307	0.473658	0.469754	0.474199
286.08	0.467604	0.395626	0.459567	0.348603	0.465431	0.457953	0.463826
286.18	0.489828	0.403357	0.457618	0.34453	0.456479	0.445613	0.452697
286.28	0.503358	0.409019	0.459169	0.342175	0.450886	0.437371	0.445803
286.38	0.513888	0.41256	0.460465	0.343807	0.450263	0.435496	0.443644
286.48	0.528611	0.419463	0.464694	0.349691	0.454187	0.436978	0.445843
286.58	0.551729	0.43231	0.473867	0.358857	0.460976	0.442044	0.450983
286.68	0.572788	0.439484	0.479711	0.364405	0.468123	0.448749	0.456164
286.78	0.589852	0.450655	0.488062	0.372992	0.475451	0.452137	0.463557
286.88	0.600759	0.454331	0.491514	0.377274	0.479766	0.454455	0.465945

286.98	0.610242	0.461044	0.497919	0.38344	0.48492	0.458762	0.471102
287.08	0.620005	0.46888	0.505425	0.389882	0.490823	0.463988	0.47636
287.18	0.63384	0.479066	0.515504	0.398257	0.498111	0.46876	0.483031
287.28	0.647516	0.490613	0.524232	0.405905	0.504043	0.472827	0.487974
287.38	0.665562	0.505976	0.535084	0.413239	0.510292	0.477447	0.493119
287.48	0.683175	0.521162	0.546528	0.421627	0.515497	0.482263	0.497056
287.58	0.704336	0.538821	0.560468	0.430866	0.522383	0.487691	0.502748
287.68	0.726965	0.559165	0.576499	0.441655	0.53081	0.493515	0.509803
287.78	0.750191	0.584573	0.5931	0.456555	0.542036	0.50245	0.520245
287.88	0.777641	0.6109	0.611352	0.467106	0.55363	0.511293	0.530038
287.98	0.820543	0.643821	0.632854	0.481883	0.566087	0.519184	0.539588
288.08	0.868688	0.686014	0.660383	0.501055	0.577784	0.528862	0.551336
288.18	0.900911	0.71359	0.67811	0.51165	0.584376	0.534155	0.558175
288.28	0.902789	0.714814	0.679694	0.51226	0.584499	0.535525	0.559289
288.38	0.874547	0.695496	0.668249	0.503794	0.579245	0.53413	0.553844
288.48	0.844367	0.673137	0.653829	0.493539	0.573733	0.530228	0.548734
288.58	0.815379	0.651187	0.639194	0.483973	0.567848	0.527492	0.544291
288.68	0.79929	0.641351	0.633977	0.478986	0.567652	0.526255	0.543924
288.78	0.790334	0.63726	0.632718	0.478014	0.570415	0.52764	0.545581
288.88	0.783335	0.635259	0.632763	0.477959	0.57216	0.528889	0.546555
288.98	0.781781	0.637974	0.636129	0.479643	0.576099	0.530756	0.549436
289.08	0.78423	0.642884	0.642171	0.483943	0.58093	0.534689	0.553667
289.18	0.787926	0.648849	0.649374	0.488127	0.587494	0.542905	0.558738
289.28	0.793651	0.656081	0.656644	0.493034	0.594374	0.547819	0.563928
289.38	0.797248	0.662851	0.664953	0.49763	0.598071	0.553469	0.569711
289.48	0.801479	0.670807	0.674339	0.503298	0.606077	0.561794	0.576954
289.58	0.808365	0.680026	0.685177	0.511845	0.618046	0.567987	0.586782
289.68	0.814664	0.69106	0.698278	0.52668	0.63231	0.578767	0.601161
289.78	0.82358	0.710551	0.717457	0.556749	0.657515	0.594932	0.62762
289.88	0.837909	0.737075	0.743536	0.592707	0.691135	0.612037	0.661664
289.98	0.844649	0.75229	0.758263	0.616629	0.709725	0.625624	0.679628
290.08	0.847295	0.75386	0.760768	0.616564	0.711709	0.632026	0.680989
290.18	0.848196	0.745102	0.756971	0.60058	0.704658	0.634184	0.67422
290.28	0.851897	0.739088	0.754907	0.585669	0.700016	0.644097	0.670835
290.38	0.850065	0.730125	0.751006	0.572647	0.698935	0.650071	0.668691
290.48	0.853668	0.728633	0.753744	0.569318	0.703968	0.660729	0.67487
290.58	0.854667	0.729237	0.755406	0.570976	0.708916	0.67345	0.681166
290.68	0.8596	0.730632	0.763131	0.575012	0.719175	0.685554	0.694934
290.78	0.854278	0.726532	0.764798	0.577334	0.724678	0.700431	0.703089
290.88	0.851456	0.726744	0.76875	0.584205	0.733875	0.713685	0.71499
290.98	0.849833	0.732271	0.776341	0.595609	0.743788	0.72883	0.731842
291.08	0.849814	0.736662	0.783446	0.605352	0.75763	0.746644	0.747479
291.18	0.855219	0.747761	0.795371	0.61973	0.774496	0.764386	0.767482
291.28	0.853205	0.751487	0.801247	0.629247	0.783902	0.780396	0.781264
291.38	0.861518	0.766824	0.815201	0.646259	0.801196	0.798865	0.800599

291.48	0.866853	0.772584	0.821154	0.655518	0.811207	0.812165	0.811118
291.58	0.871541	0.783767	0.831381	0.667959	0.824469	0.821929	0.824209
291.68	0.873407	0.785601	0.83331	0.673966	0.829804	0.828323	0.831124
291.78	0.876908	0.793362	0.842453	0.684909	0.84028	0.839912	0.841619
291.88	0.879649	0.796237	0.846213	0.691225	0.844956	0.844142	0.846494
291.98	0.885935	0.802482	0.851841	0.698784	0.852318	0.855136	0.853387
292.08	0.885809	0.806437	0.854302	0.70457	0.857793	0.856363	0.858963
292.18	0.886755	0.810547	0.858795	0.711751	0.861132	0.861482	0.863967
292.28	0.892572	0.818423	0.864552	0.720874	0.869389	0.869222	0.870584
292.38	0.89163	0.821248	0.867328	0.723211	0.871911	0.868906	0.873257
292.48	0.893673	0.824435	0.868677	0.727077	0.876286	0.873026	0.876205
292.58	0.897698	0.828315	0.871573	0.732536	0.879543	0.880479	0.879919
292.68	0.901926	0.83386	0.875492	0.739148	0.883981	0.882613	0.885457
292.78	0.90205	0.83563	0.876389	0.740099	0.88545	0.883651	0.886291
292.88	0.901169	0.835156	0.87689	0.742332	0.887012	0.882308	0.885768
292.98	0.910564	0.843697	0.88376	0.750964	0.894032	0.890989	0.891461
293.08	0.912699	0.847	0.888872	0.75582	0.895002	0.892209	0.892659
293.18	0.91432	0.849536	0.889981	0.763491	0.895203	0.891771	0.892872
293.28	0.912737	0.851102	0.891856	0.761682	0.894015	0.894287	0.891285
293.38	0.909208	0.849514	0.887677	0.760026	0.890695	0.888654	0.888059
293.48	0.915339	0.857032	0.89468	0.765025	0.893029	0.890833	0.890934
293.58	0.915752	0.858023	0.892546	0.766878	0.892078	0.891574	0.889605
293.68	0.915898	0.861841	0.889156	0.765636	0.891664	0.888406	0.890108
293.78	0.918842	0.867656	0.892864	0.768626	0.894116	0.889962	0.891651
293.88	0.914021	0.86688	0.891454	0.767423	0.894662	0.886636	0.888167
293.98	0.919058	0.873151	0.896497	0.773514	0.897941	0.885452	0.890468
294.08	0.917796	0.878079	0.89724	0.77618	0.895695	0.887708	0.888703
294.18	0.922322	0.881365	0.901543	0.779753	0.898202	0.890081	0.891991
294.28	0.917521	0.878644	0.899313	0.778549	0.893507	0.891463	0.887261
294.38	0.917306	0.880633	0.899795	0.781525	0.889071	0.890736	0.887313
294.48	0.918743	0.883024	0.901056	0.7841	0.889093	0.889742	0.887233
294.58	0.919736	0.889425	0.90524	0.789393	0.89402	0.889961	0.890944
294.68	0.918357	0.88689	0.903482	0.789321	0.892672	0.889724	0.88731
294.78	0.922287	0.891078	0.909482	0.795093	0.894995	0.890388	0.889506
294.88	0.923927	0.897669	0.910873	0.802195	0.898897	0.885861	0.890437
294.98	0.926408	0.896041	0.912715	0.803958	0.89826	0.888727	0.892347
295.08	0.926792	0.896865	0.913989	0.807078	0.898018	0.889473	0.893483
295.18	0.928832	0.898584	0.91477	0.813057	0.900803	0.892839	0.895458
295.28	0.931261	0.904045	0.916033	0.817325	0.905566	0.894813	0.896918
295.38	0.931744	0.905664	0.916483	0.82108	0.904616	0.89731	0.898849
295.48	0.933574	0.909305	0.917665	0.827275	0.909034	0.900512	0.901144
295.58	0.934977	0.909146	0.922974	0.83237	0.912005	0.905375	0.904036
295.68	0.940286	0.917155	0.925834	0.845509	0.918638	0.909293	0.91156
295.78	0.942745	0.921068	0.92895	0.855886	0.924028	0.911545	0.916207
295.88	0.947283	0.927389	0.936276	0.865183	0.927595	0.916992	0.921766

295.98	0.950922	0.930689	0.938338	0.872219	0.929512	0.921585	0.924198
296.08	0.951537	0.934635	0.942257	0.875388	0.933666	0.923718	0.928112
296.18	0.955867	0.941978	0.947348	0.888523	0.938489	0.926908	0.93433
296.28	0.965626	0.95396	0.95621	0.899328	0.947795	0.933846	0.944148
296.38	0.964574	0.959648	0.95779	0.909639	0.950133	0.939786	0.947006
296.48	0.968599	0.964158	0.963707	0.925054	0.95754	0.946376	0.956005
296.58	0.973927	0.976085	0.972021	0.941048	0.966482	0.953633	0.966541
296.68	0.976858	0.978232	0.974543	0.957748	0.970161	0.959504	0.970719
296.78	0.980122	0.98204	0.978522	0.963453	0.97444	0.961795	0.973901
296.88	0.982137	0.983958	0.980485	0.965888	0.974183	0.959387	0.974006
296.98	0.987868	0.987159	0.982071	0.957168	0.97479	0.958344	0.973233
297.08	0.981329	0.977746	0.975531	0.943016	0.966069	0.955235	0.964825
297.18	0.971218	0.967251	0.969176	0.91913	0.956089	0.946284	0.957738
297.28	0.964355	0.960169	0.962679	0.913695	0.950534	0.945523	0.951562
297.38	0.961035	0.955688	0.958736	0.904795	0.947181	0.941654	0.948814
297.48	0.95808	0.952298	0.956175	0.901705	0.944791	0.940235	0.94574
297.58	0.961042	0.954809	0.955881	0.902578	0.94548	0.943734	0.942824
297.68	0.957453	0.948999	0.95486	0.897574	0.943819	0.940397	0.939986
297.78	0.9583	0.947232	0.953562	0.895479	0.942762	0.939572	0.940898
297.88	0.959518	0.949658	0.952932	0.897634	0.946198	0.943316	0.941587
297.98	0.96178	0.949377	0.95605	0.899919	0.949805	0.94491	0.944554
298.08	0.961895	0.951126	0.958073	0.906598	0.951394	0.947343	0.947413
298.18	0.963709	0.953855	0.958229	0.913691	0.95425	0.950582	0.948513
298.28	0.96232	0.953354	0.961159	0.920318	0.955843	0.95281	0.953887
298.38	0.969904	0.962571	0.965728	0.937437	0.963727	0.963227	0.962864
298.48	0.971747	0.968508	0.972881	0.947401	0.967106	0.96711	0.968482
298.58	0.977107	0.975274	0.976173	0.953659	0.974383	0.970477	0.973742
298.68	0.979483	0.978743	0.978769	0.959541	0.978572	0.974015	0.977421
298.78	0.986341	0.988665	0.98686	0.96844	0.987143	0.977083	0.98542
298.88	0.986382	0.995107	0.991981	0.979358	0.992701	0.981012	0.991696
298.98	0.990376	0.997432	0.993935	0.987668	0.995546	0.982538	0.995028
299.08	0.994902	1.00707	1.001751	1.005352	1.004097	0.991754	1.004292
299.18	0.99684	1.01198	1.004362	1.019656	1.010357	0.997135	1.010929
299.28	1.003155	1.017699	1.009189	1.033701	1.012653	1.00267	1.017778
299.38	1.009864	1.019912	1.01469	1.038834	1.012276	1.004959	1.020255
299.48	1.010825	1.019631	1.012112	1.035138	1.010506	1.004493	1.014606
299.58	1.011739	1.016917	1.009407	1.025348	1.007165	1.001833	1.01
299.68	1.011606	1.013069	1.00939	1.016423	1.007612	0.998732	1.00811
299.78	1.007036	1.005225	1.003402	1.005638	1.001051	0.995444	1.001516
299.88	1.003773	1.001068	1.000813	0.999411	0.998368	0.98761	0.997671
299.98	1.006552	1.001289	1.001047	0.996732	1.00023	0.990363	0.998025
300.08	0.997735	0.995599	0.996555	0.990399	0.996191	0.987398	0.993645
300.18	0.999949	0.996657	0.995002	0.990356	0.994639	0.989034	0.991961
300.28	0.996578	0.9916	0.994025	0.985785	0.994533	0.988454	0.99173
300.38	0.996449	0.989129	0.992768	0.985461	0.993552	0.988571	0.990613

300.48	0.996345	0.992549	0.992962	0.984815	0.995244	0.990344	0.993567
300.58	0.992796	0.987099	0.991656	0.980992	0.992214	0.987371	0.989961
300.68	0.998382	0.991932	0.995224	0.982954	0.995647	0.990612	0.993473
300.78	0.994249	0.988788	0.992768	0.979939	0.993443	0.987137	0.991235
300.88	0.997466	0.988826	0.993585	0.983829	0.992527	0.992889	0.99144
300.98	0.993724	0.988	0.993413	0.981683	0.99227	0.99131	0.991311
301.08	0.993946	0.988909	0.994446	0.983729	0.993509	0.992454	0.992523
301.18	0.999671	0.992202	0.996854	0.987792	0.996578	0.994734	0.994861
301.28	0.994039	0.990264	0.994775	0.988904	0.995181	0.995874	0.994373
301.38	0.993348	0.990694	0.994812	0.98599	0.995605	0.993318	0.996151
301.48	0.998125	0.994816	0.998237	0.991017	0.999086	0.996388	0.999423
301.58	0.992965	0.991356	0.996239	0.991263	0.995823	0.997098	0.996103
301.68	0.997428	0.994826	0.997395	0.991516	0.997273	0.998706	0.996004
301.78	0.996651	0.993391	0.998043	0.989591	0.997442	0.997277	0.996928
301.88	0.996192	0.994226	0.998304	0.98845	0.996636	0.99813	0.99566
301.98	0.99742	0.995565	0.998794	0.993166	0.998516	1.001969	0.996583
302.08	1.000731	0.99966	0.999142	0.996408	0.997222	1.002112	0.999462
302.18	0.997662	0.996206	0.999216	0.995513	0.998556	1.003075	0.998259
302.28	0.999026	0.996926	1.000508	1.001796	0.999389	1.003358	0.998981
302.38	1.000482	0.996023	1.001209	1.003206	0.999549	1.003756	0.999526
302.48	1.0017	0.999862	1.003682	1.003809	1.003016	1.004368	1.002512
302.58	1.001368	1.000612	1.000621	1.002735	0.999549	1.004954	1.000187
302.68	1.002932	1.002144	1.00204	1.004206	1.000386	1.004991	1.001218
302.78	1.000278	0.999327	1.00161	1.002055	1.000045	1.002948	1.001944
302.88	1.003326	0.999643	1.001236	1.003136	1.001114	1.005331	1.00265
302.98	1.005407	1.003787	1.004026	1.0018	1.005832	1.006362	1.005351
303.08	1.001808	1.000327	1.001438	0.999935	1.004075	1.003725	1.002571
303.18	1.002836	1.00093	1.001702	1.005352	1.004009	1.006457	1.002767
303.28	1.004216	1.004666	1.002973	1.010699	1.00298	1.007572	1.00293
303.38	1.001203	1.000858	1.001965	1.010035	1.003343	1.008039	1.002468
303.48	1.00252	1.001962	1.003052	1.010693	1.003636	1.011068	1.003683
303.58	1.0037	1.002282	1.002276	1.011142	1.002702	1.011992	1.003175
303.68	1.004281	1.00576	1.004412	1.011066	1.003117	1.01189	1.005991
303.78	1.001179	1.00462	1.002508	1.009608	1.001237	1.011479	1.004099
303.88	1.000479	1.002994	1.000164	1.00661	1.000334	1.012012	1.002937
303.98	1.001814	1.003124	1.000267	1.008668	1.004142	1.012035	1.003534
304.08	0.999975	1.006378	1.002422	1.010968	1.006385	1.011949	1.005754
304.18	0.996481	1.002011	1.000125	1.011795	1.003255	1.009927	1.002765
304.28	1.000861	1.006398	1.002148	1.013849	1.005855	1.010147	1.005466
304.38	0.997804	1.001979	0.999412	1.012157	1.00306	1.007273	1.002903
304.48	0.998423	1.002409	0.998729	1.015638	1.000837	1.010968	1.001999
304.58	1.000422	1.00563	1.001297	1.016898	0.999185	1.011977	1.004395
304.68	1.000923	1.005765	1.000904	1.01747	1.000835	1.011812	1.004455
304.78	0.99804	1.004442	1.000887	1.018557	1.000969	1.011497	1.003909
304.88	0.999801	1.005924	1.000679	1.020572	1.002753	1.011444	1.003997

304.98	0.996639	1.002239	0.998291	1.021409	1.000479	1.01113	1.002184
305.08	0.994845	1.001807	0.996419	1.021524	0.999886	1.007864	1.000745
305.18	0.99521	1.001746	0.996289	1.021691	1.00002	1.008971	1.000766
305.28	0.996622	1.001807	0.995976	1.02292	1.000252	1.009509	1.000942
305.38	0.997618	1.005181	0.997896	1.023332	1.002662	1.011549	1.002837
305.48	0.99915	1.002082	0.995134	1.023462	0.99959	1.01122	1.000253
305.58	0.995529	1.000727	0.993638	1.022891	0.997809	1.010187	0.99865
305.68	0.996677	1.001447	0.993418	1.022697	1.000174	1.009476	0.998363
305.78	0.997585	1.004526	0.995192	1.02141	1.001264	1.00918	1.000946
305.88	0.998026	1.002397	0.992802	1.023033	0.997676	1.00913	1.000265
305.98	0.993631	1.002105	0.991906	1.024025	0.996498	1.009986	0.996978
306.08	0.994085	1.001383	0.991128	1.026668	0.996024	1.010457	0.99607
306.18	0.993181	1.001006	0.990339	1.027732	0.994712	1.00958	0.996905
306.28	0.986959	0.999162	0.987939	1.025277	0.991569	1.007643	0.992683
306.38	0.992706	1.003352	0.989992	1.026934	0.994741	1.006812	0.994883
306.48	0.992554	1.003113	0.989415	1.027596	0.993196	1.00632	0.993993
306.58	0.98828	0.999681	0.986266	1.027796	0.990285	1.004488	0.990423
306.68	0.991956	1.001444	0.986811	1.029307	0.989806	1.005039	0.990432
306.78	0.988138	1.000451	0.984448	1.028953	0.987642	1.002526	0.98934
306.88	0.986936	0.999937	0.983074	1.026803	0.986472	0.998812	0.988635
306.98	0.987029	0.999233	0.982093	1.029142	0.98396	0.998653	0.986482
307.08	0.987574	0.998773	0.981569	1.028795	0.982527	0.998258	0.987301
307.18	0.985218	1.000928	0.981886	1.030796	0.982974	0.997993	0.985211
307.28	0.987578	1.001167	0.982071	1.031192	0.982773	0.995354	0.984905
307.38	0.987325	1.004334	0.982389	1.032136	0.98255	0.996464	0.984862
307.48	0.983174	1.001065	0.979452	1.032176	0.979452	0.992773	0.980461
307.58	0.98855	1.001867	0.979536	1.034599	0.979926	0.993509	0.979649
307.68	0.983226	1.002907	0.978369	1.034409	0.977505	0.99179	0.977798
307.78	0.982512	1.002109	0.977627	1.034254	0.976348	0.990516	0.975727
307.88	0.988171	1.006969	0.979467	1.037653	0.976896	0.992824	0.977533
307.98	0.98369	1.001908	0.976177	1.033851	0.972929	0.987976	0.973028
308.08	0.984597	1.005043	0.977039	1.036875	0.97427	0.987445	0.973996
308.18	0.985901	1.005222	0.976537	1.034356	0.974347	0.983536	0.97254
308.28	0.985084	1.006569	0.977035	1.034888	0.975421	0.982922	0.971469
308.38	0.986717	1.004086	0.976312	1.036581	0.972196	0.981238	0.968381
308.48	0.987362	1.004677	0.975668	1.038079	0.969954	0.979747	0.965694
308.58	0.990124	1.008628	0.977042	1.039298	0.9716	0.981547	0.966922
308.68	0.989852	1.008003	0.976019	1.039529	0.969083	0.978927	0.964646
308.78	0.990154	1.008015	0.975239	1.039725	0.967653	0.977535	0.963264
308.88	0.992013	1.008027	0.974459	1.03992	0.966224	0.976144	0.961882

Fig. 3.1.

	LG 18 HA	LG 19 HA	LG 18 FA	LG 19 FA	LG 20 FA		LG 20 HA
280.0612	0.001418	-0.0017	0.763619	0.005937	-0.02669	280.14	-0.00154

280.1006	0.0014	-0.0043	0.770304	0.007091	-0.02238	280.179	-0.00214
280.14	0.001686	-0.0058	0.77449	0.007806	-0.01663	280.219	-0.00241
280.1794	0.003108	-0.00475	0.770343	0.007046	-0.01133	280.258	-0.00238
280.2188	0.003639	-0.00309	0.770633	0.005465	-0.00632	280.298	-0.00199
280.2582	0.004105	-0.00188	0.769881	0.004115	-0.00149	280.337	-0.00137
280.2977	0.00449	-0.00062	0.768502	0.00315	0.002683	280.376	-0.00064
280.3371	0.004802	0.000772	0.766684	0.002294	0.005873	280.416	-5.4E-05
280.3765	0.004879	0.001866	0.765528	0.001502	0.008083	280.455	0.000401
280.4159	0.004802	0.002518	0.765183	0.000808	0.009447	280.495	0.000753
280.4553	0.004713	0.002907	0.766774	0.000162	0.010018	280.534	0.001062
280.4947	0.004733	0.003255	0.769449	-0.00048	0.009728	280.573	0.001312
280.5341	0.004776	0.003566	0.77245	-0.00111	0.008539	280.613	0.001491
280.5735	0.004637	0.003647	0.774162	-0.00168	0.006635	280.652	0.001481
280.6129	0.00432	0.003343	0.774909	-0.00211	0.00445	280.692	0.001362
280.6523	0.00388	0.002659	0.774602	-0.00234	0.002453	280.731	0.001202
280.6917	0.003457	0.001731	0.773084	-0.00234	0.000909	280.771	0.001266
280.7311	0.002966	0.000752	0.769352	-0.00214	-0.00018	280.81	0.001445
280.7705	0.002441	-4.3E-05	0.764315	-0.00186	-0.00091	280.849	0.001632
280.81	0.001885	-0.00045	0.758838	-0.00165	-0.00122	280.889	0.001521
280.8494	0.001482	-0.00043	0.75478	-0.0016	-0.00095	280.928	0.001183
280.8888	0.001187	-0.00018	0.752286	-0.00173	-6.4E-05	280.968	0.000719
280.9282	0.000953	9.32E-05	0.752113	-0.00203	0.00125	281.007	0.000241
280.9676	0.000652	0.000319	0.753847	-0.00251	0.002748	281.046	-0.00018
281.007	0.00032	0.000613	0.75688	-0.00321	0.004417	281.086	-0.00049
281.0464	4.91E-06	0.001044	0.760257	-0.00405	0.006413	281.125	-0.00045
281.0858	-0.00023	0.001513	0.763772	-0.00483	0.008675	281.165	-0.00015
281.1252	-0.00039	0.001866	0.767133	-0.0054	0.010716	281.204	0.000276
281.1646	-0.0005	0.002074	0.77039	-0.00572	0.011923	281.243	0.000443
281.204	-0.00056	0.00222	0.772311	-0.00583	0.012021	281.283	0.000456
281.2434	-0.00055	0.002302	0.772837	-0.00577	0.011152	281.322	0.000454
281.2828	-0.00033	0.002149	0.771387	-0.00553	0.009538	281.362	0.001171
281.3223	-9.8E-06	0.001569	0.768835	-0.00504	0.007275	281.401	0.002244
281.3617	0.000336	0.000553	0.765527	-0.0043	0.004494	281.44	0.003194
281.4011	0.000473	-0.0007	0.761846	-0.00338	0.001569	281.48	0.002298
281.4405	0.000457	-0.00195	0.757651	-0.00236	-0.00099	281.519	8.43E-05
281.4799	0.000337	-0.00302	0.753419	-0.00129	-0.00285	281.559	-0.00257
281.5193	0.00028	-0.00384	0.749852	-0.00016	-0.00405	281.598	-0.00335
281.5587	0.000133	-0.00438	0.747952	0.000989	-0.00478	281.637	-0.00252
281.5981	-0.0001	-0.00456	0.747543	0.002039	-0.00518	281.677	-0.00081
281.6375	-0.00051	-0.00429	0.748309	0.002898	-0.00521	281.716	0.000194
281.6769	-0.00083	-0.00354	0.749858	0.003572	-0.00486	281.756	0.000416
281.7163	-0.00106	-0.0023	0.751975	0.00415	-0.00433	281.795	0.000108
281.7557	-0.00108	-0.00063	0.7549	0.004679	-0.00398	281.835	-0.00028
281.7951	-0.00111	0.0013	0.757991	0.005084	-0.00408	281.874	-0.00065
281.8345	-0.00121	0.003169	0.760699	0.005236	-0.00461	281.913	-0.00095

281.874	-0.00154	0.004624	0.761856	0.005124	-0.0054	281.953	-0.00106
281.9134	-0.00194	0.005449	0.761408	0.004907	-0.00634	281.992	-0.001
281.9528	-0.00234	0.005621	0.759713	0.004775	-0.00745	282.032	-0.00085
281.9922	-0.00257	0.005208	0.757273	0.004754	-0.00873	282.071	-0.00079
282.0316	-0.00281	0.004284	0.75393	0.004663	-0.01012	282.11	-0.00082
282.071	-0.00306	0.002985	0.750121	0.004295	-0.01168	282.15	-0.0009
282.1104	-0.00336	0.00156	0.746508	0.003624	-0.01358	282.189	-0.00089
282.1498	-0.0035	0.000305	0.744405	0.002824	-0.01601	282.229	-0.00079
282.1892	-0.00348	-0.00057	0.743999	0.002087	-0.01898	282.268	-0.00072
282.2286	-0.00341	-0.00102	0.74541	0.001445	-0.02235	282.307	-0.00101
282.268	-0.00347	-0.00109	0.748133	0.000773	-0.0258	282.347	-0.00168
282.3074	-0.00368	-0.00088	0.751517	-5.8E-05	-0.02892	282.386	-0.00246
282.3468	-0.00397	-0.00047	0.754795	-0.00105	-0.03134	282.426	-0.00274
282.3863	-0.00425	1.87E-05	0.757465	-0.00208	-0.03297	282.465	-0.00237
282.4257	-0.00447	0.000383	0.75935	-0.00302	-0.03428	282.504	-0.00162
282.4651	-0.00467	0.000348	0.760235	-0.00383	-0.03593	282.544	-0.00101
282.5045	-0.00485	-0.00024	0.759613	-0.00455	-0.03824	282.583	-0.00077
282.5439	-0.00494	-0.00128	0.757544	-0.00522	-0.04097	282.623	-0.00076
282.5833	-0.00478	-0.00251	0.754476	-0.00585	-0.04368	282.662	-0.00067
282.6227	-0.0043	-0.00371	0.75109	-0.0064	-0.04616	282.701	-0.00036
282.6621	-0.00364	-0.00488	0.747782	-0.00677	-0.04834	282.741	6.94E-06
282.7015	-0.00303	-0.00607	0.744613	-0.00691	-0.04995	282.78	-5.5E-05
282.7409	-0.0026	-0.00721	0.741722	-0.00685	-0.05051	282.82	-0.00081
282.7803	-0.00232	-0.00817	0.739261	-0.00667	-0.04987	282.859	-0.00185
282.8197	-0.00221	-0.00891	0.737349	-0.00647	-0.04848	282.899	-0.00232
282.8591	-0.00238	-0.0095	0.736093	-0.00628	-0.04707	282.938	-0.00155
282.8986	-0.00294	-0.01005	0.735427	-0.00611	-0.04602	282.977	-5.3E-05
282.938	-0.00375	-0.01049	0.735209	-0.00598	-0.04515	283.017	0.001388
282.9774	-0.0046	-0.01064	0.735298	-0.00589	-0.04419	283.056	0.001953
283.0168	-0.00529	-0.0104	0.735888	-0.00584	-0.04321	283.096	0.001953
283.0562	-0.00583	-0.00989	0.737265	-0.00576	-0.04266	283.135	0.001868
283.0956	-0.0062	-0.00932	0.73993	-0.0056	-0.04288	283.174	0.002365
283.135	-0.00647	-0.00882	0.743248	-0.0053	-0.04377	283.214	0.003114
283.1744	-0.00666	-0.00837	0.746656	-0.00486	-0.04492	283.253	0.003595
283.2138	-0.00674	-0.00788	0.749229	-0.00431	-0.04606	283.293	0.002763
283.2532	-0.00674	-0.00732	0.751274	-0.00368	-0.04709	283.332	0.001234
283.2926	-0.00673	-0.00676	0.752755	-0.00303	-0.04783	283.371	-0.00023
283.332	-0.00687	-0.00623	0.753506	-0.00245	-0.04784	283.411	0.000134
283.3714	-0.00717	-0.00573	0.753005	-0.00199	-0.04666	283.45	0.001693
283.4108	-0.00759	-0.00524	0.751881	-0.00163	-0.0442	283.49	0.003787
283.4503	-0.00818	-0.00478	0.750827	-0.00129	-0.0408	283.529	0.004593
283.4897	-0.00883	-0.0043	0.751087	-0.00087	-0.03686	283.568	0.004609
283.5291	-0.00935	-0.00371	0.752725	-0.00025	-0.03253	283.608	0.00437
283.5685	-0.00933	-0.00279	0.756351	0.00063	-0.02769	283.647	0.004934
283.6079	-0.00869	-0.00128	0.761585	0.001795	-0.02214	283.687	0.006397

283.6473	-0.00753	0.001049	0.768024	0.00319	-0.01578	283.726	0.008824
283.6867	-0.00622	0.00441	0.77491	0.004768	-0.00864	283.766	0.012459
283.7261	-0.0046	0.008971	0.782083	0.006579	-0.00105	283.805	0.017266
283.7655	-0.00262	0.014873	0.789381	0.008754	0.006439	283.844	0.023181
283.8049	-9.5E-05	0.022274	0.796318	0.011392	0.013296	283.884	0.029772
283.8443	0.00275	0.031393	0.802357	0.014467	0.019291	283.923	0.037299
283.8837	0.006054	0.042531	0.80812	0.017889	0.024505	283.963	0.04627
283.9231	0.010089	0.055976	0.81419	0.021614	0.02912	284.002	0.050747
283.9626	0.015295	0.0719	0.821876	0.025649	0.033428	284.041	0.06513
284.002	0.021675	0.090328	0.832235	0.029969	0.037969	284.081	0.082343
284.0414	0.029116	0.111202	0.847615	0.034492	0.044133	284.12	0.102105
284.0808	0.037444	0.134259	0.869509	0.039193	0.052622	284.16	0.124507
284.1202	0.046715	0.159462	0.897591	0.044228	0.063259	284.199	0.14976
284.1596	0.057225	0.186995	0.930497	0.049902	0.075071	284.238	0.178621
284.199	0.069062	0.216958	0.967556	0.056508	0.087325	284.278	0.211519
284.2384	0.082135	0.249335	1.008876	0.064247	0.100132	284.317	0.247851
284.2778	0.096204	0.284144	1.054751	0.073319	0.113978	284.357	0.285534
284.3172	0.111083	0.321351	1.104062	0.084063	0.128885	284.396	0.322933
284.3566	0.126848	0.360522	1.156143	0.096941	0.144236	284.435	0.360259
284.396	0.143618	0.400657	1.211442	0.112326	0.159396	284.475	0.397801
284.4354	0.161375	0.440518	1.271081	0.130317	0.174267	284.514	0.43547
284.4749	0.17991	0.479137	1.336072	0.150826	0.18909	284.554	0.47299
284.5143	0.199197	0.515938	1.406362	0.173856	0.203755	284.593	0.509905
284.5537	0.219296	0.550542	1.481564	0.199625	0.217584	284.632	0.545138
284.5931	0.240204	0.582651	1.56059	0.228391	0.229933	284.672	0.578351
284.6325	0.261401	0.612094	1.642633	0.260162	0.240908	284.711	0.609284
284.6719	0.281743	0.638925	1.726022	0.294542	0.251347	284.751	0.637183
284.7113	0.300876	0.663382	1.810244	0.33081	0.262059	284.79	0.661936
284.7507	0.318702	0.685675	1.893894	0.36819	0.27314	284.83	0.683698
284.7901	0.33571	0.705925	1.974002	0.406232	0.284153	284.869	0.703497
284.8295	0.351326	0.724266	2.048711	0.444968	0.294902	284.908	0.720747
284.8689	0.364913	0.7409	2.116599	0.484607	0.305854	284.948	0.734859
284.9083	0.375242	0.756057	2.177682	0.52622	0.317749	284.987	0.74446
284.9477	0.382945	0.769785	2.230622	0.566522	0.330945	285.027	0.74993
284.9871	0.387975	0.781801	2.272734	0.605112	0.345295	285.066	0.752086
285.0266	0.390638	0.791633	2.302368	0.640267	0.360397	285.105	0.755103
285.066	0.390249	0.798777	2.318838	0.670702	0.375508	285.145	0.757734
285.1054	0.387219	0.802697	2.320614	0.695431	0.389273	285.184	0.757829
285.1448	0.382276	0.802954	2.307025	0.713531	0.400104	285.224	0.750135
285.1842	0.376683	0.799619	2.277408	0.724371	0.407255	285.263	0.735565
285.2236	0.370296	0.793463	2.234037	0.727995	0.411393	285.302	0.716797
285.263	0.362484	0.785555	2.178992	0.725162	0.413816	285.342	0.698293
285.3024	0.352951	0.776617	2.115171	0.717054	0.41526	285.381	0.680706
285.3418	0.342282	0.766827	2.046723	0.704894	0.415697	285.421	0.663074
285.3812	0.331216	0.756219	1.976826	0.689682	0.415063	285.46	0.643444

285.4206	0.32006	0.745061	1.908363	0.672072	0.413682	285.499	0.62176
285.46	0.309101	0.733712	1.843525	0.65233	0.411819	285.539	0.599497
285.4994	0.298534	0.722259	1.783719	0.630315	0.409131	285.578	0.578296
285.5389	0.288964	0.710507	1.730663	0.605635	0.404908	285.618	0.558886
285.5783	0.2807	0.698309	1.68446	0.578037	0.398901	285.657	0.541163
285.6177	0.273626	0.685857	1.644066	0.547755	0.391708	285.696	0.524841
285.6571	0.267514	0.673651	1.60874	0.5155	0.384269	285.736	0.509432
285.6965	0.262207	0.662208	1.57877	0.482216	0.376998	285.775	0.495491
285.7359	0.257799	0.651782	1.554075	0.448859	0.369497	285.815	0.483701
285.7753	0.254497	0.642343	1.535339	0.416336	0.361104	285.854	0.474633
285.8147	0.252466	0.633782	1.521762	0.385544	0.351598	285.894	0.468219
285.8541	0.251514	0.626137	1.51276	0.357357	0.341294	285.933	0.464529
285.8935	0.251515	0.619651	1.50721	0.332551	0.33073	285.972	0.465246
285.9329	0.252277	0.614566	1.506046	0.311665	0.320546	286.012	0.468964
285.9723	0.253739	0.610878	1.508883	0.294885	0.311556	286.051	0.474316
286.0117	0.256016	0.608341	1.515672	0.282088	0.304591	286.091	0.478617
286.0512	0.258967	0.606693	1.52535	0.272943	0.29999	286.13	0.481857
286.0906	0.262374	0.605891	1.538514	0.266928	0.297376	286.169	0.484099
286.13	0.265947	0.606047	1.557038	0.263393	0.296016	286.209	0.485405
286.1694	0.26949	0.607154	1.581954	0.261726	0.295198	286.248	0.48583
286.2088	0.272939	0.608922	1.611735	0.261456	0.294222	286.288	0.485412
286.2482	0.276376	0.610881	1.644417	0.26217	0.292342	286.327	0.484376
286.2876	0.279537	0.612572	1.678173	0.263413	0.289062	286.366	0.482668
286.327	0.282291	0.613627	1.712055	0.264731	0.284509	286.406	0.480074
286.3664	0.284524	0.613723	1.745623	0.265757	0.2793	286.445	0.4761
286.4058	0.286225	0.612576	1.77677	0.266235	0.274071	286.485	0.470609
286.4452	0.287297	0.610043	1.80428	0.265983	0.269222	286.524	0.463932
286.4846	0.287558	0.606149	1.82743	0.264865	0.264993	286.563	0.4567
286.524	0.286696	0.601025	1.845932	0.26279	0.2615	286.603	0.449369
286.5634	0.284725	0.594832	1.859783	0.259745	0.258558	286.642	0.441641
286.6029	0.281833	0.587714	1.868622	0.255854	0.255635	286.682	0.432832
286.6423	0.278271	0.579813	1.871612	0.251432	0.252198	286.721	0.421877
286.6817	0.274126	0.571307	1.86845	0.246946	0.24813	286.76	0.409879
286.7211	0.269443	0.5624	1.859779	0.242851	0.243755	286.8	0.398085
286.7605	0.264235	0.553321	1.847191	0.239366	0.239509	286.839	0.38914
286.7999	0.258659	0.54434	1.831097	0.236408	0.235766	286.879	0.381881
286.8393	0.252725	0.535744	1.811271	0.233768	0.232966	286.918	0.375235
286.8787	0.246257	0.527789	1.785481	0.231351	0.231553	286.958	0.365888
286.9181	0.239333	0.520622	1.755321	0.229221	0.231497	286.997	0.35499
286.9575	0.232204	0.514266	1.722575	0.227431	0.231979	287.036	0.343894
286.9969	0.225066	0.508704	1.689145	0.2259	0.231865	287.076	0.335517
287.0363	0.218241	0.503974	1.655682	0.224488	0.230567	287.115	0.329814
287.0757	0.211907	0.500143	1.623791	0.223205	0.22833	287.155	0.326253
287.1152	0.20623	0.497237	1.595066	0.222307	0.225714	287.194	0.324422
287.1546	0.201544	0.495191	1.572959	0.222168	0.22314	287.233	0.323941

287.194	0.19789	0.493866	1.556993	0.22306	0.221064	287.273	0.3242
287.2334	0.195392	0.493138	1.545837	0.225056	0.220213	287.312	0.323677
287.2728	0.194136	0.492977	1.538385	0.228094	0.221201	287.352	0.321784
287.3122	0.193929	0.493416	1.535152	0.232073	0.223828	287.391	0.31944
287.3516	0.194469	0.494471	1.537217	0.23689	0.227031	287.43	0.318198
287.391	0.195435	0.496158	1.545786	0.242441	0.22968	287.47	0.319272
287.4304	0.196914	0.498625	1.561004	0.248655	0.231342	287.509	0.32231
287.4698	0.19899	0.502225	1.583295	0.255507	0.232283	287.549	0.326779
287.5092	0.201626	0.507346	1.614093	0.263	0.23298	287.588	0.331796
287.5486	0.204955	0.514105	1.653714	0.271135	0.233874	287.627	0.337837
287.588	0.209347	0.522249	1.701548	0.279901	0.235495	287.667	0.345473
287.6274	0.215514	0.531459	1.757135	0.289293	0.238498	287.706	0.355818
287.6669	0.223814	0.541777	1.819486	0.299324	0.24338	287.746	0.368991
287.7063	0.234196	0.553685	1.88896	0.310044	0.250212	287.785	0.385176
287.7457	0.246709	0.567738	1.967327	0.321568	0.2587	287.824	0.40487
287.7851	0.261376	0.584165	2.054232	0.334114	0.268397	287.864	0.428393
287.8245	0.278141	0.602936	2.149373	0.347976	0.278838	287.903	0.456003
287.8639	0.297242	0.624049	2.251901	0.363411	0.289694	287.943	0.48933
287.9033	0.318398	0.647544	2.360425	0.380506	0.30105	287.982	0.528908
287.9427	0.341465	0.673232	2.473848	0.399164	0.313536	288.022	0.573603
287.9821	0.366258	0.700523	2.590195	0.419168	0.328013	288.061	0.619567
288.0215	0.392475	0.728523	2.705749	0.44023	0.345042	288.1	0.664429
288.0609	0.419856	0.756282	2.818894	0.461982	0.36467	288.14	0.708079
288.1003	0.448088	0.782979	2.928078	0.483962	0.386741	288.179	0.750436
288.1397	0.476507	0.808098	3.031587	0.505711	0.411327	288.219	0.790464
288.1792	0.505883	0.831572	3.128413	0.526924	0.438863	288.258	0.827227
288.2186	0.534785	0.85365	3.217094	0.547499	0.469914	288.297	0.859859
288.258	0.56294	0.874473	3.295641	0.56741	0.504611	288.337	0.885914
288.2974	0.589844	0.893802	3.363869	0.586568	0.542329	288.376	0.906149
288.3368	0.614892	0.9112	3.420981	0.604852	0.582132	288.416	0.9219
288.3762	0.637557	0.926448	3.467291	0.622181	0.623185	288.455	0.938009
288.4156	0.657064	0.939633	3.502574	0.638479	0.664437	288.494	0.953544
288.455	0.672594	0.950776	3.525855	0.653544	0.70409	288.534	0.967255
288.4944	0.683501	0.959557	3.536002	0.666968	0.739637	288.573	0.975591
288.5338	0.689168	0.965596	3.534544	0.6782	0.768685	288.613	0.97858
288.5732	0.689305	0.968975	3.521967	0.686732	0.789777	288.652	0.977334
288.6126	0.683436	0.970338	3.499223	0.692327	0.802443	288.691	0.974952
288.652	0.671788	0.970396	3.466617	0.695161	0.807036	288.731	0.971971
288.6915	0.655448	0.969344	3.425449	0.695726	0.804664	288.77	0.967408
288.7309	0.635518	0.966888	3.376399	0.694557	0.796841	288.81	0.958719
288.7703	0.612985	0.962822	3.321396	0.691972	0.784911	288.849	0.944837
288.8097	0.588889	0.95747	3.263254	0.688031	0.769724	288.888	0.928164
288.8491	0.564058	0.951587	3.204051	0.682774	0.751824	288.928	0.911932
288.8885	0.539329	0.94585	3.145603	0.676519	0.731902	288.967	0.898938
288.9279	0.515741	0.940495	3.088865	0.669865	0.710838	289.007	0.888204

288.9673	0.493637	0.935436	3.034874	0.663372	0.68934	289.046	0.878802
289.0067	0.473373	0.930586	2.984508	0.657271	0.667832	289.086	0.869461
289.0461	0.455201	0.925854	2.939623	0.651523	0.646837	289.125	0.860311
289.0855	0.439313	0.920869	2.899745	0.646113	0.627409	289.164	0.85145
289.1249	0.426339	0.915025	2.864988	0.641267	0.610955	289.204	0.842625
289.1643	0.416642	0.908012	2.83444	0.637307	0.598349	289.243	0.834136
289.2037	0.409496	0.900218	2.807917	0.63434	0.589319	289.283	0.826449
289.2432	0.404127	0.892515	2.784916	0.632123	0.582874	289.322	0.820384
289.2826	0.400008	0.885684	2.766236	0.63028	0.578165	289.361	0.816067
289.322	0.396933	0.880106	2.751491	0.62859	0.57486	289.401	0.813547
289.3614	0.394801	0.875903	2.740446	0.627094	0.572866	289.44	0.813582
289.4008	0.393177	0.873112	2.732384	0.626003	0.571955	289.48	0.816576
289.4402	0.391981	0.871628	2.727308	0.625567	0.571767	289.519	0.821409
289.4796	0.391289	0.871167	2.725724	0.625985	0.572028	289.558	0.826203
289.519	0.391343	0.87137	2.72906	0.62733	0.572646	289.598	0.828847
289.5584	0.39219	0.871958	2.736614	0.62951	0.573582	289.637	0.830118
289.5978	0.393691	0.872788	2.747267	0.632316	0.574634	289.677	0.830967
289.6372	0.395667	0.873805	2.759432	0.635541	0.575411	289.716	0.834605
289.6766	0.397923	0.874978	2.772195	0.639063	0.575614	289.755	0.839603
289.716	0.400446	0.876257	2.78491	0.642807	0.575328	289.795	0.844249
289.7555	0.403184	0.877572	2.796439	0.646663	0.574945	289.834	0.842945
289.7949	0.406152	0.878875	2.805487	0.650488	0.574741	289.874	0.836647
289.8343	0.409386	0.880181	2.812619	0.654206	0.574551	289.913	0.827658
289.8737	0.412994	0.881553	2.818817	0.657845	0.573895	289.952	0.820885
289.9131	0.416989	0.883076	2.825029	0.661447	0.572397	289.992	0.817255
289.9525	0.421336	0.884849	2.831037	0.664935	0.570013	290.031	0.815871
289.9919	0.425984	0.886975	2.836413	0.668143	0.566925	290.071	0.815042
290.0313	0.430917	0.889494	2.840979	0.670961	0.56345	290.11	0.813776
290.0707	0.436116	0.892298	2.844623	0.673448	0.560196	290.15	0.812608
290.1101	0.441544	0.895145	2.846945	0.675783	0.558128	290.189	0.812439
290.1495	0.447123	0.89781	2.846187	0.67812	0.558116	290.228	0.814905
290.1889	0.452773	0.900207	2.843277	0.680533	0.560209	290.268	0.819131
290.2283	0.458504	0.902357	2.839684	0.683072	0.563552	290.307	0.824101
290.2678	0.464252	0.904297	2.839523	0.685786	0.567082	290.347	0.826903
290.3072	0.470113	0.906106	2.842924	0.688653	0.570186	290.386	0.828302
290.3466	0.476148	0.90799	2.848796	0.691514	0.572647	290.425	0.829325
290.386	0.482519	0.910275	2.854554	0.694134	0.57422	290.465	0.832391
290.4254	0.489224	0.913282	2.860596	0.696326	0.574656	290.504	0.837564
290.4648	0.496245	0.917206	2.866281	0.698027	0.574155	290.544	0.844437
290.5042	0.503671	0.922123	2.870928	0.699271	0.573499	290.583	0.852888
290.5436	0.511586	0.92804	2.871419	0.700127	0.573569	290.622	0.862989
290.583	0.519658	0.934927	2.868726	0.700678	0.574739	290.662	0.873919
290.6224	0.527357	0.942739	2.864699	0.701053	0.576781	290.701	0.88388
290.6618	0.53378	0.951359	2.863033	0.701452	0.579359	290.741	0.890682
290.7012	0.539117	0.96048	2.864597	0.702123	0.582603	290.78	0.895193

290.7406	0.543649	0.969613	2.869023	0.703282	0.587235	290.819	0.898693
290.78	0.548232	0.978217	2.876211	0.705024	0.594007	290.859	0.904378
290.8195	0.552584	0.985814	2.885593	0.707286	0.602951	290.898	0.911191
290.8589	0.556609	0.991984	2.896478	0.709906	0.613325	290.938	0.917889
290.8983	0.559894	0.996367	2.907389	0.71273	0.624237	290.977	0.920575
290.9377	0.56303	0.998801	2.917597	0.715665	0.635114	291.016	0.919749
290.9771	0.565927	0.999401	2.927556	0.718647	0.645548	291.056	0.91687
291.0165	0.568548	0.99849	2.938842	0.721603	0.654984	291.095	0.914621
291.0559	0.570115	0.996575	2.951767	0.724472	0.663004	291.135	0.913764
291.0953	0.570985	0.994405	2.965291	0.727268	0.670033	291.174	0.914525
291.1347	0.571634	0.992905	2.977502	0.730082	0.677362	291.214	0.917901
291.1741	0.573043	0.992811	2.986473	0.733026	0.686113	291.253	0.92534
291.2135	0.575279	0.994268	2.99352	0.736188	0.696097	291.292	0.9351
291.2529	0.578127	0.996885	2.999576	0.739608	0.705744	291.332	0.944699
291.2923	0.581169	1.000202	3.00783	0.743234	0.713359	291.371	0.948988
291.3318	0.584323	1.004032	3.016286	0.74688	0.718416	291.411	0.949552
291.3712	0.587613	1.008379	3.024548	0.750299	0.721483	291.45	0.948145
291.4106	0.591	1.013128	3.030678	0.753322	0.723268	291.489	0.949243
291.45	0.594463	1.017954	3.037218	0.755926	0.724279	291.529	0.952525
291.4894	0.598171	1.022552	3.043752	0.758169	0.725353	291.568	0.95729
291.5288	0.602492	1.026857	3.050546	0.760092	0.727958	291.608	0.962763
291.5682	0.607748	1.030902	3.05379	0.761709	0.733289	291.647	0.968638
291.6076	0.61369	1.034434	3.054846	0.763094	0.741028	291.686	0.973989
291.647	0.620022	1.036809	3.055421	0.764465	0.749441	291.726	0.976453
291.6864	0.626438	1.037444	3.059787	0.766144	0.756727	291.765	0.973794
291.7258	0.632758	1.036368	3.06763	0.768431	0.762187	291.805	0.968259
291.7652	0.638784	1.034271	3.077385	0.771469	0.766209	291.844	0.962855
291.8046	0.643959	1.032029	3.085965	0.775157	0.769438	291.883	0.963261
291.8441	0.648218	1.030246	3.092537	0.779161	0.77215	291.923	0.96742
291.8835	0.651795	1.029194	3.097349	0.783054	0.774309	291.962	0.973224
291.9229	0.655138	1.029039	3.100299	0.786528	0.775967	292.002	0.974171
291.9623	0.658468	1.030004	3.101469	0.789505	0.777368	292.041	0.971235
292.0017	0.661749	1.032364	3.101818	0.792053	0.778646	292.08	0.966677
292.0411	0.664798	1.036301	3.103206	0.794226	0.779611	292.12	0.966479
292.0805	0.667721	1.041621	3.107558	0.796001	0.780059	292.159	0.972008
292.1199	0.670568	1.047597	3.113721	0.79739	0.780271	292.199	0.980693
292.1593	0.673446	1.053203	3.119998	0.798587	0.781086	292.238	0.987734
292.1987	0.676394	1.057652	3.12425	0.799996	0.783406	292.278	0.988992
292.2381	0.679298	1.060751	3.126816	0.802098	0.787715	292.317	0.986305
292.2775	0.682138	1.062691	3.127915	0.805209	0.794077	292.356	0.982053
292.3169	0.684703	1.0636	3.127464	0.809199	0.80227	292.396	0.979509
292.3563	0.687254	1.063492	3.125069	0.813421	0.811682	292.435	0.978529
292.3958	0.689859	1.062593	3.121777	0.817045	0.821317	292.475	0.978922
292.4352	0.692759	1.061495	3.118778	0.819607	0.830105	292.514	0.980975
292.4746	0.695762	1.060738	3.118413	0.821287	0.837284	292.553	0.984173

292.514	0.698899	1.060275	3.120526	0.822643	0.842436	292.593	0.987556
292.5534	0.702229	1.059463	3.125881	0.824061	0.845249	292.632	0.98869
292.5928	0.706131	1.05763	3.134137	0.825448	0.845602	292.672	0.98668
292.6322	0.710324	1.054586	3.143982	0.826521	0.843946	292.711	0.98303
292.6716	0.714437	1.050619	3.153875	0.827322	0.841317	292.75	0.980157
292.711	0.717662	1.046203	3.161288	0.828323	0.838817	292.79	0.980658
292.7504	0.720028	1.041848	3.16669	0.829942	0.83709	292.829	0.98358
292.7898	0.721744	1.038079	3.170247	0.832049	0.836296	292.869	0.98783
292.8292	0.72301	1.035325	3.171668	0.83403	0.836406	292.908	0.9923
292.8686	0.72401	1.033703	3.170396	0.83529	0.837324	292.947	0.996535
292.9081	0.724984	1.032996	3.16779	0.835652	0.838822	292.987	0.999867
292.9475	0.726355	1.032903	3.166211	0.835363	0.840561	293.026	0.999863
292.9869	0.728578	1.033268	3.168572	0.834835	0.842317	293.066	0.996619
293.0263	0.731447	1.034083	3.173441	0.834424	0.844205	293.105	0.991722
293.0657	0.734709	1.035334	3.178698	0.83438	0.846602	293.144	0.988066
293.1051	0.738076	1.03686	3.181565	0.83487	0.849792	293.184	0.98719
293.1445	0.741476	1.038345	3.182781	0.835939	0.853713	293.223	0.988363
293.1839	0.744841	1.039412	3.183203	0.837491	0.85803	293.263	0.990624
293.2233	0.748086	1.039805	3.1851	0.839372	0.862361	293.302	0.993886
293.2627	0.751064	1.039477	3.187714	0.841516	0.866319	293.342	0.997199
293.3021	0.753781	1.038399	3.190963	0.843973	0.869386	293.381	0.999599
293.3415	0.756071	1.036447	3.19478	0.846774	0.871001	293.42	0.997043
293.3809	0.758106	1.033716	3.200285	0.849781	0.87105	293.46	0.990571
293.4204	0.760022	1.030919	3.206303	0.852683	0.870222	293.499	0.982585
293.4598	0.762094	1.029247	3.211494	0.855159	0.869667	293.539	0.978314
293.4992	0.764391	1.029566	3.212534	0.857056	0.870156	293.578	0.979351
293.5386	0.7669	1.031693	3.21034	0.858409	0.87154	293.617	0.984119
293.578	0.769607	1.034573	3.206006	0.859304	0.873009	293.657	0.990303
293.6174	0.772676	1.037153	3.201456	0.859716	0.87381	293.696	0.996471
293.6568	0.776053	1.039013	3.197291	0.859523	0.873616	293.736	1.002074
293.6962	0.779536	1.04024	3.193664	0.858692	0.872279	293.775	1.00651
293.7356	0.78283	1.04093	3.191025	0.857442	0.869578	293.814	1.007634
293.775	0.785648	1.041012	3.189531	0.856185	0.865509	293.854	1.006153
293.8144	0.787993	1.040496	3.188879	0.85529	0.860707	293.893	1.003229
293.8538	0.78975	1.039696	3.188386	0.854912	0.856371	293.933	1.001523
293.8932	0.79098	1.039014	3.187598	0.855034	0.853605	293.972	1.001429
293.9326	0.791823	1.038464	3.186957	0.85567	0.852825	294.011	1.002341
293.9721	0.792459	1.037559	3.18728	0.856966	0.853847	294.051	1.003241
294.0115	0.793077	1.035778	3.189855	0.859033	0.856225	294.09	1.003455
294.0509	0.79371	1.033127	3.193845	0.861669	0.859378	294.13	1.00309
294.0903	0.794411	1.030264	3.19845	0.864319	0.862623	294.169	1.00232
294.1297	0.795283	1.028021	3.201042	0.866425	0.865338	294.208	1.00111
294.1691	0.796432	1.026797	3.202437	0.867783	0.867138	294.248	0.999662
294.2085	0.797794	1.0264	3.203351	0.868543	0.867784	294.287	0.998218
294.2479	0.799353	1.026384	3.20594	0.868917	0.867066	294.327	0.99708

294.2873	0.800936	1.026408	3.209625	0.868994	0.865002	294.366	0.996328
294.3267	0.802507	1.026282	3.214124	0.868854	0.862159	294.406	0.996171
294.3661	0.803985	1.02583	3.218667	0.868746	0.859545	294.445	0.997533
294.4055	0.805342	1.024932	3.224476	0.869007	0.858034	294.484	1.001391
294.4449	0.806613	1.02376	3.230813	0.869731	0.857816	294.524	1.006346
294.4844	0.807813	1.022853	3.236486	0.870616	0.858473	294.563	1.010429
294.5238	0.808893	1.022786	3.237802	0.871226	0.859481	294.603	1.009669
294.5632	0.809873	1.023711	3.234443	0.871379	0.860545	294.642	1.005508
294.6026	0.810866	1.025289	3.22816	0.871244	0.861542	294.681	0.999551
294.642	0.812069	1.027007	3.222095	0.871111	0.862303	294.721	0.995676
294.6814	0.813651	1.028462	3.218411	0.871103	0.862617	294.76	0.993709
294.7208	0.815551	1.029374	3.216627	0.871137	0.862402	294.8	0.992777
294.7602	0.817797	1.029463	3.216165	0.871105	0.861796	294.839	0.990853
294.7996	0.820404	1.028504	3.21713	0.871036	0.861058	294.878	0.986781
294.839	0.823112	1.02652	3.218736	0.871032	0.860399	294.918	0.981955
294.8784	0.825663	1.023765	3.220123	0.871078	0.859935	294.957	0.978346
294.9178	0.827137	1.020604	3.218074	0.871032	0.859664	294.997	0.980031
294.9572	0.827792	1.017495	3.213249	0.870818	0.859382	295.036	0.985241
294.9967	0.827957	1.01501	3.207151	0.870598	0.858733	295.075	0.992082
295.0361	0.828264	1.013674	3.202626	0.870699	0.857436	295.115	0.995732
295.0755	0.828813	1.013649	3.20084	0.871356	0.85548	295.154	0.996314
295.1149	0.829691	1.014637	3.201623	0.872538	0.853043	295.194	0.994682
295.1543	0.830941	1.016141	3.204712	0.874024	0.850268	295.233	0.992487
295.1937	0.833225	1.01775	3.211296	0.875622	0.847277	295.272	0.990367
295.2331	0.836214	1.019132	3.220096	0.877291	0.844469	295.312	0.988324
295.2725	0.839544	1.019891	3.229785	0.879059	0.842667	295.351	0.986326
295.3119	0.842457	1.019634	3.237481	0.880855	0.842709	295.391	0.983476
295.3513	0.844725	1.018289	3.242541	0.8825	0.844776	295.43	0.980369
295.3907	0.846435	1.016264	3.245353	0.883843	0.848229	295.47	0.977647
295.4301	0.847618	1.014207	3.246535	0.884856	0.852104	295.509	0.977919
295.4695	0.848442	1.012568	3.24652	0.885581	0.85569	295.548	0.980796
295.5089	0.849028	1.011351	3.245393	0.885992	0.858712	295.588	0.98489
295.5484	0.849547	1.010258	3.243121	0.885948	0.861086	295.627	0.987009
295.5878	0.850175	1.009064	3.239983	0.8853	0.862737	295.667	0.985508
295.6272	0.85092	1.007871	3.236113	0.884058	0.86369	295.706	0.981848
295.6666	0.85179	1.007083	3.231621	0.882449	0.864159	295.745	0.978125
295.706	0.852674	1.007092	3.225463	0.880834	0.864389	295.785	0.977765
295.7454	0.853719	1.007962	3.218601	0.879578	0.864342	295.824	0.979669
295.7848	0.85501	1.009471	3.212197	0.878983	0.863517	295.864	0.982614
295.8242	0.857068	1.011352	3.20926	0.879255	0.861254	295.903	0.983544
295.8636	0.859801	1.013357	3.210613	0.880436	0.857391	295.942	0.982495
295.903	0.862822	1.015103	3.215084	0.882371	0.852636	295.982	0.980086
295.9424	0.865449	1.015992	3.220792	0.884766	0.848236	296.021	0.977464
295.9818	0.867105	1.015529	3.226538	0.887334	0.845174	296.061	0.975125
296.0212	0.867956	1.013745	3.232058	0.889879	0.843605	296.1	0.973065

296.0607	0.868142	1.011181	3.237018	0.892263	0.843025	296.139	0.971225
296.1001	0.867688	1.008518	3.240454	0.894347	0.84288	296.179	0.968931
296.1395	0.866588	1.006319	3.241719	0.89602	0.842926	296.218	0.966616
296.1789	0.865233	1.005072	3.241579	0.897278	0.843059	296.258	0.964795
296.2183	0.864319	1.005186	3.241743	0.898191	0.843028	296.297	0.965452
296.2577	0.86465	1.006727	3.243968	0.898797	0.842554	296.336	0.968495
296.2971	0.865876	1.009179	3.246984	0.899025	0.841715	296.376	0.972708
296.3365	0.86759	1.011635	3.249141	0.898755	0.841071	296.415	0.975862
296.3759	0.868925	1.013323	3.247184	0.897929	0.841303	296.455	0.976576
296.4153	0.870014	1.013987	3.241861	0.896572	0.842772	296.494	0.9753
296.4547	0.871057	1.013747	3.234089	0.894731	0.845447	296.534	0.972572
296.4941	0.872673	1.012773	3.224761	0.892517	0.849054	296.573	0.967407
296.5335	0.874799	1.011234	3.214689	0.890228	0.853111	296.612	0.960928
296.5729	0.877248	1.009457	3.204905	0.888359	0.857012	296.652	0.954709
296.6124	0.87963	1.007965	3.197399	0.887402	0.860248	296.691	0.953446
296.6518	0.88187	1.007169	3.194158	0.88759	0.862578	296.731	0.957791
296.6912	0.883941	1.007028	3.194074	0.888799	0.863955	296.77	0.965572
296.7306	0.885829	1.007082	3.195837	0.890736	0.864294	296.809	0.972821
296.77	0.887164	1.006832	3.19679	0.893179	0.863534	296.849	0.975455
296.8094	0.888102	1.006066	3.197367	0.895985	0.862034	296.888	0.974825
296.8488	0.888935	1.004886	3.198063	0.898915	0.860786	296.928	0.972577
296.8882	0.890299	1.00351	3.200698	0.90155	0.860967	296.967	0.972228
296.9276	0.892491	1.002115	3.204843	0.903454	0.863079	297.006	0.97341
296.967	0.895355	1.000793	3.209929	0.904419	0.866572	297.046	0.975481
297.0064	0.898899	0.999593	3.214527	0.904556	0.870294	297.085	0.977065
297.0458	0.903001	0.998549	3.218716	0.904167	0.873202	297.125	0.97774
297.0852	0.907249	0.997675	3.222386	0.903521	0.874681	297.164	0.977808
297.1247	0.911211	0.996967	3.22541	0.902745	0.874304	297.203	0.9777
297.1641	0.913537	0.99642	3.227431	0.901922	0.871808	297.243	0.978754
297.2035	0.914506	0.996058	3.22789	0.901203	0.867536	297.282	0.98028
297.2429	0.914474	0.995968	3.227187	0.900806	0.862611	297.322	0.981461
297.2823	0.913945	0.996239	3.22527	0.900908	0.858441	297.361	0.979325
297.3217	0.913068	0.996812	3.223618	0.901546	0.855966	297.4	0.974117
297.3611	0.912139	0.997384	3.222563	0.902619	0.85535	297.44	0.967244
297.4005	0.911464	0.997496	3.223236	0.904009	0.856328	297.479	0.961175
297.4399	0.912188	0.996814	3.225969	0.905692	0.858586	297.519	0.956682
297.4793	0.913954	0.995357	3.22999	0.907714	0.861794	297.558	0.953853
297.5187	0.916371	0.993437	3.234596	0.910023	0.865517	297.598	0.9529
297.5581	0.918713	0.99139	3.239026	0.912364	0.869281	297.637	0.955855
297.5975	0.920677	0.989385	3.24313	0.914373	0.872818	297.676	0.961709
297.637	0.922273	0.987466	3.245834	0.915777	0.876206	297.716	0.968875
297.6764	0.923512	0.985695	3.244776	0.916531	0.879749	297.755	0.973327
297.7158	0.924413	0.984183	3.237106	0.916806	0.88367	297.795	0.974272
297.7552	0.924976	0.982982	3.224929	0.916862	0.887905	297.834	0.972684
297.7946	0.925197	0.982015	3.210488	0.916898	0.89214	297.873	0.970228

297.834	0.92503	0.981183	3.198546	0.916955	0.896015	297.913	0.967734
297.8734	0.924528	0.980572	3.189489	0.916947	0.899254	297.952	0.96548
297.9128	0.923744	0.980583	3.183237	0.916805	0.901599	297.992	0.963762
297.9522	0.922666	0.981714	3.180579	0.916576	0.902851	298.031	0.963439
297.9916	0.921362	0.984057	3.181429	0.916381	0.903138	298.07	0.964421
298.031	0.919955	0.987032	3.184517	0.916288	0.903094	298.11	0.966442
298.0704	0.91857	0.989633	3.187927	0.91624	0.903671	298.149	0.969251
298.1098	0.917395	0.990998	3.188562	0.916112	0.905589	298.189	0.973017
298.1492	0.916492	0.990778	3.18741	0.915846	0.908909	298.228	0.977142
298.1887	0.915927	0.988962	3.185447	0.915506	0.913174	298.267	0.980764
298.2281	0.916098	0.985651	3.185924	0.915227	0.917841	298.307	0.98245
298.2675	0.916882	0.981194	3.188291	0.915152	0.92253	298.346	0.982505
298.3069	0.918036	0.976362	3.191538	0.915391	0.926957	298.386	0.981326
298.3463	0.919116	0.972143	3.193545	0.915984	0.930759	298.425	0.97959
298.3857	0.91983	0.969207	3.193798	0.916846	0.933482	298.464	0.977368
298.4251	0.920208	0.967492	3.192262	0.91776	0.934645	298.504	0.974904
298.4645	0.920281	0.966374	3.188928	0.918479	0.933704	298.543	0.972633
298.5039	0.919847	0.96522	3.181909	0.918898	0.930347	298.583	0.970932
298.5433	0.919078	0.96383	3.172063	0.91908	0.925004	298.622	0.969676
298.5827	0.918222	0.9624	3.160998	0.919156	0.918801	298.662	0.96873
298.6221	0.917769	0.9612	3.152017	0.919215	0.912956	298.701	0.967939
298.6615	0.917996	0.960397	3.147057	0.919337	0.908281	298.74	0.967266
298.701	0.918829	0.960146	3.145367	0.919684	0.905326	298.78	0.966581
298.7404	0.920297	0.960705	3.146268	0.920524	0.904803	298.819	0.965508
298.7798	0.9225	0.962252	3.148421	0.922115	0.907242	298.859	0.96363
298.8192	0.925094	0.964515	3.151593	0.924531	0.912083	298.898	0.961416
298.8586	0.927717	0.966713	3.15554	0.927593	0.917495	298.937	0.959478
298.898	0.929192	0.968	3.159853	0.930988	0.921406	298.977	0.958992
298.9374	0.92962	0.968023	3.16434	0.934413	0.922807	299.016	0.959737
298.9768	0.929398	0.967049	3.168859	0.93762	0.92204	299.056	0.961282
299.0162	0.929268	0.965635	3.173686	0.940412	0.920117	299.095	0.962416
299.0556	0.929649	0.964288	3.178737	0.942681	0.918106	299.134	0.962915
299.095	0.930483	0.963396	3.183212	0.944483	0.917074	299.174	0.963414
299.1344	0.931711	0.963342	3.186283	0.946037	0.918331	299.213	0.964773
299.1738	0.933273	0.964436	3.18538	0.947606	0.923009	299.253	0.968237
299.2133	0.935214	0.966585	3.181118	0.949365	0.931101	299.292	0.973299
299.2527	0.93737	0.969203	3.174147	0.951377	0.941344	299.331	0.97928
299.2921	0.939459	0.971535	3.164844	0.953625	0.952049	299.371	0.984434
299.3315	0.941077	0.973151	3.153537	0.955972	0.961947	299.41	0.988354
299.3709	0.942412	0.974172	3.141403	0.958117	0.970401	299.45	0.991055
299.4103	0.943675	0.975078	3.12966	0.959665	0.977047	299.489	0.9927
299.4497	0.94589	0.976328	3.121406	0.96037	0.981561	299.528	0.992859
299.4891	0.948616	0.978111	3.116412	0.960354	0.98379	299.568	0.991785
299.5285	0.951351	0.980406	3.114371	0.959984	0.983754	299.607	0.989851
299.5679	0.952732	0.983155	3.115902	0.95953	0.981618	299.647	0.987233

299.6073	0.952466	0.986302	3.120354	0.958919	0.977769	299.686	0.984178
299.6467	0.951011	0.989723	3.126574	0.957839	0.972741	299.726	0.981308
299.6861	0.949038	0.993186	3.132962	0.956108	0.96703	299.765	0.980133
299.7255	0.947315	0.996426	3.137645	0.953953	0.961134	299.804	0.98154
299.765	0.945854	0.999257	3.140398	0.951899	0.955856	299.844	0.984694
299.8044	0.944666	1.001588	3.140978	0.950363	0.952527	299.883	0.988426
299.8438	0.94382	1.003388	3.137485	0.949346	0.952514	299.923	0.991543
299.8832	0.943405	1.004708	3.130359	0.948502	0.956289	299.962	0.993819
299.9226	0.943305	1.005638	3.12103	0.947526	0.963179	300.001	0.994944
299.962	0.943261	1.006233	3.111955	0.946511	0.971923	300.041	0.993512
300.0014	0.942844	1.006527	3.105668	0.946002	0.98127	300.08	0.988945
300.0408	0.942355	1.006628	3.101639	0.946706	0.990149	300.12	0.982791
300.0802	0.942108	1.006757	3.099323	0.949016	0.997462	300.159	0.977462
300.1196	0.943299	1.007151	3.097808	0.952663	1.002234	300.198	0.976167
300.159	0.945675	1.007909	3.096839	0.956804	1.004175	300.238	0.977999
300.1984	0.94876	1.008956	3.096104	0.960544	1.003752	300.277	0.981928
300.2378	0.951536	1.010121	3.094978	0.963477	1.001718	300.317	0.985791
300.2773	0.953407	1.011222	3.092817	0.965836	0.99873	300.356	0.989438
300.3167	0.954656	1.012099	3.089939	0.968172	0.995248	300.395	0.992677
300.3561	0.955593	1.012612	3.08666	0.970817	0.991629	300.435	0.995167
300.3955	0.95717	1.012658	3.083366	0.973582	0.988241	300.474	0.995953
300.4349	0.95914	1.012226	3.080481	0.976031	0.985543	300.514	0.995604
300.4743	0.961289	1.011328	3.078328	0.978038	0.984133	300.553	0.994726
300.5137	0.963132	1.009972	3.078039	0.979979	0.984603	300.592	0.995373
300.5531	0.964611	1.008289	3.07979	0.982377	0.987173	300.632	0.997473
300.5925	0.965704	1.006692	3.083014	0.985393	0.991609	300.671	1.00012
300.6319	0.966448	1.005874	3.086963	0.988642	0.997503	300.711	1.001265
300.6713	0.966245	1.006433	3.090917	0.991487	1.004352	300.75	0.998351
300.7107	0.965402	1.008403	3.094469	0.993539	1.011198	300.79	0.993079
300.7501	0.964244	1.011288	3.097192	0.994877	1.016345	300.829	0.987478
300.7896	0.963577	1.014454	3.097542	0.995835	1.017961	300.868	0.986023
300.829	0.96372	1.017389	3.095203	0.996666	1.015406	300.908	0.988239
300.8684	0.964442	1.019673	3.091035	0.997418	1.009866	300.947	0.992846
300.9078	0.965479	1.020866	3.086215	0.998049	1.003696	300.987	0.997226
300.9472	0.966234	1.020676	3.082834	0.99862	0.999048	301.026	1.000078
300.9866	0.966797	1.019299	3.080649	0.999327	0.996927	301.065	1.001909
301.026	0.967262	1.017406	3.07941	1.000388	0.99747	301.105	1.0034
301.0654	0.967951	1.015767	3.078484	1.001844	1.000553	301.144	1.00617
301.1048	0.968898	1.014854	3.077788	1.003457	1.00575	301.184	1.009897
301.1442	0.969961	1.01479	3.077439	1.004801	1.012056	301.223	1.013898
301.1836	0.9709	1.015548	3.077568	1.005491	1.017995	301.262	1.016451
301.223	0.971362	1.017016	3.078223	1.005381	1.022384	301.302	1.016646
301.2624	0.971484	1.018912	3.079594	1.004562	1.025175	301.341	1.015169
301.3018	0.971409	1.020766	3.081877	1.003148	1.027465	301.381	1.013031
301.3413	0.971692	1.022085	3.086951	1.001169	1.030547	301.42	1.011711

301.3807	0.972276	1.022589	3.094166	0.998679	1.03481	301.459	1.011302
301.4201	0.972917	1.02225	3.102078	0.99592	1.039393	301.499	1.011615
301.4595	0.973118	1.021153	3.108206	0.993321	1.04279	301.538	1.011796
301.4989	0.972416	1.019444	3.109968	0.991291	1.043934	301.578	1.011245
301.5383	0.971035	1.01734	3.107823	0.990003	1.042946	301.617	1.010346
301.5777	0.969198	1.015137	3.102235	0.989375	1.040961	301.657	1.009765
301.6171	0.96706	1.013132	3.093308	0.989263	1.039274	301.696	1.010382
301.6565	0.964849	1.011498	3.081658	0.989658	1.038636	301.735	1.011818
301.6959	0.962875	1.010275	3.068193	0.990702	1.03933	301.775	1.013691
301.7353	0.961751	1.00945	3.054166	0.99254	1.04151	301.814	1.015348
301.7747	0.962086	1.009011	3.040999	0.995142	1.045007	301.854	1.01669
301.8141	0.963606	1.008968	3.028924	0.998262	1.048716	301.893	1.017743
301.8536	0.966041	1.009349	3.018192	1.001569	1.050377	301.932	1.018503
301.893	0.969272	1.010188	3.009636	1.004826	1.047758	301.972	1.018487
301.9324	0.972929	1.011518	3.003166	1.007955	1.040581	302.011	1.017984
301.9718	0.976594	1.013409	2.998613	1.010953	1.031032	302.051	1.017391
302.0112	0.979366	1.015959	2.995774	1.013778	1.022413	302.09	1.017753
302.0506	0.980563	1.019173	2.994528	1.016331	1.017167	302.129	1.019262
302.09	0.980544	1.022888	2.994656	1.018568	1.015802	302.169	1.02163
302.1294	0.979644	1.026829	2.995946	1.02056	1.017431	302.208	1.024405
302.1688	0.978123	1.030673	2.99748	1.022399	1.020847	302.248	1.02815
302.2082	0.976351	1.033981	2.99948	1.024008	1.02499	302.287	1.032233
302.2476	0.974758	1.036076	3.002374	1.025071	1.028805	302.326	1.035792
302.287	0.974456	1.03618	3.0074	1.025222	1.031172	302.366	1.035869
302.3264	0.976232	1.033904	3.015466	1.024317	1.031338	302.405	1.031744
302.3659	0.979412	1.02959	3.025687	1.022518	1.029301	302.445	1.025244
302.4053	0.983323	1.024101	3.037122	1.020125	1.025608	302.484	1.019296
302.4447	0.986205	1.018372	3.048104	1.01738	1.02095	302.523	1.017305
302.4841	0.988065	1.013156	3.058031	1.014505	1.015963	302.563	1.018505
302.5235	0.989117	1.009142	3.066408	1.011859	1.011253	302.602	1.021948
302.5629	0.989743	1.007013	3.072452	1.009937	1.007425	302.642	1.025754
302.6023	0.990249	1.007064	3.075501	1.009166	1.005014	302.681	1.029895
302.6417	0.990618	1.008858	3.075447	1.00967	1.004502	302.721	1.03402
302.6811	0.99084	1.011384	3.072183	1.011234	1.006495	302.76	1.037452
302.7205	0.991014	1.013595	3.063978	1.013362	1.011514	302.799	1.038884
302.7599	0.991061	1.014856	3.05176	1.015392	1.019472	302.839	1.038555
302.7993	0.99088	1.014889	3.036852	1.016636	1.029623	302.878	1.036897
302.8387	0.989928	1.013535	3.02151	1.016552	1.040951	302.918	1.034571
302.8781	0.98788	1.010802	3.007649	1.014898	1.052461	302.957	1.031424
302.9176	0.985354	1.007049	2.995328	1.01175	1.063134	302.996	1.027933
302.957	0.98299	1.002946	2.984623	1.007393	1.071743	303.036	1.02494
302.9964	0.98326	0.999182	2.975621	1.002245	1.077127	303.075	1.023836
303.0358	0.985676	0.99615	2.968443	0.996857	1.078766	303.115	1.024168
303.0752	0.989329	0.993948	2.963197	0.991929	1.07676	303.154	1.025347
303.1146	0.992497	0.992564	2.960317	0.98824	1.071446	303.193	1.026174

303.154	0.993721	0.99193	2.960291	0.986464	1.063435	303.233	1.026587
303.1934	0.993454	0.991875	2.962488	0.987061	1.053948	303.272	1.026394
303.2328	0.992125	0.992128	2.96619	0.990229	1.044909	303.312	1.025232
303.2722	0.989981	0.992426	2.969952	0.995779	1.038227	303.351	1.021408
303.3116	0.987638	0.99266	2.973275	1.003028	1.034689	303.39	1.01608
303.351	0.985705	0.99288	2.975952	1.010883	1.033846	303.43	1.010571
303.3904	0.985676	0.993191	2.977197	1.018258	1.034746	303.469	1.007884
303.4299	0.98872	0.99369	2.97648	1.024538	1.036523	303.509	1.008451
303.4693	0.993852	0.994474	2.974481	1.02965	1.038544	303.548	1.011034
303.5087	1.000101	0.995678	2.971962	1.033776	1.040259	303.587	1.01393
303.5481	1.005122	0.997435	2.972005	1.037052	1.041182	303.627	1.014019
303.5875	1.008676	0.999785	2.974118	1.039671	1.041089	303.666	1.011824
303.6269	1.010943	1.002649	2.977139	1.042243	1.040067	303.706	1.00841
303.6663	1.012242	1.005882	2.978565	1.045717	1.03834	303.745	1.006595
303.7057	1.012968	1.009306	2.975644	1.050656	1.036125	303.785	1.007371
303.7451	1.013077	1.012687	2.969959	1.056576	1.033561	303.824	1.010045
303.7845	1.012528	1.015682	2.96312	1.062109	1.030694	303.863	1.013502
303.8239	1.011	1.017956	2.960249	1.065885	1.027562	303.903	1.016517
303.8633	1.008555	1.019437	2.961462	1.067103	1.02432	303.942	1.018908
303.9027	1.005443	1.020411	2.965092	1.06531	1.021332	303.982	1.020435
303.9422	1.001872	1.021361	2.969158	1.060069	1.019111	304.021	1.020329
303.9816	0.998118	1.022683	2.970719	1.051164	1.018077	304.06	1.017532
304.021	0.994496	1.024488	2.969287	1.039148	1.018362	304.1	1.013247
304.0604	0.991324	1.02667	2.96438	1.025544	1.019941	304.139	1.009089
304.0998	0.989332	1.029057	2.952635	1.012372	1.022697	304.179	1.008322
304.1392	0.988648	1.03142	2.934929	1.0014	1.026191	304.218	1.010649
304.1786	0.98923	1.033415	2.913496	0.993789	1.0295	304.257	1.014931
304.218	0.991057	1.03458	2.891652	0.990204	1.031376	304.297	1.01889
304.2574	0.994383	1.034554	2.874119	0.990687	1.030754	304.336	1.022106
304.2968	0.998893	1.033312	2.859906	0.99432	1.027138	304.376	1.023797
304.3362	1.004274	1.031125	2.847988	0.99941	1.020362	304.415	1.023122
304.3756	1.010582	1.028355	2.834832	1.004327	1.010388	304.454	1.016017
304.415	1.017402	1.025333	2.819943	1.008262	0.997651	304.494	1.003403
304.4544	1.023971	1.022382	2.805106	1.011246	0.983309	304.533	0.988615
304.4939	1.029331	1.019864	2.792302	1.013507	0.969015	304.573	0.977682
304.5333	1.031125	1.018076	2.786753	1.014983	0.956386	304.612	0.976116
304.5727	1.030045	1.017074	2.787829	1.015649	0.946745	304.651	0.981245
304.6121	1.026752	1.016708	2.794854	1.016085	0.941523	304.691	0.990149
304.6515	1.02169	1.016773	2.809593	1.017354	0.942164	304.73	0.99515
304.6909	1.015519	1.017048	2.830989	1.020108	0.94887	304.77	0.995518
304.7303	1.009122	1.01727	2.855235	1.023838	0.959629	304.809	0.992586
304.7697	1.003465	1.017107	2.878266	1.02707	0.970573	304.849	0.989143
304.8091	1.001916	1.016241	2.887676	1.028328	0.977917	304.888	0.987024
304.8485	1.003447	1.014493	2.88609	1.026993	0.98011	304.927	0.985924
304.8879	1.006901	1.011776	2.876566	1.023333	0.977787	304.967	0.985597

304.9273	1.010211	1.008038	2.86354	1.017957	0.972384	305.006	0.986276
304.9667	1.011806	1.003335	2.851062	1.011404	0.965323	305.046	0.988288
305.0062	1.012076	0.997946	2.83974	1.004104	0.957897	305.085	0.990537
305.0456	1.011384	0.99236	2.830184	0.996579	0.951498	305.124	0.991223
305.085	1.010157	0.987059	2.825045	0.989525	0.947231	305.164	0.986863
305.1244	1.008912	0.982222	2.822999	0.98351	0.944914	305.203	0.97878
305.1638	1.007845	0.977673	2.823142	0.978676	0.942878	305.243	0.968784
305.2032	1.007809	0.97307	2.823605	0.974822	0.938918	305.282	0.960774
305.2426	1.009083	0.968177	2.82402	0.971752	0.931779	305.321	0.955424
305.282	1.010921	0.963041	2.824532	0.969645	0.922213	305.361	0.952344
305.3214	1.012594	0.957929	2.825221	0.969143	0.912707	305.4	0.950992
305.3608	1.011481	0.953171	2.827482	0.970923	0.905947	305.44	0.950198
305.4002	1.007841	0.949097	2.830294	0.975082	0.903175	305.479	0.950087
305.4396	1.00265	0.946105	2.832718	0.980939	0.903916	305.518	0.951112
305.479	0.997284	0.944686	2.832791	0.987411	0.906856	305.558	0.954754
305.5185	0.99368	0.945075	2.827959	0.993548	0.910698	305.597	0.963972
305.5579	0.991591	0.946786	2.819653	0.99875	0.914598	305.637	0.976361
305.5973	0.990768	0.948581	2.809396	1.002631	0.918053	305.676	0.988641
305.6367	0.991042	0.94908	2.800693	1.004873	0.920727	305.715	0.992286
305.6761	0.992033	0.947588	2.794401	1.005398	0.922535	305.755	0.987246
305.7155	0.993497	0.944374	2.790019	1.004593	0.923618	305.794	0.976797
305.7549	0.995059	0.940315	2.787083	1.003217	0.924125	305.834	0.967126
305.7943	0.996502	0.936363	2.784764	1.002007	0.924098	305.873	0.962736
305.8337	0.997753	0.933229	2.782897	1.001259	0.923511	305.913	0.962067
305.8731	0.998719	0.931453	2.781331	1.000793	0.922298	305.952	0.96366
305.9125	0.999216	0.931475	2.780005	1.000296	0.920443	305.991	0.964719
305.9519	0.998945	0.933365	2.779026	0.999699	0.918152	306.031	0.965348
305.9913	0.998115	0.936664	2.777907	0.999309	0.915985	306.07	0.965007
306.0307	0.996925	0.94054	2.776162	0.999588	0.914871	306.11	0.962767
306.0702	0.995747	0.944191	2.772823	1.000693	0.915636	306.149	0.954545
306.1096	0.994773	0.947253	2.767688	1.002197	0.918234	306.188	0.942375
306.149	0.993971	0.949766	2.760819	1.003298	0.921595	306.228	0.929198
306.1884	0.993579	0.951879	2.751746	1.003365	0.924203	306.267	0.922836
306.2278	0.993439	0.953694	2.740267	1.002423	0.925018	306.307	0.927216
306.2672	0.993273	0.95529	2.727196	1.001133	0.924134	306.346	0.93834
306.3066	0.992813	0.956778	2.71336	1.000216	0.922631	306.385	0.950326
306.346	0.990668	0.958288	2.699723	0.999898	0.921785	306.425	0.951844
306.3854	0.987145	0.959866	2.686763	0.999922	0.922306	306.464	0.943729
306.4248	0.983034	0.961389	2.675237	0.999998	0.924177	306.504	0.92971
306.4642	0.979352	0.962563	2.66611	1.000201	0.926954	306.543	0.917389
306.5036	0.978026	0.963109	2.663108	1.000944	0.929956	306.582	0.910652
306.543	0.978615	0.962994	2.664542	1.002452	0.932221	306.622	0.908082
306.5825	0.98069	0.962424	2.668646	1.004257	0.932425	306.661	0.90825
306.6219	0.984074	0.961695	2.672378	1.005344	0.92924	306.701	0.907731
306.6613	0.98823	0.961069	2.673445	1.004808	0.922151	306.74	0.906357

306.7007	0.992502	0.9607	2.672183	1.002466	0.911721	306.779	0.904789
306.7401	0.996181	0.960624	2.668647	0.998954	0.899095	306.819	0.904208
306.7795	0.997042	0.960791	2.661883	0.995288	0.885417	306.858	0.90803
306.8189	0.99568	0.961109	2.653491	0.992143	0.87161	306.898	0.914973
306.8583	0.992838	0.961507	2.644717	0.9895	0.858585	306.937	0.922856
306.8977	0.989641	0.961993	2.638334	0.986961	0.847364	306.977	0.924936
306.9371	0.9873	0.962694	2.635047	0.984318	0.838648	307.016	0.917986
306.9765	0.985664	0.963863	2.634405	0.98187	0.832341	307.055	0.905441
307.0159	0.98458	0.965883	2.636051	0.980242	0.827663	307.095	0.89221
307.0553	0.98386	0.96908	2.639774	0.979889	0.823668	307.134	0.885226
307.0947	0.98314	0.973379	2.645937	0.980732	0.81975	307.174	0.883521
307.1342	0.98244	0.978214	2.653889	0.982173	0.815792	307.213	0.885105
307.1736	0.981484	0.982749	2.663334	0.983544	0.812043	307.252	0.886223
307.213	0.980343	0.986315	2.672723	0.984634	0.808962	307.292	0.884383
307.2524	0.97935	0.98876	2.681374	0.985675	0.807124	307.331	0.880385
307.2918	0.978844	0.99039	2.688605	0.986868	0.807382	307.371	0.875125
307.3312	0.979912	0.991639	2.692685	0.988027	0.810597	307.41	0.870189
307.3706	0.98262	0.992831	2.693599	0.988676	0.816677	307.449	0.865613
307.41	0.986504	0.994113	2.691298	0.988467	0.823868	307.489	0.861748
307.4494	0.991089	0.995515	2.685934	0.987559	0.82896	307.528	0.85901
307.4888	0.995923	0.997014	2.676483	0.986641	0.828869	307.568	0.858245
307.5282	1.000744	0.998528	2.663382	0.986446	0.822612	307.607	0.858884
307.5676	1.005107	0.999934	2.647835	0.987195	0.811406	307.646	0.860185
307.607	1.008194	1.001111	2.63058	0.988621	0.797419	307.686	0.860184
307.6465	1.008754	1.002033	2.613533	0.990385	0.782815	307.725	0.857632
307.6859	1.007488	1.002849	2.597714	0.992492	0.769416	307.765	0.853529
307.7253	1.00503	1.00392	2.584109	0.995384	0.75896	307.804	0.849245
307.7647	1.002146	1.005627	2.575736	0.999518	0.752903	307.843	0.847409
307.8041	0.999616	1.007989	2.572002	1.004714	0.751535	307.883	0.847782
307.8435	0.997707	1.010437	2.572195	1.009896	0.75394	307.922	0.849351
307.8829	0.997054	1.011882	2.575235	1.013617	0.758848	307.962	0.85026
307.9223	0.998504	1.011358	2.582323	1.014991	0.765245	308.001	0.848161
307.9617	1.001289	1.008842	2.592344	1.014042	0.772382	308.041	0.844109
308.0011	1.004726	1.005294	2.603853	1.011239	0.779473	308.08	0.839255
308.0405	1.007451	1.002085	2.615094	1.006942	0.785556	308.119	0.836714
308.0799	1.008889	1.000338	2.623652	1.001344	0.789853	308.159	0.837053
308.1193	1.009238	1.000543	2.628979	0.994851	0.792183	308.198	0.839318
308.1588	1.008709	1.002728	2.630535	0.988411	0.792879	308.238	0.841975
308.1982	1.007634	1.006634	2.624337	0.983304	0.792494	308.277	0.843723
308.2376	1.006123	1.011587	2.611981	0.98045	0.791612	308.316	0.844364
308.277	1.004325	1.016516	2.595706	0.979927	0.790716	308.356	0.843524
308.3164	1.002428	1.02026	2.578789	0.981206	0.790018	308.395	0.840412
308.3558	1.000769	1.022125	2.565877	0.983588	0.789336	308.435	0.832321
308.3952	0.999292	1.022346	2.556123	0.986409	0.78811	308.474	0.821999
308.4346	0.997943	1.021972	2.548643	0.989126	0.785467	308.513	0.812064

308.474	0.996464	1.022214	2.542054	0.991366	0.78058	308.553	0.808703
308.5134	0.994675	1.023746	2.534815	0.992975	0.773322	308.592	0.811816
308.5528	0.992886	1.02653	2.527114	0.994012	0.764531	308.632	0.818829
308.5922	0.99138	1.030172	2.519041	0.994553	0.755723	308.671	0.825924
308.6316	0.991097	1.034246	2.510671	0.994518	0.748299	308.71	0.829596
308.671	0.992119	1.038393	2.50287	0.99368	0.74265	308.75	0.830285
308.7105	0.994162	1.042284	2.495928	0.991794	0.738031	308.789	0.828674
308.7499	0.997129	1.045593	2.490993	0.988818	0.733125	308.829	0.826091
308.7893	1.00044	1.048022	2.487659	0.98514	0.726933	308.868	0.822513
308.8287	1.003705	1.049276	2.485647	0.981514	0.719565	308.907	0.818464
308.8681	1.006539	1.048917	2.484677	0.978733	0.71222	308.947	0.814491
308.9075	1.007488	1.046487	2.483874	0.977251	0.706467	308.986	0.811658
308.9469	1.006451	1.041935	2.48385	0.977035	0.703392	309.026	0.809846
308.9863	1.004055	1.03586	2.484543	0.977805	0.703157	309.065	0.808525
309.0257	1.001057	1.029326	2.486102	0.979442	0.705198	309.105	0.806873
309.0651	0.999265	1.023426	2.48845	0.982155	0.708623	309.144	0.804198
309.1045	0.998532	1.018917	2.490947	0.986186	0.712516	309.183	0.800719
309.1439	0.998516	1.016283	2.493273	0.991419	0.71609	309.223	0.796674
309.1833	0.99892	1.01587	2.494551	0.997284	0.718878	309.262	0.79228
309.2228	0.998832	1.017676	2.495244	1.002936	0.720877	309.302	0.786914
309.2622	0.998382	1.021138	2.4951	1.007569	0.722338	309.341	0.78119
309.3016	0.997679	1.025272	2.493889	1.010683	0.723503	309.38	0.775943
309.341	0.996394	1.029075	2.49113	1.01218	0.72439	309.42	0.772982
309.3804	0.995101	1.03197	2.486045	1.012221	0.724644	309.459	0.772289
309.4198	0.99416	1.033845	2.479181	1.010868	0.723618	309.499	0.773106
309.4592	0.994141	1.034792	2.470745	1.007978	0.720546	309.538	0.774121
309.4986	0.996349	1.034913	2.462985	1.003537	0.715077	309.577	0.774898
309.538	1.000236	1.03423	2.455915	0.998081	0.708038	309.617	0.775326
309.5774	1.005156	1.032633	2.44884	0.992795	0.7016	309.656	0.775171
309.6168	1.009978	1.029915	2.441096	0.989042	0.698523	309.696	0.773509
309.6562	1.013672	1.025985	2.428817	0.987636	0.700611	309.735	0.769354
309.6956	1.016406	1.021076	2.413757	0.9886	0.707695	309.774	0.76388
309.7351	1.018329	1.015653	2.397528	0.99152	0.71824	309.814	0.758521
309.7745	1.019284	1.010242	2.378984	0.996685	0.730356	309.853	0.755174
309.8139	1.019557	1.005031	2.361183	1.005283	0.743151	309.893	0.753693
309.8533	1.01953	0.99994	2.347957	1.016035	0.756551	309.932	0.754148
309.8927	1.017846	0.996115	2.311874	1.024095	0.767038	309.971	0.755935
309.9321	1.019053	0.995269	2.324828	1.0266	0.769492		
309.9715	1.021191	0.99631	2.354206	1.025971	0.766699		

Fig. 3.2.a.

	cluster 1	cluster 2	cluster 3
280	0.678175	2.0233	1.40966
280.3	0.670952	2.0283	1.4075

280.6	0.673479	2.0152	1.41538
280.9	0.668502	2.00806	1.39886
281.2	0.666344	1.99455	1.39753
281.5	0.670784	2.00703	1.39975
281.8	0.658403	1.99304	1.39214
282.1	0.654894	1.98315	1.39656
282.4	0.660711	2.00391	1.39018
282.5	0.643897	1.97635	1.39076
282.6	0.647611	1.97815	1.38906
282.7	0.650691	1.9742	1.38829
282.8	0.647687	1.97621	1.38712
282.9	0.652265	1.98026	1.39336
283	0.655597	1.99756	1.39556
283.1	0.655565	1.98913	1.40145
283.2	0.65905	1.98864	1.39166
283.3	0.666567	2.00858	1.3947
283.4	0.662934	2.00335	1.39281
283.5	0.679869	1.99498	1.39857
283.6	0.678366	2.00804	1.39887
283.7	0.722558	2.06843	1.43489
283.8	0.730334	2.04203	1.41491
283.9	0.798478	2.06623	1.44213
284	0.87662	2.08522	1.45861
284.1	1.01294	2.14855	1.50791
284.2	1.19723	2.19945	1.53945
284.3	1.36714	2.23474	1.56904
284.4	1.58449	2.30559	1.62165
284.5	1.75149	2.34271	1.66877
284.6	1.9061	2.4044	1.71571
284.7	2.05552	2.45397	1.76742
284.8	2.12212	2.51831	1.81566
284.9	2.20704	2.56525	1.86942
285	2.24768	2.61472	1.89897
285.1	2.27617	2.62963	1.91807
285.2	2.32242	2.68414	1.96234
285.3	2.28832	2.71042	1.95791
285.4	2.24452	2.63154	1.91424
285.5	2.19502	2.59794	1.85478
285.6	2.11444	2.52669	1.82196
285.7	2.02868	2.46332	1.75269
285.8	1.94736	2.38777	1.70195
285.9	1.90257	2.3462	1.6585
286	1.87536	2.31731	1.62282
286.1	1.86113	2.30993	1.62184
286.2	1.86252	2.28904	1.62258

286.3	1.86966	2.30022	1.62305
286.4	1.86795	2.31493	1.66226
286.5	1.88819	2.34866	1.69997
286.6	1.85684	2.38412	1.73862
286.7	1.85127	2.41894	1.75855
286.8	1.82377	2.42604	1.78184
286.9	1.81698	2.45001	1.79269
287	1.78282	2.43813	1.78916
287.1	1.74689	2.43159	1.79865
287.2	1.77497	2.49612	1.85152
287.3	1.7711	2.55737	1.95133
287.4	1.79342	2.5782	2.00875
287.5	1.83129	2.65638	2.08152
287.6	1.87233	2.66208	2.12207
287.7	1.89791	2.67599	2.10442
287.8	1.8933	2.67173	2.08972
287.9	1.94117	2.65009	2.06964
288.1	2.07404	2.65675	2.0713
288.2	2.13466	2.65556	2.09139
288.3	2.17598	2.67426	2.09292
288.4	2.20773	2.66501	2.09868
288.5	2.27681	2.70385	2.15125
288.6	2.30184	2.73745	2.19419
288.7	2.32327	2.7544	2.19885
288.8	2.31174	2.73421	2.18885
288.9	2.29374	2.72923	2.16929
289	2.24422	2.67438	2.13094
289.1	2.2177	2.67775	2.11276
289.2	2.18088	2.66651	2.08373
289.3	2.1706	2.67274	2.09061
289.4	2.12795	2.64583	2.07633
289.5	2.13726	2.64181	2.09758
289.6	2.13223	2.62508	2.09795
289.7	2.13812	2.65556	2.09546
289.8	2.12664	2.64609	2.10196
289.9	2.13802	2.66423	2.10683
290	2.15151	2.66458	2.10803
290.1	2.17505	2.71008	2.13493
290.2	2.21289	2.71546	2.15722
290.3	2.2335	2.73185	2.17141
290.4	2.23567	2.7433	2.17975
290.5	2.23433	2.72117	2.1661
290.6	2.23107	2.70886	2.16265
290.7	2.23975	2.69833	2.16689
290.8	2.26245	2.7473	2.18234

290.9	2.31512	2.78641	2.22721
291	2.30844	2.78742	2.22438
291.1	2.31622	2.78349	2.21878
291.2	2.34875	2.7781	2.22899
291.3	2.3333	2.77171	2.21158
291.4	2.34481	2.78692	2.22176
291.5	2.3623	2.79573	2.22808
291.6	2.37074	2.79816	2.24302
291.7	2.4028	2.81601	2.24383
291.8	2.39186	2.82019	2.24446
291.9	2.37474	2.81875	2.23136
292	2.37657	2.80372	2.23074
292.3	2.38906	2.80337	2.21408
292.6	2.37237	2.78397	2.19619
292.9	2.40324	2.8042	2.21202
293.2	2.4067	2.80259	2.2074
293.5	2.40266	2.79832	2.20729
293.8	2.39554	2.79768	2.20595
294.1	2.40468	2.79637	2.18677
294.4	2.37648	2.79403	2.17922
294.7	2.38056	2.7708	2.18081
295	2.37928	2.75532	2.15642
295.3	2.36568	2.75095	2.15087
295.6	2.34591	2.73855	2.13646
295.9	2.31702	2.71931	2.10883
296.2	2.35531	2.73241	2.12819
296.5	2.37077	2.73118	2.12314
296.8	2.3638	2.74783	2.14634
297.1	2.37647	2.76019	2.14622
297.4	2.38267	2.76663	2.13431
297.7	2.37528	2.77005	2.14518
298	2.39732	2.76089	2.1468
298.3	2.3893	2.77244	2.14586
298.6	2.43021	2.81626	2.16569
298.9	2.44696	2.84343	2.17783
299.2	2.47661	2.84145	2.18749
299.5	2.47101	2.85123	2.19041
299.8	2.49081	2.85323	2.21722
300	2.52189	2.88967	2.23449
300.5	2.53957	2.93234	2.252
301	2.59769	2.9586	2.27913
301.5	2.61435	3.02262	2.31852
302	2.66319	3.02871	2.3405
302.5	2.70995	3.07204	2.37239
303	2.73971	3.08939	2.42569

303.5	2.79072	3.20622	2.47238
304	2.81824	3.21816	2.46036
304.5	2.89522	3.24989	2.49673
305	2.9102	3.25487	2.49397
305.5	2.88853	3.26675	2.5013
306	2.79992	3.33593	2.48445
306.5	2.83417	3.27622	2.46382
307	2.7582	3.23444	2.4144
307.5	2.74407	3.22551	2.39846
308	2.75869	3.14168	2.38576
308.5	2.70707	3.10475	2.36518
309	2.70088	3.10163	2.34598
309.5	2.62587	3.10875	2.31584
310	2.59894	3.09484	2.33278

Fig. 3.2.b.

	HA	HA-FIT
280	0.249207	0.165637
280.3	0.256157	0.15895
280.6	0.255539	0.170757
280.9	0.245126	0.167587
281.2	0.239679	0.174366
281.5	0.241833	0.160294
281.8	0.23716	0.157724
282.1	0.23026	0.15973
282.4	0.226668	0.145892
282.5	0.225025	0.139818
282.6	0.22552	0.13247
282.7	0.230092	0.145788
282.8	0.232371	0.13251
282.9	0.230065	0.145029
283	0.223765	0.136257
283.1	0.219959	0.137744
283.2	0.218358	0.13799
283.3	0.21814	0.145064
283.4	0.215852	0.133553
283.5	0.211182	0.156849
283.6	0.211383	0.147587
283.7	0.220723	0.16611
283.8	0.236327	0.182317
283.9	0.260431	0.228728
284	0.301505	0.271106
284.1	0.362821	0.355967
284.2	0.445177	0.479473

284.3	0.550301	0.590945
284.4	0.672821	0.749967
284.5	0.813151	0.821886
284.6	0.968633	0.95037
284.7	1.123	1.06049
284.8	1.25609	1.12991
284.9	1.35656	1.20561
285	1.40377	1.23016
285.1	1.3997	1.26046
285.2	1.35878	1.30643
285.3	1.29693	1.28989
285.4	1.21357	1.2504
285.5	1.13095	1.17564
285.6	1.06531	1.13555
285.7	1.02058	1.07089
285.8	0.994433	1.01699
285.9	0.989793	0.962135
286	1.00066	0.957132
286.1	1.02437	0.94736
286.2	1.05122	0.946542
286.3	1.07586	0.949827
286.4	1.0924	0.993035
286.5	1.09629	1.02511
286.6	1.08035	1.03306
286.7	1.04998	1.03442
286.8	1.00982	1.02585
286.9	0.96128	1.04374
287	0.906995	1.03239
287.1	0.858288	1.02617
287.2	0.825416	1.09165
287.3	0.814629	1.16583
287.4	0.820025	1.25255
287.5	0.83563	1.31865
287.6	0.865693	1.38834
287.7	0.929673	1.39801
287.8	1.03476	1.40837
287.9	1.18199	1.43783
288.1	1.57543	1.54037
288.2	1.79075	1.61435
288.3	1.99239	1.65164
288.4	2.15762	1.6674
288.5	2.25328	1.76987
288.6	2.2482	1.78003
288.7	2.13516	1.79352
288.8	1.95703	1.77018

288.9	1.75939	1.74818
289	1.58356	1.68803
289.1	1.44697	1.65319
289.2	1.3653	1.61665
289.3	1.32146	1.61182
289.4	1.29633	1.5805
289.5	1.28126	1.60844
289.6	1.27979	1.59624
289.7	1.28743	1.60151
289.8	1.29978	1.60155
289.9	1.31781	1.60229
290	1.34274	1.60739
290.1	1.37309	1.62965
290.2	1.40676	1.6834
290.3	1.44154	1.69202
290.4	1.48003	1.71224
290.5	1.52486	1.7049
290.6	1.57619	1.71136
290.7	1.61488	1.74682
290.8	1.64014	1.73349
290.9	1.65975	1.78777
291	1.673	1.78962
291.1	1.6746	1.77583
291.2	1.67547	1.81255
291.3	1.68838	1.79002
291.4	1.70417	1.80408
291.5	1.72262	1.8065
291.6	1.75319	1.86264
291.7	1.79236	1.85084
291.8	1.82764	1.83007
291.9	1.84796	1.82254
292	1.86396	1.81381
292.3	1.90263	1.83795
292.6	1.94491	1.82469
292.9	1.97121	1.82722
293.2	2.00797	1.82382
293.5	2.03534	1.81937
293.8	2.07613	1.80722
294.1	2.07096	1.80422
294.4	2.07516	1.79257
294.7	2.07576	1.77341
295	2.08873	1.78934
295.3	2.10222	1.74561
295.6	2.10112	1.72686
295.9	2.1102	1.70235

296.2	2.08913	1.73287
296.5	2.08647	1.73248
296.8	2.10391	1.72867
297.1	2.13905	1.74209
297.4	2.11969	1.73591
297.7	2.13013	1.7117
298	2.09358	1.72534
298.3	2.05636	1.72514
298.6	2.0294	1.75908
298.9	2.03576	1.75555
299.2	2.02417	1.77349
299.5	2.0413	1.7751
299.8	2.00001	1.79813
300	1.97598	1.78224
300.5	1.98925	1.80072
301	1.95681	1.79258
301.5	1.92729	1.84273
302	1.90042	1.90994
302.5	1.88444	1.88354
303	1.82309	1.94272
303.5	1.82311	1.97314
304	1.77068	1.92313
304.5	1.82528	1.88763
305	1.7263	1.82902
305.5	1.62966	1.83977
306	1.59202	1.69381
306.5	1.48677	1.69572
307	1.46178	1.82275
307.5	1.45304	1.85422
308	1.42922	1.72707
308.5	1.35558	1.75451
309	1.33306	1.73193
309.5	1.26746	1.6825
310	1.30231	1.66258

Fig. 3.2.d.

	FA	FIT
280	0.748218	0.702756
280.3	0.768413	0.694703
280.6	0.77477	0.714273
280.9	0.752002	0.703307
281.2	0.772175	0.710698
281.5	0.751499	0.693249
281.8	0.758357	0.687847
282.1	0.747459	0.695368

282.4	0.758217	0.66482
282.5	0.759753	0.662633
282.6	0.753088	0.64843
282.7	0.744721	0.669748
282.8	0.738241	0.646325
282.9	0.735413	0.66941
283	0.735573	0.654752
283.1	0.740261	0.654477
283.2	0.748421	0.646965
283.3	0.752955	0.664039
283.4	0.752253	0.644708
283.5	0.751377	0.678333
283.6	0.760442	0.665143
283.7	0.777333	0.69196
283.8	0.795436	0.706221
283.9	0.810579	0.764468
284	0.831703	0.801949
284.1	0.882395	0.902045
284.2	0.968376	1.03788
284.3	1.08181	1.15468
284.4	1.21694	1.34063
284.5	1.3801	1.39623
284.6	1.57486	1.5635
284.7	1.78552	1.69423
284.8	1.99344	1.80083
284.9	2.16528	1.92168
285	2.28372	1.95012
285.1	2.32124	1.99886
285.2	2.26157	2.09165
285.3	2.1197	2.08899
285.4	1.94404	2.0078
285.5	1.78315	1.87244
285.6	1.66122	1.82055
285.7	1.57621	1.74785
285.8	1.5263	1.65499
285.9	1.50672	1.56041
286	1.51325	1.55153
286.1	1.5424	1.54193
286.2	1.60481	1.52792
286.3	1.68889	1.52834
286.4	1.77238	1.62261
286.5	1.83526	1.69316
286.6	1.86812	1.73261
286.7	1.8651	1.76022
286.8	1.83117	1.76205

286.9	1.76966	1.78702
287	1.6865	1.80746
287.1	1.60573	1.81861
287.2	1.55495	1.95258
287.3	1.53569	2.09589
287.4	1.54865	2.29445
287.5	1.60628	2.39725
287.6	1.71765	2.50982
287.7	1.87741	2.53971
287.8	2.08921	2.53318
287.9	2.3512	2.55479
288.1	2.92683	2.71152
288.2	3.17673	2.82457
288.3	3.36807	2.89192
288.4	3.48987	2.87068
288.5	3.5365	3.05027
288.6	3.50762	3.07209
288.7	3.4153	3.10519
288.8	3.27805	3.0571
288.9	3.12868	3.01656
289	2.99286	2.91446
289.1	2.88648	2.85544
289.2	2.81033	2.80705
289.3	2.75925	2.80956
289.4	2.73251	2.76787
289.5	2.72682	2.81555
289.6	2.74791	2.80016
289.7	2.77971	2.81187
289.8	2.80649	2.81448
289.9	2.82293	2.81466
290	2.8374	2.8251
290.1	2.84647	2.85749
290.2	2.84233	2.94448
290.3	2.84203	2.95545
290.4	2.85671	3.00725
290.5	2.8705	2.97969
290.6	2.86714	2.98623
290.7	2.86451	3.04756
290.8	2.88064	3.02584
290.9	2.90783	3.11301
291	2.93401	3.11928
291.1	2.96682	3.09195
291.2	2.9913	3.12869
291.3	3.00942	3.09982
291.4	3.02923	3.12709

291.5	3.04555	3.11548
291.6	3.05481	3.21855
291.7	3.06207	3.19131
291.8	3.08505	3.15956
291.9	3.09882	3.1449
292	3.10182	3.12774
292.3	3.12784	3.15527
292.6	3.13583	3.14334
292.9	3.16843	3.1211
293.2	3.1838	3.11478
293.5	3.21252	3.08984
293.8	3.18902	3.08859
294.1	3.19927	3.07246
294.4	3.22356	3.05677
294.7	3.21733	3.00463
295	3.20669	3.03303
295.3	3.23535	2.95245
295.6	3.23888	2.91049
295.9	3.2146	2.88345
296.2	3.24163	2.91853
296.5	3.22331	2.90269
296.8	3.19726	2.89776
297.1	3.2236	2.92642
297.4	3.22322	2.9216
297.7	3.24096	2.87162
298	3.18191	2.89423
298.3	3.19089	2.88822
298.6	3.1568	2.91876
298.9	3.16006	2.89719
299.2	3.18289	2.93637
299.5	3.11554	2.94366
299.8	3.14102	2.97653
300	3.10583	2.94022
300.5	3.07793	2.95443
301	3.08012	2.95119
301.5	3.10996	3.02959
302	2.99641	3.14294
302.5	3.06162	3.08008
303	2.97493	3.19554
303.5	2.97255	3.29534
304	2.97043	3.2069
304.5	2.79091	3.16513
305	2.84142	3.09489
305.5	2.83085	2.96285
306	2.77757	2.65223

306.5	2.66313	2.76718
307	2.6351	2.96965
307.5	2.67311	2.99067
308	2.60345	2.84226
308.5	2.53734	2.89204
309	2.48499	2.85797
309.5	2.46277	2.79425
310	2.3854	2.76374

Fig. 3.3.b.

	cluster 1	cluster 2	cluster 3
280.3	1.69891	1.26226	0.770979
280.6	1.68971	1.24934	0.762587
281.8	1.71132	1.27317	0.760183
282.1	1.69134	1.25835	0.751852
282.4	1.69747	1.26404	0.759405
282.5	1.69271	1.26143	0.757621
282.6	1.70193	1.25686	0.756963
282.7	1.69504	1.25635	0.758619
282.8	1.68563	1.24374	0.745831
282.9	1.68286	1.24533	0.759531
283	1.70471	1.27398	0.771852
283.1	1.6821	1.24622	0.755184
283.2	1.69284	1.25541	0.758887
283.3	1.69934	1.25279	0.81081
283.4	1.68876	1.24781	0.755047
283.5	1.6847	1.24698	0.756772
283.6	1.69349	1.25291	0.772398
283.7	1.70394	1.25497	0.787892
283.8	1.72967	1.27865	0.813196
283.9	1.7553	1.29218	0.850317
284	1.76372	1.30714	0.916201
284.1	1.80365	1.33474	1.02676
284.2	1.86439	1.39542	1.18211
284.3	1.88787	1.41963	1.32114
284.4	1.94546	1.47567	1.48851
284.5	1.99389	1.52079	1.65014
284.6	2.07866	1.59468	1.81788
284.7	2.12837	1.66959	1.97069
284.8	2.19314	1.72301	2.09534
284.9	2.25613	1.78738	2.1943
285	2.31658	1.85808	2.28339

285.1	2.35606	1.90833	2.33686
285.2	2.37514	1.92846	2.3631
285.3	2.33666	1.91139	2.3225
285.4	2.29901	1.86246	2.27623
285.5	2.23887	1.79104	2.19815
285.6	2.13695	1.71073	2.08474
285.7	2.11004	1.67758	2.03514
285.8	2.05279	1.63113	1.96524
285.9	1.97789	1.56302	1.88105
286	1.95303	1.53808	1.8623
286.1	1.92543	1.52162	1.8525
286.2	1.91235	1.50779	1.84745
286.3	1.96373	1.56506	1.91048
286.4	1.9671	1.57825	1.90403
286.5	2.02584	1.64037	1.93675
286.6	2.06125	1.67767	1.94643
286.7	2.0941	1.72459	1.93282
286.8	2.13841	1.76991	1.94153
286.9	2.15068	1.77865	1.9037
287	2.15997	1.77803	1.87871
287.1	2.16984	1.79038	1.84445
287.2	2.22262	1.83679	1.83974
287.3	2.27389	1.90424	1.83775
287.4	2.37598	2.01351	1.88774
287.5	2.45986	2.11615	1.94104
287.6	2.497	2.16644	1.96897
287.7	2.51988	2.19878	2.00719
287.8	2.49242	2.18385	2.02393
287.9	2.50775	2.19885	2.10638
288	2.55847	2.26438	2.24218
288.1	2.59226	2.31007	2.39678
288.2	2.59513	2.35103	2.49773
288.3	2.64475	2.42034	2.6443
288.4	2.69125	2.47011	2.74893
288.5	2.73627	2.5339	2.82679
288.6	2.73223	2.55487	2.873
288.7	2.76401	2.57807	2.91252
288.8	2.73698	2.53177	2.86668
288.9	2.69839	2.47045	2.82327
289	2.64392	2.4132	2.7481
289.1	2.61815	2.38055	2.69162
289.2	2.60317	2.37465	2.63194
289.3	2.57978	2.32859	2.5793
289.4	2.55989	2.30646	2.52723
289.5	2.60923	2.35645	2.56311

289.6	2.59229	2.32654	2.52324
289.7	2.59055	2.3327	2.52931
289.8	2.58857	2.34004	2.53474
289.9	2.6233	2.35726	2.53173
290.1	2.65214	2.3854	2.56063
290.2	2.64496	2.37776	2.57331
290.3	2.65014	2.39126	2.57608
290.4	2.63386	2.39731	2.60381
290.5	2.65634	2.43403	2.64411
290.6	2.64522	2.42318	2.64702
290.7	2.70582	2.46966	2.70762
290.8	2.6955	2.45902	2.70774
290.9	2.71307	2.47803	2.73528
291	2.72378	2.48204	2.76726
291.1	2.74515	2.52971	2.80127
291.2	2.73142	2.48723	2.78338
291.3	2.7017	2.47233	2.78325
291.4	2.71498	2.48398	2.78884
291.5	2.73385	2.49401	2.81835
291.6	2.79805	2.56685	2.88801
291.7	2.80086	2.5589	2.92274
291.8	2.76793	2.52799	2.88763
291.9	2.76779	2.5433	2.90737
292	2.84209	2.61461	2.99615
292.3	2.84939	2.588	2.992
292.6	2.90362	2.67641	3.09325
292.9	2.82496	2.57947	2.98789
293.2	2.80542	2.57878	2.98435
293.5	2.87654	2.61226	3.05224
293.8	2.84261	2.58942	3.0192
294.1	2.8369	2.58532	3.03734
294.4	2.81843	2.56499	2.99673
294.7	3.75755	3.01367	3.34986
295	3.46696	3.07953	3.83196
295.3	3.78164	3.3611	4.21525
295.6	3.48382	3.06387	3.74841
295.9	3.72847	3.26402	4.26096
296.2	3.44968	3.08309	3.73836
296.8	3.21684	2.85568	3.45317
297.1	3.47576	3.03381	3.84701
297.4	3.49096	3.0571	3.86974
297.7	3.37108	2.98267	3.68429
298	3.30649	2.92202	3.57121
298.3	3.48944	3.03241	3.85119
298.6	3.28888	2.91643	3.56659

298.9	3.5887	3.09473	4.08836
299.2	3.60236	3.06159	4.00397
299.5	3.26912	2.87846	3.5552
299.8	3.45191	3.00818	3.782
300	3.52503	3.00295	3.85387
300.5	3.34135	2.89484	3.69027
301	3.17375	2.76689	3.40076
301.5	3.34449	2.85511	3.71766
302	3.22039	2.7843	3.46833
302.5	3.22467	2.72175	3.49524
303	3.1413	2.66891	3.34223
303.5	3.39981	2.85515	3.7686
304	3.2959	2.787	3.50394
305	3.29584	2.82612	3.54211
305.5	3.38814	2.89793	3.63928
306	3.53777	2.9651	3.76771
306.5	3.43856	2.90445	3.86974
307	3.1957	2.69806	3.43804
307.5	3.03372	2.51942	3.02011
308	3.21853	2.60733	3.29696
308.5	3.31969	2.76686	3.67214
309	3.08453	2.56026	3.13507
309.5	3.26849	2.68649	3.30957
310	3.35508	2.71947	3.48299

Fig. 3.3.c.

	HA	FIT
280.3	0.256157	0.319902
280.6	0.255539	0.308776
281.8	0.23716	0.299453
282.1	0.23026	0.301897
282.4	0.226668	0.304457
282.5	0.225025	0.300969
282.6	0.22552	0.294595
282.7	0.230092	0.297497
282.8	0.232371	0.289158
282.9	0.230065	0.297391
283	0.223765	0.309465
283.1	0.219959	0.291676
283.2	0.218358	0.302026

283.3	0.21814	0.308011
283.4	0.215852	0.291076
283.5	0.211182	0.294513
283.6	0.211383	0.298071
283.7	0.220723	0.297182
283.8	0.236327	0.310928
283.9	0.260431	0.325346
284	0.301505	0.356312
284.1	0.362821	0.402139
284.2	0.445177	0.47053
284.3	0.550301	0.534489
284.4	0.672821	0.61563
284.5	0.813151	0.686998
284.6	0.968633	0.780429
284.7	1.123	0.868506
284.8	1.25609	0.927959
284.9	1.35656	0.996302
285	1.40377	1.05551
285.1	1.3997	1.10552
285.2	1.35878	1.12655
285.3	1.29693	1.11629
285.4	1.21357	1.07414
285.5	1.13095	1.00671
285.6	1.06531	0.950638
285.7	1.02058	0.920259
285.8	0.994433	0.872735
285.9	0.989793	0.825035
286	1.00066	0.816762
286.1	1.02437	0.806433
286.2	1.05122	0.808039
286.3	1.07586	0.855355
286.4	1.0924	0.874393
286.5	1.09629	0.912954
286.6	1.08035	0.935018
286.7	1.04998	0.960545
286.8	1.00982	0.980919
286.9	0.96128	0.970822
287	0.906995	0.963492
287.1	0.858288	0.9502
287.2	0.825416	0.973381
287.3	0.814629	1.02019
287.4	0.820025	1.08861
287.5	0.83563	1.16894
287.6	0.865693	1.21338
287.7	0.929673	1.25124

287.8	1.03476	1.25188
287.9	1.18199	1.28126
288	1.36647	1.36742
288.1	1.57543	1.44953
288.2	1.79075	1.51973
288.3	1.99239	1.60771
288.4	2.15762	1.6766
288.5	2.25328	1.75217
288.6	2.2482	1.77738
288.7	2.13516	1.7936
288.8	1.95703	1.75807
288.9	1.75939	1.70188
289	1.58356	1.65318
289.1	1.44697	1.60786
289.2	1.3653	1.58353
289.3	1.32146	1.53904
289.4	1.29633	1.50133
289.5	1.28126	1.53801
289.6	1.27979	1.50784
289.7	1.28743	1.52047
289.8	1.29978	1.52396
289.9	1.31781	1.51702
290.1	1.37309	1.53984
290.2	1.40676	1.53977
290.3	1.44154	1.55927
290.4	1.48003	1.58207
290.5	1.52486	1.61825
290.6	1.57619	1.6068
290.7	1.61488	1.6522
290.8	1.64014	1.64252
290.9	1.65975	1.66036
291	1.673	1.67746
291.1	1.6746	1.70871
291.2	1.67547	1.68895
291.3	1.68838	1.67795
291.4	1.70417	1.68248
291.5	1.72262	1.69223
291.6	1.75319	1.74534
291.7	1.79236	1.76266
291.8	1.82764	1.72808
291.9	1.84796	1.75322
292	1.86396	1.79983
292.3	1.90263	1.78411
292.6	1.94491	1.85658
292.9	1.97121	1.79829

293.2	2.00797	1.787
293.5	2.03534	1.81161
293.8	2.07613	1.79581
294.1	2.07096	1.79756
294.4	2.07516	1.7656
294.7	2.07576	1.55811
295	2.08873	2.25332
295.3	2.10222	2.29204
295.6	2.10112	2.21899
295.9	2.1102	2.53305
296.2	2.08913	2.18072
296.8	2.10391	1.98861
297.1	2.13905	2.19102
297.4	2.11969	2.18531
297.7	2.13013	2.10063
298	2.09358	2.02558
298.3	2.05636	2.19017
298.6	2.0294	2.01624
298.9	2.03576	2.23715
299.2	2.02417	2.16567
299.5	2.0413	1.99764
299.8	2.00001	2.1303
300	1.97598	2.09258
300.5	1.98925	2.03426
301	1.95681	1.89322
301.5	1.92729	1.97471
302	1.90042	1.89726
302.5	1.88444	1.81658
303	1.82309	1.79743
303.5	1.82311	1.82397
304	1.77068	1.85662
305	1.7263	1.9103
305.5	1.62966	1.87306
306	1.59202	1.91815
306.5	1.48677	1.68111
307	1.46178	1.71125
307.5	1.45304	1.55931
308	1.42922	1.49328
308.5	1.35558	1.24528
309	1.33306	1.55122
309.5	1.26746	1.51139
310	1.30231	1.07654

Fig. 3.3.d.

	FA	FIT
280.3	0.768413	0.838537
280.6	0.77477	0.819891
281.8	0.758357	0.822894
282.1	0.747459	0.817486
282.4	0.758217	0.820569
282.5	0.759753	0.817348
282.6	0.753088	0.809352
282.7	0.744721	0.812826
282.8	0.738241	0.799617
282.9	0.735413	0.80919
283	0.735573	0.832238
283.1	0.740261	0.802569
283.2	0.748421	0.819394
283.3	0.752955	0.828371
283.4	0.752253	0.803669
283.5	0.751377	0.80776
283.6	0.760442	0.813885
283.7	0.777333	0.813348
283.8	0.795436	0.838593
283.9	0.810579	0.86334
284	0.831703	0.903304
284.1	0.882395	0.969974
284.2	0.968376	1.07094
284.3	1.08181	1.15617
284.4	1.21694	1.27161
284.5	1.3801	1.37102
284.6	1.57486	1.50779
284.7	1.78552	1.63391
284.8	1.99344	1.72158
284.9	2.16528	1.82512
285	2.28372	1.91801
285.1	2.32124	1.99082
285.2	2.26157	2.02034
285.3	2.1197	2.00016
285.4	1.94404	1.93602
285.5	1.78315	1.83527
285.6	1.66122	1.73974
285.7	1.57621	1.69582
285.8	1.5263	1.62193
285.9	1.50672	1.54358

286	1.51325	1.52526
286.1	1.5424	1.50616
286.2	1.60481	1.50353
286.3	1.68889	1.57748
286.4	1.77238	1.60261
286.5	1.83526	1.66574
286.6	1.86812	1.70405
286.7	1.8651	1.747
286.8	1.83117	1.78456
286.9	1.76966	1.77629
287	1.6865	1.76922
287.1	1.60573	1.75405
287.2	1.55495	1.79746
287.3	1.53569	1.8713
287.4	1.54865	1.98505
287.5	1.60628	2.11111
287.6	1.71765	2.17837
287.7	1.87741	2.23516
287.8	2.08921	2.22821
287.9	2.3512	2.26748
288	2.64318	2.39009
288.1	2.92683	2.50218
288.2	3.17673	2.59422
288.3	3.36807	2.71888
288.4	3.48987	2.81653
288.5	3.5365	2.92559
288.6	3.50762	2.9586
288.7	3.4153	2.9857
288.8	3.27805	2.92999
288.9	3.12868	2.84627
289	2.99286	2.77152
289.1	2.88648	2.70608
289.2	2.81033	2.67533
289.3	2.75925	2.60879
289.4	2.73251	2.55474
289.5	2.72682	2.61588
289.6	2.74791	2.57131
289.7	2.77971	2.58888
289.8	2.80649	2.59447
289.9	2.82293	2.59314
290.1	2.84647	2.62994
290.2	2.84233	2.62561
290.3	2.84203	2.65141
290.4	2.85671	2.6795
290.5	2.8705	2.73287

290.6	2.86714	2.71489
290.7	2.86451	2.78602
290.8	2.88064	2.77124
290.9	2.90783	2.79603
291	2.93401	2.82328
291.1	2.96682	2.86959
291.2	2.9913	2.83579
291.3	3.00942	2.81631
291.4	3.02923	2.82373
291.5	3.04555	2.84077
291.6	3.05481	2.92676
291.7	3.06207	2.94801
291.8	3.08505	2.89428
291.9	3.09882	2.93067
292	3.10182	3.00672
292.3	3.12784	2.98533
292.6	3.13583	3.09225
292.9	3.16843	2.99639
293.2	3.1838	2.9779
293.5	3.21252	3.02742
293.8	3.18902	2.99776
294.1	3.19927	2.99487
294.4	3.22356	2.95049
294.7	3.21733	2.79584
295	3.20669	3.71988
295.3	3.23535	3.57191
295.6	3.23888	3.66649
295.9	3.2146	4.15029
296.2	3.24163	3.62741
296.8	3.19726	3.30477
297.1	3.2236	3.62633
297.4	3.22322	3.61646
297.7	3.24096	3.48858
298	3.18191	3.38001
298.3	3.19089	3.62086
298.6	3.1568	3.35471
298.9	3.16006	3.65379
299.2	3.18289	3.5862
299.5	3.11554	3.32897
299.8	3.14102	3.53102
300	3.10583	3.49318
300.5	3.07793	3.38104
301	3.08012	3.16752
301.5	3.10996	3.29828
302	2.99641	3.1646

302.5	3.06162	3.03925
303	2.97493	3.01017
303.5	2.97255	2.98661
304	2.97043	3.10637
305	2.84142	3.20698
305.5	2.83085	3.1616
306	2.77757	3.19264
306.5	2.66313	2.69774
307	2.6351	2.88459
307.5	2.67311	2.68928
308	2.60345	2.57486
308.5	2.53734	2.03437
309	2.48499	2.67406
309.5	2.46277	2.60563
310	2.3854	1.70894

Fig. 3.4.b.

	cluster 1	cluster 2
280	2.37552	1.17418
280.3	2.38603	1.18938
280.6	2.38462	1.17876
280.9	2.37908	1.17452
281.2	2.38264	1.17669
281.5	2.38745	1.1705
281.8	2.38427	1.17736
282.1	2.39098	1.17491
282.4	2.39683	1.17248
282.5	2.38846	1.17122
282.6	2.39671	1.17358
282.7	2.39004	1.16917
282.8	2.39572	1.17465
282.9	2.38554	1.17743
283	2.38928	1.18064
283.1	2.39146	1.1836
283.2	2.40475	1.19184
283.3	2.40262	1.19997
283.4	2.39595	1.20934
283.5	2.39345	1.23233
283.6	2.4119	1.26053

283.7	2.40326	1.30358
283.8	2.41006	1.38711
283.9	2.41688	1.52944
284	2.41817	1.73655
284.1	2.42721	1.98216
284.2	2.42735	2.15999
284.3	2.45162	2.33541
284.4	2.44045	2.43434
284.5	2.45896	2.52789
284.6	2.44917	2.57386
284.7	2.462	2.61522
284.8	2.45086	2.61296
284.9	2.44258	2.60669
285	2.44707	2.61747
285.1	2.45096	2.61222
285.2	2.44734	2.5965
285.3	2.46804	2.60276
285.4	2.47405	2.6077
285.5	2.4671	2.5887
285.6	2.47858	2.58118
285.7	2.47672	2.58176
285.8	2.49882	2.58912
285.9	2.49371	2.59645
286	2.4931	2.60035
286.1	2.50033	2.60462
286.2	2.5074	2.6197
286.3	2.51746	2.61922
286.4	2.53552	2.61086
286.5	2.54006	2.60062
286.6	2.55693	2.59142
286.7	2.54623	2.55452
286.8	2.54686	2.52223
286.9	2.55478	2.50189
287	2.57022	2.49565
287.1	2.58247	2.47557
287.2	2.60474	2.48652
287.3	2.63154	2.50431
287.4	2.63838	2.51244
287.5	2.65951	2.53584
287.6	2.64391	2.53951
287.7	2.65713	2.56353
287.8	2.63484	2.57881
287.9	2.63448	2.62793
288	2.63687	2.66251
288.1	2.64989	2.71513

288.2	2.65528	2.7489
288.3	2.65351	2.79545
288.4	2.66519	2.81139
288.5	2.66616	2.83072
288.6	2.66572	2.82259
288.7	2.64997	2.81724
288.8	2.66195	2.81763
288.9	2.66491	2.79903
289	2.65961	2.78762
289.1	2.65919	2.77901
289.2	2.65895	2.76005
289.3	2.65527	2.75217
289.4	2.66208	2.74852
289.5	2.65337	2.74253
289.6	2.65686	2.73434
289.7	2.67496	2.75377
289.8	2.67424	2.75959
289.9	2.66018	2.73785
290	2.67281	2.75175
290.1	2.65967	2.7377
290.2	2.66044	2.74532
290.3	2.62851	2.72239
290.4	2.65717	2.74861
290.5	2.63766	2.74662
290.6	2.63084	2.74385
290.7	2.63373	2.74274
290.8	2.63991	2.74557
290.9	2.62711	2.75865
291	2.65547	2.78012
291.1	2.66371	2.80128
291.2	2.64749	2.79398
291.3	2.67668	2.82861
291.4	2.66552	2.84928
291.5	2.66949	2.86647
291.6	2.64418	2.81682
291.7	2.68615	2.89003
291.8	2.68349	2.86139
291.9	2.69595	2.86815
292	2.69887	2.85667
292.3	2.70394	2.88098
292.6	2.71289	2.89641
292.9	2.70903	2.87168
293.2	2.7226	2.89123
293.5	2.72763	2.90788
293.8	2.72338	2.90347

294.1	2.70795	2.87418
294.4	2.71191	2.8664
294.7	2.73179	2.90097
295	2.73966	2.91698
295.3	2.74195	2.91194
295.6	2.74433	2.9097
295.9	2.73189	2.89348
296.2	2.71847	2.87025
296.5	2.71633	2.86765
296.8	2.7361	2.8839
297.1	2.73412	2.90148
297.4	2.73211	2.89949
297.7	2.71688	2.87484
298	2.72868	2.88878
298.3	2.72625	2.89709
298.6	2.72513	2.89828
298.9	2.73672	2.9137
299.2	2.73504	2.91622
299.5	2.75343	2.94138
299.8	2.74589	2.91737
300.1	2.74008	2.90462
300.4	2.75277	2.98201
300.7	2.73781	2.96452
301	2.72949	2.90728
301.3	2.73242	2.97628
301.6	2.73503	2.94925
301.9	2.71754	2.88511
302.2	2.67942	2.8974
302.5	2.65926	2.8187
302.8	2.65469	2.78147
303.1	2.62685	2.78044
303.4	2.61581	2.75406
303.7	2.62133	2.74903
304	2.58268	2.68843
304.3	2.59366	2.71237
304.6	2.54576	2.65011
304.9	2.53531	2.64223
305	2.46001	2.56704
305.5	2.47376	2.55299
306	2.45641	2.52728
306.5	2.48761	2.57889
307	2.47012	2.52332
307.5	2.42807	2.48404
308	2.47931	2.51609
308.5	2.46617	2.51817

309	2.50287	2.54865
309.5	2.54706	2.58313
310	2.52103	2.54235

Fig. 3.4.c.

	HA	FIT
280	0.0045	-0.03828
280.3	-0.00053	-0.04467
280.6	0.003487	-0.01738
280.9	-9.9E-05	-0.07292
281.2	0.002208	-0.08128
281.5	-0.00347	-0.01683
281.8	0.001532	-0.01269
282.1	0.001942	-0.04002
282.4	0.00016	-0.08191
282.5	-0.00015	-0.04995
282.6	-0.00303	-0.05202
282.7	-0.00602	-0.00749
282.8	-0.00856	0.00892
282.9	-0.01012	0.018623
283	-0.01052	0.016161
283.1	-0.00926	0.029662
283.2	-0.00806	0.011899
283.3	-0.00666	0.003448
283.4	-0.00538	0.006678
283.5	-0.00415	0.006599
283.6	-0.00163	-0.01609
283.7	0.005818	-0.00641
283.8	0.021315	0.03075
283.9	0.047855	0.094555
284	0.089298	0.195493
284.1	0.146439	0.308908
284.2	0.217852	0.401368
284.3	0.304859	0.48909
284.4	0.404744	0.55782
284.5	0.502974	0.616002
284.6	0.587902	0.653492
284.7	0.656671	0.68792
284.8	0.710663	0.697338
284.9	0.752899	0.707382
285	0.785309	0.701775
285.1	0.802337	0.701675
285.2	0.797502	0.704928
285.3	0.77718	0.691159
285.4	0.751018	0.686113

285.5	0.722053	0.665297
285.6	0.691454	0.675127
285.7	0.661229	0.655442
285.8	0.636859	0.649574
285.9	0.618695	0.645036
286	0.608982	0.654586
286.1	0.60584	0.760588
286.2	0.60847	0.677677
286.3	0.61297	0.674203
286.4	0.612827	0.665382
286.5	0.604303	0.66019
286.6	0.588245	0.653793
286.7	0.567266	0.630423
286.8	0.544299	0.612437
286.9	0.523833	0.596881
287	0.508328	0.58695
287.1	0.498257	0.58581
287.2	0.493718	0.601634
287.3	0.493216	0.615241
287.4	0.496665	0.62646
287.5	0.506012	0.645641
287.6	0.524898	0.650021
287.7	0.551621	0.655073
287.8	0.590899	0.676757
287.9	0.645391	0.768822
288	0.713138	0.753051
288.1	0.782878	0.798505
288.2	0.843409	0.830761
288.3	0.894936	0.871651
288.4	0.934739	0.904146
288.5	0.960623	0.916437
288.6	0.970116	0.922198
288.7	0.968933	0.919003
288.8	0.958882	0.902874
288.9	0.944251	0.892632
289	0.931423	0.890989
289.1	0.918792	0.860828
289.2	0.900957	0.85904
289.3	0.883028	0.859059
289.4	0.873159	0.866531
289.5	0.87119	0.844068
289.6	0.872836	0.879376
289.7	0.875731	0.856458
289.8	0.879049	0.850522
289.9	0.882558	0.846565

290	0.887469	0.843834
290.1	0.894393	0.83555
290.2	0.900833	0.857667
290.3	0.905797	0.853942
290.4	0.911265	0.863366
290.5	0.921546	0.872008
290.6	0.938165	0.873892
290.7	0.960176	0.8901
290.8	0.982203	0.886957
290.9	0.996537	0.899929
291	0.999055	0.921215
291.1	0.994199	0.940241
291.2	0.993602	0.93583
291.3	1.00092	0.973604
291.4	1.01184	0.985591
291.5	1.02371	1.017
291.6	1.03379	0.985534
291.7	1.03726	1.04897
291.8	1.0323	1.02144
291.9	1.02902	1.03526
292	1.03222	1.10023
292.3	1.06334	1.125
292.6	1.05717	1.16236
292.9	1.03307	1.11582
293.2	1.03965	1.16514
293.5	1.02959	1.16517
293.8	1.04076	1.19067
294.1	1.02964	1.17918
294.4	1.02508	1.11464
294.7	1.02897	1.13605
295	1.01485	1.12795
295.3	1.01982	1.10626
295.6	1.00869	1.07237
295.9	1.01498	1.0675
296.2	1.00496	1.0644
296.5	1.01259	1.0395
296.8	1.00629	1.05223
297.1	0.997393	1.04287
297.4	0.997498	0.977228
297.7	0.984764	0.991755
298	0.984631	0.993988
298.3	0.977219	0.967169
298.6	0.961852	0.983989
298.9	0.968034	0.995696
299.2	0.965749	0.99712

299.5	0.978694	0.997898
299.8	1.00136	1.00306
300.1	1.00692	1.0042
300.4	1.01263	1.07289
300.7	1.00773	1.06511
301	1.01872	1.03941
301.3	1.02067	1.04627
301.6	1.01397	1.04797
301.9	1.0104	1.01196
302.2	1.03336	1.07827
302.5	1.0114	0.985545
302.8	1.01488	0.967647
303.1	0.992973	0.979606
303.4	0.993295	0.943239
303.7	1.00878	0.939399
304	1.02348	0.909431
304.3	1.03316	0.909708
304.6	1.01675	0.902209
304.9	1.01073	0.900317
305	0.998856	0.854064
305.5	0.944671	0.854051
306	0.937467	0.837419
306.5	0.963084	0.856381
307	0.964971	0.833625
307.5	0.997438	0.801113
308	1.00539	0.814357
308.5	1.02307	0.803663
309	1.03364	0.798723
309.5	1.0349	0.793822
310	0.998252	0.792076

Fig. 3.4.d.

	FA	FIT
280	0.003305	-0.07802
280.3	0.003094	-0.08403
280.6	-0.00198	-0.01172
280.9	-0.0018	-0.13482
281.2	-0.00583	-0.1573
281.5	-0.00072	-0.01113
281.8	0.005112	0.00097
282.1	0.003824	-0.04895
282.4	-0.00242	-0.13099
282.5	-0.00447	-0.07098
282.6	-0.0061	-0.071
282.7	-0.00691	0.005699

282.8	-0.00657	0.04452
282.9	-0.0061	0.059679
283	-0.00586	0.062436
283.1	-0.00557	0.086723
283.2	-0.00452	0.061779
283.3	-0.00292	0.036061
283.4	-0.00172	0.039536
283.5	-0.00072	0.019017
283.6	0.001543	-0.03263
283.7	0.005355	-0.04171
283.8	0.011048	-0.01906
283.9	0.019411	0.027561
284	0.029765	0.101683
284.1	0.041629	0.184537
284.2	0.0567	0.252272
284.3	0.079186	0.315242
284.4	0.114048	0.377809
284.5	0.165323	0.429927
284.6	0.233615	0.457937
284.7	0.32029	0.497206
284.8	0.415799	0.503117
284.9	0.517025	0.517972
285	0.617147	0.499487
285.1	0.692259	0.498747
285.2	0.726682	0.511996
285.3	0.717686	0.49
285.4	0.681675	0.491133
285.5	0.629917	0.476685
285.6	0.561621	0.50559
285.7	0.479223	0.477016
285.8	0.39679	0.470505
285.9	0.328751	0.463306
286	0.28552	0.472512
286.1	0.26584	0.673265
286.2	0.261396	0.500281
286.3	0.263816	0.485939
286.4	0.266198	0.469354
286.5	0.264172	0.453565
286.6	0.256156	0.459144
286.7	0.245016	0.426142
286.8	0.236397	0.412958
286.9	0.230169	0.394237
287	0.225792	0.38404
287.1	0.22261	0.364464
287.2	0.223289	0.363049

287.3	0.230744	0.362396
287.4	0.243835	0.348494
287.5	0.26119	0.367941
287.6	0.282651	0.380281
287.7	0.30823	0.381941
287.8	0.339132	0.419341
287.9	0.378944	0.554871
288	0.428579	0.485744
288.1	0.483876	0.532981
288.2	0.537866	0.558313
288.3	0.587726	0.595653
288.4	0.632252	0.616364
288.5	0.668758	0.612128
288.6	0.690827	0.626222
288.7	0.695621	0.621153
288.8	0.689108	0.595375
288.9	0.674627	0.601478
289	0.658314	0.618465
289.1	0.644243	0.575101
289.2	0.634568	0.58128
289.3	0.629503	0.584615
289.4	0.626024	0.598261
289.5	0.626567	0.560673
289.6	0.632473	0.632285
289.7	0.641275	0.58035
289.8	0.65099	0.566742
289.9	0.660264	0.562433
290	0.668765	0.563921
290.1	0.675185	0.550582
290.2	0.68123	0.586983
290.3	0.688136	0.576865
290.4	0.694966	0.580523
290.5	0.699159	0.591124
290.6	0.700861	0.585608
290.7	0.702097	0.619069
290.8	0.706108	0.617135
290.9	0.712873	0.630513
291	0.72037	0.665372
291.1	0.727587	0.698614
291.2	0.735093	0.690608
291.3	0.743955	0.747913
291.4	0.752564	0.757675
291.5	0.758707	0.827162
291.6	0.762842	0.77605
291.7	0.766872	0.872048

291.8	0.774686	0.832938
291.9	0.78455	0.857709
292	0.791939	0.990303
292.3	0.807376	1.01717
292.6	0.825662	1.08034
292.9	0.83565	1.02926
293.2	0.838212	1.10234
293.5	0.857091	1.09933
293.8	0.855581	1.1632
294.1	0.864899	1.15275
294.4	0.86895	1.03859
294.7	0.871114	1.06935
295	0.870594	1.06281
295.3	0.88032	1.02254
295.6	0.884975	0.956748
295.9	0.882201	0.956243
296.2	0.897814	0.965645
296.5	0.892194	0.911027
296.8	0.895287	0.947913
297.1	0.903247	0.909887
297.4	0.903982	0.805323
297.7	0.916752	0.843051
298	0.916353	0.849961
298.3	0.915327	0.800308
298.6	0.919184	0.817575
298.9	0.931175	0.85297
299.2	0.948754	0.849381
299.5	0.960287	0.854321
299.8	0.950506	0.860248
300.1	0.950695	0.883943
300.4	0.973869	0.98748
300.7	0.993062	0.994903
301	0.999645	0.949202
301.3	1.00324	0.976749
301.6	0.989248	0.976222
301.9	1.00541	0.910801
302.2	1.0237	1.05
302.5	1.01342	0.924208
302.8	1.01665	0.90947
303.1	0.989438	0.926286
303.4	1.01988	0.877964
303.7	1.04982	0.877456
304	1.04587	0.830926
304.3	0.99469	0.82615
304.6	1.01598	0.823988

304.9	1.02186	0.833902
305	1.00533	0.755551
305.5	0.990745	0.774351
306	0.999313	0.752527
306.5	1.00085	0.780448
307	0.980797	0.760838
307.5	0.986514	0.719813
308	1.01133	0.746486
308.5	0.992491	0.738153
309	0.978274	0.737055
309.5	1.00335	0.734824
310	1.02355	0.752824

Fig. 3.5.b.

	cluster 1	cluster 2	cluster 3
280	1.88274	1.0881	0.731307
280.3	1.87693	1.09838	0.729971
280.6	1.87216	1.08031	0.742129
280.9	1.86804	1.07728	0.713719
281.2	1.86701	1.07689	0.708013
281.5	1.86308	1.07223	0.685187
281.8	1.86117	1.05776	0.687861
282.1	1.86581	1.07606	0.715033
282.4	1.85337	1.06491	0.708354
282.5	1.86409	1.06983	0.73781
282.6	1.85651	1.07695	0.740728
282.7	1.85801	1.07654	0.745629
282.8	1.85832	1.0852	0.75279
282.9	1.85801	1.09286	0.752797
283	1.85567	1.09416	0.747643
283.1	1.86098	1.10266	0.723963
283.2	1.85845	1.09517	0.712891
283.3	1.85937	1.09225	0.71886
283.4	1.86419	1.09975	0.708485
283.5	1.86829	1.10276	0.70366
283.6	1.8655	1.11635	0.714948
283.7	1.8764	1.13483	0.717882
283.8	1.87995	1.16544	0.721046
283.9	1.88492	1.22025	0.709673
284	1.9049	1.31219	0.740123
284.1	1.91422	1.4076	0.762762
284.2	1.9314	1.49683	0.776681
284.3	1.93071	1.57471	0.791458
284.4	1.94516	1.65529	0.821701

284.5	1.95821	1.70839	0.845871
284.6	1.96172	1.74278	0.854456
284.7	1.96389	1.764	0.872583
284.8	1.96803	1.77001	0.876249
284.9	1.97357	1.79087	0.880346
285	1.97121	1.78056	0.882193
285.1	1.98313	1.79364	0.899262
285.2	1.98662	1.78009	0.891262
285.3	1.97813	1.77084	0.8879
285.4	1.98057	1.77531	0.881525
285.5	1.97832	1.76329	0.881475
285.6	1.9755	1.7731	0.888486
285.7	1.97614	1.75267	0.884341
285.8	1.97536	1.75881	0.879991
285.9	1.97066	1.75877	0.890512
286	1.97993	1.76363	0.902251
286.1	1.98061	1.7773	0.895157
286.2	1.98973	1.78855	0.901037
286.3	2.01698	1.79632	0.922567
286.4	2.04173	1.80273	0.931326
286.5	2.05654	1.78462	0.940185
286.6	2.07608	1.78444	0.949297
286.7	2.07681	1.77478	0.945877
287	2.00915	1.64695	0.898846
287.1	2.07279	1.69018	0.940105
287.2	2.15558	1.72374	0.931729
287.3	2.18607	1.7748	0.995874
287.4	2.20864	1.84452	1.03032
287.5	2.21838	1.84897	1.05518
287.6	2.22131	1.85602	1.04325
287.7	2.22255	1.85192	1.05443
287.8	2.23369	1.83721	1.02598
287.9	2.22521	1.86614	1.03426
288	2.23026	1.88632	1.01936
288.1	2.23355	1.90716	0.989706
288.2	2.21849	1.90268	0.987573
288.3	2.23393	1.95443	1.00221
288.4	2.2361	2.00304	1.0115
288.5	2.24074	2.01868	1.05294
288.6	2.2365	2.02812	1.05357
288.7	2.2382	2.03947	1.05494
288.8	2.23249	2.02672	1.0676
288.9	2.24287	2.02983	1.06025
289	2.22665	2.01	1.06078
289.1	2.21756	1.97077	1.06204

289.2	2.2126	1.96851	1.0639
289.3	2.2097	1.96229	1.05222
289.4	2.20531	1.95959	1.05805
289.5	2.21928	1.97247	1.08432
289.6	2.22201	1.96624	1.06811
289.7	2.22868	1.98295	1.08655
289.8	2.22408	1.98144	1.07778
289.9	2.22665	1.9725	1.06755
290	2.24172	1.98458	1.10045
290.1	2.23793	1.985	1.11472
290.2	2.22258	1.97654	1.09872
290.3	2.22911	1.99218	1.11016
290.4	2.21797	1.99216	1.09419
290.5	2.2115	1.98493	1.11256
290.6	2.2075	1.97556	1.10688
290.7	2.20849	1.98229	1.11791
290.8	2.2201	1.99853	1.10867
290.9	2.22487	2.00897	1.10058
291	2.22914	2.00797	1.12078
291.1	2.22226	2.01861	1.10676
291.2	2.22873	2.01998	1.1171
291.3	2.23754	2.02303	1.0917
291.4	2.22796	2.02215	1.10417
291.5	2.24134	2.02416	1.0914
291.6	2.24625	2.05066	1.08437
291.7	2.22487	2.00792	1.08569
291.8	2.24794	2.04481	1.06281
291.9	2.25225	2.01591	1.07476
292	2.24412	2.00446	1.06876
292.3	2.24977	2.01242	1.06055
292.6	2.25182	2.01771	1.05224
292.9	2.2568	2.02418	1.06818
293.2	2.2496	2.02745	1.06623
293.5	2.24495	2.0247	1.06164
293.8	2.23865	2.0214	1.04755
294.1	2.23865	2.02275	1.02813
294.4	2.24383	2.01244	1.03891
294.7	2.24473	2.02855	1.04867
295	2.24191	2.02598	1.02605
295.3	2.2307	2.01652	1.02746
295.6	2.22952	2.01865	1.03043
295.9	2.23004	2.02829	1.05234
296.2	2.22839	2.03588	1.04459
296.5	2.2269	2.02384	1.06185
296.8	2.21748	2.0301	1.06051

297.1	2.21555	2.02585	1.06541
297.4	2.21363	2.01517	1.07322
297.7	2.2106	2.01371	1.05856
298	2.19855	2.01809	1.0763
298.3	2.19126	2.01134	1.07719
298.6	2.19357	2.02844	1.09026
298.9	2.19543	2.03086	1.10393
299.2	2.19099	2.0338	1.09916
299.5	2.19483	2.02518	1.07629
299.8	2.18915	2.01975	1.08477
300.1	2.19653	2.03332	1.05365
300.4	2.19956	2.0381	1.06795
300.7	2.19396	2.02921	1.07045
301	2.17968	2.01353	1.09338
301.3	2.18418	2.00669	1.05319
301.6	2.17619	2.00692	1.06631
301.9	2.17578	2.01099	1.03262
302.2	2.16713	2.02018	1.06158
302.5	2.1687	2.00265	1.0537
302.8	2.16269	1.97748	1.02997
303.1	2.14619	1.95206	1.03259
303.4	2.13654	1.95783	1.03033
303.7	2.13139	1.94279	1.02729
304	2.11546	1.94688	1.01654
304.3	2.11864	1.9316	0.991271
304.6	2.1033	1.90829	0.992967
304.9	2.08782	1.86818	0.985637
305	2.03845	1.84367	0.94297
305.5	2.05932	1.85713	0.93703
306	2.08905	1.88193	0.953649
306.5	2.10427	1.90736	0.976541
307	2.03625	1.85857	0.950381
307.5	2.10055	1.90352	0.974136
308	2.10508	1.91291	0.97534
308.5	2.09488	1.89335	0.979285
309	2.07071	1.86182	0.955405
309.5	2.09525	1.848	0.929603
310	2.07992	1.80617	0.92767

Fig. 3.5.c.

	HA	FIT
280	0.003631	-0.09839
280.3	-0.00196	-0.08058
280.6	0.001439	-0.07497
280.9	0.001446	-0.07565

281.2	0.000229	-0.0721
281.5	0.001331	-0.08955
281.8	6.38E-05	-0.11411
282.1	-0.0008	-0.14099
282.4	-0.00262	-0.13979
282.5	-0.00171	-0.1339
282.6	-0.00074	-0.11862
282.7	-0.00037	-0.10039
282.8	-0.00034	-0.08512
282.9	-0.00231	-0.06514
283	0.000793	-0.05058
283.1	0.001945	-0.03735
283.2	0.002815	-0.04194
283.3	0.002537	-0.04031
283.4	-0.00016	-0.03353
283.5	0.004116	-0.03198
283.6	0.004439	-0.01618
283.7	0.007098	-0.00203
283.8	0.01663	0.035473
283.9	0.032788	0.101699
284	0.050575	0.204744
284.1	0.091688	0.327814
284.2	0.150524	0.418964
284.3	0.231541	0.517477
284.4	0.326821	0.602851
284.5	0.421967	0.644166
284.6	0.516202	0.670016
284.7	0.600763	0.708407
284.8	0.667659	0.712112
284.9	0.717328	0.7165
285	0.746757	0.720373
285.1	0.754647	0.722122
285.2	0.755716	0.696905
285.3	0.717837	0.695958
285.4	0.672365	0.694366
285.5	0.621132	0.679165
285.6	0.567313	0.681146
285.7	0.52324	0.664712
285.8	0.48781	0.681912
285.9	0.467468	0.689484
286	0.467519	0.6933
286.1	0.479459	0.704378
286.2	0.485198	0.707269
286.3	0.485161	0.699951
286.4	0.480527	0.67919

286.5	0.468203	0.659067
286.6	0.449903	0.640395
286.7	0.428133	0.623302
287	0.354197	0.565216
287.1	0.331742	0.551066
287.2	0.324263	0.597886
287.3	0.323919	0.654303
287.4	0.319047	0.68345
287.5	0.321435	0.659297
287.6	0.333522	0.64972
287.7	0.353975	0.640332
287.8	0.392221	0.615999
287.9	0.453584	0.651317
288	0.548475	0.687801
288.1	0.664634	0.704534
288.2	0.771849	0.704979
288.3	0.861933	0.815861
288.4	0.916299	0.903485
288.5	0.955825	0.954574
288.6	0.978216	0.94443
288.7	0.974335	0.96365
288.8	0.961236	0.954478
288.9	0.92323	0.949405
289	0.889944	0.932556
289.1	0.866137	0.898527
289.2	0.843462	0.893061
289.3	0.823593	0.880072
289.4	0.813591	0.875361
289.5	0.818825	0.877665
289.6	0.828937	0.863358
289.7	0.832796	0.86516
289.8	0.844406	0.868085
289.9	0.830945	0.858019
290	0.816792	0.84933
290.1	0.814152	0.854311
290.2	0.812865	0.853885
290.3	0.823174	0.848672
290.4	0.828714	0.851604
290.5	0.836925	0.835743
290.6	0.857064	0.836579
290.7	0.883624	0.835278
290.8	0.897119	0.85564
290.9	0.911572	0.841274
291	0.920512	0.839979
291.1	0.914441	0.863507

291.2	0.916439	0.855661
291.3	0.937088	0.825666
291.4	0.949783	0.841874
291.5	0.94991	0.854056
291.6	0.961609	0.922725
291.7	0.975212	0.843631
291.8	0.969113	0.871567
291.9	0.96455	0.867938
292	0.974253	0.85157
292.3	0.987952	0.822913
292.6	0.98791	0.846263
292.9	0.991332	0.865035
293.2	0.987425	0.85731
293.5	0.982429	0.863316
293.8	1.00761	0.851141
294.1	1.00342	0.892665
294.4	0.996155	0.876279
294.7	0.997403	0.929379
295	0.9803	0.912652
295.3	0.988912	0.920047
295.6	0.985744	0.934238
295.9	0.983541	0.960404
296.2	0.967683	0.956058
296.5	0.974993	0.919216
296.8	0.971206	0.973145
297.1	0.977428	0.948539
297.4	0.974149	0.943551
297.7	0.965831	0.951818
298	0.963589	0.94573
298.3	0.982306	0.978759
298.6	0.970341	0.947765
298.9	0.961303	0.973608
299.2	0.964226	0.971349
299.5	0.992895	0.952083
299.8	0.981281	0.972417
300.1	0.986028	0.93918
300.4	0.993024	0.96078
300.7	1.00111	0.947703
301	0.998323	0.930614
301.3	1.0167	0.90196
301.6	1.01078	0.896249
301.9	1.0179	0.893387
302.2	1.02382	0.883472
302.5	1.01801	0.859578
302.8	1.0389	0.832244

303.1	1.02387	0.839767
303.4	1.01471	0.830934
303.7	1.00902	0.813431
304	1.02058	0.833338
304.3	1.01917	0.842532
304.6	0.975643	0.802499
304.9	0.986575	0.76861
305	0.986102	0.807021
305.5	0.950503	0.819042
306	0.964901	0.845009
306.5	0.931458	0.885504
307	0.921884	0.856347
307.5	0.860883	0.875745
308	0.848239	0.883558
308.5	0.815379	0.84974
309	0.810899	0.796202
309.5	0.773132	0.736993
310	0.758138	0.696561

Fig. 3.5.d.

	FA	FIT
280	-0.0304	-0.13737
280.3	0.002906	-0.11085
280.6	0.005205	-0.10341
280.9	0.000271	-0.1099
281.2	0.012038	-0.10942
281.5	-0.00355	-0.13318
281.8	-0.00412	-0.16613
282.1	-0.01307	-0.2283
282.4	-0.0335	-0.19966
282.5	-0.03791	-0.18651
282.6	-0.0448	-0.15542
282.7	-0.04985	-0.13122
282.8	-0.04931	-0.10433
282.9	-0.04596	-0.07953
283	-0.04362	-0.06952
283.1	-0.04297	-0.05754
283.2	-0.04566	-0.06355
283.3	-0.04785	-0.0668
283.4	-0.04504	-0.06978
283.5	-0.03578	-0.06775
283.6	-0.02328	-0.05095
283.7	-0.00613	-0.04414
283.8	0.01249	-0.01465
283.9	0.026497	0.041337

284	0.037758	0.129666
284.1	0.057604	0.237878
284.2	0.087649	0.313825
284.3	0.12226	0.402699
284.4	0.16093	0.469925
284.5	0.198524	0.500254
284.6	0.231908	0.511922
284.7	0.258981	0.562413
284.8	0.28685	0.547876
284.9	0.315089	0.546603
285	0.350218	0.550517
285.1	0.387396	0.562439
285.2	0.409266	0.53191
285.3	0.415201	0.555302
285.4	0.414505	0.555929
285.5	0.409072	0.550566
285.6	0.395069	0.554859
285.7	0.376334	0.549457
285.8	0.355262	0.553584
285.9	0.328985	0.563816
286	0.306474	0.591244
286.1	0.29693	0.588826
286.2	0.294454	0.593854
286.3	0.287777	0.587108
286.4	0.274862	0.556292
286.5	0.263548	0.543334
286.6	0.25584	0.506528
286.7	0.246159	0.496844
287	0.23181	0.476121
287.1	0.226776	0.41817
287.2	0.220858	0.456485
287.3	0.222842	0.539517
287.4	0.230157	0.572133
287.5	0.232839	0.536646
287.6	0.23625	0.49995
287.7	0.248951	0.471204
287.8	0.272206	0.388852
287.9	0.300036	0.458449
288	0.335412	0.45373
288.1	0.386651	0.379586
288.2	0.454818	0.508056
288.3	0.544734	0.643299
288.4	0.648341	0.705198
288.5	0.744318	0.751634
288.6	0.799243	0.766234

288.7	0.80344	0.792917
288.8	0.773693	0.778193
288.9	0.725901	0.792132
289	0.671611	0.780936
289.1	0.620934	0.75492
289.2	0.58999	0.750882
289.3	0.576509	0.743393
289.4	0.571964	0.742781
289.5	0.572304	0.743059
289.6	0.574681	0.732843
289.7	0.575502	0.72859
289.8	0.574715	0.736254
289.9	0.572984	0.731676
290	0.56623	0.715798
290.1	0.558556	0.726115
290.2	0.561018	0.723823
290.3	0.569669	0.717215
290.4	0.574507	0.705922
290.5	0.573577	0.699316
290.6	0.575509	0.684942
290.7	0.582487	0.699644
290.8	0.598277	0.686665
290.9	0.624777	0.662228
291	0.651158	0.672639
291.1	0.670852	0.675982
291.2	0.692579	0.657409
291.3	0.714564	0.619882
291.4	0.722923	0.631856
291.5	0.725891	0.606734
291.6	0.73933	0.580391
291.7	0.758837	0.612957
291.8	0.769097	0.582467
291.9	0.77506	0.487124
292	0.778586	0.625556
292.3	0.798524	0.668958
292.6	0.845454	0.684223
292.9	0.83846	0.6877
293.2	0.85978	0.689584
293.5	0.870177	0.687549
293.8	0.862579	0.709555
294.1	0.863354	0.728759
294.4	0.858175	0.725305
294.7	0.86258	0.756318
295	0.858649	0.753766
295.3	0.842504	0.761116

295.6	0.86311	0.768728
295.9	0.853021	0.792924
296.2	0.843062	0.792745
296.5	0.849608	0.767124
296.8	0.862456	0.805385
297.1	0.874758	0.801775
297.4	0.856297	0.806506
297.7	0.882035	0.807421
298	0.903156	0.808174
298.3	0.926212	0.834192
298.6	0.916222	0.82113
298.9	0.921548	0.840201
299.2	0.928009	0.839293
299.5	0.984006	0.813079
299.8	0.952796	0.8547
300.1	1.0002	0.829219
300.4	0.987909	0.853463
300.7	1.00935	0.834647
301	0.996812	0.813813
301.3	1.02736	0.8108
301.6	1.03996	0.806682
301.9	1.04678	0.774085
302.2	1.02409	0.73707
302.5	1.01404	0.715717
302.8	1.02981	0.713608
303.1	1.07376	0.711105
303.4	1.0351	0.724259
303.7	1.03649	0.710846
304	1.01805	0.701137
304.3	1.02669	0.663552
304.6	0.942644	0.618268
304.9	0.976453	0.607214
305	0.959117	0.680019
305.5	0.908805	0.692085
306	0.915649	0.717142
306.5	0.929653	0.793184
307	0.829345	0.772444
307.5	0.827737	0.79279
308	0.779298	0.794875
308.5	0.776091	0.766963
309	0.703608	0.713191
309.5	0.714839	0.633211
310	0.761382	0.592164

Fig. 4.1.a.

	char	char+water	char+vermiculite	char+kaolinite	char+goethite	char+pyrophyllite
273.58	0.000401	0.001459	0.007017	0.006395	-0.00395	0.004173968
274.08	0.00063	5.36E-05	0.004769	0.001761	0.007032	0.001967459
274.58	0.000341	-0.00014	0.001512	0.002377	0.008005	0.002227349
275.08	3.71E-05	0.000806	-0.00131	0.000638	-0.00018	3.99371E-05
275.58	-7.6E-05	0.000143	-0.00058	-0.00269	-0.00134	-0.000380305
276.08	-0.00023	0.001165	-0.00083	0.001892	-0.00152	-0.001499777
276.58	-0.0004	0.000896	-0.00066	-0.00109	-0.00517	-0.00192002
277.08	-0.00038	0.000134	7E-06	-0.00338	-0.00235	-0.000127995
277.58	-0.00036	0.000151	-0.00028	-0.00115	-0.00129	-0.000521796
278.08	-0.00035	-0.00015	0.002795	0.001034	-0.00356	0.000806034
278.58	-0.0003	0.000229	0.002582	0.001212	0.000284	0.001659387
279.08	-0.0001	-1.7E-06	-0.00146	0.001131	0.000922	-0.000497177
279.58	0.000294	-7.4E-05	-0.0018	-0.00496	0.006193	0.000231314
280.08	0.000905	-0.00048	-0.005	-0.00947	0.00814	-0.001250993
280.58	0.001867	-0.00049	-0.00872	-0.00765	0.009328	-0.00086624
281.08	0.003335	-8.7E-05	-0.01248	-0.01325	0.005895	-0.002795114
281.58	0.006095	0.000396	-0.01318	-0.01885	0.01213	-0.000268605
281.68	0.006759	-5.4E-05	-0.01192	-0.01745	0.009518	-0.002242923
281.78	0.007498	-2E-05	-0.01571	-0.01557	0.007992	-0.003068506
281.88	0.008397	0.000249	-0.01555	-0.01426	0.007738	-0.002917226
281.98	0.009602	0.000413	-0.01456	-0.01959	0.008823	-0.004214349
282.08	0.010957	0.000997	-0.0138	-0.02112	0.00778	-0.004030751
282.18	0.012348	0.002407	-0.01097	-0.02076	0.010357	-0.001464487
282.28	0.014334	0.003539	-0.01265	-0.01732	0.011885	-0.000804943

282.38	0.01647	0.005316	-0.01084	-0.01113	0.0065	-0.00275135
282.48	0.019254	0.006943	-0.00967	-0.0114	0.013345	0.000298205
282.58	0.022868	0.009105	-0.00811	-0.00954	0.013126	-0.000371668
282.68	0.02694	0.011488	-0.00845	-0.0014	0.006985	-0.002059536
282.78	0.032925	0.014707	-0.0052	0.00582	0.01257	-0.000644943
282.88	0.040535	0.01737	-0.00287	0.011562	0.009061	-0.004308575
282.98	0.048709	0.021145	-0.00086	0.023088	0.010754	-0.004997544
283.08	0.063597	0.025467	0.00415	0.037169	0.008371	-0.008788976
283.18	0.087058	0.033	0.010561	0.052781	0.004945	-0.013751176
283.28	0.090973	0.042356	0.021456	0.054845	0.014134	-0.010180136
283.38	0.091802	0.06097	0.035624	0.065404	0.031613	0.000278897
283.48	0.119441	0.09087	0.055088	0.088383	0.053537	0.02323151
283.58	0.138806	0.136713	0.078586	0.119253	0.097122	0.066905394
283.68	0.18991	0.199099	0.115081	0.159228	0.150625	0.11918009
283.78	0.227634	0.270164	0.159871	0.223756	0.22644	0.19260353
283.88	0.284517	0.355836	0.212754	0.295134	0.305492	0.27320729
283.98	0.350782	0.436784	0.256411	0.368837	0.376766	0.3438664
284.08	0.424102	0.516701	0.310653	0.433254	0.443279	0.4125991
284.18	0.487978	0.583238	0.355237	0.491726	0.497695	0.47017351
284.28	0.553299	0.651941	0.392956	0.548833	0.543759	0.52030319
284.38	0.601924	0.706443	0.426687	0.586084	0.580307	0.56354928
284.48	0.637208	0.750796	0.459428	0.613039	0.604753	0.59588829
284.58	0.662427	0.776405	0.475139	0.615849	0.631519	0.62572857
284.68	0.681598	0.801618	0.498097	0.6288	0.660287	0.65378112
284.78	0.690979	0.806056	0.509101	0.631766	0.684342	0.66893466
284.88	0.687169	0.795454	0.513368	0.627543	0.700523	0.66789281
284.98	0.67776	0.778461	0.505414	0.605208	0.710811	0.66758252
285.08	0.664685	0.754573	0.495596	0.586107	0.706645	0.6606222
285.18	0.642375	0.727807	0.483786	0.551639	0.705187	0.64870999
285.28	0.617677	0.697072	0.468855	0.540141	0.68313	0.62648414
285.38	0.584272	0.660796	0.446514	0.510681	0.646769	0.60015547
285.48	0.563653	0.631835	0.428966	0.492179	0.612459	0.57953228

285.58	0.52508	0.60542	0.411196	0.475921	0.580388	0.55900897
285.68	0.49945	0.588252	0.402208	0.460268	0.560297	0.5454662
285.78	0.478802	0.57841	0.40006	0.439659	0.548183	0.53524624
285.88	0.461337	0.571636	0.397038	0.421767	0.544102	0.53069063
285.98	0.446595	0.567083	0.392135	0.423288	0.543109	0.53026575
286.08	0.434469	0.562839	0.388604	0.423784	0.540592	0.52905498
286.18	0.416055	0.55796	0.386105	0.409628	0.535651	0.5255247
286.28	0.402024	0.551691	0.386037	0.400818	0.538321	0.52594889
286.38	0.391702	0.545624	0.382792	0.387127	0.541548	0.525477
286.48	0.382522	0.537694	0.379245	0.378259	0.547802	0.52533857
286.58	0.377472	0.53414	0.384144	0.392759	0.55605	0.52621227
286.68	0.373599	0.534097	0.384796	0.385031	0.573023	0.53734377
286.78	0.367646	0.538549	0.392734	0.395519	0.584616	0.55391486
286.88	0.353706	0.542891	0.401242	0.407688	0.590962	0.57646024
286.98	0.344326	0.548486	0.410384	0.418452	0.590905	0.59339123
287.08	0.336742	0.552735	0.419189	0.435801	0.58846	0.61037217
287.18	0.335346	0.558792	0.431532	0.443072	0.586915	0.61818526
287.28	0.340765	0.563928	0.435406	0.458849	0.585354	0.62178096
287.38	0.346346	0.569926	0.443442	0.469688	0.588524	0.62244899
287.48	0.354668	0.578081	0.45641	0.482087	0.60256	0.62627384
287.58	0.363034	0.584753	0.466739	0.509094	0.613029	0.63206711
287.68	0.372969	0.595328	0.483154	0.51999	0.632816	0.63955997
287.78	0.37934	0.607934	0.501511	0.550013	0.656631	0.64742742
287.88	0.390791	0.619652	0.519475	0.56933	0.681398	0.65683582
287.98	0.394747	0.631388	0.533842	0.583967	0.711326	0.66377783
288.08	0.401343	0.642646	0.554114	0.603589	0.74666	0.67607422
288.18	0.41855	0.649636	0.574694	0.633295	0.778006	0.69056378
288.28	0.426147	0.652913	0.589937	0.644652	0.785672	0.69057519
288.38	0.43266	0.652141	0.591283	0.636015	0.784657	0.68984623
288.48	0.434093	0.6486	0.585484	0.621438	0.775298	0.68455466
288.58	0.434139	0.643376	0.573659	0.610723	0.758297	0.67770746
288.68	0.430634	0.638753	0.565169	0.597452	0.740915	0.67109088

288.78	0.436577	0.639588	0.562275	0.590703	0.73135	0.67052057
288.88	0.443608	0.646353	0.564743	0.590785	0.728849	0.67277509
288.98	0.452929	0.651401	0.566271	0.594217	0.722032	0.67332267
289.08	0.459533	0.658039	0.570786	0.596457	0.721856	0.68208767
289.18	0.46779	0.662676	0.573317	0.605455	0.726891	0.68316701
289.28	0.476048	0.670703	0.576455	0.605364	0.729877	0.69276197
289.38	0.487584	0.678646	0.581404	0.614868	0.735088	0.69973923
289.48	0.498005	0.685182	0.584776	0.634145	0.739062	0.70414726
289.58	0.513302	0.694465	0.589711	0.643258	0.74041	0.70937057
289.68	0.527481	0.705588	0.598997	0.656681	0.747614	0.71641833
289.78	0.542356	0.71246	0.601157	0.665437	0.750239	0.7189593
289.88	0.558952	0.723566	0.607818	0.679159	0.755626	0.72207758
289.98	0.581268	0.734884	0.617278	0.697245	0.770872	0.73115252
290.08	0.594005	0.745078	0.626841	0.706185	0.778233	0.73460426
290.18	0.604146	0.752345	0.635307	0.715314	0.796672	0.74596638
290.28	0.614156	0.761901	0.643719	0.74319	0.807478	0.75236927
290.38	0.629401	0.772465	0.652559	0.76676	0.817693	0.76384157
290.48	0.641119	0.783598	0.660607	0.781766	0.826349	0.77354083
290.58	0.656441	0.796565	0.67048	0.801043	0.844293	0.78826396
290.68	0.672331	0.812572	0.685881	0.817845	0.853865	0.79723167
290.78	0.687361	0.826363	0.696221	0.827257	0.866985	0.80914906
290.88	0.697169	0.837583	0.704757	0.833653	0.877431	0.82026
290.98	0.711319	0.854727	0.718201	0.847882	0.899864	0.83792841
291.08	0.723968	0.86887	0.728533	0.856465	0.911238	0.85357846
291.18	0.72903	0.884967	0.742319	0.865163	0.917602	0.8630133
291.28	0.752606	0.897861	0.753118	0.875329	0.933093	0.87825057
291.38	0.768583	0.910201	0.765729	0.890208	0.947481	0.89205118
291.48	0.780668	0.921021	0.779934	0.89714	0.950485	0.89955727
291.58	0.795828	0.929417	0.785385	0.898402	0.963618	0.91097081
291.68	0.806624	0.937064	0.793004	0.901454	0.966285	0.91472809
291.78	0.815821	0.94452	0.801314	0.902532	0.976955	0.92434361
291.88	0.823258	0.950359	0.807808	0.905117	0.981231	0.92987834

291.98	0.832416	0.955356	0.813882	0.9076	0.988823	0.93493712
292.08	0.828673	0.961244	0.819616	0.915314	0.988302	0.93573737
292.18	0.84191	0.965831	0.824169	0.91756	0.997533	0.94285858
292.28	0.851448	0.969357	0.831054	0.917895	0.998965	0.94316672
292.38	0.859913	0.975851	0.837669	0.915888	1.007203	0.95034376
292.48	0.864506	0.978837	0.840382	0.915113	1.007243	0.95081201
292.58	0.868922	0.979656	0.845891	0.91466	1.010748	0.95465596
292.68	0.87578	0.980579	0.846188	0.913689	1.009531	0.95500082
292.78	0.87852	0.979915	0.846522	0.91186	1.003678	0.9518892
292.88	0.88017	0.984996	0.850802	0.911603	1.01223	0.95944817
292.98	0.872974	0.986132	0.851145	0.915754	1.007985	0.95710923
293.08	0.880129	0.986584	0.850065	0.925218	1.013565	0.96191094
293.18	0.884424	0.987079	0.854271	0.91844	1.012961	0.9616976
293.28	0.884667	0.986679	0.857179	0.927028	1.01455	0.96135939
293.38	0.885059	0.9864	0.857924	0.919813	1.014342	0.96034692
293.48	0.884388	0.98492	0.85899	0.918738	1.014267	0.96091066
293.58	0.885122	0.982514	0.859742	0.919563	1.010118	0.95632567
294.08	0.87513	0.978684	0.864377	0.931582	0.997895	0.94948002
294.58	0.883332	0.976286	0.864423	0.945571	0.992589	0.94760242
295.08	0.886985	0.976117	0.870608	0.933026	0.991079	0.9495368
295.58	0.892014	0.978604	0.884891	0.936263	0.988881	0.95265516
296.08	0.911145	0.982264	0.90045	0.945192	0.991213	0.95713967
296.58	0.932005	0.986442	0.935268	0.957298	0.994778	0.96437849
297.08	0.951051	0.989836	1.096095	1.030654	0.998591	0.97964376
297.58	0.943774	0.990682	0.927846	0.954615	0.994303	0.97033612
298.08	0.942225	0.995111	0.93222	0.954221	0.995396	0.97411699
298.58	0.953033	0.995233	0.93436	0.96997	0.995206	0.97757762
299.08	0.972312	0.998081	0.96997	0.984655	0.99787	0.98475769
299.58	0.995193	0.998202	1.074886	1.019455	0.998285	0.99348311
300.08	0.994161	0.999103	1.014087	1.002496	1.001634	0.99483577
300.58	0.989454	1.000404	0.985399	1.007569	0.995778	0.98979989
301.08	0.991111	0.9999	0.977738	0.980071	1.000372	0.99740008

301.58	1.001135	1.002869	0.98284	0.988816	1.003326	1.0023605
302.08	1.004899	1.004277	0.988871	0.987	1.006501	1.0061238
302.58	1.011289	1.00371	0.995105	0.99837	1.002447	1.0073736
303.08	1.014359	0.999747	0.996513	0.996818	1.001867	1.0102511
303.58	1.016213	0.998245	0.998062	1.007796	0.997275	1.0092593
304.08	1.018812	0.995463	0.998563	1.013186	0.994644	1.0098701
304.58	1.0197	0.989326	0.999473	1.012227	0.991163	1.0105647
305.08	1.013231	0.982253	0.997574	1.008799	0.983764	1.0088501
305.58	1.012253	0.974061	1.00051	1.008606	0.977932	1.0073045
306.08	1.002839	0.964504	1.004561	1.002553	0.969505	1.0066741
306.58	1.004271	0.957195	1.005891	1.009836	0.966113	1.0027149
307.08	0.998166	0.948868	1.007846	1.004728	0.958679	0.99891446
307.58	0.988899	0.938441	1.006615	0.996782	0.948032	0.99225684
308.08	0.982189	0.927263	0.999999	0.989389	0.936621	0.98579312
308.58	0.969514	0.917302	0.995496	0.98085	0.929763	0.9814124

Fig. 4.1.b.

	char	char+water	char+vermiculite	char+kaolinite	char+goethite	char+pyrophyllite
273.58	0.010422	0.007493	0.013729	0.007823	-0.01347	0.002687958
274.08	0.004565	0.004206	0.008922	0.00195	-0.00028	0.002310571
274.58	0.002094	0.001669	0.004859	0.00125	0.004774	0.002781152
275.08	0.000597	0.001043	-0.00209	0.001834	-0.00033	-0.001697445
275.58	-0.00049	-0.0006	-0.00138	-0.00047	0.000534	0.000634703
276.08	-0.00346	-0.00129	-0.00092	-0.00045	-0.00296	-0.001750081
276.58	-0.00314	-0.00129	-0.00324	-0.0009	-0.00332	-0.002401122
277.08	-0.00265	-0.00127	-0.00044	-0.00278	-0.00462	-0.002414837
277.58	-0.00147	-0.00035	0.000468	-0.00182	-0.00094	0.001035333
278.08	-0.00201	-6.5E-05	0.001277	-7.3E-05	0.007118	0.003561919
278.58	-0.00048	0.001231	0.002209	0.00136	0.010937	0.003315958
279.08	0.000222	0.000931	-0.00074	0.002063	0.016819	-0.000325473
279.58	0.002003	-1.8E-05	-0.00153	-0.00038	0.03039	-0.002737262
280.08	0.004124	-0.00089	-0.00483	-0.00303	0.04038	-0.006722562

280.58	0.005625	-0.00232	-0.00841	-0.00411	0.048981	-0.008833692
281.08	0.008589	-0.00508	-0.01381	-0.00655	0.056577	-0.014588741
281.58	0.010883	-0.00526	-0.011	-0.00958	0.067759	-0.0178629
281.68	0.009778	-0.00577	-0.01225	-0.0102	0.065559	-0.019754936
281.78	0.009977	-0.00568	-0.0136	-0.01162	0.065619	-0.021778399
281.88	0.011758	-0.0059	-0.01508	-0.01183	0.067393	-0.022934089
281.98	0.013707	-0.00707	-0.01399	-0.01245	0.071772	-0.023603684
282.08	0.012989	-0.0066	-0.01681	-0.01167	0.07154	-0.023844794
282.18	0.014388	-0.00565	-0.01196	-0.01361	0.079489	-0.024908667
282.28	0.01668	-0.00532	-0.01262	-0.01409	0.084648	-0.025191185
282.38	0.021469	-0.00698	-0.01889	-0.0133	0.085115	-0.025147839
282.48	0.023714	-0.00548	-0.01418	-0.01408	0.091609	-0.02554198
282.58	0.026942	-0.00578	-0.01576	-0.01446	0.093896	-0.02730079
282.68	0.030371	-0.00621	-0.02383	-0.01159	0.088129	-0.029498886
282.78	0.038156	-0.00559	-0.017	-0.01091	0.103452	-0.030425932
282.88	0.044206	-0.00705	-0.02225	-0.00886	0.10186	-0.031682443
282.98	0.055853	-0.00712	-0.01996	-0.00984	0.114425	-0.034714104
283.08	0.068564	-0.00987	-0.0187	-0.01157	0.122729	-0.037490115
283.18	0.077916	-0.01354	-0.02476	-0.01311	0.135112	-0.040408354
283.28	0.094393	-0.01374	-0.0164	-0.0224	0.142406	-0.041573047
283.38	0.106331	-0.00775	-0.01103	-0.02396	0.156297	-0.03631587
283.48	0.122767	0.010032	-0.0015	-0.01036	0.157654	-0.017464209
283.58	0.148	0.046395	0.025084	0.014751	0.18056	0.01463087
283.68	0.182793	0.093975	0.062359	0.061676	0.204309	0.066288613
283.78	0.239272	0.159831	0.132423	0.115366	0.242424	0.12939302
283.88	0.297871	0.231302	0.201417	0.180174	0.285638	0.20291248
283.98	0.356702	0.299837	0.275054	0.248607	0.340967	0.27525912
284.08	0.418592	0.367692	0.350944	0.318915	0.39933	0.33635913
284.18	0.469464	0.425114	0.414811	0.37403	0.454188	0.39640774
284.28	0.51159	0.482642	0.466929	0.425858	0.498327	0.44448397
284.38	0.53855	0.53194	0.501748	0.469837	0.540738	0.48610414
284.48	0.546288	0.565279	0.512806	0.50346	0.580334	0.52236824

284.58	0.538363	0.594659	0.52223	0.525905	0.607353	0.54946133
284.68	0.529502	0.620429	0.527926	0.546453	0.636699	0.57609533
284.78	0.514981	0.6334	0.525327	0.556337	0.655316	0.59472495
284.88	0.497749	0.634527	0.507919	0.563295	0.650412	0.60127599
284.98	0.483913	0.629988	0.483709	0.554851	0.63105	0.6087326
285.08	0.47379	0.617003	0.467144	0.546612	0.599562	0.60604241
285.18	0.470441	0.603223	0.4536	0.53068	0.578476	0.59859388
285.28	0.470865	0.58149	0.443543	0.512865	0.549812	0.58194373
285.38	0.467104	0.555586	0.429341	0.491824	0.509184	0.55657445
285.48	0.470249	0.532343	0.424203	0.46942	0.47669	0.53562145
285.58	0.475322	0.511055	0.425648	0.448593	0.44502	0.51427238
285.68	0.482558	0.496921	0.431656	0.433917	0.425471	0.5005442
285.78	0.491826	0.487194	0.440172	0.423428	0.416967	0.4892051
285.88	0.491446	0.480246	0.44334	0.414414	0.417756	0.48464074
285.98	0.485231	0.47366	0.438511	0.407229	0.417386	0.48095495
286.08	0.471591	0.468215	0.430339	0.39996	0.419491	0.47387729
286.18	0.452477	0.46164	0.418209	0.392406	0.422688	0.46800587
286.28	0.432319	0.456487	0.406345	0.38604	0.427105	0.46459914
286.38	0.412615	0.450624	0.395943	0.380656	0.431417	0.46091335
286.48	0.393785	0.447353	0.385078	0.377324	0.436256	0.46016394
286.58	0.381054	0.446874	0.378543	0.379686	0.447347	0.46030031
286.68	0.370741	0.449761	0.375477	0.384921	0.463843	0.46955548
286.78	0.364696	0.457959	0.380405	0.39402	0.478865	0.48179383
286.88	0.359367	0.46419	0.388188	0.401062	0.488123	0.49593337
286.98	0.357463	0.470901	0.399777	0.410214	0.485033	0.50647039
287.08	0.359021	0.475865	0.410648	0.417003	0.485578	0.51637909
287.18	0.370807	0.481685	0.428834	0.427885	0.488952	0.5233172
287.28	0.392389	0.484605	0.443418	0.432752	0.504261	0.52639354
287.38	0.423527	0.490656	0.471012	0.442211	0.532031	0.53265832
287.48	0.46042	0.500108	0.504252	0.452441	0.572522	0.53797431
287.58	0.500358	0.507379	0.539405	0.462114	0.625461	0.54445333
287.68	0.545608	0.517386	0.583935	0.4762	0.705123	0.55358067

287.78	0.592277	0.530504	0.62873	0.490307	0.801254	0.56343896
287.88	0.630497	0.542421	0.673676	0.504237	0.918302	0.57239707
287.98	0.656755	0.553023	0.711239	0.516107	1.008449	0.58051621
288.08	0.686865	0.568481	0.756089	0.533431	1.083218	0.5944055
288.18	0.715382	0.582817	0.795713	0.55287	1.130795	0.61222676
288.28	0.728088	0.5879	0.810548	0.561773	1.132517	0.61448034
288.38	0.721191	0.592241	0.806046	0.562641	1.100597	0.61626223
288.48	0.698866	0.590033	0.773577	0.557328	1.047015	0.61302473
288.58	0.669657	0.586657	0.729093	0.553224	0.983402	0.6075692
288.68	0.63662	0.584428	0.68097	0.54561	0.917003	0.6023171
288.78	0.614328	0.586121	0.649783	0.544716	0.867174	0.60303138
288.88	0.602122	0.594368	0.635977	0.549807	0.831999	0.60764523
288.98	0.592341	0.596481	0.618044	0.555677	0.803263	0.60755295
289.08	0.587039	0.604747	0.613161	0.560053	0.784772	0.6157261
289.18	0.583414	0.606954	0.606084	0.566002	0.775823	0.61962702
289.28	0.584765	0.614745	0.603467	0.571133	0.770378	0.6254111
289.38	0.588836	0.621393	0.604718	0.578589	0.77391	0.63378229
289.48	0.593354	0.627261	0.604672	0.585335	0.772118	0.63854917
289.58	0.59949	0.63379	0.604619	0.593623	0.773299	0.64364912
289.68	0.607999	0.642062	0.613605	0.602532	0.781585	0.65173226
289.78	0.610876	0.648413	0.612758	0.6079	0.784097	0.65433331
289.88	0.616864	0.6584	0.621992	0.618013	0.794537	0.66128222
289.98	0.624665	0.669016	0.631732	0.628299	0.80605	0.67017372
290.08	0.632038	0.676147	0.642326	0.640375	0.820564	0.67919304
290.18	0.640942	0.688991	0.650443	0.649092	0.827753	0.68972466
290.28	0.648582	0.699492	0.658646	0.660717	0.839261	0.7003427
290.38	0.655514	0.710937	0.666446	0.672197	0.844382	0.71217417
290.48	0.663177	0.72228	0.67591	0.684094	0.853956	0.72656756
290.58	0.67194	0.735497	0.684834	0.699981	0.859805	0.74088893
290.68	0.683204	0.749975	0.697993	0.713136	0.865601	0.75506447
290.78	0.690948	0.763192	0.706461	0.727102	0.86627	0.76626942
290.88	0.697547	0.771873	0.708872	0.738828	0.873081	0.78124972

290.98	0.708997	0.790414	0.727823	0.753895	0.881319	0.7971302
291.08	0.715265	0.805715	0.737587	0.766398	0.878914	0.80992846
291.18	0.72572	0.818339	0.742932	0.780825	0.880057	0.81720324
291.28	0.731779	0.832302	0.751318	0.792891	0.881128	0.83305491
291.38	0.742953	0.849989	0.766125	0.807556	0.877306	0.84875715
291.48	0.753106	0.8608	0.77636	0.819428	0.876639	0.85906013
291.58	0.761449	0.870613	0.781403	0.829595	0.873134	0.8470837
291.68	0.769166	0.87602	0.784995	0.838462	0.874454	0.85255452
291.78	0.776831	0.886945	0.792731	0.845265	0.875424	0.86404393
291.88	0.784324	0.894133	0.798151	0.852674	0.876634	0.87089562
291.98	0.791078	0.899672	0.8025	0.858994	0.878643	0.8791876
292.08	0.802021	0.90316	0.805202	0.865283	0.882113	0.87843459
292.18	0.807871	0.911262	0.813534	0.870873	0.883222	0.88624948
292.28	0.81432	0.911904	0.815269	0.875914	0.886888	0.88911158
292.38	0.822838	0.921198	0.827648	0.878716	0.890894	0.89435016
292.48	0.828257	0.92547	0.83179	0.884526	0.893434	0.89659114
292.58	0.831888	0.927642	0.84	0.885459	0.897646	0.90044704
292.68	0.836559	0.930625	0.844069	0.889187	0.902116	0.90371963
292.78	0.838908	0.927959	0.844584	0.891338	0.902627	0.9028766
292.88	0.845202	0.935435	0.848837	0.895116	0.91311	0.90782892
292.98	0.852507	0.933437	0.848679	0.894515	0.915211	0.90301971
293.08	0.854281	0.937115	0.859181	0.89792	0.921758	0.9083393
293.18	0.861047	0.939114	0.866848	0.900243	0.925597	0.9076259
293.28	0.866118	0.939852	0.871137	0.901734	0.9292	0.90933577
293.38	0.869255	0.939301	0.874503	0.903287	0.933464	0.91046233
293.48	0.873673	0.941607	0.879441	0.903108	0.940233	0.91186615
293.58	0.876701	0.939684	0.882602	0.903062	0.940921	0.90881769
294.08	0.896718	0.933963	0.893563	0.90155	0.944533	0.90690341
294.58	0.90955	0.934471	0.907735	0.904498	0.95119	0.9078823
295.08	0.922466	0.935685	0.915205	0.907772	0.961381	0.90762975
295.58	0.932229	0.941698	0.922751	0.916772	0.971274	0.91440218
296.08	0.939167	0.950436	0.931378	0.930382	0.978678	0.92707439

296.58	0.94462	0.964754	0.944741	0.94676	0.982205	0.94210505
297.08	0.950014	1.034288	0.997861	1.040622	0.984759	1.0427858
297.58	0.955897	0.963768	0.94209	0.946924	0.987261	0.94779317
298.08	0.965938	0.965755	0.960387	0.948604	0.995048	0.95183807
298.58	0.970464	0.971386	0.967042	0.955884	0.995453	0.95889316
299.08	0.971888	0.987413	0.978373	0.976102	0.999228	0.99408421
299.58	0.976985	1.026439	1.007099	1.020193	0.994002	1.0274533
300.08	0.982526	1.000831	0.983116	0.998203	1.000047	1.0005555
300.58	0.988659	0.990245	0.985024	0.987534	0.995396	0.98258563
301.08	0.995953	0.99202	0.99336	0.990745	0.999296	0.9854801
301.58	1.005368	0.995994	1.002209	0.996853	1.005604	0.99011912
302.08	1.01154	1.001423	1.007974	1.001663	1.010375	0.99800237
302.58	1.019392	1.002821	1.012349	1.005612	1.008989	0.99884984
303.08	1.022128	1.000715	1.014426	1.006808	1.002682	1.0026787
303.58	1.023677	1.001879	1.016456	1.009863	0.995934	1.002554
304.08	1.024472	1.000221	1.014995	1.008817	0.988449	1.0051064
304.58	1.022263	0.998255	1.012684	1.009504	0.976674	1.0065155
305.08	1.018221	0.993005	1.010236	1.007095	0.9631	1.0057553
305.58	1.013123	0.989682	1.007935	1.005493	0.950712	1.0066946
306.08	1.006225	0.983672	1.000887	1.002193	0.933968	1.0054806
306.58	0.998582	0.980623	0.996622	1.002381	0.924434	1.0071005
307.08	0.992027	0.975403	0.996314	1.000208	0.91423	1.0032256
307.58	0.98434	0.970212	0.991378	0.995901	0.901283	0.99655116
308.08	0.974738	0.961035	0.985063	0.990074	0.889719	0.9912036
308.58	0.967894	0.952983	0.983502	0.984758	0.88864	0.99000407